From deposit to product

A probabilistic approach to the value chain of underground iron ore mining

by

Steinar Løve Ellefmo

This thesis has been submitted

to

Department of Geology and Mineral Resources Engineering
Norwegian University of Science and Technology

in partial fulfilment of the requirements for
the Norwegian academic degree

DOKTOR INGENIØR

January 2005

New spring in mining

Identify and assess

Certainty and risk

Preface

The following work has been carried out at the Department of Geology and Mineral Resources Engineering, NTNU, in cooperation with the Norwegian iron ore mining company Rana Gruber AS. Although it has been conducted as a stand-alone doctoral project without any regular or direct contact with a research unit or group, it constitutes a part of a vision regarding the effective utilisation of in-situ quality variations in mineral deposits. This vision was coined and developed by Associate Professor Erik Ludvigsen and documented in a series of doctoral projects.

This work in particular was initiated in 2001, partly as a spin off from the IT-Development Programme for the Norwegian Mining Industry, headed by Per Helge Fredheim.

I would like to especially acknowledge:

- Associate Professor Erik Ludvigsen for his ability to see the best in any situation, for his encouragement and support.
- Rana Gruber AS for financial support and interesting discussions.
- Roar Sandøy for reviewing the scientific content and for proofreading.
- Maria Thornhill at the Department of Geology and Mineral Resources Engineering for her editorial assistance.
- My colleagues and the staff at the Department of Geology and Mineral Resources Engineering for valuable discussions and assistance.
- Susanne for her infinite patience and kindness.
- Family and friends who gave me a refuge from the scientific work and made me laugh whenever I needed it.

Steinar Løve Ellefmo

Trondheim, January 2005

Abstract

Mining activities will eventually deplete any deposit. In a sustainability perspective, the deposit should therefore be utilised optimally during production. A prerequisite to achieve this is the deliberate and consistent utilisation of the variations in the deposit.

In an ideal world everything is certain. In the real world nothing is certain. In the real world everything is more or less probable.

Therefore, the question asked is how an underground iron ore mining company like Rana Gruber AS can benefit from knowing and exploiting the uncertainty and variability of decisive ore parameters. The perspective is the value chain from in-situ ore to product, whereas the focus is on deposit characterisation and production.

In order to answer this question the existing database with geodata from the Kvannevann Iron Ore is reviewed and estimation techniques based on kriging and geostatistical simulation algorithms (Turning Band) are implemented to identify and assess the ore deposit uncertainties and variations and associated risks. Emphasise is on total iron in the ore (FeTot), total iron in the ore originating from magnetite (FeMagn), manganese oxide (MnO) and joint parameters. Due to insufficient number of assays of MnO, a geochemical MnO-signature is developed using cluster analysis. This geochemical signature is applied as input in the kriging with inequalities procedure. This procedure is based on soft data (lithologies) and a conditional expectation of the MnO level in the different lithologies.

A cut-off based on both hematite and magnetite is estimated. A process analysis is performed to visualise the working processes, related inputs, outputs and controlling-, supporting- and risk elements. The process analysis is based on the IDEF process modelling methodology. Given the identified deposit uncertainties and variations, systems to evaluate potential mining stope performance are developed and implemented for one of the mining stopes. To test the possibility to decrease the ore-related uncertainty, a method for collection of drill cuttings has been developed and tested. The correlation between magnetic susceptibility and FeMagn and the correlation between ore density and FeTot are both investigated.

The results show that an illustrative and useful overview can be won by using the IDEF-based process modelling methodology. A non-linear relationship between density and FeTot is established and it is shown that the density can be used as a FeTot indicator. This relationship is also used in the reserve and resource estimation. As expected a positive correlation between FeMagn and magnetic susceptibility measured on cores could be established. However, the deviation from other reported relationships is considerable. The importance of magnetite is emphasised and quantified by the cut-off estimation. The cluster analysis reveals that the MnO levels in the different lithologies are significantly different. This result is implemented into the kriging with inequalities procedure and immediate effects can be observed.

The development of the geodata collector and the collection of drill cuttings show that it is possible to obtain precise analysis of collected drill cutting material. Although high- and low assay values have been correlated with geological observation in the mine, the accuracy has been difficult to assess.

The estimation and the simulation of the ore properties illustrate and quantify the uncertainties and variations in the ore deposit well. The structural analysis performed prior to the estimation and the simulation reveals anisotropies for all ore decisive parameters. The quantification of ore variations provides a useful input into the a-priori assessment of stope performance. It is also shown that the probability that a SMU is above or below some cut-off value can be assessed using the simulation results and the systems developed in standard software.

It is concluded that the process analysis approach offers valuable input to gain an overview of the mining value chain. It is also an approach that constitutes an important step in the identification and assessment of IT-requirements, bottlenecks, input- and output requirements and role- and skill requirements along the value chain. However, the process analysis approach requires sufficient organisational resources, which also is the case regarding the implementation of the grade- and stability issues that are presented. Further it is concluded that the ore variations can be utilised to some extent by using standard software.

The ore in question is a Neoproterozoic (600 to 700 Ma) metasedimentary magnetite-hematite ore deposited under shallow marine conditions. Primary precipitate was probably ferric hydroxide.

Applied methods have been chosen to handle the uncertainty along the value chain of Rana Gruber AS. Every aspect of these methods may therefore not be directly applicable to other mining operations. However, the general aspects have a broad area of use.

Table of contents

1. Introduction

Where is the Life we have lost in living?

Where is the wisdom we have lost in knowledge?

Where is the knowledge we have lost in information?

Eliot, T.C. (1934)

1.1. General introduction

Modern society is urged to struggle for industrial and economic development that can be sustained without harming the environment or depleting the natural resources (The Brundtland report "Our common future" 1987).

It is a fact that mining will eventually deplete any deposit. The task is therefore to utilise the deposit optimally during production. Deliberate and consistent utilisation of deposit variations is one way to reach this goal.

Three fundamental issues are considered here in order to exploit deposit variations during production:

- Decisive parameters related to the ore geology
- Variability and uncertainty, amalgamated as "verity"
- The value chain perspective

1.1.1. Ore geology

Ore geology, in this context, comprises ore characteristics including parameters related to mineralogy, geochemistry and rock mechanics. The knowledge of the ore characteristics is captured in the three-dimensional ore model. The ore model must be dynamic to achieve optimal exploitation of ore variations. This means that the ore model must be updated with geoinformation collected during production.

Utilisation of deposit variations in connection with selective mining (ore blending or campaign production) has been shown to be useful by a number of authors (e.g. Morley et al. 1999).

1.1.2. Verity

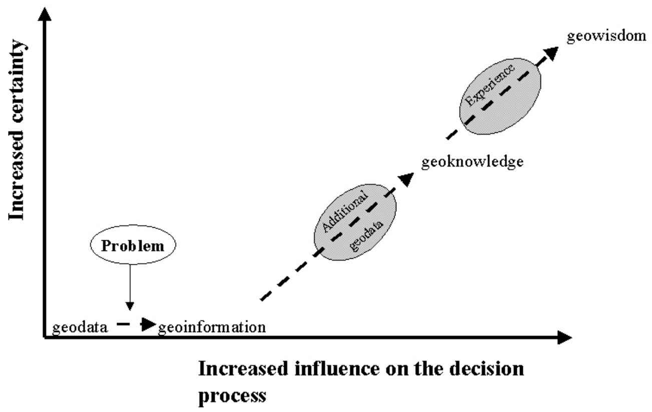

Figure 1 From geodata to geowisdom.

Geodata is data with a geographical location. Geodata can carry information about topics such as mineral content, grade or geophysical signatures. Without a problem to solve, the geodata is stand-alone crude information of limited value. If the geodata is relevant to a problem and organised and analysed accordingly, it can be defined as geoinformation, i.e. information positioned in the three-dimensional space (see Figure 1). Neither geodata nor the geoinformation is known with certainty. If more geodata relevant to the problem is collected and the new set of geodata confirms the geoinformation, the total information base can be termed geoknowledge. The geoknowledge is known with a higher degree of certainty than the geoinformation. As experience is added the level of geowisdom can be reached. Reaching the level of geowisdom is no guarantee that the correct decision is made. The reason for this is the verity or the total uncertainty in the mining system defined by the mining value chain. Verity is an amalgamation of variability and uncertainty, used by Vose (2000). Similar hierarchies from "data to wisdom" have been termed "Knowledge Hierarchy" (Ackoff 1989) and "Information Hierarchy" (Cleveland 1982) respectively. In Longley et al. (2001) it is termed the hierarchy of decision-making infrastructure.

1.1.3. Value chain perspective

The value chain perspective is based on a process view of organisations. According to Porter (1985) the value chain consists of the following primary activities:

- Inbound logistics
- Operations (production, processing, i.e. value creating activities)
- Outbound logistics
- Marketing and sales
- Service

These primary activities are sustained by four support activities (Porter 1985):

- Procurement
- Technology development
- Human resource management
- Firm infrastructure

A thorough understanding of the value chain and how the different working processes interact with each other through inputs and outputs is imperative to achieve an optimisation of the workflow.

1.2. Objective of this thesis

The English macroeconomist John Maynard Keynes has formulated one of the basic ideas of this thesis:

"I would rather be approximately right than precisely wrong"

The aim of this thesis is to evaluate the financial- and geological effects of knowing the verity of the decisive ore parameters, introduced to the value chain by the deposit.

The question asked is how can an underground iron ore company, exemplified by Rana Gruber AS, benefit from knowing and exploiting the verity of decisive parameters, such as ore grade, costs and tonnage.

The answer will constitute important decision input in the customisation of the delivered ore qualities seen in relation with the products that are to be produced.

The objective of this thesis is to:

- Identify and characterise the decisive parameters in the iron ore mining process.
- Establish and apply systems and routines to handle ore verity and its associated risk.
- Model, visualise and utilise the value chain perspective.

1.3. Scope

The idea captured in the above quotation by John Maynard Keynes is used in this thesis in a more microeconomic manner compared with the macroeconomic context from which it originates. As Figure 2 illustrates the focus is on deposit characterisation and production. The perspective is the whole value chain of iron ore mining as a whole from deposit to product.

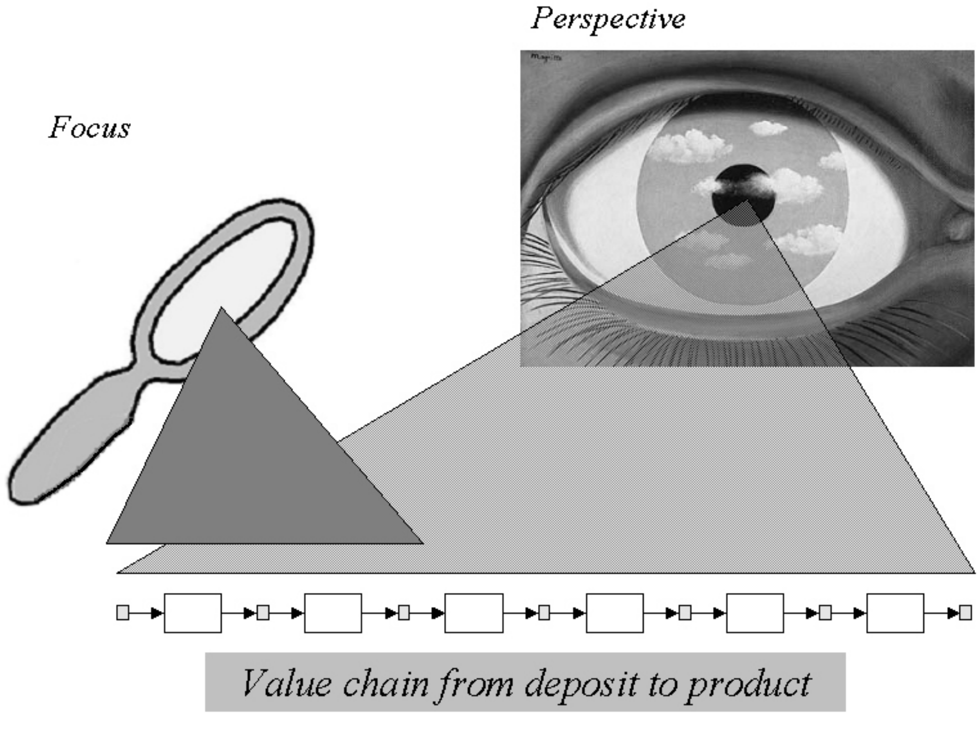

Figure 2 Focus on deposit characterisation and production. The perspective is the whole value chain from deposit to product.

The emphasis is on the working processes and the characteristics of the corresponding inputs and outputs. The important aspect is that every working process has certain requirements for the input. In order to maximise the total added value along the value chain the output must satisfy these requirements.

The cooperative company, Rana Gruber AS, produces hematite- and magnetite products from an underground mine. Methods applied will be specially chosen for this company to handle the uncertainty along their value chain. The special features of the methods will therefore not necessarily be applicable to all kinds of mining, but the general aspects will have a broad area of use.

Iron deposits can be formed from magmatic-, metamorphic- and sedimentary processes. This thesis concentrates on a deposit originally formed through sedimentary processes. Iron deposits like skarn-iron, bog iron and orthomagmatic iron are therefore not discussed any further.

The terminology used when referring to iron formations is disputed in the international geoscience community. Two commonly used terms are cherty- and noncherty iron formations. The majority of cherty and noncherty iron formations were formed during Precambrian and Paleozoic respectively. The iron formations studied in this thesis belong to a group of iron formations that have an assumed enigmatic Neoproterozoic age.

1.4. Outline of this thesis

The thesis is organised as a monograph. It contains the following chapters:

1. Introduction

   The chapter gives a general introduction and defines objectives and scope.

2. Background

   This chapter reviews issues related to the cooperative mining company. Terminology related to iron ores, the regional geology and specific information about the Kvannevann Iron Ore is discussed.

3. Revitalisation of the existing database

   Existing geological material is reviewed and new approaches are applied to the material in order to update and extend its area of use.

4. Methodology

   Methods for collection, evaluation and presentation of deposit geodata used in the thesis are presented.

5. Results

   The results are presented.
6. Discussion
7. Conclusions and recommendations
8. References
9. Appendices

2. Background

2.1. Rana Gruber AS

2.1.1. Coordinates and general introduction

Mo i Rana is a town in Nordland county, northern Norway, UTM WGS 84 33 W 464690 7357963, about 70 kilometres south of the Artic Circle. The ore dressing plant at Rana Gruber AS is situated in Mo i Rana. The mine is near the small mining community Storforshei, 27 kilometres north of Mo i Rana (see Figure 3).

The ore dressing plant in Gullsmedvik is situated close to the Rana Fjord and has its own established quay structure for the shipment of products.

The iron-formations are located in the Dunderlandsdalen Valley.

After stoping, the ore is transported to the gyratory crusher and crushed to about minus two hundred millimetres (adjustable) and stored in a silo with a capacity of 115 000 tonnes. The crushed ore is transported by rail to the plant in Gullsmedvik. The transportation length from the silo down to Gullsmedvik is 37 kilometres. One train contains about 35 wagons, and carry in total about 2200 tonnes of ore.

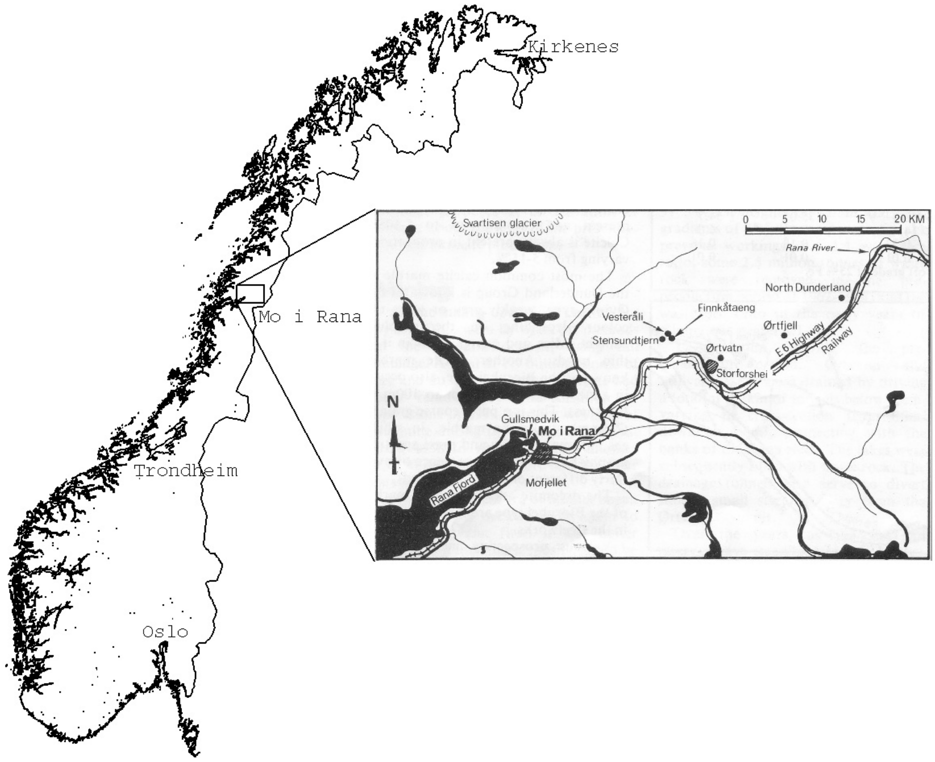

Figure 3 Mo i Rana, located in Nordland county, about 70 kilometres south of the polar circle.

Rana Gruber AS has about 150 employees in the mine and ore dressing plant, including laboratories used to analyse product quality, plant feed and drill cuttings.

2.1.2. Mining method

The mining method is sub-level stoping. The stopes are about 40 metres wide, 100 metres high and from 50 to 70 metres long.

Figure 4 illustrates the mining method.

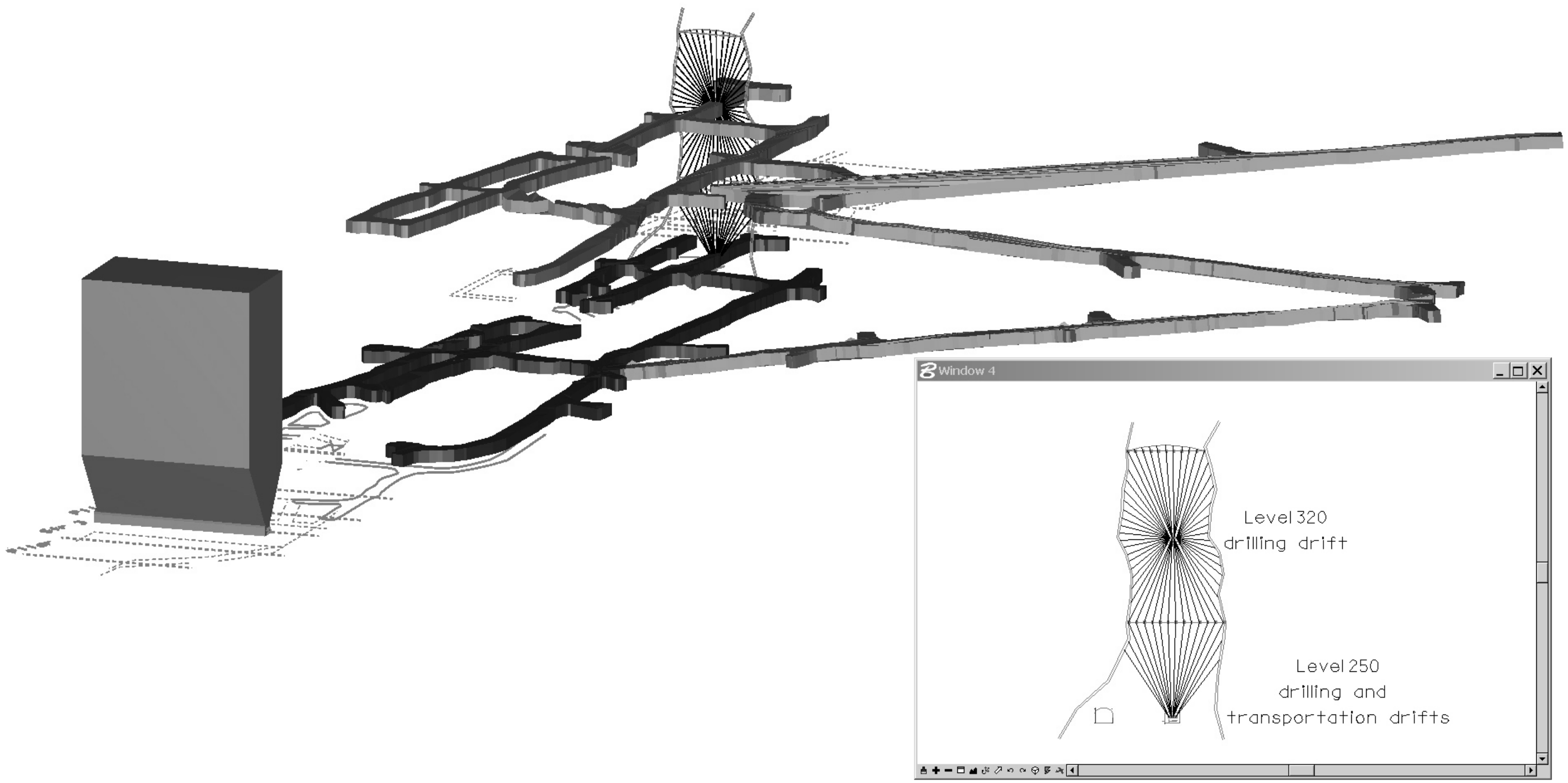

Figure 4 Sub-level stoping at Rana Gruber AS. Drilling from level 320 (320 metre above sea level) and drilling, loading and transportation from level 250.

2.1.3. Dressing plant

The ore dressing follows mainly two streams:

- Production of hematite products
- Production of magnetite products

Upon arrival at the dressing plant, the ore is stored in silos. From the silos the ore is transported on belts to an autogenous mill. Further dressing includes sieving, grinding and magnetic separation. Figure 5 illustrates the main dressing processes in the plant.

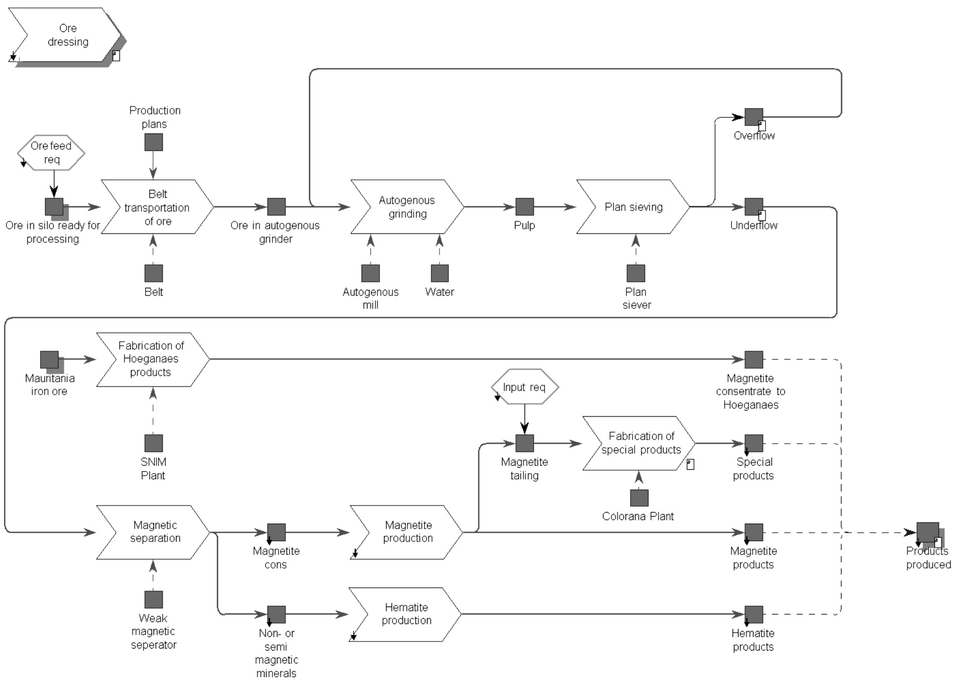

Figure 5 A process model illustrating the main processes in the dressing plant.

The products include:

- o Hematite concentrates in different fractions for steel production.
- o Magnetite concentrates for special applications, like.
  - o Water cleansing
  - o Products used in catalysers
  - o Products used as fillers
  - o Abrasives

- Black and red pigments used in
  - Paint
  - Plastic
  - Rubber.
- Toner carrier.

The magnetite-based products give the highest value-add to the mining value chain, whereas the hematite-based products for steel production are most important in tonnage.

The product development department is constantly working with new products. High value-add hematite-based products are currently under development.

2.1.4. Rana Gruber AS – The Story

This review is based on Rana Gruber (1984), Berg (1995) and Nordvik (2000).

Rana Gruber AS has historical lines that with certainty can be followed back to 1799 when the first claims on iron ores near Mo i Rana where registered by Mostadsmarkens Iron Company (Mostadsmarkens Jernverk) situated near Trondheim.

Ole Tobias Olsen was a vicar in Nordland County and known as the initiator of the railway track through the county. In the 1870's he claimed the rights for 48 iron ore findings in the Dunderlandsdalen Valley.

In the 1880's consul Nils Persson from Helsingborg, Sweden, got rights and claims in the Rana district, including Storforshei. Persson was known as the "Ore King of Norway" due to his involvement in the mines in and around Sulitjelma.

Persson had hired the Swedish engineer Alfred Hasselbom to explore and assess the Rana district for iron ore. Hasselbom estimated the resources to comprise over a billion tonnes of iron ore. Neither grade nor cut-off is reported.

In 1899 consul Persson sold all his rights to Edison Ore Milling Syndicate, which had been founded to utilize an invention by Thomas Alva Edison. The invention made enrichment of iron ore possible. To be in charge of the development work and the following iron ore production and ore dressing, Dunderland Iron Ore Co Ltd (DIOC) was established in 1902.

DIOC carried through extensive development work including quay structure, briquette plant, a power station in Gullsmedvik and a railway track between Storforshei and Gullsmedvik. The development work employed 2000 men, and the investments during this period reached about 4 million British pounds. In 1906 iron ore excavation started from the Ørtvann Iron Ore. The same year the first shipment of iron briquettes went from Mo i Rana to England.

After two years and a production of 87.200 tonnes of briquettes, the production ceased in 1908 due to low iron recovery and dust problems at the dressing plant in Storforshei.

In the following years, research was initiated to develop new dressing processes that improved the iron recovery. In 1917 a new dressing plant was build in Gullsmedvik. The separation of magnetite was achieved by wet magnetic separation, whereas the hematite was separated using a shaking table. This new plant was periodically in production towards the Second World War. The iron recovery was 81% and the concentrates contained 67% iron. The production stopped in September 1939 due to the Second World War outbreak.

In 1947, the Norwegian State bought DIOC's rights, properties and installations. The railway tracks were transferred to NSB (Norwegian State Railways).

In 1937 the iron ore company A/S Sydvaranger in Kirkenes (see fig. 1) and the German Vereinigte Stahlwerke founded Rana Gruber AS. The basis for the establishment of Rana Gruber AS was sixteen iron ore claims bought from the inheritors after Ole Tobias Olsen. After the war in 1945 the Norwegian State expropriated all the German shares in A/S Sydvaranger and Rana Gruber AS. In 1951 the Norwegian State obtained all the Norwegian shares in Rana Gruber AS. The Norwegian State was thereby the sole owner of Rana Gruber AS.

After intensive testing and research on the Rana ore and alternative dressing processes, a new dressing plant was erected in Storforshei. This plant was in production from 1958 to 1962. Based on the experience won from this period a new ore dressing plant was built in Gullsmedvik.

In 1955 Norsk Jernverk AS started production of steel in Mo i Rana. In 1961, the Norwegian Parliament approved a completely new plan for the production of steel at Norsk Jernverk AS. This resulted in the inclusion of Rana Gruber AS into Norsk Jernverk AS. From 1961 to 1989 Rana Gruber AS functioned as the mine department and main supplier of iron oxide concentrate to Norsk Jernverk AS.

In 1989, Norsk Jernverk AS closed down, and Rana Gruber AS was sold to the employees and was once again without governmental ownership. Due to the closure of Norsk Jernverk AS, Rana Gruber AS lost their main customer. Thanks to governmental contributions and an effective and successful product development department, Rana Gruber AS managed to develop new products that made continued production possible.

2.2. Iron – the metal of prosperity

With iron we plough the cultivated land, plant trees, trim gardens, form rocks, cut timbers and perform all sorts of useful work.

Plinius, 1th century AC

Technically and economically, iron is the most important metal of mankind.

Iron has been known since about 4000 BC. The first utilisation of iron dates back to about 2800 BC, but iron was not important before about 1350 BC when precursors to the modern steel started to replace bronze in the Middle East. Iron metal is relatively soft and is therefore not suitable for weapons and tools, but iron / carbon alloys are twice as hard as bronze.

The knowledge about the use of iron alloys spread quickly and iron was adopted in Italy and Greece around 1000 BC as the dominating raw material for production of tools and weapons. Iron based tools made it possible to increase productivity, especially in agriculture and has later only increased its importance.

Iron is the most abundant element in the Earth with about 37 weight percent. The majority of this is in the core. In the Earth crust iron is one of the top four elements with 4.6 weight percent. Only oxygen, silicon and aluminium are more abundant.

The chief iron bearing minerals are the iron oxides:

- Hematite, Fe_2O_3
- Magnetite, Fe_3O_4
- Ilmenite, $FeTiO_3$
- Goethite, FeOOH

Other iron minerals are the iron carbonate siderite, the iron silicate chamosite and iron sulphides like pyrite.

2.3. Iron ore in a global perspective

2.3.1. Production

The world production of iron ore has increased from about 95 Mt in 1904 to 1.300 Mt in 2004 (Kelly and Jorgenson 2004, AME 2004).. Forecasts for future production tonnages predict, that by 2009 the annual world iron production will be 1.900 Mt (AME 2004).

In 2003 Brazil was the largest producer with 245 Mt. Australia is the second largest and the largest exporter (Info Comm 2004). Other major iron ore producing countries are China, Ukraine, Russia, India and USA.

2.3.2. Resources

The world resources are estimated to exceed more than 800 billion tonnes of crude ore with more than 230 billion tonnes of iron. (U.S. Geological Survey 2003).

2.3.3. Prices

About 98 % of all iron ore is used to produce steel (U.S. Geological Survey 2003). Iron ore prices are therefore controlled by what the iron ore producing companies can supply compared to what the steel making companies demand and what these companies are willing to pay.

In 1990 Japan, China and USA in this order were the largest consumers of iron ore. From 1992 China was the largest consumer of iron ore. This trend has continued from 1992 until present and the high demand is now pushing the prices due to a supply-demand unbalance.

In 2003 the iron ore prices increased with about 9 %, while industry analysts expected a 2 to 3 % increase. Due to China's high level of steel consumption, the price increase has continued. AME (2004) predicts a price increase of 20% in 2005.

2.3.4. Future trends

There will not be any drastic change in the global supply pattern. The major iron ore producing countries will continue to produce at high rates. However, in the long run, it is likely that Africa will become more dominant.

As in other branches, huge mergers are common, and will probably continue to be so also within the iron ore industry. Large companies grow larger. After acquisition performed by the Brazilian CVRD, it now controls over 95% of Brazils iron ore production and all of its production of pellets. Rio Tinto, the owner of the gigantic Hamersley iron ore, has also made take-overs making them the world's second largest producer of iron ore. Recently, BHP merged with Billiton.

CVRD, Rio Tinto and BHP Billiton controls 30% of world iron ore production and 70% of global export. Being so dominant, these companies can to a great extent control the price negotiations. Smaller companies are thus forced to follow the prices these companies negotiate.

2.4. Terminology

2.4.1. Ore

Many definitions have been applied to the term “ore”. Common for all of them is that they state that “ore” is an economic term.

Evans (1994) discusses the meaning of the term and quotes UK Institution of Mining and Metallurgy (IMM):

“Ore is a solid naturally-occurring mineral aggregate of economic interest from which one or more valuable constituents may be recovered by treatment”

Lane (1988):

“An ore is a material in the ground that can be extracted to the overall economic benefit of a particular mining operation, governed by the financial determinants at the time of examination.”

The definition of IMM includes the metallic ores and industrial minerals, while the definition of Lane restricts the time span interval where the definition is valid.

2.4.2. Iron formation

In this section iron formation is used with or without hyphen dependent on what the referenced authors prefer. At the end of this section a decision is made regarding the use of hyphen.

Iron formations are enigmatic. Different definitions and different categorising schemes have been developed to create a common basis for discussion.

Definitions of iron formation

Kimberley (1978 and 1994) defines iron formation as

> *“a mappable rock unit composed mostly of iron-rich chemical sedimentary rock (ironstone), with the uppermost and lowermost beds being ironstone”*.

“Ironstone” is defined as

> *“any chemical sedimentary rock which contains over 15% Fe”*.

He goes further and defines a chemical sedimentary rock as

> *“a rock containing over 50 wt-% inorganic and/or organic chemical precipitates from a surficial water body and/or diagenetic replacements of those precipitates.”*

Trendall (2002) draws attention towards how the term is used globally rather than discussing a formal definition. In this perspective he focuses on the chemical composition and states the following characteristics:

- 25 to 35 % Fe
- CO_2 significant minor
- Al_2O_3, MgO and alkalies are minor
- Low on trace elements
- Hematite and magnetite are the principal iron minerals
- Iron carbonates can be present in form of ankerite or siderite
- Iron silicates can be present in form of stilpnomelane, greenalite or riebeckite.
- Microcrystalline quartz called chert constitutes the silica.
- Typically fine grained
- Typically hard, heavy and resistant
- Typically banded with alternating bands of silica and iron oxides.

Based on these characteristics, Trendall (2002) defines iron-formation as

> *"an iron-rich (± 30%) and siliceous (± 50% SiO_2) sedimentary rock which results from extreme compaction and diagenesis of a chemical precipitate in which those components were major constituents."*

James (1954), Gross (1966) and Trendall (1983) have proposed similar definitions.

Kimberley (1989a) discusses the definition and whether the term iron formation should have a hyphen or not. Brandt et al. (1973 in Kimberley 1989a)) suggest that the lithologic meaning of the word should be written with a hyphen, whereas the stratigraphic meaning of the word should be written without. Kimberley (1989a) argues against this by pointing out that there is an lack of logic when to use and when not to use hyphen, and that the hyphen would be lost in oral communication.

Classification of iron formations

Iron can exist in different valence states. Different iron minerals will be formed dependent on varying Eh (redox-potential) and pH conditions and on the geochemical composition of the solution from which the minerals precipitate. Mineralogy can therefore indicate different environments. James (1954) defines four major iron-formation end-member facies in his description of the iron ores in the Lake Superior district: oxide-, carbonate-, silicate- and sulphide facies. See Table 1.

FACIES	CHARACTERISTICS
Oxide facies	Hematite or magnetite, 30-35% iron, carbonates may be present.
Carbonate facies	Interbanded chert and siderite (iron carbonate) in equal proportions. The siderite lacks oolitic or granular texture
Silicate facies	Generally associated with magnetite, siderite and chert. Primary iron silicates may include greenalite, chamosite (iron rich chlorite) and glauconite (mica mineral only found in sedimentary rocks) and some minnesotaite and stilpnomelane , ferrous (2+) iron (mostly)
Sulphide facies	Pyritic carbonaceous argillites, formed under anaerobic conditions.

Table 1 James' (James 1954) four major iron-formation end-member facies and their characteristics.

The oxide facies indicates a positive Eh, whereas the sulphide facies indicates a strongly negative Eh. The carbonate and the silicate facies indicate an intermediate Eh (e.g. Maynard 1983).

Gross (1966) introduces the Lake Superior-, Algoma-, Minette- and Clinton type iron formation. According to Gross the Lake Superior type is associated with sedimentary or metasedimentary rocks deposited on continental shelves. The Algoma type is associated to volcanic rocks from tectonically more unstable areas (e.g. Kimberley 1989a; Maynard 1983). This classification had validity describing the iron formations in North America when it came, but in a global perspective, it looses its validity (Trendall 2002). The Minette- and the Clinton type ores are mostly Phanerozoic, noncherty and show typically an oolittic structure.

Kimberley (1989a) classifies iron formations according to paleoenvironmental conditions during deposition. His classification scheme is summarised in Table 2.

	ACRONYM	EXPLANATION
1	SVOP-IF	Shallow-volcanic-platform iron formation
2	MECS-IF	Metazoan-poor (metazoan = multi-celled animal / organism), extensive, chemical-sediment-rich shelf

		sea iron formation
3	SCOS-IF	Sandy, clayey and oolitic, shallow island-dotted-sea iron formation
4	DWAT-IF	Deep-water iron formation
5	SOPS-IF	Sandy, oolite-poor, shallow sea iron formation
6	COSP-IF	Coal-swamp iron formation

Table 2 Classification scheme for iron formations. From Kimberley (1989a).

Trendall (2002) divides iron-formations into banded iron formations (BIF) and granular iron formations (GIF). This classification into lithological types is purely a descriptive classification. A BIF follows the definition stated above and is mostly older than 2.0 Ga. A GIF can be considered to be a BIF deposited or reworked at shallow water (Trendall 2002). The main differences between the two types are textural.

Their characteristics are given in Table 3 (Trendall 2002).

ACRONYM	EXPLANATION
BIF	• Occurs in greenstone belts sequences of all main old cratons • Mostly tectonically deformed, but do also exist in little metamorphosed supracrustal rock sequences. • Stratigraphic, sharply bounded units • Distinct mesobanding • No current generated structures • Epiclastic components are almost absent • Uniform chemical composition, but varying mineralogy. • Considerable lateral continuity
GIF	• Form sharply bounded units, but relative to BIF they are more interstratified with coarse to medium-grained epiclastic sediments and partly associated to vulcanogenic rocks. • Do not have the regular mesobanding like BIF. The alternations of iron-rich and silica-rich bands tend to

	be coarser and less regular. • Current generated structures are common. • The iron-rich bands tend to be granular or oolithic. • Uniform chemical composition. Varying mineralogy. • Not the same lateral continuity as BIF
Table 3 BIF and GIF characteristics. From Trendall (2002).	

The BIF and GIF can co-exist in one iron-formation (Trendall 2002).

Iron formation with or without hyphen

Iron formation as a noun is in this thesis used without hyphen. Iron formation must be understood in a stratigraphic sense, i.e. it comprises a rock unit with a certain place in the stratigraphic column. Although "ironstone" has been used to term Phanerozoic iron-rich rock units (Maynard 1983, Evans 1994, Gross 1991), I choose to follow the definition of iron formations posted by Kimberley (1978) (see page 16). In accordance with the same author, hyphen is used if the two nouns "iron" and "formation" are combined to produce an adjective, e.g. iron-formation classification. This use of hyphen is also grammatically correct.

2.5. Geological background

2.5.1. The geology and genesis of iron formations

Introduction

The formation of iron ores is disputed. There is however a general acceptance that iron formations are chemical or biochemical precipitates (e.g. Gross 1983, Kimberley 1989b, Evans 1994, Trendall 2002).

Iron formations can roughly be categorized into cherty iron formations, mostly Precambrian, and noncherty iron formations, mostly oolitic and deposited during Phanerozoic.

What is common for all types, no matter when or how they have been deposited, are that the iron in them originates from somewhere (i.e. there is a source), the iron has been transported and probably deposited through chemical or biochemical precipitation. Their final characteristics prior to diagenesis or metamorphism are dependent on the source and the conditions during the mechanical- or chemical liberation of iron, any precipitation during transport and the conditions at the place and time of precipitation.

Any complete and precise genetic classification scheme must take all these aspects into consideration. This is a difficult, if not impossible, task.

The simple binary classification into cherty and noncherty iron formations used here is no exact classification. Especially since noncherty oolitic iron formations have been formed during Precambrian (Kimberley 1989b). Nevertheless it is applied here as basis for the discussion.

How iron formations are distributed in time

The vast majority of iron formations were formed during Precambrian. Figure 6 is an assemblage of figures from different authors illustrating major peaks of iron formation deposition.

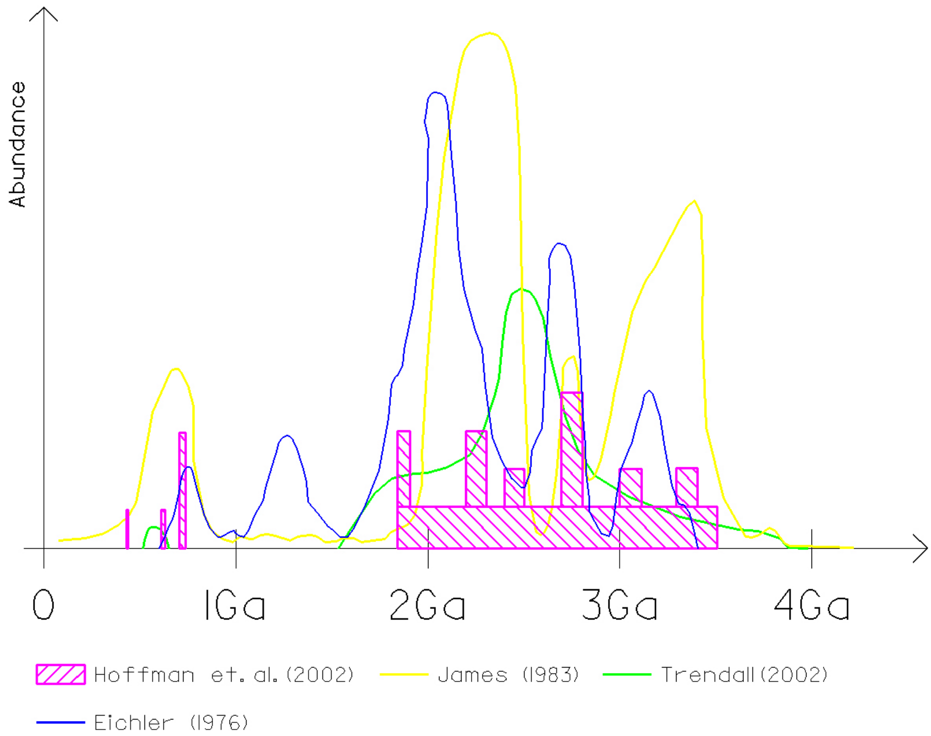

Figure 6 Assemblage of figures from different authors showing major peaks of iron formation deposition. Vertical axis is unquantified.

There are two major issues illustrated in Figure 6 worth emphasising:

- Most of the iron formations were deposited during a period of about 1.6 Ga, from about 3.5 Ga to 1.9 Ga ago. The oldest known iron formation is the Isua Iron Formation on Greenland. This is estimated to about 3.8 Ga (Trendall 2002).

- There is an apparent significant gap in the formation of iron formations from about 1.9 Ga to about 800 Ma ago. This gap is not apparent in Eichler (1976).

Hoffman et al. (2002) emphasise the correlation between the deposition of iron formations and major glacial periods. Further they emphasis the rise of metazoan starting at about 650 Ma. Since the MECS-IF of Kimberley (1989a) is termed a metazoan-poor iron formation, this could, at least, indicate a minimum depositional age for this type. Hoffman et al. (2002) also emphasise the increase in atmospheric oxygen levels that occurred as a consequence of the evolution of the green-plant photosynthesis.

Gross (1991) has estimated that 90% (10^{15} tons) of all iron deposited during Precambrian was precipitated in the relatively short time interval from 2.5 Ga to 1.9 Ga ago.

Cherty iron formations

The cherty iron formations are mostly banded, although also granular cherty iron formations have been reported (Trendall 2002, Maynard 1986). The banding occurs on mainly three different scales:

- Macrobanding
    - The macrobanding consist of a resistant iron formation in alternation with a low iron shale. The shale consist of a matrix with stilpnomelane or chlorite, with varying amounts of quartz, feldspar, siderite and pyrite.
- Mesobanding
    - The iron formation macrobands can be further divided into mesobands, which vary in thickness from 1 to 80 mm. Dales Gorge member of the Hammersley Basin has a mesobanding consisting of chert, magnetite, stilpnomelane and carbonates (Maynard 1986). Mesobanding of the iron ore from Syd-Varanger is illustrated in Figure 7.

Figure 7 Banded Iron Formation from Syd-Varanger, northern part of Norway.

- Microbanding
  - The chert mesobands may contain microbands, which vary from 0.5 to 1 mm in thickness. They consist of iron rich and iron poor laminae.

Noncherty iron formations

The noncherty iron formations are typically not banded, but oolitic. Kimberley (1989a) divides noncherty iron formations into the oolitic SCOS-IF, the oolite-poor SOPS-IF and the coal-swamp COSP-IF. The oolitic variant is significantly more abundant than the other two. The COSP-IF contains siderite as the chief iron mineral and differs from the other two by a distinct banding. The main difference between the SCOS-IF and the SOPS-IF is that the latter contain more glauconite and tend to grade to sedimentary rocks scarce on iron minerals.

The majority of these iron formations were deposited during the Phanerozoic, from early Cambrian to present. One of the largest noncherty oolitic iron formations is the Kerch Iron Formation of Russia from Pliocene, only 5 Ma old (Kimberley 1989b).

Iron-bearing minerals in noncherty iron formations comprise mostly oxides and hydroxides, e.g. hematite and goethite. The iron carbonate siderite and the aluminous iron silicate chamosite can be present in relatively significant amount. Pyrite is the only iron sulphide in noncherty iron formation (Maynard 1983).

The noncherty iron formations are insignificant compared to the cherty iron formations both in size, in-situ tonnage and economic importance.

2.5.2. Regional setting of the Dunderland Formation

Iron ore province

The two iron formations Storsforshei- and Lasken Iron Formation are parts of the Dunderland Formation (Søvegjarto et al. 1989). The Dunderland Formation constitutes a part of an iron ore province from Tromsø in the north down to Eiterådalen in the south (see Figure 8), containing iron formations in two sub-provinces.

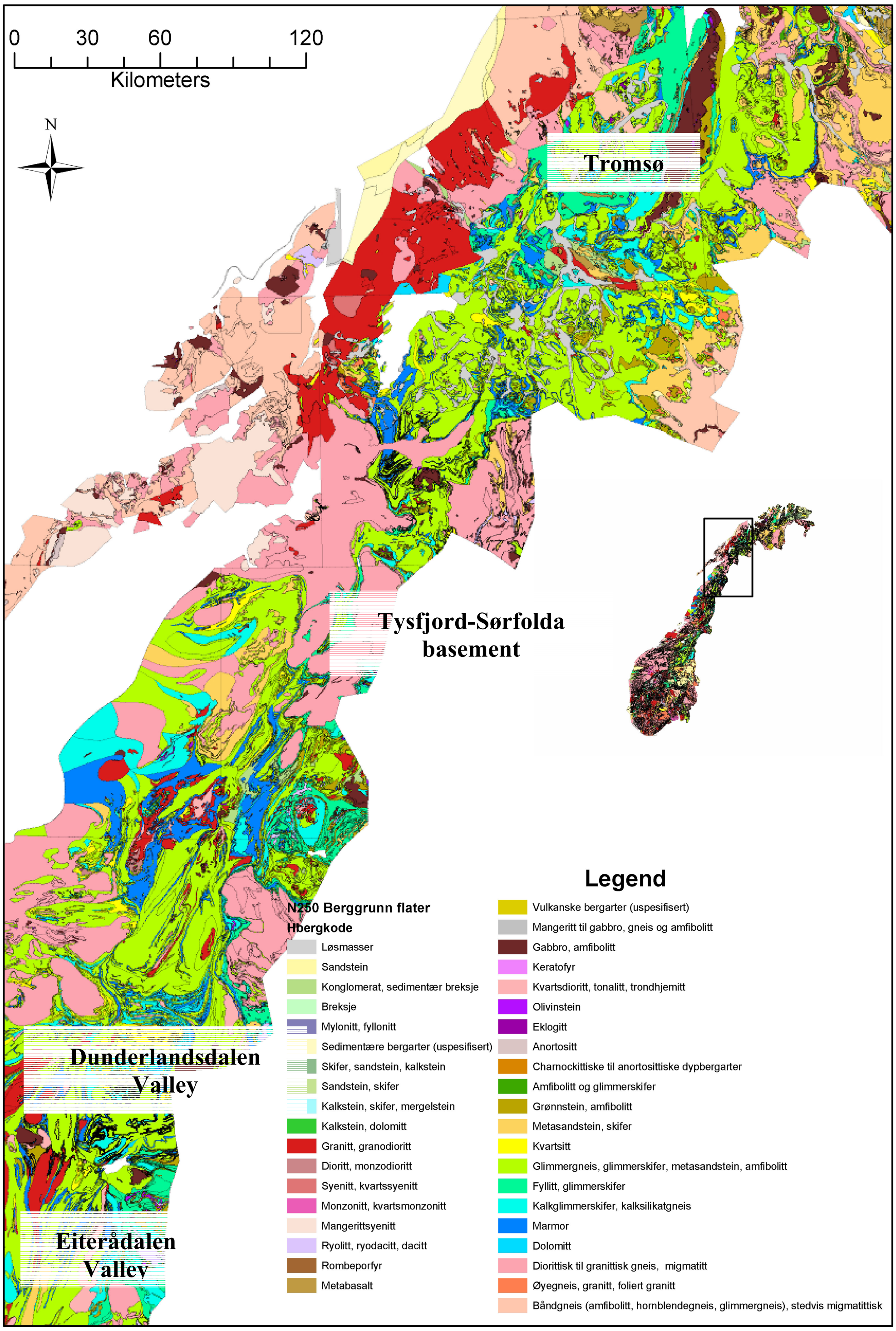

Figure 8 Caledonian iron ore province from Tromsø in the north to Eiterådalen in the south. Scale applies to detail map. (NGU 2005)

This comprises a total distance of about 510 kilometres. The province consists of thick metasedimentary sequences of marble and mica schist. The iron formations are from north to south the following:

- Northern sub province (north of Tysfjord-Soerfolda basement)
  - Tromsøsundet Iron Formation
  - Sørreisa Iron Formation
  - Salangen Iron Formation
  - Lavangen- og Gratangen Iron Formation
  - Bogen Iron Formation
  - Dyrøy Iron Formation
  - Andørja Iron Formation
  - Rolløy Iron Formation
  - Håfjell Iron Formation
  - Sjåfjell Iron Formation (The Skjomen-, the Beisfjord and the Fagernes Iron Formation probably represent a continuation)
- Southern sub province (south of Tysfjord-Soerfolda basement)
  - Neverhaugen Iron Formation
  - Grønlivann Iron Formation
  - Storforshei Iron Formation
  - Lasken-Grønlifjell-Nevernes Iron Formations
  - Alternes-Øyjord Iron Formation
  - Ormlid-Fuglevik-Bjørnå Iron Formations
  - Seljelid Iron Formation
  - Fuglestrand Iron Formation
  - Elsfjordstrand Iron Formation
  - Formo Iron Formation
  - Dolstadåsen Iron Formation
  - Herringbotn Iron Formation
  - Eiterådalen Iron Formation
  - Rapen Iron Formation

The iron formations are predominantly composed of magnetite and hematite in varying ratios and quartz, calcite- and dolomite marble, hornblende, garnet and epidote. They are banded in terms of mineralogy, grain size, grain shape and iron content, but lack the typical mesobanding of the Precambrian BIFs; for example like the Syd-Varanger Iron Formation.

The two sub provinces given above show different mineralogical characteristics. One difference is that magnetite is the dominating ore mineral in the northern sub province whereas in the southern sub province hematite and magnetite occur side by side in varying ratios. Further, the iron grade is different. The formations is generally richer in the southern province with grades in the interval 30 to 33%, which is about ten percentage points above corresponding values in the northern province.

The content of manganese oxide is generally around 0.15 to 0.40 %, but extreme values may reach 15% (for example Håfjell- and Gratangen Iron Formation).

The phosphorus content is in average around 0.2 %, but may in some cases show values around 2%. The content of sulphur and titanium dioxide are commercially negligible, but can locally represent a problem as contaminant.

Regional tectonostratigraphy

The Dunderland Formation belongs to the Rødingfjell Nappe Complex (RNC), which constitutes a part of the uppermost allochthon of the Scandinavian Caledonides (Stephens et al. 1985). The Rødingfjell Nappe Complex contains rocks of assumed Neoproterozoic to Cambrian-Silurian age and consists of the Beiarn Nappe, the Slagfjell Nappe, the Plura Nappe and the Ramnålia Nappe (Søvegjarto et al. 1989). Figure 9 and 10 below illustrate a schematic subdivision of the Uppermost Allochthon into nappes, groups, formations, iron formations and ores and mineralisations relevant for the Dunderland Formation.

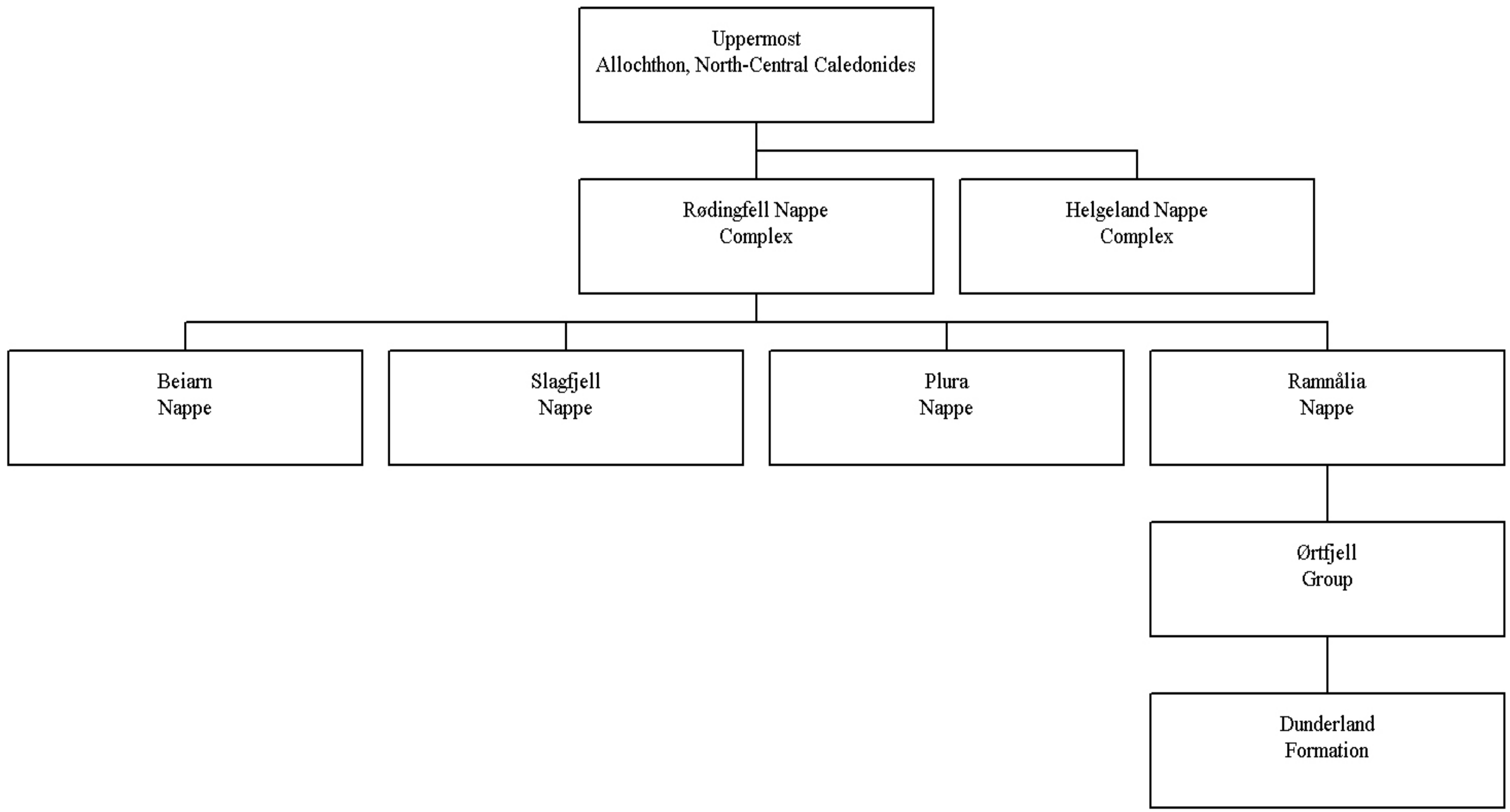

Figure 9 Schematic subdivision of the Uppermost Allochthon, North-Central Caledonides.

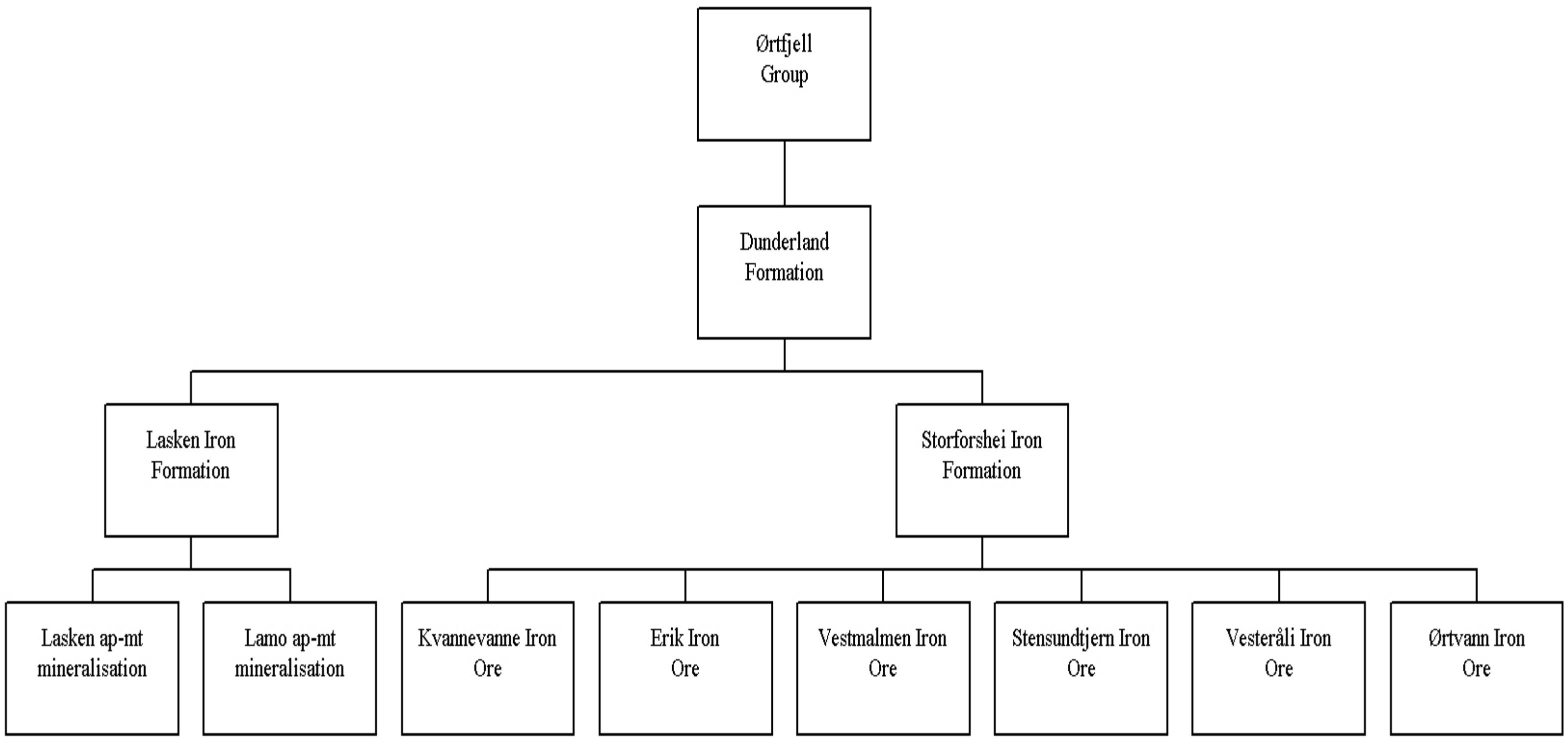

Figure 10 Schematic subdivision of the Ørtfjell Group, which is a part of the Uppermost Allochthon, North-Central Caledonides.

Dunderland Formation petrography

The Dunderland Formation, which is a part of the Ørtfjell group in the Råmnålia nappe, consists of dolomite- and calcite marble, mica schist, calcareous mica schist, graphite-mica schist, amphibolites, garnet fels, and two iron formations, Storforshei- and Lasken Iron Formation. The following overview is based on Søvegjarto (1986) and Søvegjarto et al. (1989).

The dolomite marble is fine grained (0.02 to 0.4 mm), yellowish-white to light grey. The grey colour is due to a certain content of graphite. The dolomite marble also contains quartz, tremolite and calcite.

The calcite marble is light grey to light greyish blue and medium grained (1-2 mm). A coarse grained (2-5 mm) stinkstone can be found in places. The graphite and pyrite content is higher than in the dolomite marble. Bands of mica and quartz may occur. Apatite, tremolite, titanite and rutile may be present. Baryte have been found.

The mica schist lies in direct contact with the upper ore zone, the Storforshei Type (see Figure 13). It is rich in oligoclase, quartz and muscovite. A garnet and hornblende and a hematite or magnetite impregnation may be present. The mica schist is sometimes termed gneiss due to poor schistosity.

The calcareous mica schist contains dolomite and calcite lenses. The carbonate content may reach 20%. Other minerals are quartz, oligoclase, biotite, muscovite, hornblende, epidote, garnet, chlorite, magnetite, apatite, pyrite, rutile and tourmaline.

The graphite-mica schist is a rusty mica schist containing pyrite and pyrrhotite.

The amphibolites are black and fine-grained.

The garnet fels is a fine-grained (0.02 to 0.05 mm) rock in places in direct contact to the upper ore formation. It occurs as a yellow or pink coloured fels. The matrix consists of quartz and / or mangano-calcite. Epidote is present in the yellow type. The garnet fels contain up to 26% MnO.

A geologic map showing a part of the Dunderland Formation including the central part of Kvannevann Iron Ore is given in Figure 11. The Kvannevann Iron Ore is the southern most ore in the map section in Figure 11. The vertical profile A-A’ through the Kvannevann Iron Ore is given in Figure 12.

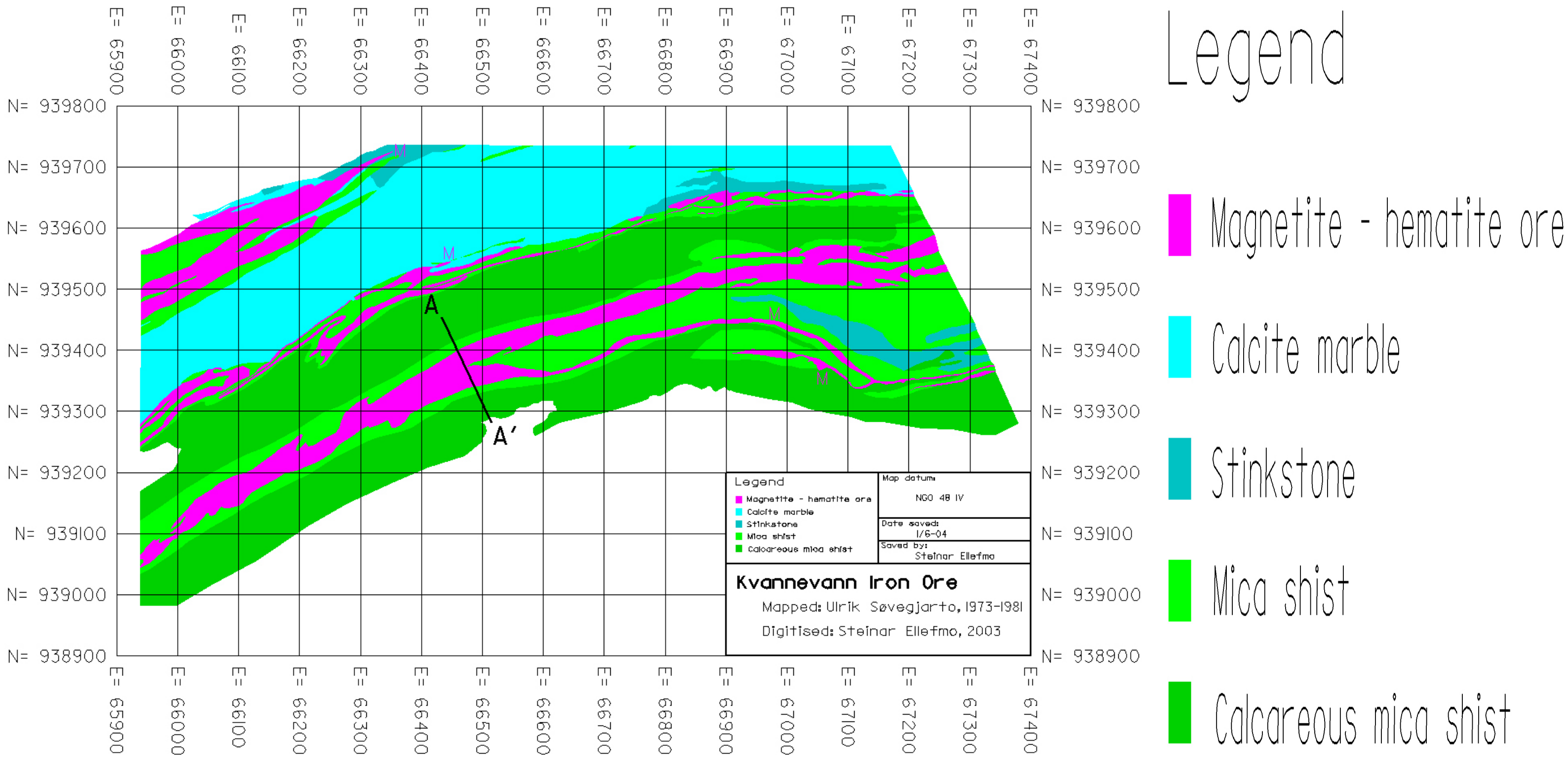

Figure 11 Geologic map showing the Kvannevann Iron Ore, which belong to Storforshei Iron Formation. The Kvannevann Iron Ore is intersected by profile A-A'. The ore in the north-western corner of the map is the Erik Iron Ore. Map first presented in Søvegjarto (1986).

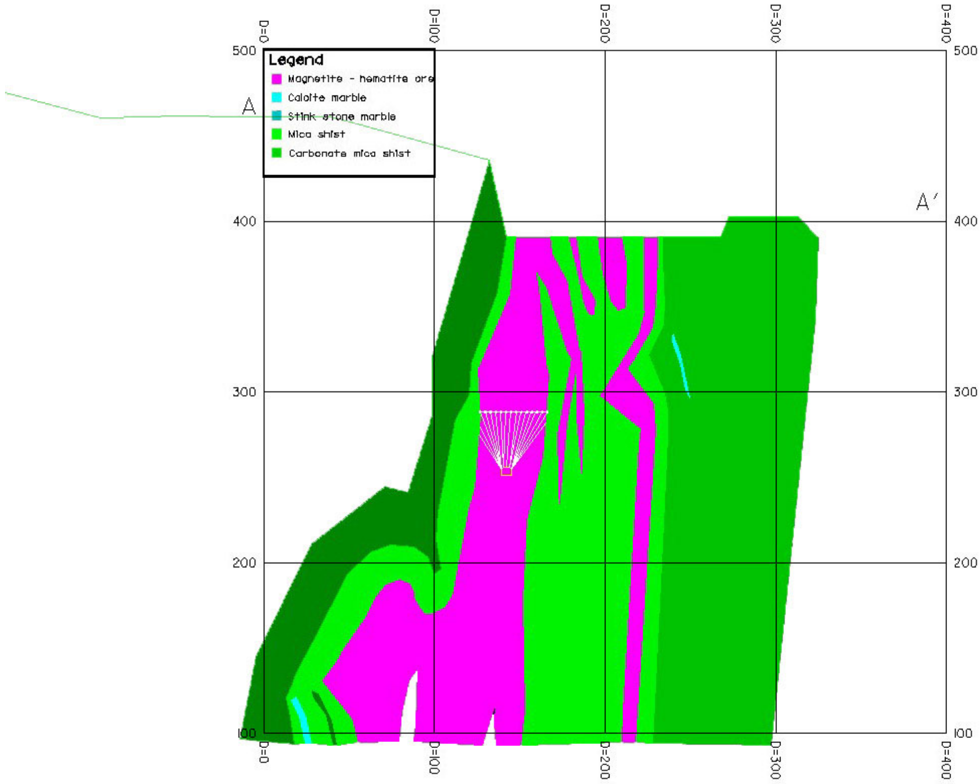

Figure 12 Vertical profile A-A’ through the Kvannevann Iron Ore.

2.5.3. Iron formations in the Dunderland Formation

Introduction

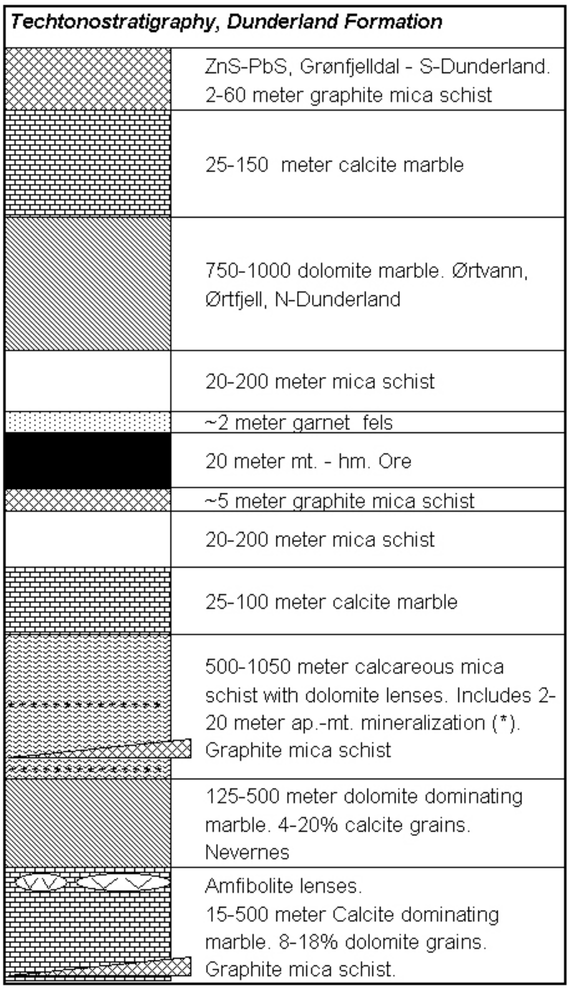

Figure 13 Tectonostratigraphy of the Dunderland Formation. From Søvegjarto (1990).

The Lasken- and Storforshei Iron Formation in the Dunderland Formation have significantly different characteristics. They occur in a mica schist- and in a calcareous mica schist formation respectively. They are separated by a calcite marble formation. See the tectonostratigraphic column in Figure 13. The Lasken Iron Formation contains an apatite-magnetite mineralisation (Søvegjarto 1990). The Storforshei Iron Formation contains the economically important magnetite-hematite iron ores. The Sjåfjell- and the Håfjell Iron Formations in the Ofoten area are geochemical and tectonostratigraphic equivalents the Lasken- and the Storforshei Iron Formations respectively (Melezhik et al. 2002, Søvegjarto 1972).

Lasken Iron Formation

The Lasken Iron Formation comprises the Lasken and Ømmervann-, Lomli- and Ørtvann-Nord-Lamo mineralisations.

The ores in this iron formation is generally fine grained (Nilsen 1990) and consist of a magnetite-hornblende schist, apatite in significant amounts and traces of pyrite (Søvegjarto et al. 1989). Compared to the Storforshei Iron Formation, the Lasken Iron Formation is higher on carbonate. It is characterised by a high content of phosphorus (0.6-2 %), 6-7 % iron silicates, 0.03-0.11 % MnO and sulphur normally around 0.2 %, but it might reach 2%. The iron content is relatively low, with total iron (FeTot) ranging from 10 to 30% and magnetic iron (FeMagn) around 15% (Søvegjarto 1990).

Storforshei Iron Formation

Introduction

The Storforshei Iron Formation contains the ores that has been economically important since production started here in 1906. The following ores belong to this type:

Ørtvann	Vesteråli	Vesteråga
Finnkåteng	Stensundtjern	Ørtfjell
Nord-Dunderland	Ørtfjellmo	Bjørnhei
Nevernes	Bjørnå	Langvatn

The Ørtfjell ore is a generic term for the Kvannevann-, the Erik- and the Vestmalmen Iron Ore. These three have all been exposed to production. Present production underground takes place in the Kvannevann Iron Ore.

Geochemistry and mineral quantification

The ores in the Storforshei Iron Formation have more FeTot than the mineralisations in the Lasken Iron Formation, whereas the FeMagn varies considerably from about 2 to as much as 25%. The ore minerals are magnetite and hematite and the formation is characterised by a garnet fels (see Figure 13). In these iron formations the average content of phosphorus is 0.20% whereas the average content of titanium dioxide, sulphur and manganese oxide is 0.29%, 0.08 and 0.29 (Søvegjarto 1990). However, the within- and between deposit variation is considerable.

Figure 14, 15 and 16, gives the average content of elements and oxides, trace elements and minerals respectively.

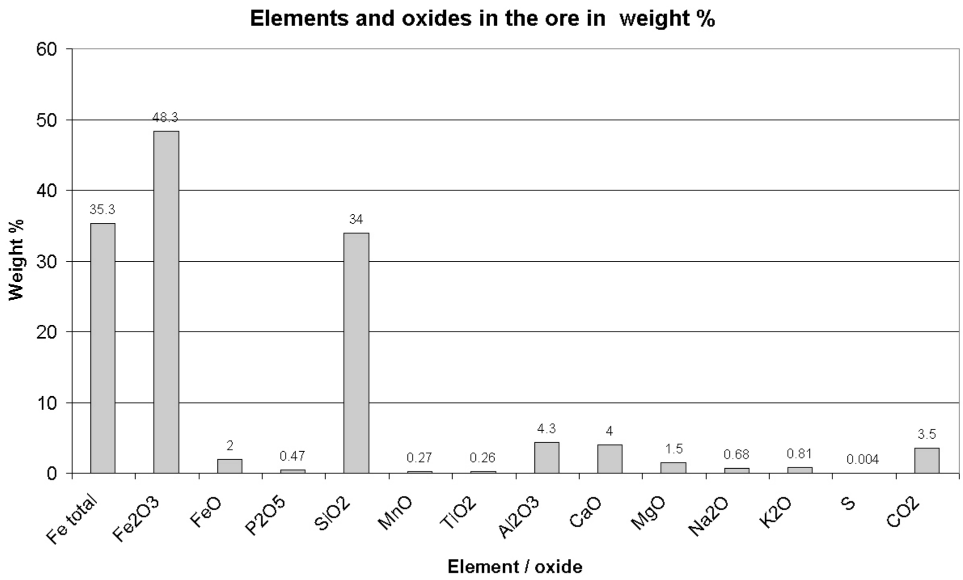

Figure 14 Bulk composition of the ore. Compiled from Ringdalen 1983.

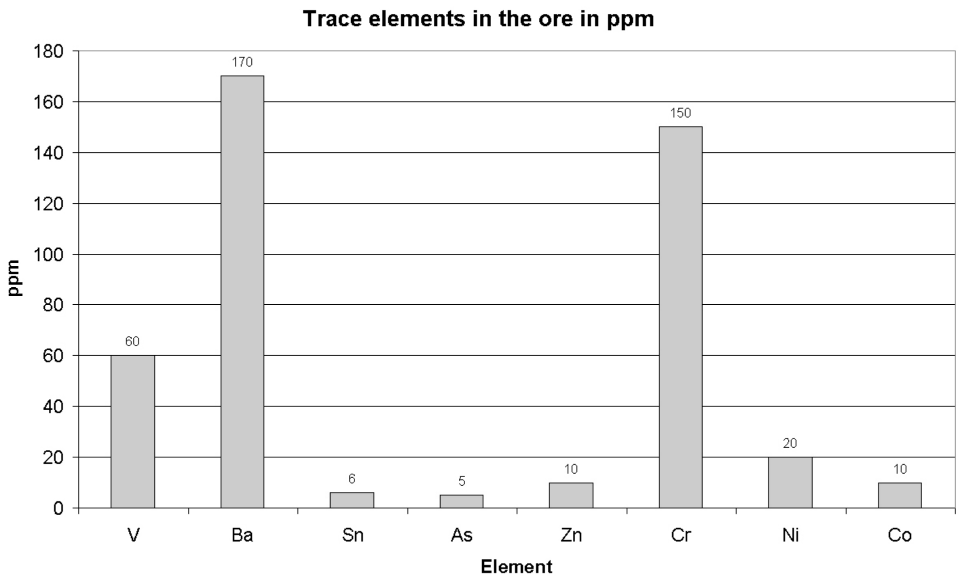

Figure 15 Bulk composition of trace elements in the ore. Compiled from Ringdalen 1983.

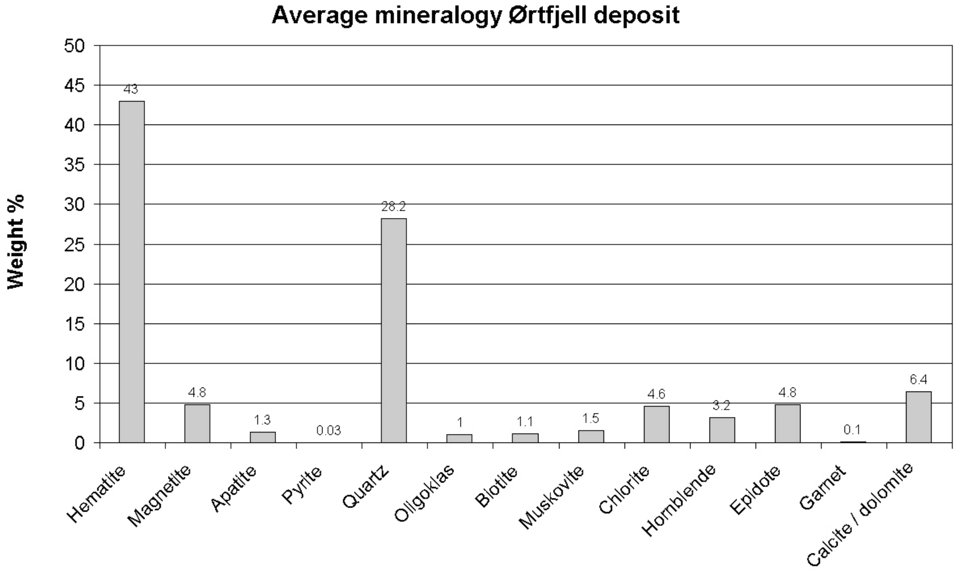

Figure 16 Average mineralogy in the Ørtfjell deposit, comprising Vestbruddet-, Erik- and Kvannevann Iron Ore. (NGU 2003a)

Ore mineralogy and textures

The main minerals in the ore in the Storforshei Iron Formation are hematite and magnetite at varying ratios, calcite and dolomite, quartz, garnet, epidote, mica (biotite and muscovite) and amphiboles.

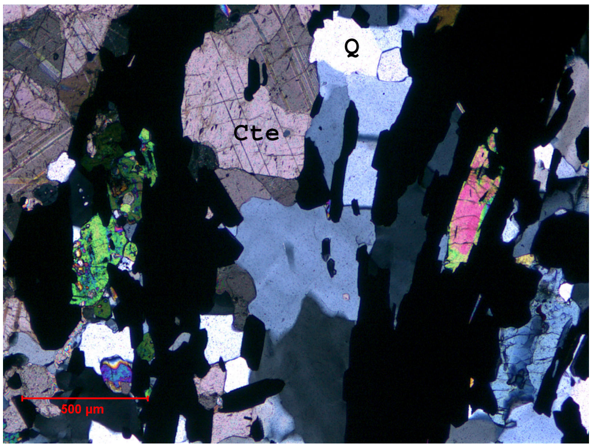

Figure 17 Gangue rock mineralogy. Mainly quartz and carbonates.

Quartz

Quartz, calcite and dolomite are the dominating gangue rock minerals. The quartz is relatively fine grained with grain sizes mostly between 0,2 and 0,5 mm. Figure 17 shows anhedral quartz grains.

Carbonate minerals

Calcite (Cte) and dolomite constitutes the carbonate minerals in the ore (See Figure 17). The carbonate mineral grains are on average finer than quartz.

Other minerals

Mica, feldspar, amphibole and apatite occur disseminated and in bands. Apatite grains vary in size from 0.1 mm to 0.4 mm (Malvik 1999).

Hematite

Hematite occurs in a number of varieties. It occurs coarse grained (0,4-0,6 x 0,05-0,1 mm) in massive or semi massive bands and in bands of gangue rock containing relatively fine-grained (0,1-0,3 mm) disseminated hematite. The hematite in the massive bands is flaky to tabular shaped whereas the disseminated hematite is typically cubic (see Figure 18).

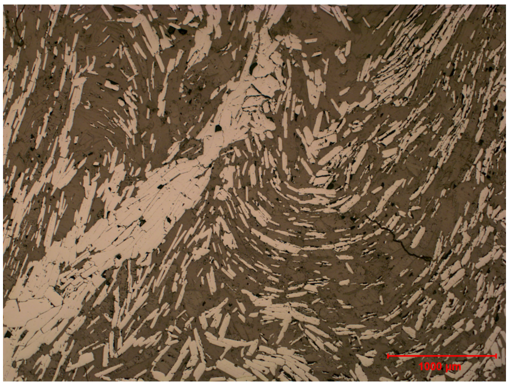

Figure 18 Disseminated hematite.

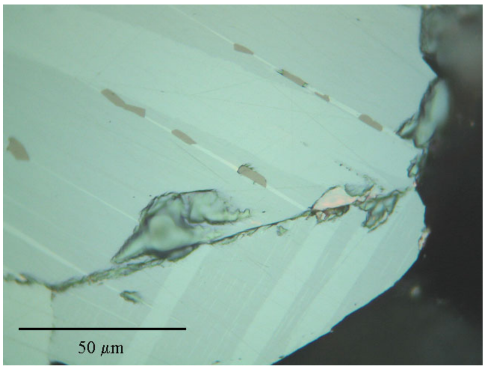

Figure 19 Magnetite grains imbedded in hematite deformation twins. Picture taken with oil immersion objective.

Metamorphism has induced deformation twins in the hematite. Often small grains of magnetite are imbedded in these deformation twins or in intersections between these deformation twins (see Figure 19). Similar twinning in the ore from the Rana district is reported in Craig & Vaughan (1994). However, no detailed information on the ore type or location is given.

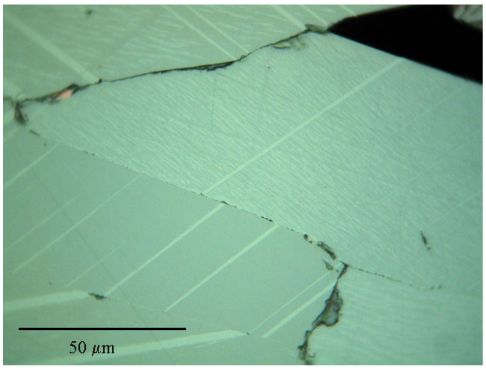

Figure 20 Small inclusions or micro twin deformations in the hematite; oil immersion, reflected light.

Some hematite minerals also contain small exsolutions or small micro twin deformations. These are parallel, sub parallel or perpendicular to the deformation twins (see Figure 20).

Ramdohr (1980) has observed the same texture, however their origin and characteristics remain unexplained in his publication. He notes though, that a number of the hematite grains in question are anomalously magnetic. McEnroe (pers. comm. 2004) has observed similar textures in Australian iron ores.

It has been observed that some of the large deformation twins actually consist of small deformation twins at high density.

Magnetite

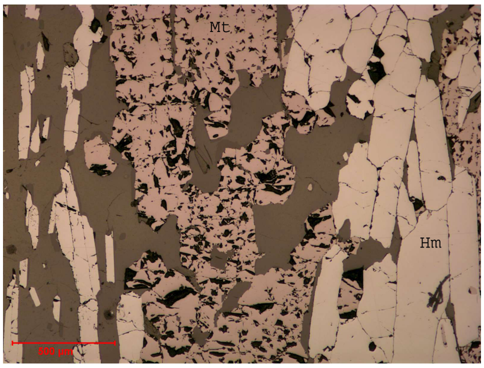

Figure 21 Magnetite (Mt) and flaky hematite (Hm).

Magnetite occurs as single anhedral to subhedral grains in hematite bands or as bands in gangue rock. The grains are at average between 0,4 and 0,6 mm, but are also found down to 0,1 mm and up to several millimetres.

Figure 21 shows bands of magnetite grains.

This is in accordance with thin section examinations performed by Ringdalen (1984), Søvegjarto (1986) and Malvik (1999).

Depositional age of the iron ores in the Dunderland Formation

Both Precambrian and Cambro-Silurian have been suggested as the depositional age of the ores in the Rana area (Svinndal 1977, Bugge 1978, Søvegjarto 1990).

Oftedahl (1981) indicates that the rocks in Rødingfjell Nappe Complex (RNC) and Helgeland Nappe Complex (HNC) (see Figure 9) might be older than Cambrian. He makes reference to incipient dating results and states that their ages could be from 600 to 1200 Ma and even older.

Dunderland Formation equivalents (Sjåfjell- and Håfjell Iron Formation) have been classified by Kimberley (1989a) as MECS-IF. MECS-IFs are defined as metazoan-poor. The rise of metazoan started at about 650 Ma (e.g. Hoffmann et al. 2002), thus an indicatively minimum depositional age could be 650 Ma.

Brattli et al. (1982) have made a Rb-Sr total rock isotope study of an orthogneiss in Simafjell in RNC. The ages 383 ± 19 MA and 362 ± 50 Ma were interpreted as secondary ages due to resetting of the Rb-Sr total rock isotope system. The estimated model age was determined to be 760 ± 120 Ma. This age is interpreted as a lower limit for the origin of the gneiss or some first rehomogenisation of the orthogneiss.

A Rb-Sr study on granitic dykes in RNC cutting the main schistosity concluded with an isochron age of 447 ± 7 Ma (Claeson 1979 in Brattli et al. 1982). Brattli et al. (1982) interpret these results as a minimum age for the major structural events (F_1 and F_2) in RNC and HNC.

Grenne et al. (1999) suggest a Neoproterozoic age for the ores. The age stands unquantified, but a roughly reading from their illustrations gives indicatively 590 to 610 Ma.

Melezhik et al. (2002) have applied carbon and strontium isotope stratigraphy to quantify the depositional ages of high-grade marble sequences in the Ofoten district. They conclude that the apparent Neoproterozioc age of the marble sequences is between 595 and 650 Ma. These marble sequences have been correlated with the marble sequences in the Dunderland district (Melezhik et al. 2002; Søvegjarto pers. comm. 2004).

Unpublished carbon and oxygen isotopes as well as Rb and Sr isotope data from the marbles in the Dunderland district indicate a depositional age consistent with that of the marbles in the Ofoten District (Melezhik pers. comm. 2003).

Based on the above, a probable depositional age would be Neoproterozoic, 600 to 700 Ma.

Ore genesis

Bugge (1948) proposed a sedimentary origin of the iron ores in the Dunderland Formation. The iron was suggestively deposited as ferric hydroxide ($Fe(OH)_3$) under relatively shallow marine conditions and varying Eh-pH conditions. The source of iron was suggested to be nearby coastal areas. The ferric hydroxide was transformed during rock consolidation to hematite. The magnetite originates, according to Bugge (1948), mainly from hematite formed by reduction during metamorphism. Subsequent authors have repeated this theory as the most probable one (e.g. Foslie 1949, Søvegjart 1972, Bugge 1978, Grenne et al. 1999). Grenne et al. (1999) point out the differences between the Lasken- and Storforshei Iron Formation and suggest that the deposition of the Lasken Iron Formation have been influenced from volcanic activity. This conclusion is made due to a higher content of carbonates and amphibole in the Lasken Iron Formation.

Kimberley (1989a) concludes that deep weathering (defined as hydration of new crust or late diagenesis of sediments) has been the source of all iron formations. Cherty iron formations have deep weathering through hydration by seawater of new crust as the source.

Trendall (2002) argues that there is a deep-water origin of BIFs in the Hamersley Group. His arguments comprise the absence of epiclastic material and current generated structures. He lists three requirements for deposition of an iron formation:

1. The development of a depository that remained tectonically stable for periods approaching 10^6 years.
2. The depository had sufficient depth of water.
3. The shape of the depository was such that ocean water with dissolved ferrous iron was able to circulate freely into and out of it.

As Trendall (2002) points out, his arguments are not necessarily valid for the Neoproterozoic iron formations formed between 800-600 Ma. According to Trendall such Neoproterozoic iron formations have been described from Australia (e.g. Braemer Iron Formation), from northwest Canada (Rapitan Group), Brazil (Jacadigo Formation) and Namibia (Damara Supergroup). Most of them show evidence of glacial association (Klein and Beukes 1993 in Trendall 2002 and Grenne et al. 1999). Hoffman et al. (2002) have developed an idea regarding an ice covered Earth (Snowball Earth), first coined by Harland (1964 in Trendall 2002) and followed up by Kirschvink (1992 in Trendall 2002). Hoffman et al. (2002)

have developed the ideas into an integrated hypothesis where iron formation deposition is one probable outcome. However, as Grenne et al. (1999) point out, it has not been possible to find any evidence of glaciogenic components in the Dunderland Formation or its Caledonian equivalents.

As illustrated in Figure 13 a garnet fels is positioned techtonostratigraphically between the magnetite-hematite iron ore and the mica schist of the Storforshei Iron Formation. The precipitation of this garnet fels is probably a result of similar precipitation mechanisms and the same source that are responsible for the iron formations. However, since dissolved Mn^{2+} remains in solution over a larger range of Eh-pH conditions than Fe^{3+} and Fe^{2+} (e.g. Maynard 1983) the Mn-mineralisations will be formed at a greater distance from the source and therefore on top of the iron formation.

The iron ores in the Dunderland Formation occur in medium metamorphosed facies. The metamorphic grade is within the lower half of amphibolite facies (Søvegjarto 1972). The Dunderland Formation is intensively deformed through four fold phases. The main metamorphism occurred during the pre-Caledonian F1 (Søvegjarto 1990). It is due to the folding that necessary thickness of iron ore has formed.

2.6. Magnetism of rocks and minerals

2.6.1. Introduction

All materials are magnetic. The magnetism originates from orbital and spin motions of electrons and how the electrons interact with each other. Dependent on how materials response to external magnetic fields, they can be divided into five classes: diamagnetism, paramagnetism, ferromagnetism, ferrimagnetism and antiferrimagnetism (e.g. Telford 1994).

Diamagnetism

Materials are diamagnetic if they have a negative response (magnetisation) to an external magnetic field. The magnetic susceptibility (see Section 2.6.2) of such materials is very low and negative. If the external magnetic field is removed, the magnetisation is reduced to zero. Diamagnetic materials are composed of atoms where there are no unpaired electrons. Examples of diamagnetic minerals are quartz, calcite, graphite and salt. Diamagnetism is independent of temperature.

Paramagnetism

Paramagnetic materials have a net magnetic moment due to unpaired electrons in partially filled orbitals. Iron has unpaired electrons. In the presence of an external field, the different atomic magnetic moments will align according to the direction of the external field and thereby respond positively (positive magnetisation). If the external magnetic field is removed, the magnetisation is reduced to zero. The different magnetic moments in paramagnetic materials do not interact magnetically. The effect of paramagnetism is therefore weak. Examples of paramagnetic minerals are biotite and pyrite. Paramagnetism is temperature-dependent.

Ferromagnetism

Ferromagnetic materials have a net magnetic moment. Adjacent magnetic moments interact magnetically very strongly through significant orbital overlap and resulting exchange coupling. Unlike diamagnetic and paramagnetic materials, the magnetisation of ferromagnetic materials is not reduced to zero if the external magnetic field is removed. Instead, the magnetisation follows a path called a hysteresis loop. Such a loop is given in Figure 22. If the ferromagnetic material is subjected to an increasing external magnetic field (H), the magnetisation (B) increases until it flattens along the line Os. The magnetisation at point s is the maximum magnetisation value for the given sample, and increasing the external field, will not result in an increased magnetisation. If H is decreased, the magnetisation follows the line connecting s and r, where r is the residual, or remanent, magnetism.

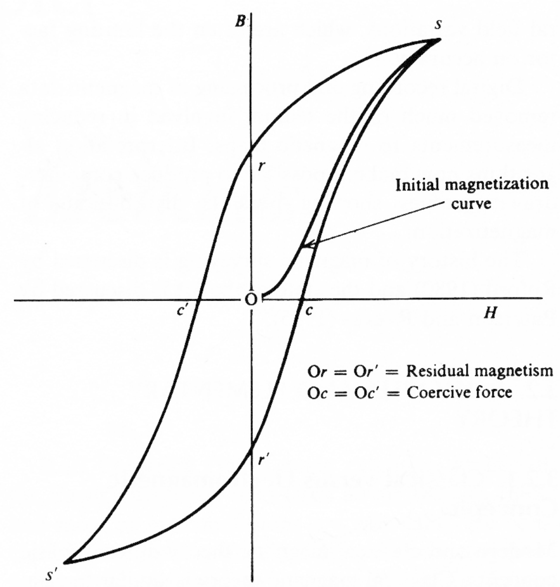

Figure 22 Hysteresis loop. From Telford 1994.

If H is reversed, the magnetisation continues to drop and equals zero at c′, the coersive force. When H is reversed further, the reversed saturation magnetisation is finally reached. Increasing H again, the magnetisation of the material follows the path indicated in Figure 22.

Ferromagnetic materials are spontaneous magnetised, i.e. they are also magnetised in the absence of an external magnetic field. Further they become paramagnetic above the Curie temperature.

Metallic iron is an example of a ferromagnetic material.

Two subgroups of ferromagnetism are ferri- and antiferromagnetism.

Ferrimagnetism

Whereas ferromagnetic materials have a parallel exchange coupling, the ferrimagnetic materials have antiparallel coupling with unequal magnetisation between layers of atomic magnetic moments.

Magnetite is the most important ferrimagnetic mineral.

The reason for this can be found in the crystal structure of magnetite.

Crystal structure of magnetite

Magnetite is an iron oxide of type AB_2O_4, the spinel group. Magnetite has the general formula Fe_3O_4 or $Fe^{3+}(Fe^{2+}\,Fe^{3+})O_4$ and is, because it is made up of oxygen and more than one type of ions with different co-ordination number, a multiple oxide. The iron ions are surrounded by four or six oxygen anions and are therefore four and six co-ordinated. Magnetite is an inverse spinel because half of the trivalent iron ions are four co-ordinated, while the rest are together with the bivalent iron ions six co-ordinated (e.g.

Ramdohr 1980, Prestvik 1992). Figure 23 illustrates the crystal structure of magnetite.

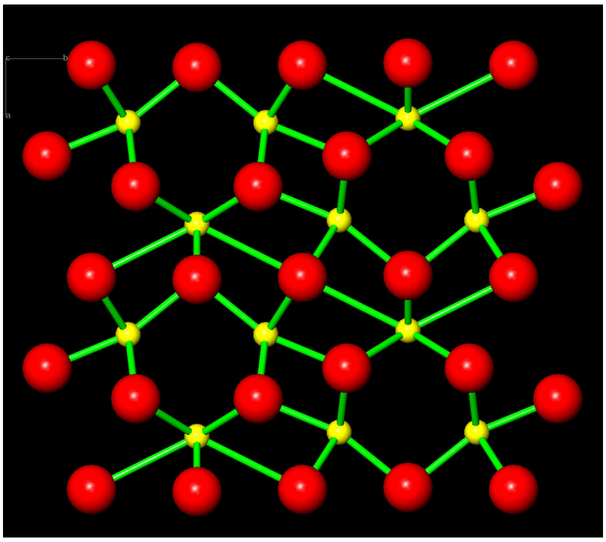

Figure 23 Magnetite crystal structure with iron ions (yellow) in octohedral and tetrahedral sites (Downs 2003)

The magnetic moments of ions in the octahedral sites are opposite in direction compared to the ions in the tetrahedral sites. This means that the total magnetic moment originating from the trivalent ions is nullified, whereas the magnetic moment contribution from the bivalent iron ions causes the magnetic properties of magnetite.

Magnetic moments of some iron minerals are given in Figure 24.

Ferrite	Postulated ion distribution: tetrahedral ions	Postulated ion distribution: octahedral ions	Magnetic moment of tetrahedral ions	Magnetic moment of octahedral ions	Magnetic moment per molecule $MeFe_2O_4$: theoretical	Magnetic moment per molecule $MeFe_2O_4$: experimental
$MnFe_2O_4$	$Fe^{III}_{0.2}+Mn^{II}_{0.8}$	$Mn^{II}_{0.2}+Fe^{III}_{1.8}$	5	5 + 5	5	4.6
Fe_3O_4	Fe^{III}	$Fe^{II}+Fe^{III}$	5	4 + 5	4	4.1
$CoFe_2O_4$	Fe^{III}	$Co^{II}+Fe^{III}$	5	3 + 5	3	3.7
$NiFe_2O_4$	Fe^{III}	$Ni^{II}+Fe^{III}$	5	2 + 5	2	2.3
$CuFe_2O_4$	Fe^{III}	$Cu^{II}+Fe^{III}$	5	1 + 5	1	1.3
$MgFe_2O_4$	Fe^{III}	$Mg^{II}+Fe^{III}$	5	0 + 5	0	1.1
$Li_{0.5}Fe_{2.5}O_4$	Fe^{III}	$Li^{I}_{0.5}+Fe^{III}_{1.5}$	5	0 + 7.5	2.5	2.6

Figure 24 Theoretical and experimental magnetic moment per iron molecule. From Yeary (2004).

Antiferromagnetism

As ferrimagnetic materials, the antiferromagnetic materials have a large concentration of interacting magnetic atoms, i.e. the exchange coupling is significant. Unlike the ferrimagnetic materials, the antiparallel coupling between the layers of atomic magnetic moments is equal. The resulting magnetisation is therefore equal to zero.

Hematite is the most important antiferromagnetic mineral.

The reason for the equal antiparallel coupling between layers of magnetic moments is found in the crystal structure of hematite.

Crystal structure of hematite

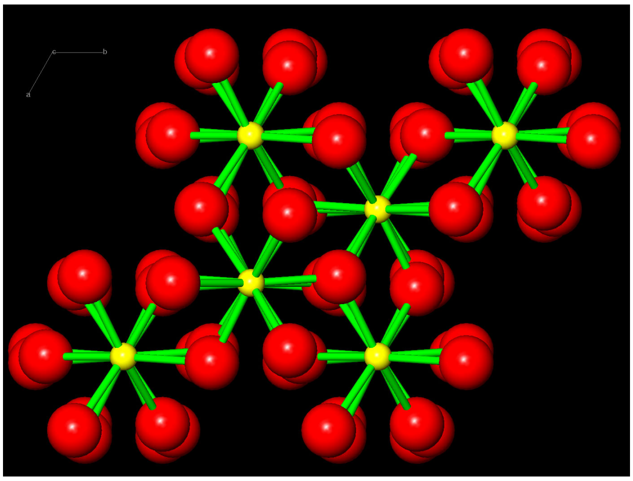

Figure 25 Image of the hematite crystal structure. Iron ions (yellow) in octahedral sites (six co-ordinated) Downs (2003).

Hematite is an iron oxide of the corundum structure type A_2O_3. This type of oxide is called single oxide because only ions of one metal are combined with the oxygen atom.

Hematite has layers of hexagonal closest-packed anions and six co-ordinated (octa-hedral) iron ions. (e.g. Ramdohr 1980, Prestvik 1992). Figure 25 illustrate the crystal structure of hematite.

2.6.2. Magnetic susceptibility

Magnetic susceptibility is the fundamental rock parameter in magnetic prospecting (Telford et al. 1994). Magnetic susceptibility is a measure of the degree to which a material can be magnetised in the presence of an external magnetic field. The volume magnetic susceptibility is dimensionless and is given by the ratio between the induced magnetisation M and the external field H:

$$\kappa = \frac{M}{H}$$ **Eq. 1**

The mass magnetic susceptibility is defined as:

$\chi = \frac{\kappa}{\rho}$, where ρ is the density of the material. **Eq. 2**

Measured, uncorrected magnetic susceptibility is only apparent. When a magnetic body is placed in an external magnetic field, positive and negative charges will appear on the surface of the body. These charges induce a magnetic field opposite in direction to the external field. This field is called the demagnetisation field, F_d. The net magnetic field inside the body is therefore less than the external field. This is called demagnetisation (Guo et al. 2001). Demagnetisation is significant, and must be accounted for, if the volume magnetic susceptibility is above 0.1 (SI units). In such a case the volume magnetic susceptibility is given by:

$$\kappa = \frac{M}{H - F_d}$$ **Eq. 3**

The correlation between magnetic susceptibility and mineralogy has been established and confirmed by many investigators. (e.g. Petruk 1965; Zablocki 1974; BVLI 1980; Eloranta 1983; Telford et al. 1994; Sandøy 1996; Clark 1997; Fallon et al. 1997; Blum 1997; Mutton 2000).

Petruk (1965) measured the specific magnetic susceptibilities of eleven chlorites using a Frantz isodynamic separator and correlated the results with the content of total iron (FeO) plus manganese oxide (MnO). The correlation found correspond to the following linear equation where χ_m being the mean mass magnetic susceptibility:

$$Total\ FeO + MnO\,(wt\%) = 0.12 + 0.559 * 10^{-6}\,\chi_m$$ **Eq. 4**

Sandøy (1996) cites Balsley & Buddington (1958) and states the following empirical correlation between the magnetic susceptibility of a rock and its content of magnetite:

$$\kappa = 33x10^{-3} * Vol\%\,magnetite$$ **Eq. 5**

Equation (5) is also given by Blum (1997), although in a slightly rearranged form:

$$Volume\ fraction\ of\ magnetite = \frac{\kappa}{3}$$ **Eq. 6**

Eloranta (1983) examined 130 two-foot samples of drill cuttings from the Biwabik Iron Formation. He found two equations, each valid for volume magnetic susceptibilities below (eq. 39) and above (eq. 40) 50 (cgs units) respectively:

$$\%Magnetic\ Iron\,(wt\%) = 0.32 * magnetic\ susceptibility - 2.56$$ **Eq. 7**

$$\%Magnetic\ Iron\,(wt\%) = 0.12 * magnetic\ susceptibility + 7.00$$ **Eq. 8**

Clark (1997) cites Puranen (1989) and states the following relationship between the observed volume susceptibility κ, and volume fraction of magnetite (f) up to a few per cent:

$$\kappa = 3.47 f$$ **Eq. 9**

The deviation from the linear relationships given in Equation (9) becomes clear at susceptibility values above approximately 0.1. In Figure 26, the linear relationship of Puranen (1989) has been extended to 30 vol% mt for illustration.

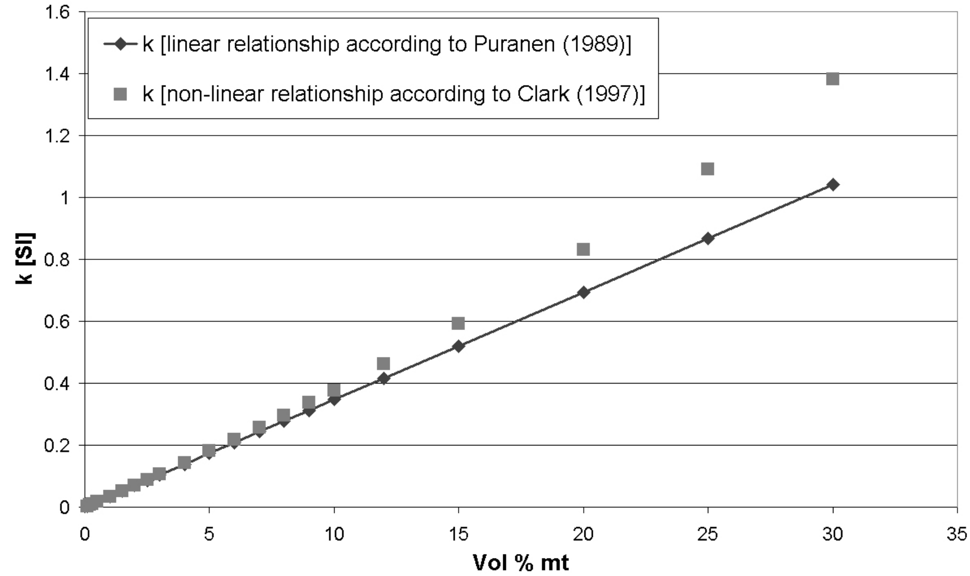

Figure 26 Departures from linear relationship between vol% mt and magnetic susceptibility due to interactions between highly magnetic grains. The linear relationship extended to 30 vol % mt for illustration.

The reason for the deviation from a linear relationship is that at high concentrations of highly magnetic material (e.g. magnetite), the magnetic susceptibility is influenced by interactions between grains and thereby increases faster than the linear relationship.

2.6.3. Magnetic susceptibility of ore minerals

Lower- and upper limits for the mass- and volume magnetic susceptibility for some of the minerals in the Kvannevann Iron Ore are given in Figure 27 and 28. Note that a logarithmic scale has been used on the y-axis.

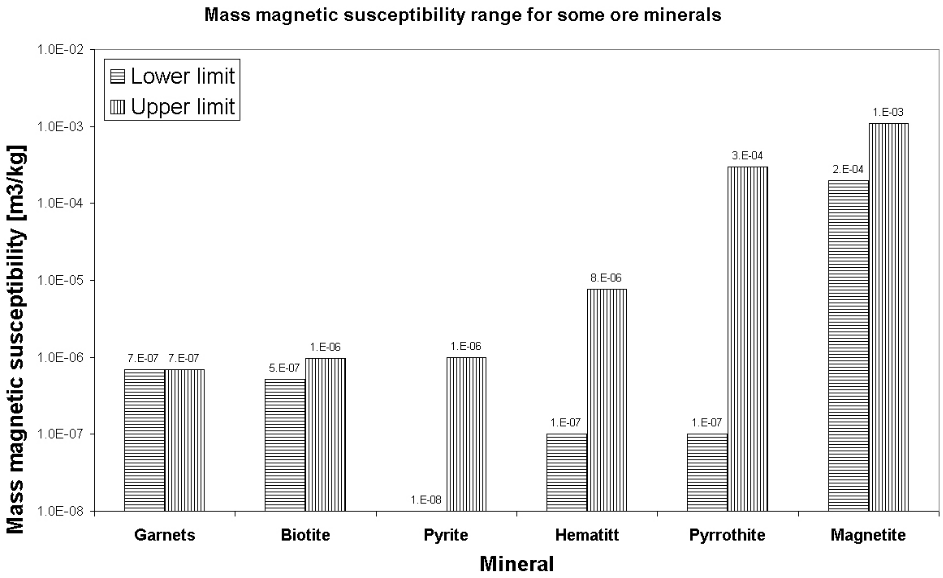

Figure 27 Mass magnetic susceptibility ranges of some ore minerals. Compiled from Hunt et al. (1995)

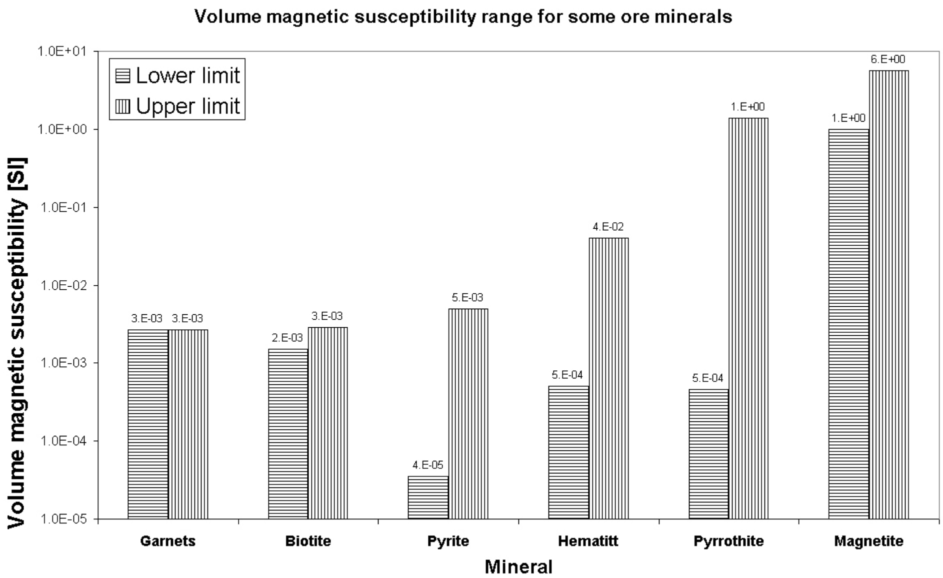

Figure 28 Volume magnetic susceptibility ranges of some ore minerals. Compiled from Hunt et al. (1995).

The content of pyrrothite in the ore is very limited, i.e. magnetite has by far the largest magnetic susceptibility. The lower limit of volume magnetic susceptibility of magnetite is twenty-five times larger than the upper limit of hematite.

3. Revitalisation of the existing database

3.1. Introduction

After years of mining Rana Gruber AS possess material, which forms an important basis for the following study. This material consists of borehole data including lithologies, assays, core loss, deviation measurements and joint densities along the boreholes, blast contours and blast assays and geologic maps and profiles. This material is reviewed and to some extent further processed in order to increase its area of application.

Rana Gruber AS personnel have logged the borehole cores. Mineralised zones have been crushed, grounded and analysed by the Rana Gruber AS' own laboratory.

Geodata can be collected directly using censors like GPS-receivers or total stations. This kind of collection is primary collection of geodata. Secondary collection comprises collection through scanning or digitising of data on paper. The existing database is on paper. Secondary collection through scanning, digitisation and simple entering of data into a computer has therefore been performed.

3.2. Surface maps

3.2.1. Topography

Ore deposit modelling and description includes the characterisation of volumes within certain boundaries. An important boundary is the terrain.

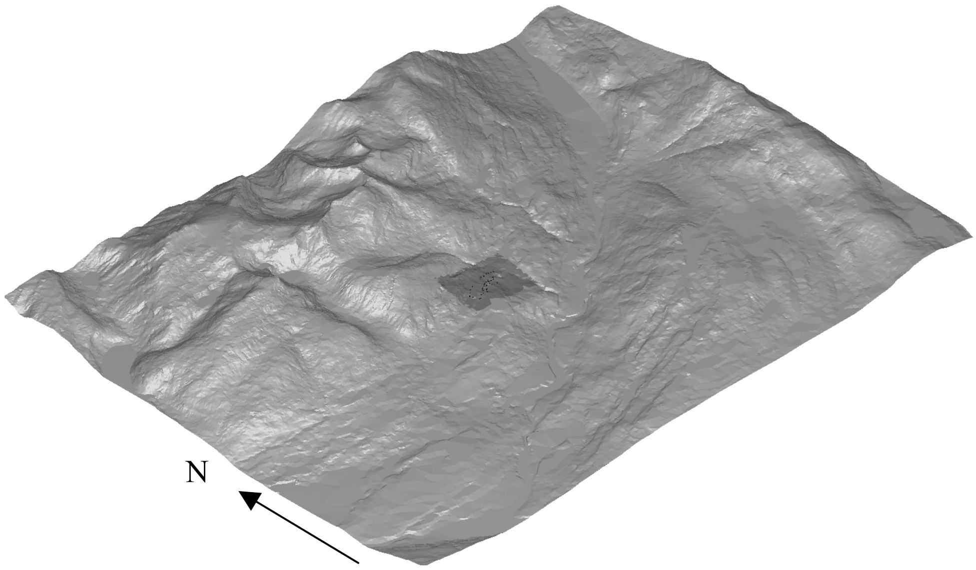

Figure 29 Topography of Dunderland Valley. Arrow indicates North. Area limited by rectangle with corner coordinates [59000.000, 933500.000], [74929.800, 945186.755], NGO48 IV. With permission from Statens Kartverk.

In Figure 29 a digital terrain model based on M711 UTM contour lines is presented. Before modelling the terrain surface, the M711 geodata was transformed into NGO 48 IV coordinates within a rectangle with corner coordinates [59000.000, 933500.000], [74929.800, 945186.755]. The terrain model will be used for the following purposes:

- Communication.
- Since ore characterisation has no meaning above the surface, the terrain model is used to delimit this process.
- Reference surface for the surface geology map.

3.2.2. Geology map

An ore modelling process should utilise all available geodata of good quality. However, an ore model cannot be more accurate than the accuracy of the geodata used in the modelling process. (e.g. Holding 1994)

To assist in the ore deposit modelling, the geology map (Søvegjarto 1986) was therefore digitised and draped onto the terrain model. The geology map is given in Figure 11.

3.3. Borehole digitising and ore type characterisation

3.3.1. Introduction

Business processes may be divided into primary-, secondary- and development processes. Exploration performed parallel to production to increase the reserve base is an example of a development process (e.g. Haugen 1998).

During the open pit mining, a considerable amount of exploration diamond drilling was performed by Rana Gruber AS. In total almost 200 kilometres of diamond core, have been drilled and logged in the Dunderland Valley district. The exploration drilling was mainly performed in two campaigns; one in the 1950's and one in the 1980's.

Geoinformation from boreholes penetrating the Kvannevann Iron Ore, including lithology, core loss, assays, deviation data and joint density, is presented in the following chapters.

3.3.2. Borehole summary statistics

Borehole summary statistics are calculated in order to obtain input necessary for the subsequent geostatistical analysis.

General borehole statistics

The borehole data is stored and organised in a database. The general features of the boreholes are summarized in Table 4.

Feature	Quantification
Number of diamond drilled boreholes in the database	99
Total length of boreholes in database	20252 metres
Total length of assays	9460 metres

Table 4 General borehole features.

The borehole collars are constrained within a strike length of about 1.2 kilometres and an elevation of about 400 meters, with groups of boreholes around 100 metres above sea-level and around 400 metres above sea-level. Figure 30 and 31 show the x-, y- and z coordinates of the borehole collars.

The boreholes with a collar with z-coordinates approximately equal to 100 are drilled from an exploration- and drainage drift.

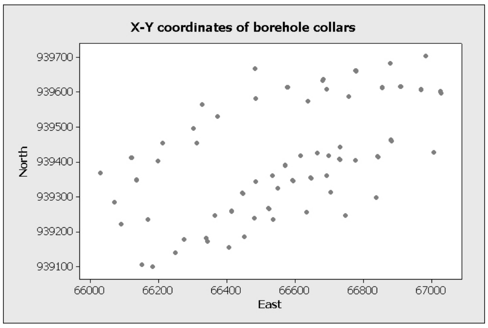

Figure 30 North vs. east coordinates of borehole collars.

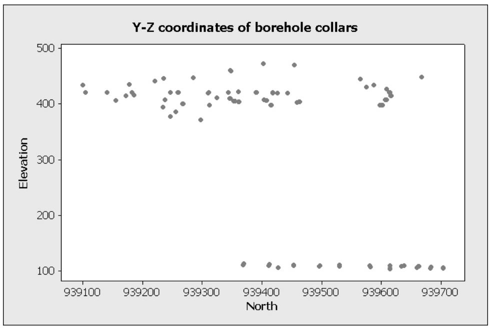

Figure 31 North coordinate vs. elevation above sea level of borehole collars.

Assay length, azimuth and inclination

The cores drilled during the exploration campaign in the 1950's had a diameter of 22 mm. Table 5 presents some basic borehole statistics from twelve boreholes originating from this exploration campaign.

# of assays	Mean length	Median length	StDev	Min	Max
62	10.30	10.00	4.51	2.10	19.90

Table 5 Summary statistics describing the assay lengths for the boreholes in 1950's exploration campaign.

The cores drilled during the exploration campaign in the 1980's had a diameter of 35 mm. Table 6 presents some basic borehole statistics. Eighty-seven of the boreholes in the database are from this exploration campaign.

# of assays	Mean length	Median length	StDev	Min	Max
1355	6.51	7.00	2.07	0.70	30.00

Table 6 Summary statistics describing the assay lengths for the boreholes in the 1980's exploration campaign.

The experimental variogram in a geostatistical analysis has the ability to reveal anisotropies in the spatially distributed data, i.e. differences in variability in different directions. It is therefore decisive to estimate experimental variogram in different directions. To achieve this at a reasonable confidence level, the borehole directions and their deviations must be known with accuracy. The boreholes drilled in the 1950 and the 1980 campaign deviate significantly. Figure 32 and 33 summarise the azimuth and the inclination of all the deviation measurements along the boreholes.

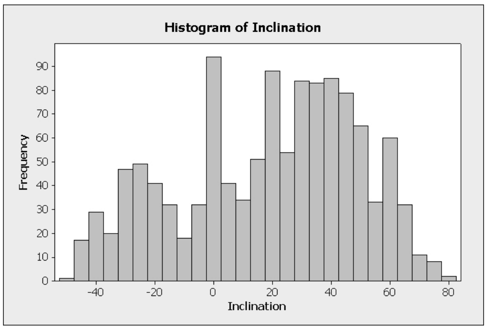

Figure 32 Inclination of all the deviation measurements in the database. Positive inclination downwards

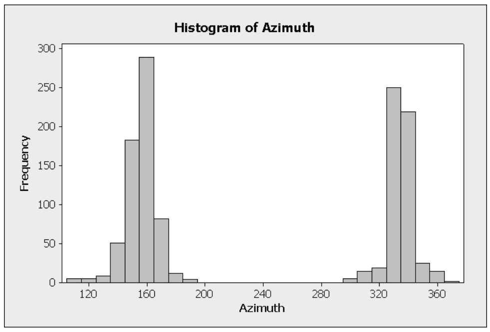

Figure 33 Azimuth of all the deviation measurements in the database. "330" means N330°E

Figure 33 shows that boreholes have been drilled in mainly two directions, namely N150E and N330E, i.e. they have been drilled from southeast to northwest and from northwest to southeast respectively. These directions are approximately perpendicular to the average strike of the mineralisation and the baseline of the local coordinate system. This baseline is oriented approximately N65°E.

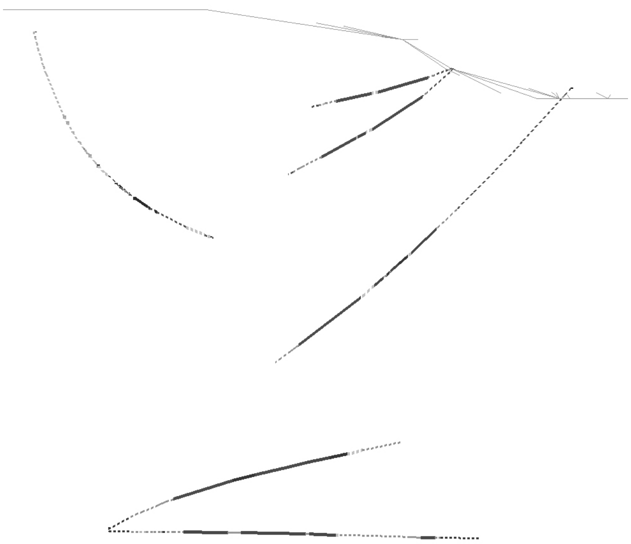

Positive inclination is defined as downwards. Figure 32 shows the variation in the borehole inclination. The histogram is characterised by three peaks, one around minus 30 degrees, one around 0 (zero) and one with a mode around 40 degrees. Figure 34 illustrates how the boreholes deviate in a cross section.

Figure 34 Borehole deviations in a cross section.

Geochemical summary statistics

Introduction

Outliers can have major influence on statistical analysis. Detection of outliers is therefore a first step in the (geo-) statistical analysis of geodata.

The database contain analysis of FeTot, which is the total iron in the samples, FeMagn, which is the amount of magnetite-bound iron in the ore samples, manganese-oxide, MnO, phosphorous, P, sulphur, S and titanium dioxide, TiO_2.

These are all important ore parameters, and are included in the database due to their importance and due to accessibility. Other important ore parameters are Al_2O_3 and Ca, however, the cores have not been analysed on these parameters.

Regularisation, size matters

Variables used in geostatistics should be additive. To achieve additivity the variables must have the same support. The support is the size and the shape of the volume under consideration. Volumes with different support have different variance structure. This is formulated in the Krige's additivity relation (e.g. Armstrong 1998):

$$\sigma^2(v \mid V') = \sigma^2(v \mid V) + \sigma^2(V \mid V') \qquad \textbf{Eq. 10}$$

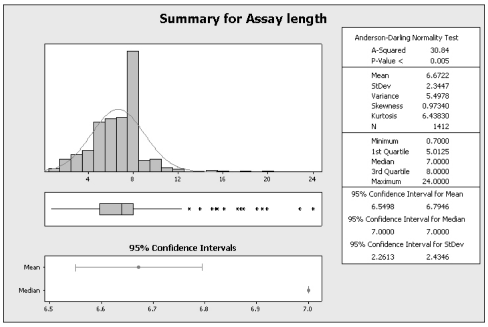

Figure 35 Sample length summary statistics, all 99 boreholes.

The Krige's additivity relation is based on experimental work done by Daniel Krige (Krige 1951). His work was based on a large number of underground development samples from the Rand goldmines in South Africa (Witwatersrand).

In Equation (10) the different v's represent different supports, where v < V < V'. V' could for example be the entire deposit, whereas V and v are blocks and diamond cores respectively. This relation states that the dispersion variance of cores in the deposit is the sum of the dispersion variance of the cores in the blocks and the dispersion variance of the blocks in the deposit.

A consequence of Krige's additivity relation is that core sections used in geostatistical analysis must have the same length, or support. In Figure 35 it can be seen that the analysed core sections vary from 0.70 to 30 metre, with an arithmetic mean of 6.7 metres and a most frequent value of 8 metres.

Composite assays of equal lengths are therefore generated to equalize the support and thereby allow a meaningful interpretation of the variance structure. Because the majority of the core sections were analysed in eight-metre composites, this was chosen as the general composite length.

Descriptive statistics

As described in Section 3.4, a 3D-model of the mineralised envelope was generated based on the geoinformation from the diamond cores. The geochemical summary statistics of eight-metre composite geodata inside the mineralised envelope is given in Table 7.

steinare - Jun 01 2004 09:50:01

Univariate Statistics

	Count	Minimum	Maximum	Mean	Variance
ASSAYS_FEMAGN	1060	0.1000	32.1890	2.5953	9.8368
ASSAYS_FETOT	1070	5.3153	48.1057	32.0275	74.5645
ASSAYS_MNO	257	0.0500	6.4052	0.6169	1.1447
ASSAYS_P	1021	0.0723	0.5827	0.2127	0.0022
ASSAYS_S	1031	0.0010	0.3222	0.0061	0.0004
ASSAYS_TIO2	624	0.0900	0.8485	0.3093	0.0218

Bivariate Statistics

	Count	Minimum	Maximum	Mean	Variance	Correlations
ASSAYS_FEMAGN	1060	0.1000	32.1890	2.5953	9.8368	-0.0868
ASSAYS_FETOT	1060	5.3153	48.1057	31.9535	74.5104	
ASSAYS_FEMAGN	257	0.1000	32.0500	2.6239	11.7090	-0.2068
ASSAYS_MNO	257	0.0500	6.4052	0.6169	1.1447	
ASSAYS_FEMAGN	1014	0.1000	32.1890	2.5452	8.6846	-0.2278
ASSAYS_P	1014	0.0723	0.5827	0.2127	0.0022	
ASSAYS_FEMAGN	1026	0.1000	32.1890	2.6027	10.1232	0.1691
ASSAYS_S	1026	0.0010	0.3222	0.0061	0.0004	
ASSAYS_FEMAGN	624	0.1000	32.1890	2.4544	7.3019	0.2241
ASSAYS_TIO2	624	0.0900	0.8485	0.3093	0.0218	
ASSAYS_FETOT	257	8.7664	45.6800	32.2810	72.4363	-0.3412
ASSAYS_MNO	257	0.0500	6.4052	0.6169	1.1447	
ASSAYS_FETOT	1021	5.3153	48.1057	31.8897	76.1159	0.4356
ASSAYS_P	1021	0.0723	0.5827	0.2127	0.0022	
ASSAYS_FETOT	1031	5.3153	48.1057	31.9320	76.6881	-0.0481
ASSAYS_S	1031	0.0010	0.3222	0.0061	0.0004	
ASSAYS_FETOT	624	5.3153	48.1057	32.1790	76.3015	-0.9060
ASSAYS_TIO2	624	0.0900	0.8485	0.3093	0.0218	
ASSAYS_MNO	242	0.0891	6.4052	0.6298	1.1720	-0.0856
ASSAYS_P	242	0.1100	0.4100	0.2060	0.0022	
ASSAYS_MNO	257	0.0500	6.4052	0.6169	1.1447	0.0098
ASSAYS_S	257	0.0010	0.3222	0.0074	0.0007	
ASSAYS_MNO	242	0.0891	6.4052	0.6298	1.1720	0.1850
ASSAYS_TIO2	242	0.0900	0.8426	0.3048	0.0218	
ASSAYS_P	1012	0.0723	0.5827	0.2126	0.0022	-0.0273
ASSAYS_S	1012	0.0010	0.3222	0.0058	0.0003	
ASSAYS_P	624	0.0723	0.5827	0.2053	0.0022	-0.4950
ASSAYS_TIO2	624	0.0900	0.8485	0.3093	0.0218	
ASSAYS_S	624	0.0010	0.3222	0.0079	0.0005	0.1219
ASSAYS_TIO2	624	0.0900	0.8485	0.3093	0.0218	

Table 7 Summary statistics for eight-metre composites inside mineralised envelope.

Important features of the summary statistics are the varying number of composites, the mean values of the different parameters and the negative correlation between FeTot and TiO_2.

In the calculation of the summary statistics, S values below detection limit have been replaced by the detection limit (DL). The average sulphur-value given in Table 7 could therefore be considered as a maximum average value of the geodata.

The variance or the standard deviation is together with the coefficient of variation (CV) commonly used parameters to quantify the dispersion in a dataset. The CV is the ratio between the mean value and the standard deviation.

The CV is given in the Table 8.

	FeMagn	FeTot	MnO	P	S	TiO_2
CV	121%	27%	173%	22%	328%	48%

Table 8 Coefficient of variation

From Table 8 given above, it can be seen that there is a large dispersion in the S, MnO and FeMagn values. This dispersion is confirmed by the histograms shown in Figure 37, 38 and 41.

Declustered histograms

A histogram of composites can be considered to be representative for the deposit, or a section of it, if the sampling is on a regular grid. As illustrated in Figure 30 and 31, the sampling is not on a regular grid and the boreholes deviate considerably. The borehole deviations are illustrated in Figure 32 and 33.

The declustered histograms calculated here take account of preferential sampling by reducing the weight of samples, which are surrounded by other samples. Enforcing a 3D-grid on the samples and calculating the average value within each block for different block sizes produce the declustered histograms. Each sample within the block is given a weight equal to 1/n, where n is the number of samples within the block. If the over-sampling is performed in high-grade zones, the block size is chosen so that the total average is minimized. If the over-sampling is in low-grade zones, the chosen block size maximizes the total average. Block-sizes were found by trial and error and are given in Appendix B.

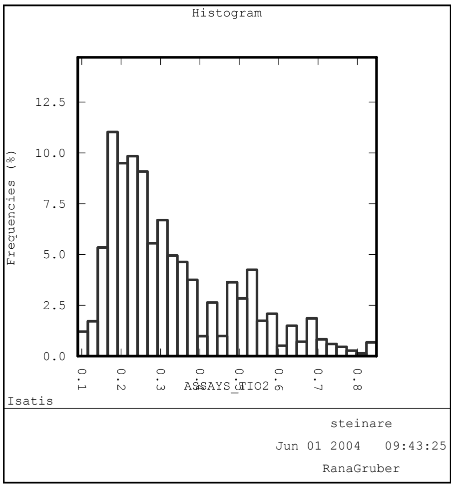

Figure 36 Declustered histogram for TiO2 inside mineralised envelope

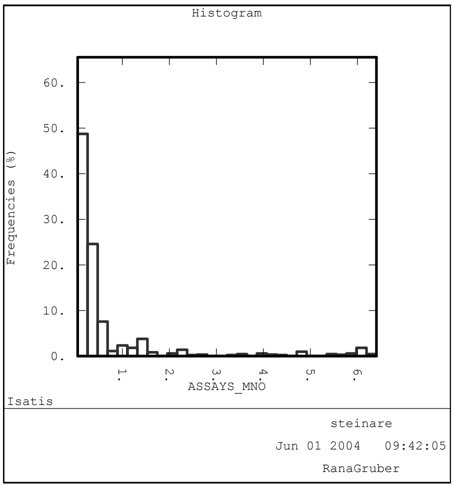

Figure 37 Declustered histogram for MnO inside mineralised envelope

The declustered histogram of TiO_2 indicates two populations. One major around 0.2% and one minor around 0.5%.

The MnO histogram is skewed, with a skewness equal to 3.56. The majority of the composite data is below 0.5%. The calculated value 2.89 equals average MnO plus two standard deviations as given in the summary statistics in Table 7. The equivalent value using the declustered summary statistics is 3.31. All MnO values above these limits can be considered to be outliers. However, since they can be explained by the presence of certain garnet containing rock types within the mineralised envelope, they cannot be excluded from future analysis.

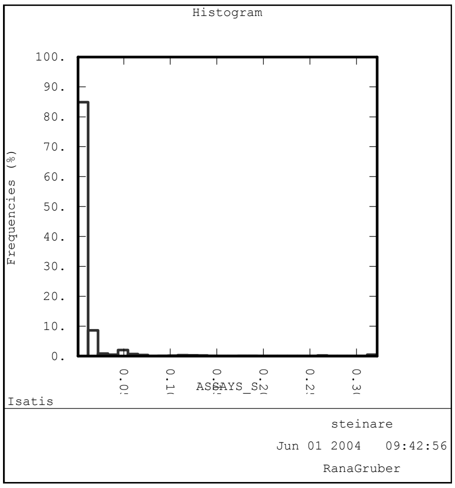

Figure 38 Declustered histogram for S inside mineralised envelope

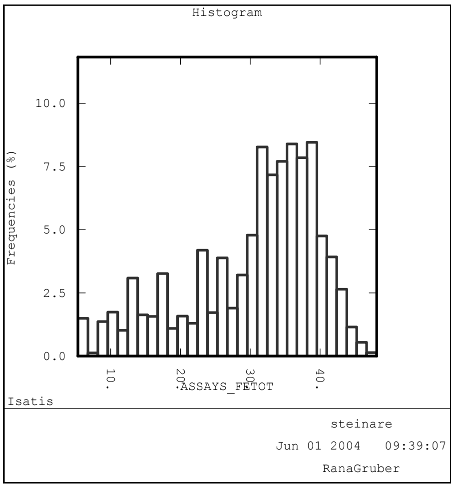

Figure 39 Declustered histogram for FeTot inside mineralised envelope

The S histogram in Figure 38 is highly skewed, with a skewness equal to 10.13 and extreme values above 0.30% S. These high values are not representative for the general %S trend in the deposit. Correlating these high %S values with the lithology produces no clear explanation. However, some of the high values correlate with high values of FeMagn, which might indicate a more reducing depositional environment. Another explanation could be that some secondary process has deposited sulphides locally.

The FeTot histogram in Figure 39 shows a negatively skewed shape, i.e. tail towards low values. This shape is common for FeTot in iron ores (e.g. Armstrong 1998). The majority of the values are centred on 35%.

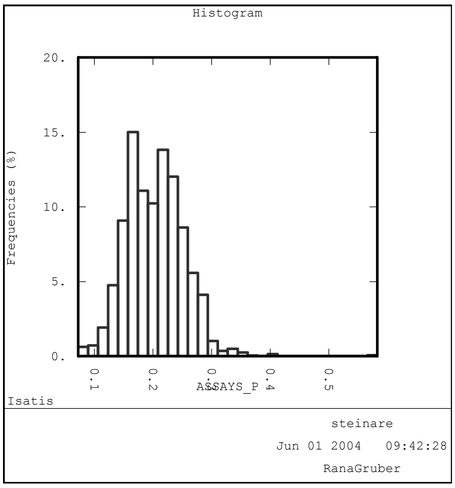

Figure 40 Declustered histogram for P inside mineralised envelope

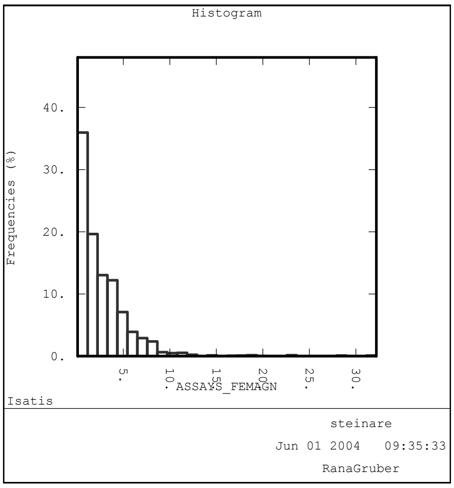

Figure 41 Declustered histogram for FeMagn inside mineralised envelope

The histogram showing the P distribution in Figure 40 shows a bell shaped distribution comparable to a normal distribution. The average value is around 0.2% P.

The FeMagn data are also positively skewed, with skewness equal to 4.28. The majority of the composite data is below 5%.

Descriptive statistics for the declustered data are given in Appendix A.

Declustered histograms of transformed data

Transformations can be used to detect special features of skewed data. A natural logarithmic transformation (ln) has been used on the FeMagn, MnO and S data. Their declustered histograms are presented in Figure 42, 43 and 44.

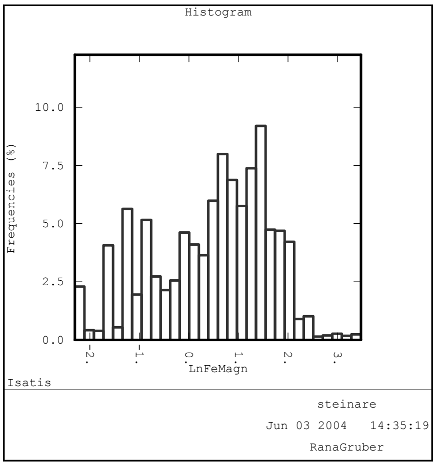

Figure 42 Histogram of ln(FeMagn), 8-metre composites inside mineralised envelope.

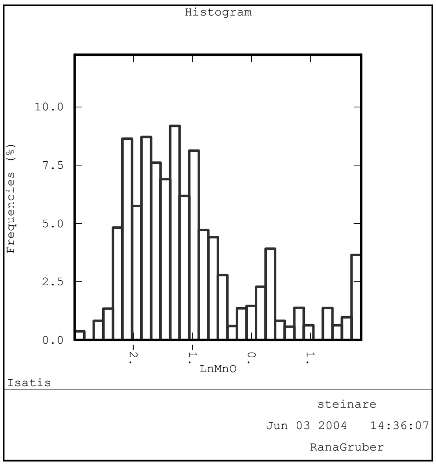

Figure 43 Histogram of ln(MnO), 8-metre composites inside mineralised envelope.

The FeMagn histogram shows a bimodal shape with modes around ln(FeMagn) = -1 and ln(FeMagn) = 1. This represents real FeMagn values of about 0.4 and 2 respectively. These values may indicate different ore types.

The main mode of the ln-transformed MnO histogram is around –1.5, which in real MnO values represent 0.2% MnO. Minor peaks occur around 0.3 and 1.8, which represent real MnO values of about 1.3 and 6.0 respectively.

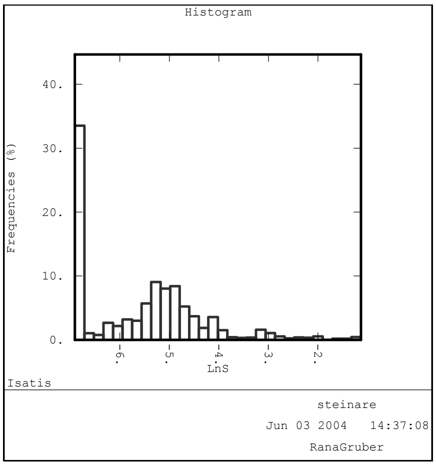

Figure 44 Histogram of ln(S), 8-metre composites inside mineralised envelope. Analyses below detection limit are equalled the detection limit before transformation.

The declustered histogram of the ln-transformed S data shows that the majority of the data is below or equal to the detection limit (DL) of 0.001% S. In the declustered histogram in Figure 37 all values below DL have been replaced by the DL. The main mode except from the very low values is centred on –5 which represent a real S% value of 0.006%. One minor mode around 0.05% S (lnS = -3) can also be discerned.

Scatter plots

Scatter diagrams are used to detect correlations, possible outliers and to assess bimodality.

The scatter diagrams in Figure 45 to 46 are included to draw attention to special features of the data.

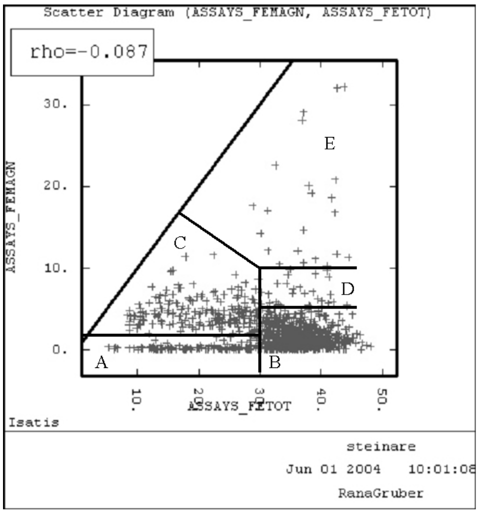

Figure 45 Scatter plot of 8-metre composites showing the relationship between FeTot and FeMagn. Black line indicates x=y, i.e. FeMagn=FeTot.

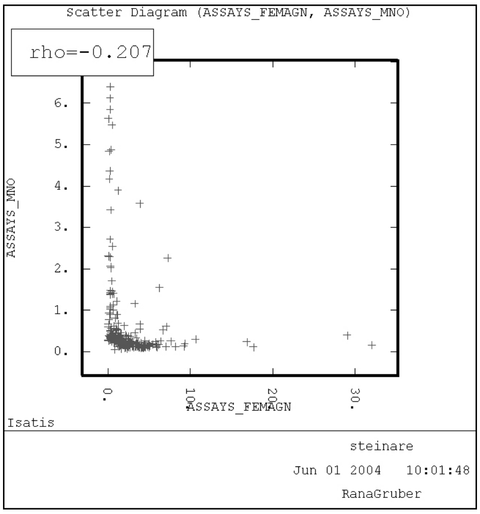

Figure 46 Scatter plot of 8-metre composites showing the relationship (or the lack of) between the MnO and FeMagn.

The following characteristics about the geochemical relationships can be extracted from the plots in Figure 45 and 46:

a. When all the data is considered there is no apparent correlation between the total iron content (FeTot) and FeMagn. The scatter plot may be interpreted to indicate different geochemical types of mineralisation, i.e. different populations. Basically five types could be extracted from the Figure 38. Letters in the following list, correspond to letters used in Figure 45.

   A. This type has FeTot below 30% and almost no FeMagn. Could be termed hematite impregnation.

   B. This type, or population, has an iron geochemistry dominated by hematite. This type could be characterised with a FeTot between 30% and 50% and a FeMagn up to 5%.

   C. A third type has FeTot values below 30% but more FeMagn compared to type B. Relative to this type, type C must be dominated by magnetite. It could be termed magnetite impregnation

   D. Type D is high on FeTot (above 30%) and relatively high on FeMagn (between 5 and 10%). This type could also be interpreted to be a part of type E (see next point). Type D and E would then be a hematite-magnetite mineralisation.

E. A fifth type is characterised by FeMagn values above 10% and FeTot values above 30%. Could be termed magnetite mineralisation.

b. As indicated in the summary statistic overview in Table 28, there is no apparent correlation between MnO and FeMagn (correlation coefficient equal to –0.20). This is seen in Figure 46. The plot indicates that if FeMagn is present, the content of MnO is very low and visa versa. Apparently, only a few samples have both FeMagn and MnO.

Figure 47 shows the scatter plots FeTot vs. TiO_2 and FeTot vs. P.

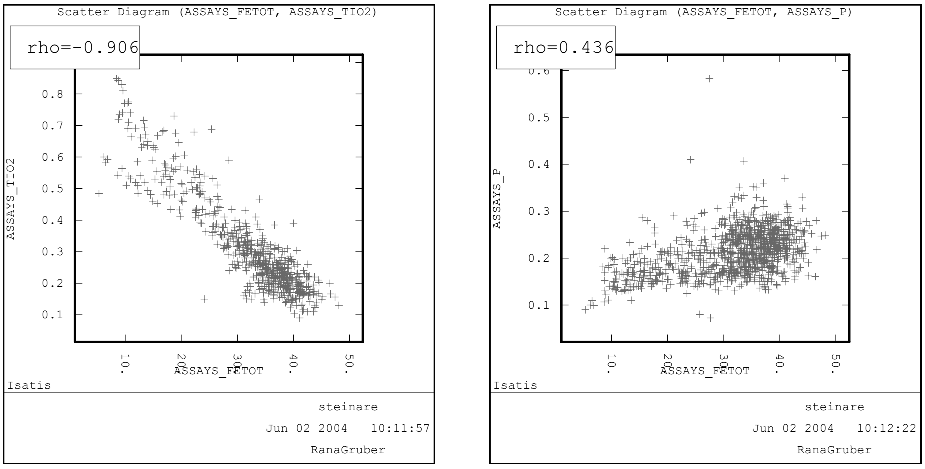

Figure 47 Scatter plot showing the relationship between P, FeTot and TiO_2. The 8-metre composites within the mineralised envelope have been used to produce these plots.

The following characteristics of the geochemical relationships can be extracted from the plots in Figure 47:

a. Strong negative correlation between FeTot and TiO_2. Similar, but not so strong correlations have been found plotting FeHm vs. TiO_2, where FeHm = FeTot – FeMagn for both FeHm above and below 30%. The reason for this correlation could be two-fold. First, it could be a result of the difference in solubility between Ti and Fe. Second, and probably the most predominant reason, it could be the result of a transition from iron rich iron ore to relatively TiO_2-rich mica schist. Results from a comparison between Bugge (1948) and Ringdalen (1984) and Malvik (1997) show that the TiO_2-content in the mica schist is significantly higher than the TiO_2-content in the hematite.

This is supported by Henry and Guidotti (2002) who have studied the incorporation of Ti in biotite.

b. Weak positive correlation between P and FeTot. An equivalent correlation (Søvegjarto 1990) has been reported from the apatite-magnetite mineralisation within the Lasken Iron Formation (see Section 2.5.3). It seems that the correlation is controlled by the FeTot values below 30%. This is confirmed in Figure 48. This figure show FeHm vs. P for samples where FeTot < 30%. Above 30% there seems to be no correlation (see Figure 47, FeTot vs. P).

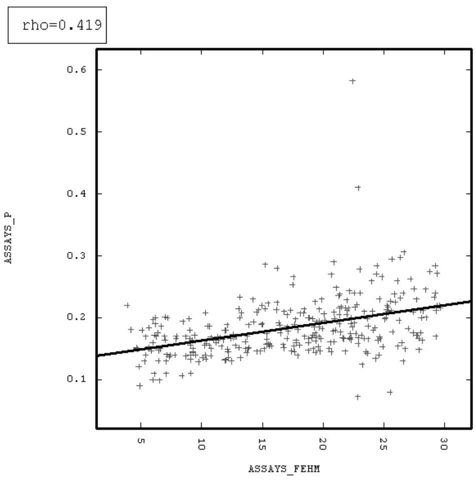

Figure 48 Scatter plot showing FeHm vs. P for FeTot < 30%. FeHm is defined as FeTot minus FeMagn.

3.3.3. Rock- and ore types

The borehole log consists of strict observations of different lithologies as “mica schist” and different types of ore, termed as “malm” (the Norwegian word for “ore”). It has not been possible to retrieve the assumed cut-off, used in the ore assignments in the borehole log.

The different ore- and rock types are described in the logs. Not all intervals have been analysed for the different decision parameters stated in the introduction of “Geochemical summary statistics” in Section 3.3.2. In particular, this applies to MnO. An attempt has therefore been made to find a geochemical signature of selected ore- and rock types defined from the descriptions in the log and assays matched with corresponding log intervals. Table 9 summarises the different rock types extracted from the log. These types have been used in the following analysis.

• Mica schist (Glimskif) o Mica schist; with and without fine-grained garnet rock.	• Yellow garnet ore o Ore with visible yellow garnet.
• Other ore o Ore not possible to assign	• Hematite ore (Hm_Malm) o Ore with granular to

to any other ore type.	sugary grained hematite. Magnetite porphyroblasts present only in limited amounts.
• Mixed ore o Ore termed "mixed ore". Not described any further in the log.	• Magnetite ore (Mt_Malm) o Ore, mainly magnetite.
• Epidote ore o Ore containing fine-grained epidote rock.	• Magnetite-hematite ore (Mt_Hm_Malm) o Granular to bladed hematite ore with magnetite porphyroblasts.
• Garnet ore (GrFels_Malm) o Ore containing fine-grained garnet.	• Impregnation, i.e low grade "ore" (Impregnasjon) o Mica schist with iron impregnation.

Table 9 Rock- and ore types defined based on the log. Abbreviations used in Section 5.5 in brackets.

3.4. Modelling of a geometric mineralised envelope

All models are wrong. Some models are useful.

George Box 1979

Hard- and soft boundaries are two important terms and concepts within spatial ore deposit characterisation (Sinclair 1998).

A hard boundary is clearly defined by for example a given lithology, whereas a soft boundary is based on estimation and given by a defined cut-off. In the Kvannevann Iron Ore the boundary between the ore and the mica schist is a hard boundary. See geology map Figure 11 and Table 9.

A geometric mineralised envelope is a constructed volume that, in this case, contains rock types with an assumed certain amount of iron. It is called a mineralised envelope instead of ore model, because it is mainly based on lithologies. If "Impregnation" is used in the log, the assays have been taken into account. The geometric mineralised envelope can be considered as a hard boundary.

The reasons for using a geometric mineralised envelope based hard boundaries are at least two-fold:

- Assays that belong to one geological domain can be excluded from the estimation of the average grade (for example) in other geological domains.
- Zones outside the hard boundary will not be included in the resource estimate.

Based on the borehole data presented in Section 3.3, a geometric mineralised envelope has been constructed by using FeMagn- and FeTot assays and lithology observations in the borehole log. The mineralised envelope is given in Figure 49.

The ore / waste rock boundaries on the digitised geology map presented in Chapter 2 has been used to assist in the construction of the envelope.

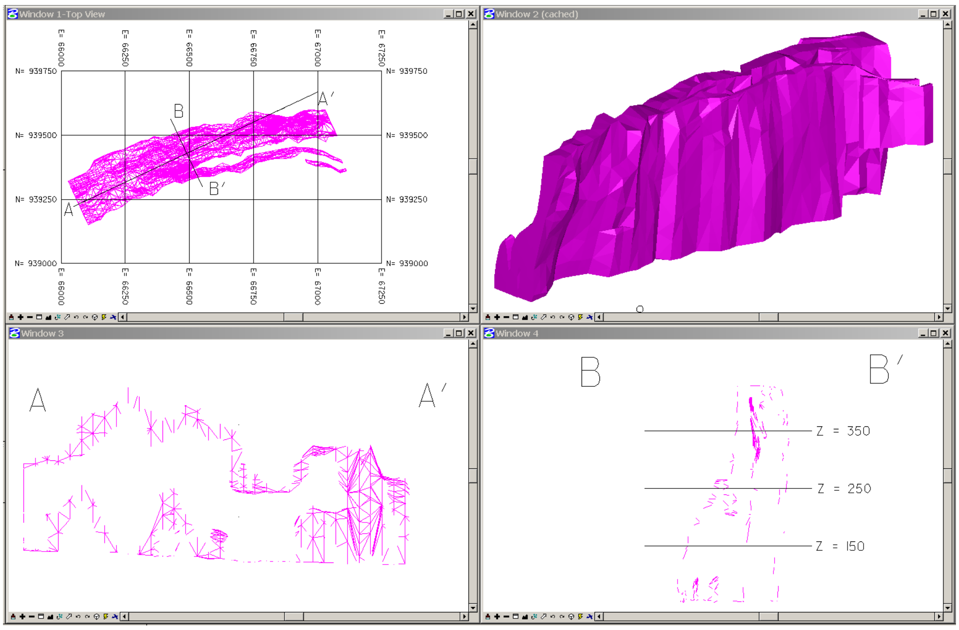

Figure 49 Mineralised envelope of the Kvannevann Iron Ore between profile 1100 and 2200. Upper left: top view. Upper right: isometric view. Lower left: profile A-A'. Lower right: profile B-B'.

3.5. 3D modelling of open pit blasts

To exploit assay results from drill cuttings collected during the open pit operation on the Kvannevann Iron Ore, the open pit blasts were digitised. Each blast outline in Figure 50 represents one blast.

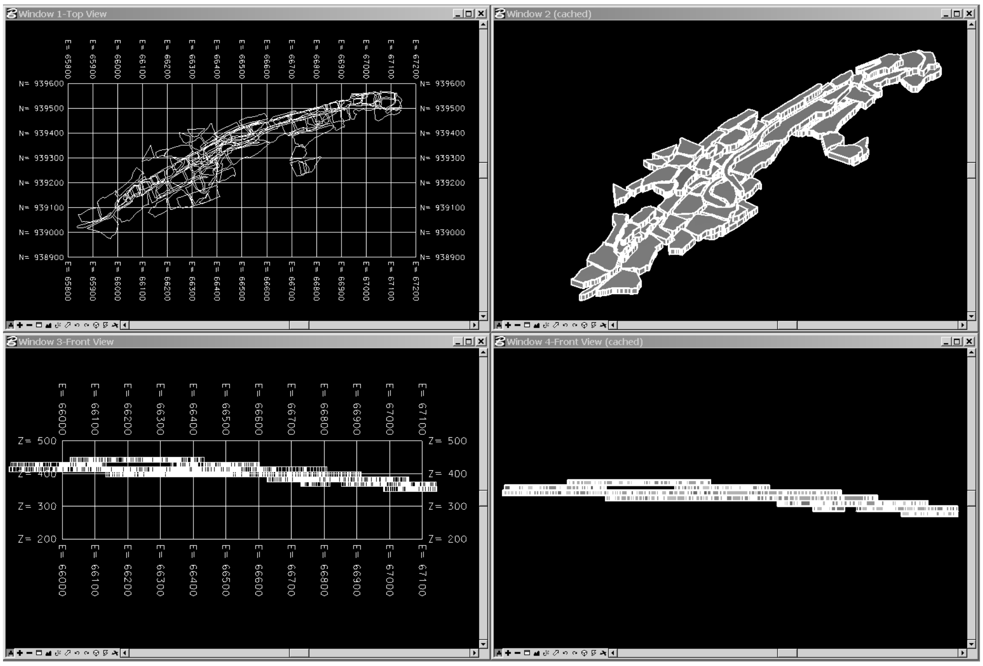

Figure 50 Blast contours in the Kvannevann open pit. Upper left: top view. Upper right: isometric view. Lower views: front views, i.e. from south, with and without grid.

Drill cutting assays were collected from the Rana Gruber AS archives and matched with the different blasts. Due to defective archives it was not possible to retrieve all the necessary drill cutting assays. Of the 101 blasts presented in Figure 50, only three were possible to match with assays. The volumes and approximate mass data of these blasts are given in Figure 51.

The arithmetic mean grades for blast 11, 12 and 13 were calculated using 9, 20 and 21 drill cutting samples respectively. In Chapter 5, these mean values will be compared to the estimated values based on borehole assays.

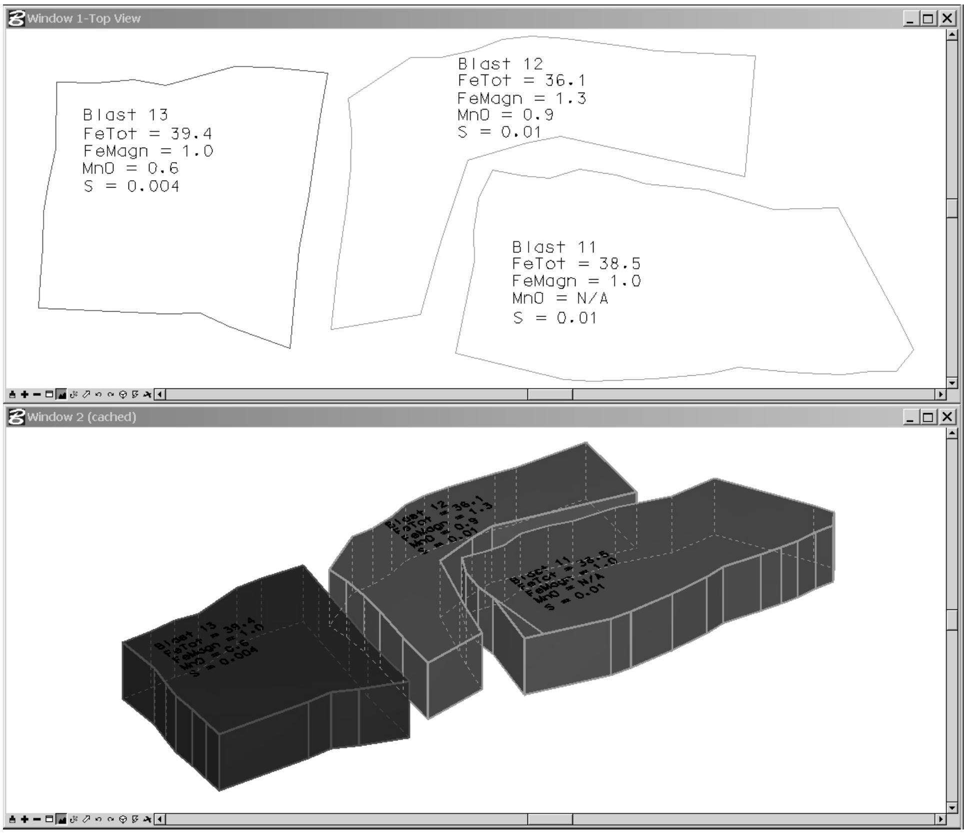

	Centre of gravity of blast				
Blast number	Centre X	Centre Y	Centre Z	Volume	Tonnage
11	67097.90	939518.00	352.50	38377.20	138158.00
12	67069.20	939544.00	352.50	29364.10	105711.00
13	67008.40	939534.00	352.50	32296.80	116268.00

Figure 51 Only 3 of the 101 digitised blasts could be assigned to assay results.

3.6. Jointing and zones of weakness

3.6.1. Joint density along borehole

Introduction

A joint is a planar or semi planar discontinuity in a rock formed through movements perpendicular to the fracture surface (e.g; Park 1989; Braathen and Gabrielsen 2000).

There are three joint sets in the area (Nilsen 1979). These sets have the following general characteristics:

Joint name	Strike	Dip	Joint set
Foliation joints	*N65°Ø – N85°Ø*	*60°N - 90°*	*1*
Steep traverse joints	*N150°Ø – N210°Ø*	*70°Ø - 90° / 70°V - 90°*	*2*
Flat traverse joints	*N150°Ø – N210°Ø*	*<25°Ø / <25°V*	*3*

Joint set 1 is the most pronounced and illustrated in Appendix C, "Jointing in Erik open pit" and "Lineament map, Rana". Tectonic lineaments in the Nordland County are described in Gabrielsen et al. (2002). Joint sets 2 and 3 are illustrated in Appendix D, "North wall of Kvannevann open pit".

Søvegjarto (197?), Dahlø (1994) and joint mapping, performed within the scope of the present thesis work, on the surface and in the mine confirm the general characteristics of these joint sets.

Joints represent zones of weakness in the rock mass. Thus, to assess the stability of the rock mass, the spatial joint distribution is an important input. Boreholes from the 1980-campaign were logged for joint density by counting the number of joints pr. metre, i.e. the support is equal to one metre. Rana Gruber AS personnel performed the logging. The boreholes penetrating the Kvannevann Iron Ore were drilled mainly in two directions: N150°E and N330°E, perpendicular to the ore strike. Consequently, the joint density in the boreholes is mainly influenced by joint set 1.

Joint density summary statistics

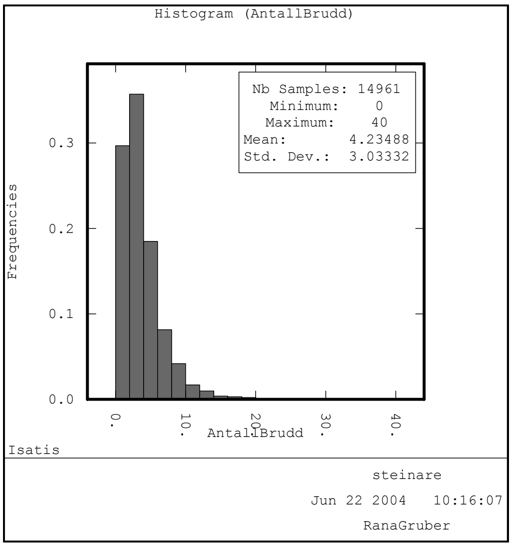

Figure 52 Joint density histogram

Summary statistics from the 14.961 joint density registrations are given in Appendix E, "Summary statistics of joint density along borehole". The frequency registrations were only available on paper and had to be digitised. Mean value, standard deviation and the minimum- and maximum values are given in the Figure 52 with the histogram. The summary statistics have been calculated on a one-metre support.

The mean joint density equals

4.2, whereas the most frequent value (35.7%) is between 2 and 4.

Characteristics of joints in joint set 1

The joints in joint set 1 are from one up to twenty metres (Nilsen 1979). The joints are mostly closed, sometimes coated with chlorite. They are discontinuous. The joints surfaces show both a varying degree of large-scale waviness (slightly undulating to undulating) and a varying degree of small-scale smoothness (rough to smooth).

These characteristics are used in the calculation of the RMi-value in Section 5.7.2.

3.6.2. Major weakness zones

Surface observation

Nilsen (1979) mapped major zones of weakness in the area around the Kvannevann Iron Ore. Weakness zones will appear more distinct due to glacial striation. The direction of glacial striation is towards southwest as indicated by the arrow in Figure 53. This direction corresponds well to the average strike of the rocks. See geologic map in Chapter 2.

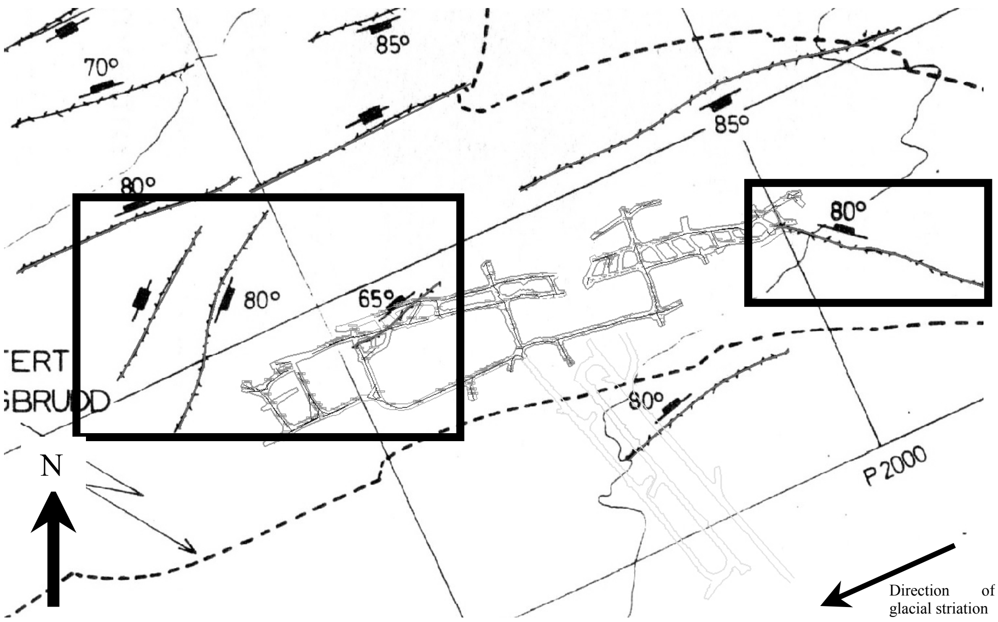

Figure 53 Major weakness zones observed on the surface above the mine. Level 255 and transportation ramp of mine map included for spatial reference. Weakness zones representing a potentially major threat located within squares. Direction of glacial striation indicated by the arrow. Figure based on Figure. 5.18 in Nilsen (1979).

Weakness zones that are at an angle to the direction of glacial striation represent, since they are indeed exposed, a potentially greater threat to the overall stability than zones parallel to the direction of glacial striation. In Figure 53, potentially dangerous zones of weakness are framed by a square. These weakness zones can then be extended into three dimensions for better correlation with the areas exposed to production underground. This has been done and in the figure in Appendix F, "Major weakness zones extended into 3D" the assumption has been made that the zones follow a constant dip. Their spatial position relative to mining operations can thereby be estimated and assessed.

3.7. Ore feed analysis

The laboratory at Rana Gruber AS collects and analyses ore feed on a daily basis. Figures 54 and 55 illustrate how the ore feed characteristics have varied from 9th of August 2004 to 19th of October 2004. The ore feed analysis are included to illustrate the varying properties of the ore feed.

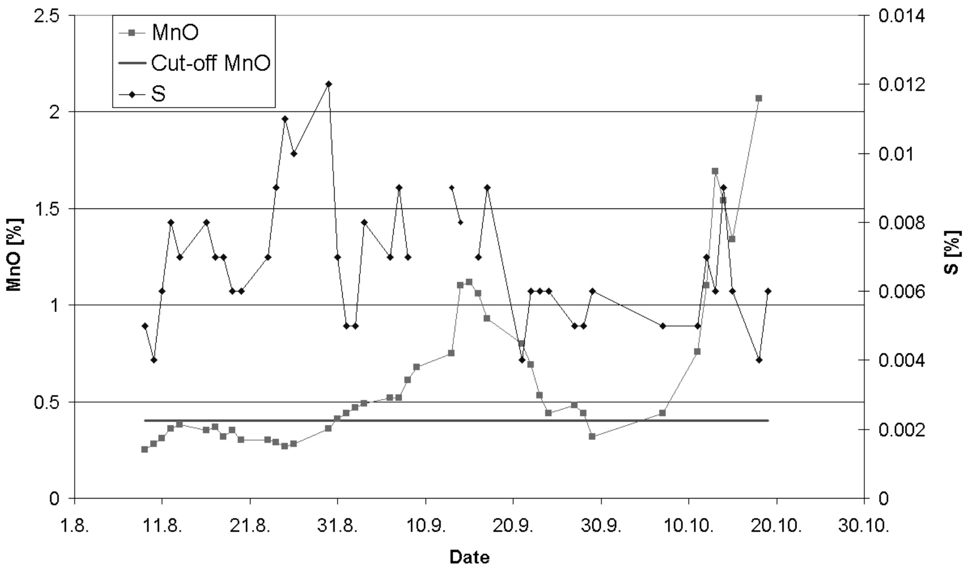

Figure 54 MnO and S vs. date. Cut-off values for MnO indicated with a red line. Notice different y-axes.

It can bee seen from Figure 54 that the MnO content of the ore feed in periods exceeds the required level.

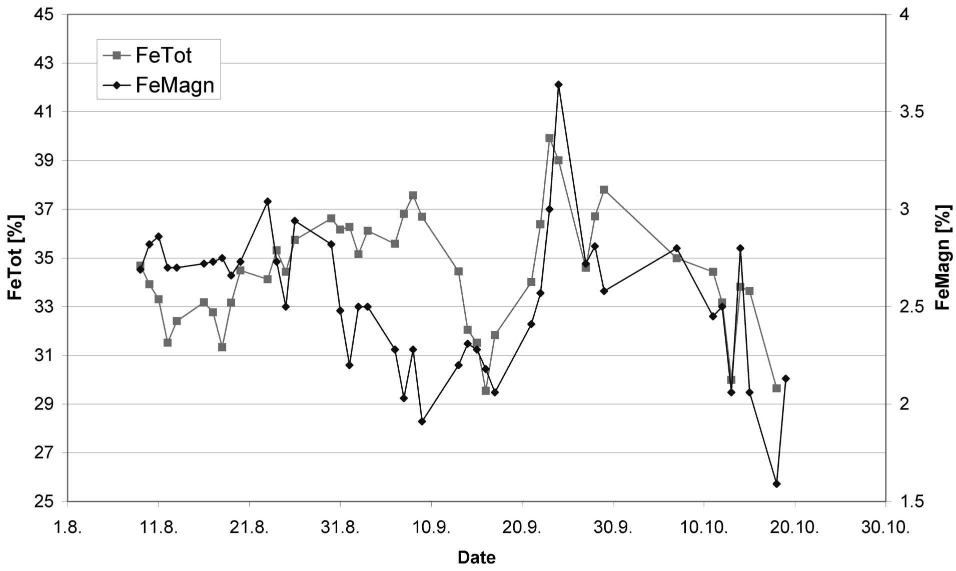

Figure 55 FeTot and FeMagn vs. date. Notice different y-axes.

Figure 55 illustrates that a relatively high content of FeTot is followed both by a relatively high (from 20th to 30th of September) and low (from 31st of August to 15th of September) content of FeMagn. This observation can be seen as a confirmation of the scatter plots in Section 3.3.2.

4. Methodology

4.1. Value chain

4.1.1. Introduction

Any mineral resource exhibits intrinsic geochemical and mineralogical variations (e.g. Watne 2001; Osland 1999). Whether these variations are utilised or not, should be a strategic decision made by the company. Utilisation of variations can follow two main approaches; 1) selective production with the aim of producing special qualities at different times and 2) selective production with the aim of delivering crushed material to the ore dressing plant with a constant, or within limits, content of specified quality parameters (equalisation). Common for both approaches is the need to know the quality variations of the deposit and to have an organisation that can utilise them (e.g. Ludvigsen 1997).

The mining value chain considered here consists of working processes executed within the company. They correspond to detail-level-two of Gether (2002). There are numerous ways to categorise such processes. The categorisations presented in the following have similarities, and they originate in Porter's (Porter 1985) definition of the value chain.

Lund et al. (2001) categorise the working processes into core processes and support processes. Core processes are defined as those in directly relationship with the customers throughout the value chain, whereas the support processes are those that support, controls, plans and adds resources to the core processes or other support processes.

Zakarian and Kusiak (2001) state that a typical process consists of three types of activities:

1. Value-adding activities defined as activities important for the customer
2. Workflow activities defined as activities which move workflow across boundaries that are primary, functional, departmental or organisational
3. Control activities defined as activities created to control value adding or workflow activities.

Further, they define strategic processes as processes essential for the company's business objectives.

Vernadat (1996) defines a business process as a partially ordered set of activities executed to achieve some desired end-result. Activity is defined as a set of elementary actions to realise some task.

Haugen (1998) categorises the working processes within a company into primary-, support- and development processes. Primary processes are the directly value adding processes for which the customer pay. The support processes are not directly value adding, but they are necessary for the execution of the primary processes. The development processes will ensure future success.

A process model will consist of working processes tied together by inputs and outputs to form the value chain. Responsibility for the value chain progress starts and ends at these output / input intersections. The blue boxes (see Figure 56) are visually used to define where the responsibility for value chain progress changes from one person or organisation to another.

Controlling and supporting elements can be considered to be outputs from supporting processes like maintenance or production planning. In the first case, the maintained drilling rig could be an output from the maintenance process and thereby a supporting element to the process "Production drilling". In the latter example the drilling plans are the output from the planning process and thereby a controlling element of the "Production drilling" process.

A value chain analysis has the following purposes:

- Set the scope of the study, i.e. emphasise and visualise the perspective and focus (see Figure 60 and Figure 83, Section 5.1.1).
- Be an aid in the assessment of competence and role requirements relevant for the business processes. A comparison of the results of these assessments with the organisation will reveal whether the organisation is capable of producing with the required level of selectivity.
- Identify primary- and secondary flows. A primary flow is the most likely or preferred progress along the value chain. The primary flow is visualised in the model by a red solid line. The secondary flow represent progress along the value chain that is unwanted or of less importance than the primary flow. The secondary flow is illustrated with a black solid line.
- Identify possible events or risk elements along the value chain.
- Identify the flow of geodata that must be taken care of by the GIS.
- Transform geodata to geoinformation by the identification of potential problems along the chain.

4.1.2. IDEF

Integrated Computer Aided Manufacturing Definition (IDEF) is a methodology initially developed by the US Air Force to describe manufacturing systems. The methodology consists of four methodologies, IDEF0, IDEF1 IDEF1x, IDEF3 for functional-, data-, dynamic analysis- and process modelling respectively (Menzel et al. 1994 in Zakarian and Kusiak 2001).

Hunt (1996 in Haugen 1999) suggests the use of the IDEF methodologies to produce and analyse working processes.

The main components in IDEF0 modelling are functions (processes, activities or transformations), inputs, outputs and controlling- and supporting (mechanisms) elements. See figure 56.

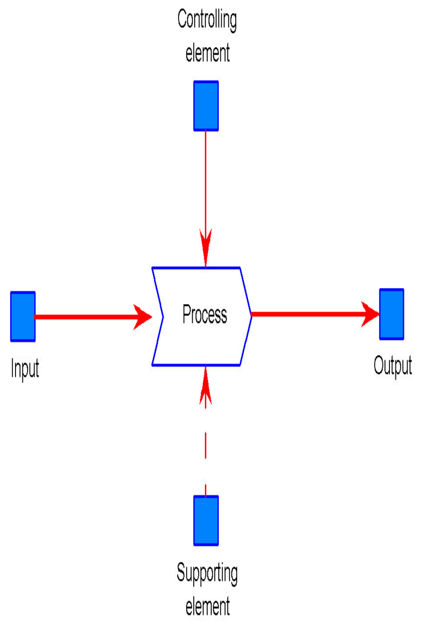

Inputs	Examples are requirements, information, problems, material or conditions. The input is used, consumed, or altered by the process.
Outputs	Examples are results, information, products or conditions. The output is created or comes out of the process.
Controlling elements	Examples are standards, regulations, legislation or plans. These elements are something that decides when and how the process might or must be executed.
Supporting elements	Examples are human resources, tools, equipment, systems or facilities. This element is used but not consumed.

Figure 56 The process model is based on working processes and their inputs, outputs and controlling- and supporting elements.

In Figure 56, the five elements are illustrated according to the IDEF0 standard (IDEF0 1994) with modifications according to Lund et al. (2001):

- The input enters the process from the left.
- The process transforms the input to an output, which exits to the right.
- The controlling elements enter the process from the top. These elements have influence on how or when the processes are performed.
- Supporting elements, or mechanisms (e.g. Gingele et al. 2002), enter the process from below. Supporting elements are tools necessary to perform the process. They are used, but not consumed.

The different elements are connected via arrows. Arrows are either horisontal or vertical. If an arrow connecting two elements is bent it must be curved only using a 90^{o} arc (see Figure 57).

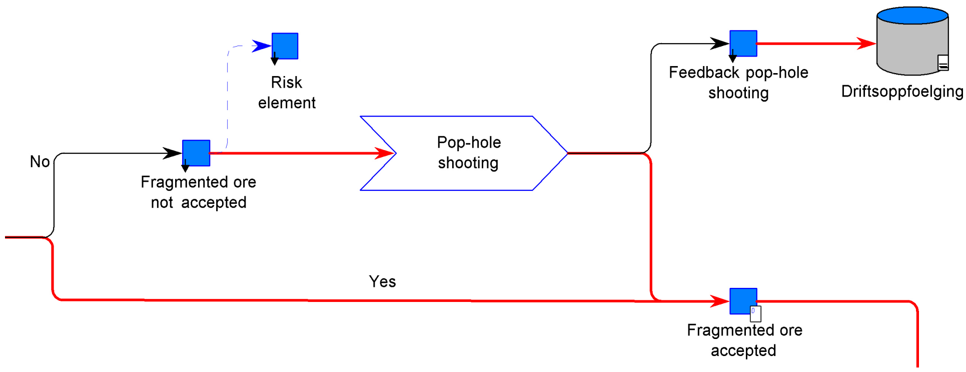

Figure 57 A segment from the "Production" process. Illustrates the arrow convention.

Processes are named using verbs or verb phrases. Inputs and outputs are labelled using nouns or noun phrases (IDEF 1994). Business objects are used in accordance with Lund et al. (2001) to better characterise the inputs and outputs. These business objects are the blue boxes in the Figure 57 and can be broken down into a more detailed description (see Figure 58).

Arrows represent relations between objects and are either solid or dashed. To enhance readability, some presentation rules should be followed when modelling the processes. These are presented in Table 10. The last column, "Relative position", indicate where the element in the "From" column is positioned compared to the element in the "To" column.

Colour	Style	Type	From	To	Relative position
Red	Solid	Flow	Input	Process	Left of
Red	Solid	Flow	Process	Output	Left of
Red	Solid	Controls	Control	Process	Above
Red	Dashed	Is used by	Mechanism	Process	Below
Black	Solid	Secondary flow	Process	Output	Left of
Black	Solid	Requirement	Requirement	Output	Above
Blue	Solid	Consist of	Output	Specifications	Left of
Blue	Dashed	Is a kind of	Output	Generalisations	Left of

Table 10 Presentation rules for relations between objects in a process model. The last column, "Relative position", indicate where the element in the "From" column is positioned compared to the element in the "To" column.

The two relations used to specify and generalise outputs are illustrated in Figure 58 and 59.

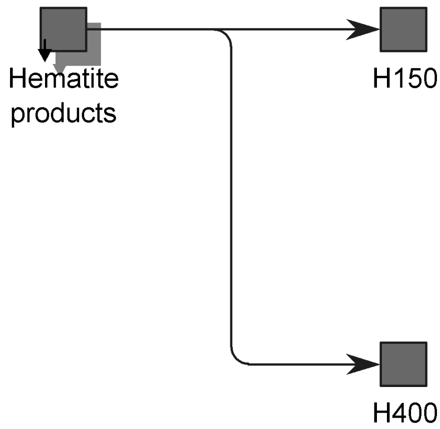

Figure 58 The object "Hematite products" consist of two products; H150 and H400. Relation type "Consist of" have been used.

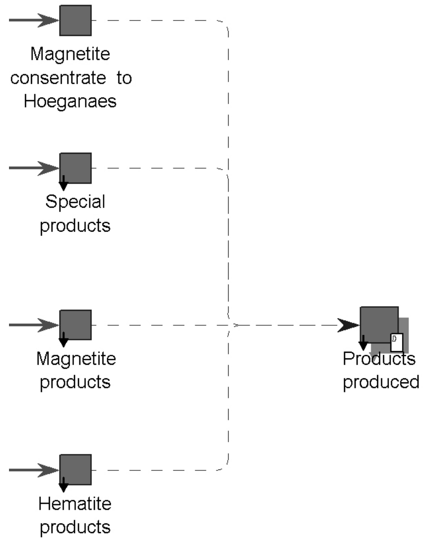

Figure 59 Products consist of four groups of products. Relation type "Is a kind of" are used.

Figure 58 should be read, "Hematite products consist of H150 and H400", whereas Figure 59 should be read "Hematite products", "Magnetite products", "Special products" and "Magnetite concentrates to Hoeganaes" are kinds of "Products produced".

A complete IDEF0 model consists of processes ordered in series. Normally a top-down approach is applied where parent processes are broken down into child-processes. The parent process is included in the top left corner of the child process. Elements originating from a higher level are shaded.

For increased readability, number of functions on one screen should be limited to between three and six.

4.1.3. Value chain definition

To define the value chain the working processes along the chain have been identified through brainstorm meetings with company representatives and through observations performed by the researcher during his stays at the mine site. Identified processes have been visualised using Business Viewer. A top-down approach has been applied. This is illustrated in Figure 60.

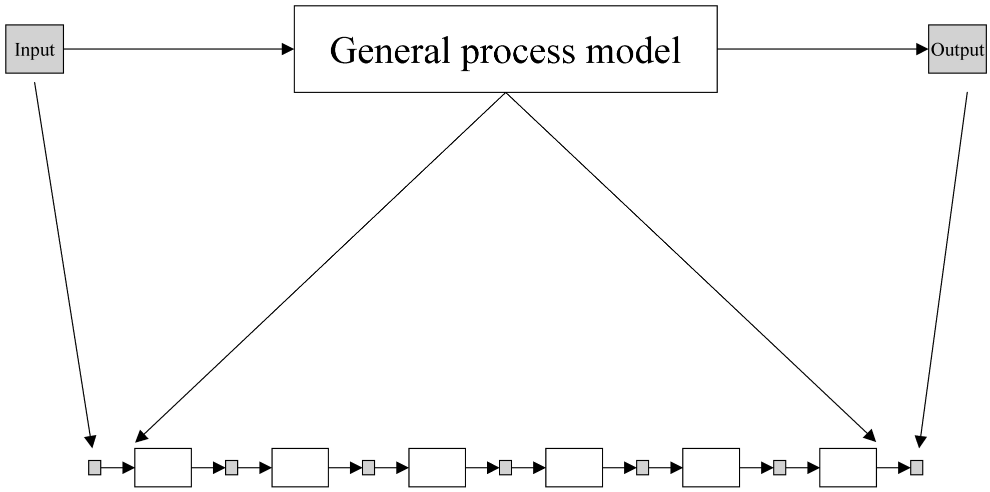

Figure 60 Top-down approach to value chain modelling starting with a general process model with general input and output and ending up with a detailed process break-down.

4.2. Cut-off

It is not the largest and the established that win, but those who adapt quickest.

Ulltveit-Moe 2004

4.2.1. Introduction

The cut-off grade is simply the grade used to distinguish ore from waste. It is the key driver of value in a mining operation (e.g. Hall 2003).

Deciding which cut-off grade to use is a fundamental issue in mining.

The following incomplete list contains elements that may influence the estimation of the cut-off.

- Costs
- Mineralogy
- Mine scheduling
- Corporate objective
- Production rates
- Comminution properties of the ore
- Limiting capacities (bottlenecks) along the value chain
- Time to depletion

Mortimer (1950 in Hall (2003)) defines the cut-off grade as

1. the average grade of rock, which provides a certain minimum profit per tonne milled and
2. the lowest grade of rock that pays for itself.

This two-fold definition is not necessarily straightforward to use. The lowest grade that pays for itself, may generate an average grade that gives a profit below the minimum profit requirement An average that produces the required profit may force the mining company to consider mineralised material with a higher grade than the lowest grade that pays for itself, as waste. Therefore the two goals in this definition could be mutually exclusive.

Lane (1988) presents a set of six equations used to estimate the cut-off used in the short term, or the cut-off policy used in the long term, that maximises the net present value (NPV) of the operation.

Other corporate goals could for example be maximum mine lifetime or maximum resource recovery. However, Lane's methodology cannot be used in these cases. Deciding which of Lane's six equations to use is dependent on the limiting capacity (bottleneck) in the mining value chain. For an underground operation, limiting capacities could be development, treating (ore excavation and ore dressing) or the market.

The use of Lane's methodology has proved to be difficult for selective stoping in large-scale underground mining (Poniewierski et al. 2003). The solution then is to calculate the value, on which the corporate goal is based (e.g. NPV or mine lifetime), for a number of different cut-offs. Each calculation requires different stoping layouts, which in turn will have a number of possible schedules. Kuchta et al. (2003) have used mixed integer programming to reduce the size of the scheduling problem at LKAB's Kiruna mine. The optimum cut-off is the one that provides the maximum value. This calculation requires a considerable amount of effort, but will increase the value of the operation significantly (Hall 2003). The effect is minor if there is a short timeframe for the mining operation.

The cost break-even cut-off is the cut-off required to generate a revenue equal to the costs. Although one is aware of the fact that this cut-off does not maximise the profit of the operation, such a calculation is used here. First, a deterministic approach is used, where all input parameters are single values. Second, a probabilistic approach is used where the input parameters are defined as distributions instead of single values. The deterministic and probabilistic approaches are presented in the following two sections.

4.2.2. Deterministic estimation of a cost break-even cut-off

For Rana Gruber AS, the two decisive ore minerals are hematite and magnetite. A tool design to support decisions related to whether different parts of the mineralised material are waste or ore must therefore be based on these two minerals. The FeMagn assay value indicates the presence of magnetite, whereas the presence of total iron is quantified by the FeTot assay value. The hematite content (FeHm) can then be derived by assuming that FeTot = FeHm + FeMagn.

The income must cover the costs to reach break-even:

$$\text{Income} - \text{Costs} = 0$$

The cut-off g that satisfies this is a function of the recovery, the product prices and the costs (Lane 1988):

$$g = \frac{h + \frac{(f + F)}{H}}{py} \qquad \textbf{Eq. 11}$$

Here, h is the variable costs, f the fixed costs, F the opportunity cost, which is introduced by Lane to maximise NPV, H is the limiting capacity, p is the product price and y the recovery. In the case of a cost break-even calculation, the opportunity cost F is set to zero.

For a two mineral case, the cost break-even cut-off calculation results in a line instead of a point, where all combinations above the line can be considered to be ore.

In the present case with magnetite and hematite as ore minerals the cut-off line can be expressed as:

$$\text{FeMagn} = a_1 * \text{FeHm} + b_1 \qquad \textbf{Eq. 12}$$

Having quantified all the variables in Equation (11) for magnetite and hematite, the required hematite iron (FeHm) and the required magnetite iron (FeMagn) can be calculated separately, assuming in turn that the grade of one of the ore minerals are equal to zero. The required grades are intersections between the linear line defined in Equation (12) and the two coordinate axes, FeMagn and FeHm. The required parameters a_1 and b_1 in Equation (12) can thereby be calculated using Equations (13) and (14).

$$a_1 = -\frac{FeMagn}{FeHm} \qquad \textbf{Eq. 13}$$

$$b_1 = FeMagn \qquad \textbf{Eq. 14}$$

FeMagn and FeHm in Equations (13) and (14) are the required grades to cover costs.

By substituting FeHm in Equation (13) with FeTot-FeMagn, the corresponding a_2 and b_2 for the case where FeMagn and FeTot are decisive ore parameters are given by:

$$a_2 = -\frac{a_1}{1+a_1} \qquad \textbf{Eq. 15}$$

$$b_2 = \frac{b_1}{1+a_1} \qquad \textbf{Eq. 16}$$

Which gives Equation (17):

$$\text{FeMagn} = a_2 * \text{FeTot} + b_2 \qquad \textbf{Eq. 17}$$

Equation (17) is illustrated in Figure 61.

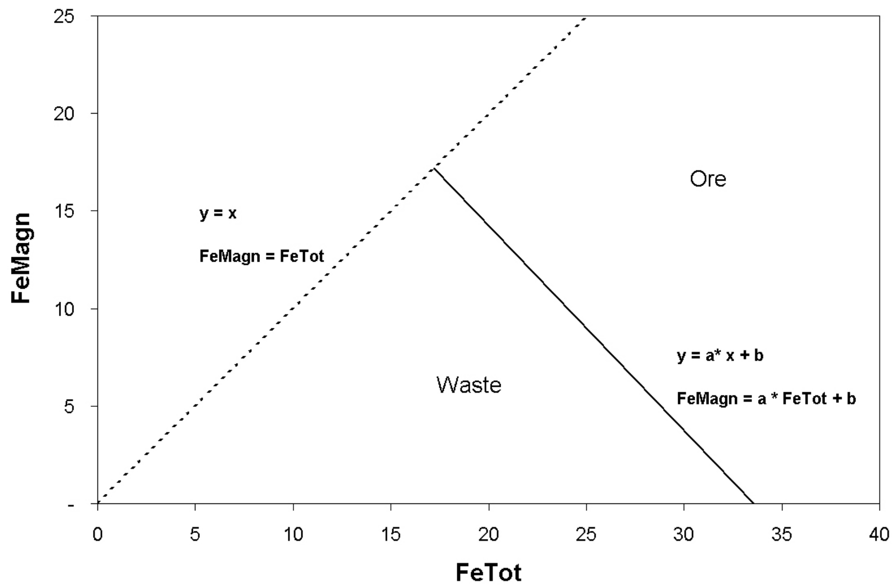

Figure 61 Linear waste-ore cut-off line for a two-mineral case with hematite and magnetite.

4.2.3. Probabilistic simulation of a cost break-even cut-off

The deterministic approach in Section 4.3.1 considers all parameters to be constant and equal to one single value. However, they are probably not. A probabilistic simulation is applied to take this verity into account. The deterministic approach also fails to consider any correlation between the input parameters.

Correlations

Recovery vs. feed FeMagn

Some magnetite will always enter the hematite product and the tailings. The FeMagn assay value of the hematite products and the tailings are normally around 0.5%, regardless of the FeMagn content of the feed. The consequence is that if the ore feed is low on FeMagn, almost 100% of the magnetite will be distributed among the hematite products and the tailings. The recovery in such a case is close to 0%. If the ore feed is high in FeMagn a low percentage of the feed magnetite will enter the hematite products and the tailing. Consequently, the recovery is high. If y is the maximum recovery (100%), G is the feed FeMagn grade and γ is the FeMagn grade of the tailing and the hematite products, the FeMagn recovery, y_{FeMagn} may be defined as (Lane 1988):

$$y_{FeMagn} = R * \frac{(G - \gamma)}{G} \qquad \textbf{Eq. 18}$$

Figure 62 illustrates this correlation for increasing FeMagn grades and a γ-value equal to 0.5%.

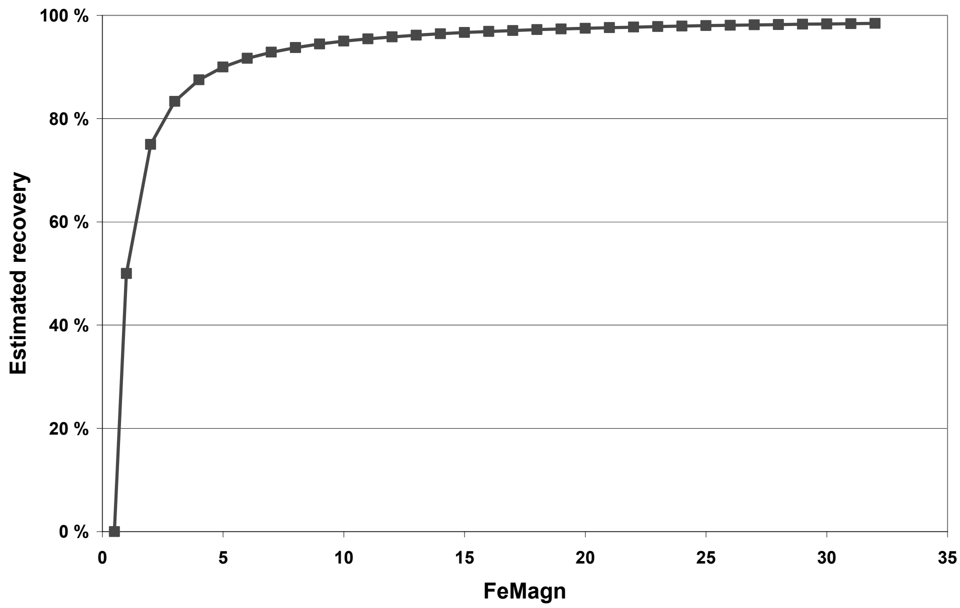

Figure 62 Correlation between FeMagn and FeMagn recovery.

Product price vs. iron content in product

The price of the hematite product is directly dependent on the percentage of iron in the product. This can be incorporated in the probabilistic model.

Feed FeMagn vs. ore dressing tonnage cost

It is more expensive to produce one tonne of magnetite product than one tonne of hematite product. Consequently, if the FeMagn is high, the total ore dressing costs will increase. This is taken into account in the model used in the probabilistic approach.

Verity

Variability and uncertainty are two important concepts in probabilistic modelling. Together they describe the total uncertainty in the system and are responsible for our insufficient ability to describe a deposit correctly and thereby predict the future. Vose (2000) amalgamate the two concepts to "verity". Verity is a synonym for truth, and the verity can conceptually be considered to be a distance measurement, which quantifies how far we are from the truth.

Variability

The variability is an intrinsic property of the system under study. The variability cannot be reduced. However, by changing the system, the contribution to the verity from the variability might be changed.

There are two types of variability:

- System dependent variability
- Ore dependent variability

System dependent variability is related to the mining operation itself, whereas the ore dependent variability is related to the intrinsic variations in the ore body. The ore dependent variability is quantified by the variogram.

This kind of variability has been termed aleatory uncertainty (Hacking (1975 in Baecher and Christian (2003)) and natural variability (Baecher and Christian 2003).

Uncertainty

The uncertainty in a system is the lack of, or deficiencies of the information made available or perceived by the assessor. The uncertainty can be changed by additional data collection or by consulting more experts. These actions might, but will not ensure a reduction of the uncertainty. The reason for this is that the new data might not be in correspondence with the existing data and thereby only increase the uncertainty.

Uncertainty as it is defined here has been termed epistemic uncertainty by others (Hacking (1975 in Baecher and Christian (2003)).

Uncertainty in inputs

The uncertainty in the parameter inputs can be quantified by two different approaches (e.g. Baecher and Christian 2003):

1. Frequentist approach
2. Degree-of-belief approach

The frequentist approach relies on a quantification of the uncertainties based on previous events similar to the one we try to describe. The degree-of-belief approach relies on a quantification of the uncertainties based on our confidence in that we know the parameter in question.

4.3. Ore density

There is no such thing as a true value…there exists only results of a procedure.

Deming 1986

4.3.1. Introduction

Resource and reserve estimates are given in terms of grade and tonnage. Economic simulations are based on the same two parameters.

The estimation process is initiated by an evaluation of volumes. The density defines the link between volume and tonnage. Since the volumes considered are large, using the imprecise and inaccurate density will lead to imprecise and inaccurate tonnage estimates, which will influence the expected economic result.

The equipment used in the mining process like loaders and trucks has certain limits when it comes to load weight. An unexpected high density may result in the following event – consequence chain:

- Event:
    - Load heavier than recommended
        - Possible consequence:

            - More wear on loader, which may lead to more heavily maintenance and an increased probability of breakdown.

- Event:
    - The total load weight transported to silo by the trucks are above maximum load weight
        - Possible consequence
            - Gearbox breakdown in spiral, which in turn lead to a production standstill.

In the planning and estimation processes at Rana Gruber AS, a grade independent density equal to 3.7 g/cm^3 has been used.

The densities of the minerals in the ore vary from about 2.7 g/cm^3 (quartz) to about 5.2 g/cm^3 (hematite). The density / iron grade correlation could thereby constitute valuable geoinformation relative to two questions:

- Knowing the iron grade: what is the density?
- Knowing the density: what is the iron grade?

The question asked here is to what degree the density can be used as an iron grade indicator.

Dependent on the purpose of the calculations including the density, different types of densities must be used. Five types of density can be defined. Definitions are given in Table 11:

Term	Definition
Specific gravity	Relative density; density relative to the density of water at 4^{o}C.
Density	Mass per unit volume
In situ bulk density	Density of in-situ material including natural water
Dry bulk density	Density of the material without water.
Grain density	Density of the solid grains only.

Table 11 Definitions of different types of density. From Lipton (2001)

Performing in-situ reserve and resource estimations, the dry bulk density should be used. If the object is to estimate the tonnage of ore that in fact will be mined, the in-situ bulk density should be used (Lipton 2001).

Mineral densities for the minerals in the ore are given in connection to average density estimation in Appendix G.

4.3.2. Theoretical correlations between grade and density

The density of a rock consisting of an ore mineral and gangue minerals is related to the rock composition according to the following equation (e.g. Sheldon 1964):

$$\rho_r = \frac{W_r}{V_r} = \frac{W_r}{V_{mh} + V_g} = \frac{W_r}{\frac{W_{mh}}{\rho_{mh}} + \frac{W_g}{\rho_g}} \qquad \textbf{Eq. 19}$$

In Equation (19) ρ_r, ρ_{mh} and ρ_g are the density of the rock, the ore minerals magnetite and hematite and the gangue respectively. W and V are the weights and volumes of the constituents indicated by the index.

The main ore minerals in the Kvannevann Iron Ore are magnetite and hematite. Defining MtHm as the weight proportion of magnetite and hematite relative to the total rock weight W_r and G as the weight proportion of the gangue, Equation (19) can be written:

$$\frac{1}{\rho_r} = \frac{MtHm}{\rho_{mh}} + \frac{G}{\rho_g} \qquad \textbf{Eq. 20}$$

Substituting MtHm = aFeTot, where the factor a is the reciprocal proportion of iron in the iron minerals, here hematite and magnetite, and G = 1 – MtHm and rearranging, gives:

$$\frac{1}{\rho_r} = \frac{1}{\rho_g} + aFeTot\left(\frac{1}{\rho_{mh}} - \frac{1}{\rho_g}\right), \qquad \textbf{Eq. 21}$$

Assuming constant density of the iron minerals hematite and magnetite and the gangue minerals, $1/\rho_r$ is a linear function of the total iron in the ore, FeTot. If hematite Fe_2O_3 was the only iron mineral present, the factor a_{hm} would be equal to 1.429:

$$a_{hm} = \frac{3 \times 16 + 2 \times 55.85}{2 \times 55.85} = 1.429 \qquad \textbf{Eq. 22}$$

Similarly, if magnetite Fe_3O_4 was the only iron mineral present, the factor a_{mt} would be equal to 1.382.

Since both iron minerals are present, the factor a must take both minerals into account. One way to achieve this would be to weight the a factors according to mineral content in the n sample data and calculate the average:

$$\bar{a} = \frac{1}{n}\sum_{i=1}^{n}\frac{\%Fe_{hm,i} \times a_{hm} + \%Fe_{mt,i} \times a_{mt}}{\%Fe_{Tot,i}}$$ **Eq. 23**

Having established the linear relationship between the reciprocal density and the FeTot grade, and thereby found the regression coefficients, the density of the gangue and the ore minerals can be found from Equation (21).

Densities are expressed in terms of volume (g/cm^3). Thus, if the grade is given in weight % the relationship between the density and the grade is a curve rather than a straight line. The reason for this is that one tonne of ore has a much less volume than a tonne of gangue.

Assuming an ore with quartz and magnetite the non-linear relationship between density and grade and the linear relationship between the reciprocal density and grade can be computed:

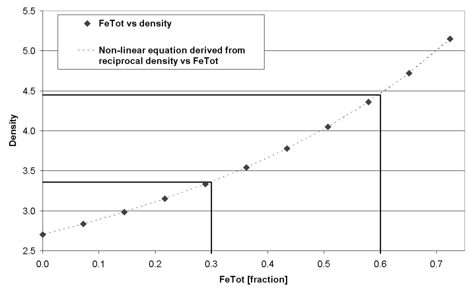

Figure 63 Non-linear relationship derived from the linear relationship in eq. 15 fit the data.

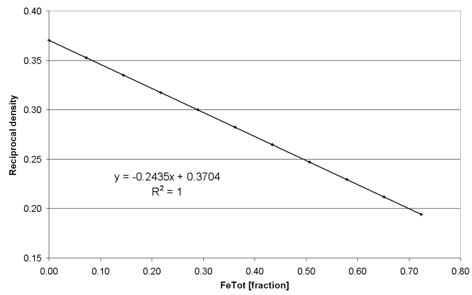

Figure 64 Linear relationship between reciprocal density and total iron.

Figure 63 and 64 have been established by calculating the total ore density of an ore containing quartz and magnetite at varying proportions. 2.7 g/cm^3 and 5.15 g/cm^3 have been used as density for quartz and magnetite respectively.

The equation describing the linear relationship between grade and reciprocal density (Equation (21)) can be rearranged to provide the equation that describes the non-linear relationship between the density and the FeTot grade. With the linear relationship given in Figure 64 the following equation is obtained:

$$\frac{1}{\rho_r} = 0.3704 - 0.2435 * Fe_{Tot} \Rightarrow$$

$$\rho_r = \frac{1}{0.3704 - 0.2435 * Fe_{Tot}}$$ **Eq. 24**

Since the relationship between density and FeTot grade is non-linear, an average density cannot be found from an average grade without knowing the grade distribution. See for example Koch and Link (1971) or summary chapter in Goovaerts (1997). An example would illustrate this.

Consider a quartz-magnetite ore with an average grade of 30-weight percent iron. According to Figure 56, this ore would have an average density of 3.37 g/cm^3 (yellow line). However if it were known that the ore consisted of 50 weight percent iron ore with 60 weight percent iron and 50-weight percent quartz the correct density would be:

$$\rho_r = \frac{4.45 + 2.70}{2} = 3.58$$ **Eq. 25**

4.3.3. Experimental tests

Water pycnometer

Tests have been made on iron ore samples to establish the correlation between density and iron grade. Samples were collected from different parts of the ore made accessible by the mining activities (see Appendix G, Section “Sample coordinates, grain density”). The ore samples were crushed, grounded and sieved into three fractions:

- -100 μm
- 100 – 300 μm
- + 300 μm

Since the density estimation is thought of as a possible iron grade indicator, the method applied to estimate the density must be possible to implement in a production situation where borehole cuttings are collected and stored for analysis. A method based on Archimedes’ Principle was used (e.g. Broch and Nilsen 2001). A jar with a surface grounded upper edge and a glass plate used as cover is weighted with and without water. The weight difference gives the volume of the jar. The jar is then weighted with grounded ore first without and then with water. The weight difference offers the volume of the grounded ore. Having the weight of the ore grains, the grain density can be obtained and correlated with the FeTot grade.

Water displacement method

The cores used in the water displacement method and the calliper method came from different parts of the ore collected especially for utilisation in this project and for stress measurements (re-use of previous collected material). Core coordinates are given in Appendix G, Section “Core sample coordinates”. The same cores have been used in the determination of the relationship between magnetic susceptibility and FeMagn (see Section 4.7).

In the water displacement method the drill cores were water-saturated and weighted in air and lowered into water. A PRECISA 3000D with a resolution of 0.1 gram (Torsvik and Olesen 1988) was used.

The dry bulk density, ρ_{db} is estimated according to the following formula where W_a and W_w are the weights of the core in air and in water respectively:

$$\rho_{db} = \frac{W_a}{W_a - W_w} \qquad \textbf{Eq. 26}$$

Calliper method

In the calliper method the drill cores are dried and weighted to obtain the weight W. The volume V of the cores are estimated using the following formula:

$$V = \pi r^2 * l \qquad \textbf{Eq. 27}$$

A calliper rule is used to make the necessary measurements of the core radius r and core length l.

The required dry bulk density ρ_{db} is obtained from the following formula:

$$\rho_{db} = \frac{W}{V} \qquad \textbf{Eq. 28}$$

Because the calliper method is based on direct measurements of radius r and length l of the core pieces, this method requires good quality drill cores.

Ore porosity

The porosity of a rock sample is defined as the proportion of void volume to total rock bulk volume.

In the calliper method the porosity is disregarded. This is not the case with the water displacement method. By using the volume found from the water displacement as the true volume of the cores the void volume can be estimated:

$$V_{void} = V_{Calliper} - V_{Water\ displacement}$$ **Eq. 29**

The porosity ϕ can thereby be estimated from:

$$\phi = \frac{V_{Void}}{V_{Calliper}}$$ **Eq. 30**

4.4. Geodata collection

4.4.1. Introduction

The mineralised envelope presented in Section 3.4 has been established based on borehole drillings. The boreholes are separated 25 to 50 metres in the horisontal plane. To supplement these geodata, a decision was made to construct a geodata collector to collect drill cuttings. It was important that the collector could be used as part of the production process without significant delay.

The mining process consist of two sub processes, which involve drilling:

1. Drift drilling
2. Production fan drilling

The production drilling involves larger and longer holes and considerable more water relative to the drift drilling. The holes in a drift blast are 4.2 metres long and have a diameter of 2 inches. The amount of water reaches about 90 litres per minute per derrick. The rig has an average penetration rate of 2.1 metres per minute. Drilling one hole takes about two minutes and produces drill slurry containing 180 litres of water and 8.5 litres of drill cuttings. This amount of drill slurry must be split into manageable volumes that can be sent to the Rana Gruber AS laboratory for analysis.

4.4.2. The collector

To handle the slurry six teats were attached to a simple steel bucket (see Figure 65). A rope was attached to the bucket grip. The bucket could thereby be fastened to the drilling face end of the drill derrick.

A hose fastened to one of the teats led the slurry into containers for decantation.

With six teats only one sixth of the total amount of drill slurry was collected and processed further before shipping to the laboratory. For one hole this would theoretically amount up to about thirty litres of slurry. It was therefore decided that only half a hole should be sampled during testing.

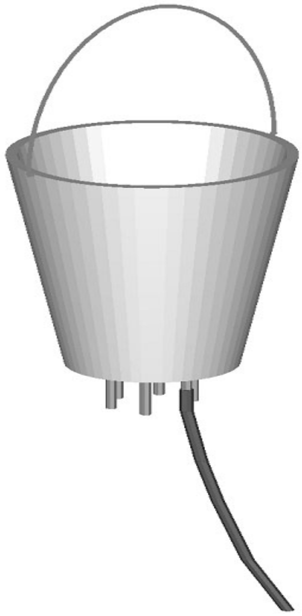

Figure 65 Drill cutting collector

4.4.3. Experimental tests

For initial tests, a hose was attached to three of the teats. This made it possible to test the quality of the splitting that takes place in the bucket. The idea and the whole prerequisite is that it does not matter, which teat is chosen, i.e. that the drill cuttings collected through one of the six teats can represent the ore in the hole and the volume around it.

To assess the repeatability the coefficient of variation (CV) can be computed from the test results. The CV is the square root of the relative variance. Where n is the number of duplicates and t_1 and t_2 is duplicate 1 and 2 respectively, the CV can be computed using Equation (31) (Dagbert et al. 2003).

$$CV = \sqrt{\frac{1}{n} \times \sum_{i=1}^{n} 2 \times \frac{(t_1 - t_2)_i^2}{(t_1 + t_2)_i^2}} \qquad \textbf{Eq. 31}$$

The sampling precision is twice the CV.

4.5. Joint density geodata

4.5.1. Introduction

As described in Chapter 3, joints per metre borehole, i.e. joint density is among the available geodata at Rana Gruber AS. Joint density data can be applied as inputs in rock mass characterisation systems.

Mainly, three classification systems are in use. These are the Q-system (Barton et al. 1974), the RMR-system (Bieniawski 1973 and 1989) and the RMi system (Palmström 1995). Nilsen et al. (2003) compare these systems for rockmass classification and support prediction. They conclude that the RMi classification system is preferred if stress induced problems are of major concern. Further it is emphasised that both RMi and RMR consider rock strength parameters and that the RMi classification do not consider groundwater conditions.

4.5.2. From joint density to RQD and RMi

The Rock Quality Designation (RQD, Deere 1966) is a parameter often used to describe the degree of jointing in a rock mass. It is defined as the length of core pieces longer than 10 cm divided by the total length of core:

$$RQD = \frac{Length\ core\ pieces > 10\ cm}{Total\ core\ length} \times 100 \qquad \textbf{Eq. 32}$$

A rock mass can be classified according to the RQD – value (Deere 1966, in Nilsen and Palmström 2000). See Table 12.

Term	RQD
Very poor	< 25
Poor	25 – 50
Fair	50 – 75
Good	75 – 90
Excellent	90 – 100

Table 12 Rock mass classification based on RQD.

Rock Mass index (RMi, Palmström 1995) is a rock mass parameter used in estimates of required support, for characterisation of rock mass strength and rock mass deformation, calculation of the constant in the Hoek Brown failure criterion for rock masses, and assessment of TBM penetration rate (Palmström 2000a). Inputs in a calculation of the RMi are:

- Jointing parameters, given by:
  - Joint condition factor, which is a function of
    - Joint roughness factor, jR
    - Joint alternation factor, jA
    - Joint size factor, jL

- Block volume (Vb), which can be estimated from
    - Joint spacing (S) or joint density
- Uniaxial compressive strength of the rock (sigma c, σ_c)

The volumetric joint count, Jv, can be estimated from the joint spacing, S_i where S_i is the spacing between joints in joint set *i* (Palmstrøm 2000a):

$$Jv = \frac{1}{S_1} + \frac{1}{S_2} + \frac{1}{S_3} + ... \qquad \textbf{Eq. 33}$$

The joint spacing can be estimated from the joint density, ρ_i:

$$S_i = \frac{1}{\rho_i} \qquad \textbf{Eq. 34}$$

The block volume, Vb used in the RMi calculation can be found from the following expression (Palmström 2000b):

$$Vb = \frac{\beta}{Jv^3} \qquad \textbf{Eq. 35}$$

The parameter β is the block factor describing the shape of the block. Where a3 and a1 is the longest and shortest dimensions of the block respectively, β is given by (Palmström 1995 in Palmström 2000b):

$$\beta = 20 + 7\frac{a3}{a1} \qquad \textbf{Eq. 36}$$

The foliation joints mainly influence the joint density registrations as presented in Chapter 3. The boreholes will not to any great extent intersect the traverse joints, since the boreholes are running parallel to these joints. To take these traverse joints into account, the joint distance can be simulated based on field data. Field mapping presented in Nilsen (1979) yields:

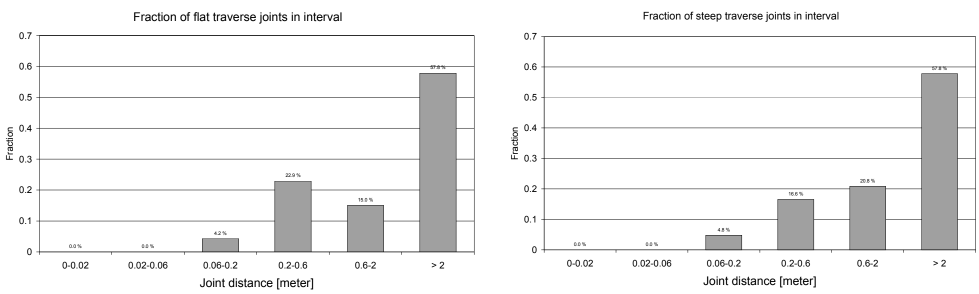

Figure 66 Field mapping results from Nilsen (1979), which assist in defining the range of possible joint distances for the traverse joints.

Given the estimated joint density from the borehole registrations and simulated values for distances between the traverse joints (data given in Figure 66), the volumetric joint count and thereby the block volume can be estimated using Equation (33).

Having the volumetric joint count from Equation (33) the RQD can be estimated (Palmström 1982 in Palmström 2000b):

$$RQD = 115 - 3.3 * Jv \qquad \textbf{Eq. 37}$$

Having only information about joint density along a scanline or borehole, the RQD can be approximated by (Priest and Hudson 1981):

$$RQD = 100e^{-0.1\lambda}(0.1\lambda + 1) \qquad \textbf{Eq. 38}$$

With the block volume, the RMi parameter can be estimated using the uniaxial compressive strength σ_c of the rock and the joint condition factors (Palmström 2000a):

$$RMi = \sigma_c * 0.2\sqrt{jL * \frac{jR}{jA}} * Vb^{0.37*\left(jL*\frac{jR}{jA}\right)^{-0.2}} \qquad \textbf{Eq. 39}$$

The rock mass can then be characterised based on the estimated RMi value (Palmström 1995 in Palmström 1996). See Table 13.

RMi-interval	**Classification class**	**Rock mass characterisation**
<0.001	Extremely low	Extremely weak
0.001 – 0.01	Very low	Very weak
0.01 – 0.1	Low	Weak
0.1 – 1	Medium	Medium
1 – 10	High	Strong
10 – 100	Very high	Very strong
> 100	Extremely high	Extremely strong

Table 13 Classification classes and rock mass characterisation based on estimated RMi-value.

4.5.3. Estimation of joint density using kriging

Mito et al. (2003) have used geostatistics simulation to predict geological conditions based on the drill energy coefficient that represents the amount of energy required for drilling a unit volume of rock. Syrjänen and Lovén (2003) have used geostatistics on estimated Geological Strength Index, GSI (Hoek et al. 1995). They conclude that rock mechanical quality parameters from drill cores can be estimated using geostatistical interpolation methods. Yu and Mostyn (1993) review concepts and models used to model the spatial correlation of joint geometric parameters. La Pointe (1980) uses geostatistics to indicate the degree of inhomogeneity in the frequencies and orientation of two distinct joint sets. Einstein (2003) reports the use of geostatistics on RQD values. Chilès (1988) and Chilès and Marsily (1993) uses geostatistical and fractal methods to model fracture systems.

Having joint density data from the boreholes, the expected joint density has been estimated using kriging. Kriging is an estimation technique, which takes the spatial correlation of the variable into account. Kriging is described in Section 4.8. From the estimated joint density, the RMi value can be estimated to classify the rockmass as described in Section 4.5.1. Once the classification has been made, a comparison between the rock masses and actual events related to instability has been performed.

4.6. Geochemical characterisation of the ore types

4.6.1. Introduction

Low content of MnO in the ore is important for the product quality. As shown in the summary statistics, only 257 out of a total of 1070 composites have been analysed for MnO. Based on these 257 analyses, an attempt has therefore been made to find a MnO geochemical signature of each ore- and rock type defined in Section 3.3.3.

4.6.2. Isatis

The grouping of assays into lithologies / ore types have been performed on the composites using Isatis. Isatis is a commercial software package offering tools for geostatistical analysis including estimation with kriging and simulation. Composites with a centre of gravity close to the centre of gravity of a lithology / ore type observation have been selected, and geochemical characteristics have been estimated on these selections.

4.6.3. MS Access

Another approach takes the advantage of queries in MS Access. Assays have been assigned to different ore- or rock units if their start and end coordinates are within a section of one lithology or ore type defined in the log. Weighted summary statistics have been calculated from the assigned assays.

The weighted average $\bar{x}$ has been calculated by weighing the different assays according to their assay lengths using Equation (40).

$$\bar{x}_w = \frac{\sum_{i=1}^{n} w_i x_i}{\sum_{i=1}^{n} w_i} \qquad \textbf{Eq. 40}$$

The weighted standard deviation, σ_w can be estimated using Equation (41) (NIST 2004):

$$\sigma_w = \sqrt{\frac{\sum_{i=1}^{n} w_i \left(x_i - \bar{x}_w\right)^2}{\frac{(n-1)}{n}\sum_{i=1}^{n} w_i}} \qquad \textbf{Eq. 41}$$

4.6.4. Cluster analysis

Cluster analysis is a multivariate statistical technique used to group objects based on some characteristics they possess. A cluster analysis consist of mainly six steps (e.g. Hair Jr. et al. (1995); Johnson and Wichern (1992).):

1. Objective definition and variable selection
2. Pre-analysis assessments
    - Detection of outliers
    - Standardisation of data
    - Similarity measurements
3. Discussion on assumptions made
    - Decision on sample representativity
    - Assessments of the impact from multicolinearity
4. Select and execute algorithm
    - Hierarchical or non-hierarchical algorithm
    - Decision on the number of clusters
5. Interpret clusters
    - Examine and name the clusters
6. Validate and profile clusters
    - Validate using different clustering algorithms
    - Profile the clusters by describing the characteristics of each cluster in detail thereby explaining how and why they differ.

Objective and variable selection

The objective of the analysis is to confirm the ore type classification given in Chapter 3. The input data used in this analysis have the following characteristics:

- Assays are organised along boreholes.
- Assays are regularised to eight-metre composites.
- All observations with %S values above 0.1 have been considered as outliers and removed.
- All assays with %S below detection limit (DL) have been replaced by DL.
- Only the observations where all variables (FeMagn, FeTot, MnO, P, S, TiO_2) are defined have been considered in the analysis.
- As described in Chapter 3, there is some degree of preferential sampling. This is taken care of in Section 3.3.2 by calculating declustered histograms. However, the dataset used in the cluster analysis from which the results are presented in Chapter 5, is not declustered.

Pre-analysis assessments

FeTot assays show values in the region above 30%, whereas S% is below 0.1% (after screening). The difference in magnitude is significant, as is the difference in variance (see Section 3.3.2). Thus standardisation is required. The assay values have been standardised by producing standard scores (subtracting the mean and dividing the difference by the standard deviation).

Basically there are three ways of measuring the similarity between objects (Hair Jr et al. 1995):

- Correlational measures
- Distance measures
- Association measures

The first one uses the correlation between objects and is applied primarily if one is interested in the patterns in the data set. Association measures are used if the object characteristics are measured on a non-metric scale. A distance measure for similarity is used in this analysis because the main interest is the magnitude of the values.

Assumptions

Sample representativeness

As in any analysis the quality of the output from a cluster analysis is mainly dependent on the quality of the input. Good quality input is a good representation of the system under study.

The system under study consists of the following:

- The iron ore, limited spatially by the mineralised envelope presented in Chapter 3 and by the surface.
- Hematite and magnetite are the two ore minerals.
- The main pollutant is manganese oxide (MnO), with phosphor, sulphur and titanium dioxide as pollutants of less importance.

Multicollinearity

Multicollinearity is to which extent a variable can be explained by other variables included in the analysis (Hair Jr et al. 1995).

There is a good negative correlation between FeTot and TiO_2. The presence of TiO_2 can therefore be estimated roughly by a low content of iron. The consequence if both FeTot and TiO_2 are included in the analysis, is that the factor explaining the presence of iron and TiO_2 is weighted more heavily than they should. Two clusters might therefore be formed, one with high iron and low TiO_2 values and one with low iron and high TiO_2 values only due to the varying total iron- and TiO_2 values.

To overcome this problem a factor analysis has been performed using a varimax rotation. Factor scores on the first factor, which explain the iron - TiO_2 variation, has replaced the FeTot and TiO_2 assays in the cluster analysis. The problem of multicollinearity is thereby eliminated.

The factor score is negatively correlated with FeTot and positively correlated with TiO_2. Consequently, a high factor score represent a low FeTot value and a high TiO_2 and vice versa.

Algorithms

There are two main groups of cluster analysis:

1. Hierarchical cluster analysis and
2. Non-hierarchical cluster analysis.

Hierarchical cluster analysis

The hierarchical clustering technique applied here performs a series of mergers. Initially, each observation is defined as a cluster. The most similar clusters are then merged to form a new cluster. At the end as the similarity between clusters decreases, the clusters are fused to form one cluster.

The similarity level is measured using a linkage method. Ward linkage method and Squared Euclidean Distance have been applied here. The objective of this linkage method is to minimise the within-cluster sum of squares.

Non-hierarchical cluster analysis

The advantage of the non-hierarchical cluster analysis is that observations already assigned to a cluster, can change cluster. Non-hierarchical cluster analysis can be used to fine-tune hierarchical cluster analysis (Hair Jr. et al. (1995)). The K-mean non-hierarchical cluster analysis has been used here. It is based on the definition of cluster seed points. These points form the initial centroids of the future clusters. Observations that are closest to the different centroids are joined with the seed points to form different clusters. New centroids are calculated every time an observation is gained or removed from a cluster. The algorithm continues until every observation is as close as possible to a cluster centroid.

4.7. Measurement of magnetic susceptibility and remanence

4.7.1. Introduction

Cores from the Kvannevann Iron Ore were collected to establish the correlation between magnetic susceptibility and the magnetite content. See Section 4.3.3 “Water displacement method” for background information on the core samples. Measurements were performed at Geological Survey of Norway (NGU). The natural remanence was also measured to further investigate the magnetic properties of the ore.

4.7.2. Magnetic susceptibility of the ore

The magnetic susceptibility was measured using a susceptibility meter consisting of a frequency oscillator, a frequency counter and pick-up coils. The sensitivity of the susceptibility meter is $1*10^{-5}$ (SI units) (Torsvik and Olesen 1988). The susceptibility is calculated by monitoring the period (reciprocal frequency) change in the pick-up coil when a sample (the core) is inserted into the coil. Pick-up coils are shown on Figure 67.

Figure 67 Pick-up coils for susceptibility measurements (to the left) in the NGU laboratory.

The apparent volume magnetic susceptibility κ_a is calculated from:

$$\kappa_a = CFAC * \left(\frac{T_1}{T_0}\right)^{\frac{1}{2}} * \left(\frac{T_1 - T_0}{Volume}\right) \qquad \textbf{Eq. 42}$$

T_1 and T_0 is the period of the empty and filled coil respectively. V is the volume of the sample and CFAC is a coil dependent constant.

As described in Section 2.6.2, demagnetisation must be accounted for if the susceptibility is above 0.1 (SI units). Due to the significant amount of magnetite in some of the cores a higher susceptibility than 0.1 must be expected. The corrected intrinsic susceptibility κ_i is obtained from Equation (43):

$$\kappa_i = \frac{\kappa_a * 4\pi}{4\pi - \frac{4\pi * \kappa_a}{3}} \qquad \textbf{Eq. 43}$$

Prior to measurements the system was tested according to instructions in Torsvik and Olesen (1988).

4.7.3. Magnetic remanence of the ore

The ore remanence was measured using a fixed Schonstedt fluxgate magnetometer positioned within a two-layered u-metal shield (see Figure 68 and 69).

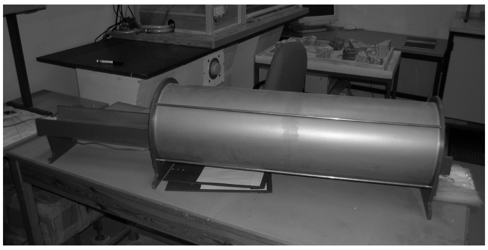

Figure 68 Fixed Schonstedt fluxgate magnetometer inside the shield in the NGU laboratory; side view.

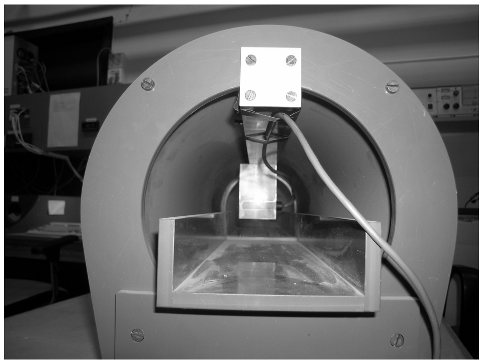

Figure 69 Fixed Schonstedt fluxgate magnetometer inside the shield in the NGU laboratory; front view.

The background magnetic field value inside the shield is first measured. Inserting the core causes a change in the magnetic field. This change is proportional to the sample remanence, SR, given in Equation (44):

$$SR = \frac{Calibration\ coefficient * Fluxgate\,output\,change}{Volume} \qquad \textbf{Eq. 44}$$

The calibration coefficient is equal to 1425 (Torsvik and Olesen 1988).

The core is measured in six directions using a cubic sample holder (see Figure 70).

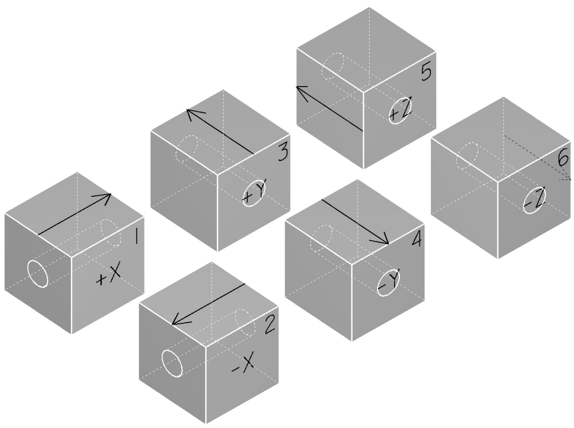

Figure 70 The cubic sample holder containing the sample (here core) is inserted into the probe in six different directions. Modified from Torsvik and Olesen (1988).

Equation (45) gives the natural remanent magnetisation or remanence, NRM:

$$NRM = \left(Xm^2 + Ym^2 + Zm^2\right)^{\frac{1}{2}} \qquad \textbf{Eq. 45}$$

Xm is calculated from X_1 and X_2, which are the remanence measurements in the two directions +X and –X in Figure 70:

$$Xm = \frac{X_1 - X_2}{2} \quad \textbf{Eq. 46}$$

Similar equations are used for Ym and Zm.

4.8. Geodata mining with linear geostatistics

Simulation strives for realism; estimations strive for accuracy.

Shibli 2004

4.8.1. Introduction

Geodata mining is a variety of data mining. Data mining involves the process of analysing a dataset to reveal its characteristics. The prefix “geo” is used to emphasise that the dataset consist of content with a geographical location, where content can be grade, density etc.

Geostatistics is a generic term for a set of estimation methods used to predict the value in unsampled points or blocks or the average of an entire deposit. It has proved to be superior to other methods, like inverse distance- and nearest point estimation, for estimating reserves in most types of mines (Armstrong 1998). Geostatistics is based on the concept of regionalised variables developed by Matheron (1963). He based his work on experimental work performed by a South-African mining engineer, Daniel Krige, who in 1951 published his M. Sc. thesis and proposed a new way of estimating the average grade of mining blocks. Geostatistics is described in many textbooks including Armstrong (1998), Journel and Huijbregts (1978), Goovaerts (1997) and Chilès and Delfiner (1999). These books have been used in the following.

A geostatistical analysis consists mainly of the following steps:

1. Structural analyses, which are used to investigate and if possible establish the spatial correlation between observations.
2. Estimation by kriging, which provides the best possible unbiased estimate by minimising the estimation variance.
3. Conditional or non-conditional simulation to investigate and quantify the true variability of the variable under study.

Prior to these steps, an initial data analysis providing the summary statistics and the modelling of a mineralised envelope should be completed.

Before the structural analysis is described any further, the concept of regionalised variables will be elaborated.

4.8.2. Regionalised variables

A grade cannot be regarded as a random variable, but a variable with a random aspect. The reason for this is that two neighbouring samples are in most cases correlated. This is the ore dependent variability in Section 4.2.3. It is intuitive to expect that two samples located in the immediate vicinity of each other collected in a high-grade zone will both show high, but not equal grades. Analogous would be expected in low-grade zones. This fact indicates that there is some spatial aspect connected to these types of data. This spatial aspect is the core of the concept of regionalised variables.

"A regionalised variable is, sensu stricto, an actual function, taking a definite value in each point of space"

(Matheron 1963)

A regionalised variable has the following characteristics (Matheron 1963):

1. The variable is localised and its variations take place in the geometric field of the regionalisation. This geometric field can be an ore or any stratigraphic unit being studied.
2. The variable is defined on a geometric support, which is defined by the geometric shape, size and orientation of the sample.
3. The variable may or may not show steady continuity in its spatial variation.
4. The variable may show anisotropies in the spatial variation. This means that there might be directions along which the variable under study varies more than along other directions, typically along directions perpendicular with each other.

These characteristics of a regionalised variable are all incorporated in geostatistics by the variogram.

4.8.3. Variogram

The variogram is the fundamental tool used in geostatistics. It is used to describe and quantify the spatial continuity in the regionalised variable. Where Z(x) is a regionalised random variable at location x and Z(x+h) is a regionalised variable at location x+h, the semi-variogram is defined as:

$$\gamma(h) = \frac{1}{2} E\left\{\left[Z(x) - Z(x+h)\right]^2\right\} \qquad \textbf{Eq. 47}$$

An estimate is almost certainly wrong. The difference between the estimate z^* and the unknown true value z is the estimation error ε:

$$\varepsilon = z - z^* \qquad \textbf{Eq. 48}$$

The estimation error can be negative or positive dependent on whether the estimator over- or underestimates the true value. In real situations neither the magnitude nor the sign of the estimation error is known. A reasonable way to estimate the magnitude of the estimation error is through the estimation variance, which is the average squared difference between the true value at a location and all possible estimates for that value. Different estimates could be obtained dependent on the number of available sample values. The estimation variance can be approximated calculating the mean squared difference between the sample values. If this mean value were large, it is intuitive to think that the difference between the estimate and the true value also is large. This is captured in the experimental calculation of the (semi-) variogram:

$$\gamma^*(h) = \frac{1}{2n}\sum_{i=1}^{n}\left[z(x) - z(x+h)\right]^2 \qquad \textbf{Eq. 49}$$

In Equation (49) n is the number of pairs involved in the calculation and z(x) is a realisation of the regionalised random variable Z(x) and z(x+h) is a realisation of the regionalised random variable Z(x+h). The scaling factor of 0.5 is used so that the variogram can be compared to the variance of all samples.

Generally the variogram value γ(h) will increase with increasing h until it reaches a certain value termed the sill c at a range a (see Figure 71).

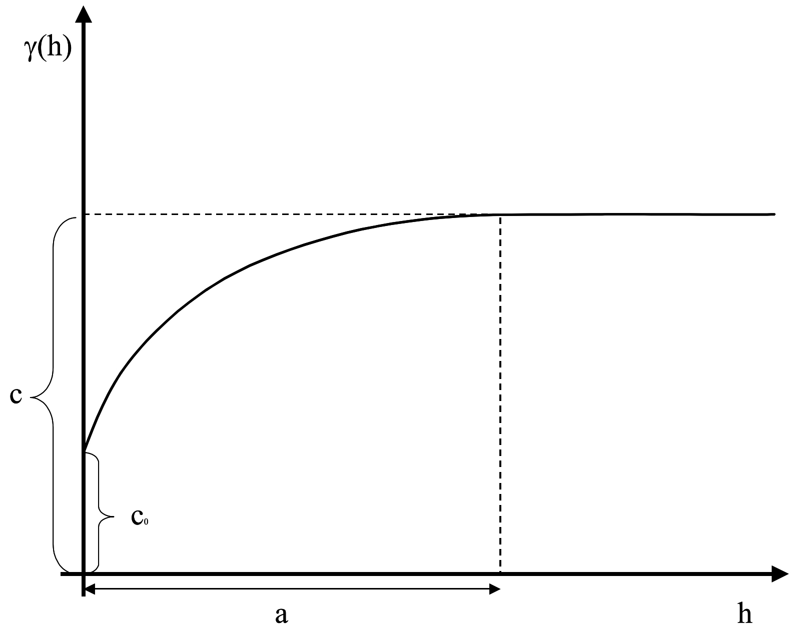

Figure 71 The general shape of a variogram.

The discontinuity c_0 at h = 0 is called the nugget effect. This effect is caused by abrupt changes in the data values at small distances. At h = 0, the variogram value $\gamma(h)$ is equal to zero by definition, but it must not necessarily be equal to zero as h approaches zero.

One of the most important aspects of the variogram function is to what rate it increases with increasing h, near h = 0. If the rate is high, the estimation variance will be high indicating that the correlation between values relatively close to one another is low.

The variogram function can in theory be calculated in all directions. If the variogram calculated in different directions show different sills and / or ranges, the variations within the geometric field are said to be anisotropic. Anisotropy is identified using a variogram map.

To use the variogram in an estimation process a variogram model must be fitted to the experimentally calculated variogram. There are a number of admissible models including the spherical-, the exponential-, the Gaussian- and the pure nugget model. For a variogram model to be admissible it must be conditionally negative definite, which means that the model ensures a positive variance.

4.8.4. Stationarity

If a variable is stationary all its moments are constant within the geometric field under study. This means that the mean, the (co-) variance and all other higher moments are constant.

With limited experimental data available, it is not possible to verify that all moments are constant. Therefore this requirement of strict stationarity is weakened by only assuming that the mean and the (co-) variance are constant. This hypothesis is called the second order- or weak stationarity.

Whenever there is a trend present, the mean is not constant, i.e. the second order stationarity hypothesis cannot be used. If the mean is constant, the (co-) variance need not necessarily be constant. Therefore Matheron (1963) developed the intrinsic hypothesis stating that the increments Z(x)-Z(x+h) are second order stationary:

$$E[Z(x)-Z(x+h)]=0 \qquad \textbf{Eq. 50}$$

$$Var[Z(x)-Z(x+h)]=2\gamma(h) \qquad \textbf{Eq. 51}$$

If the variable is stationary there is a direct relationship between the variogram and the covariance (e.g. Armstrong 1998) (see Figure 72).

$$\gamma(h)=C(0)-C(h) \qquad \textbf{Eq. 52}$$

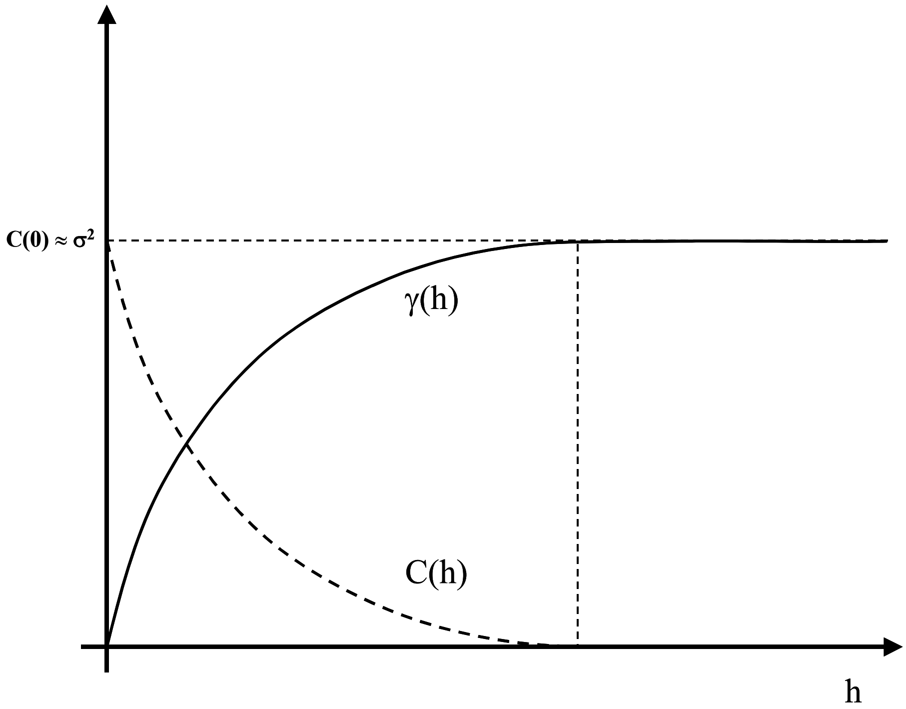

Figure 72 General relationship between covariance and variogram for stationary variables.

For stationary variables, the sill, C, is equal to the covariance at zero distance, C(0). The sill approximates the sample variance σ^2. Normally, the sample variance is smaller than the sill due to inter-correlation between samples.

To decide whether a variable is stationary or not there are three approaches commonly used. Firstly, the variable can be investigated for a trend, i.e. is the mean value constant within the geometric field. Secondly, the variogram can be calculated and if it is shown to be unbounded, i.e. it does not converge towards a sill, the variable is not stationary. Thirdly, the variance can be plotted as a function of the mean. If the variance increases with increasing mean, the variogram is said to have a proportional effect. In such a case, the variable is not stationary.

The estimation with kriging of unsampled areas, blocks or points involves the use of a search window normally smaller than the dimensions of the geometric field. If the variable is not stationary within the geometric field as a whole, the variable might be stationary within this search window. The variable is then said to be quasi-stationary.

4.8.5. Structural analysis

A fitted mathematical model of the variogram is the main output from the process of structural analysis. It involves the following three steps:

1. Validation and evaluation of input data
2. Calculation of the experimental variogram
3. Fitting of a mathematical model (theoretical variogram) to the experimental variogram. The model is fitted to the experimental variogram by testing different models and structures until a reasonable fit is obtained. How the different models perform in estimation can be tested using cross validation. Outliers are disregarded if necessary.

The mathematical model can be presented as an equation on the form:

$$\gamma(h) = Nugget + Sill \times Modeltype(Range\ dir\ 1, Range\ dir\ 2, Range\ dir\ 3) + ...$$

In the equation above, “Modeltype” could be “Sph” for a spherical model, “Gau” for a Gaussian model etc.

The spherical model is given by:

$$\gamma(h) = C * \left(\frac{3*|h|}{2*a} - \frac{|h|^3}{2*a^3} \right) \qquad \text{, for } |h| < a$$

$$\gamma(h) = C \qquad \text{, for } |h| \geq a$$

The parameters a and C are the range and the sill respectively.

If more than one basic structure is present, they are simply added to the equation after the plus sign. Dir 1, 2 and 3 are directions defined by the anisotropy.

4.8.6. Estimation by kriging

Kriging is an unbiased and exact estimation technique, which uses the variogram- or the covariance model to find the optimal weights in terms of minimum estimation variance.

Kriging is used to provide an estimate at an unsampled point or block at position x, which is as close as possible to the unknown true grade. The quality of the estimation is quantified by the estimation variance. During the kriging algorithm, the estimation variance is minimized and the corresponding weights are used in the estimation. This minimisation introduces a smoothing effect that leads to an underestimation of the true dispersion in the deposit.

The dataset consists of data values $z(x_1)$, $z(x_2)$,… $z(x_N)$ that are considered to be realisations of the regionalised variable Z(x). Where λ_i is the optimal weights, an estimate z^* of the value in an unsampled point x with support v and true value z is:

$$z_v^* = \sum_{i=1}^{n} \lambda_i z(x_i) \qquad \textbf{Eq. 53}$$

To derive the optimal weights the regionalised variable Z(x) is used:

$$Z_v^* = \sum_{i=1}^{n} \lambda_i Z(x_i) \qquad \textbf{Eq. 54}$$

This makes the estimator a moving average of available data inside a search neighbourhood centred on the point or block to be estimated. The estimator is required to be unbiased. To accomplish that the average estimation error must be equal to zero:

$$E\left[Z_v^* - Z_v\right] = 0 \qquad \textbf{Eq. 55}$$

Further the variance of the estimation error must be minimised:

$$Var\left[Z_v^* - Z_v\right] = \min \qquad \textbf{Eq. 56}$$

In case of ordinary kriging it is required that the weights sum to one and a lagrange multiplier μ is introduce to minimise the variance of the error. The kriging equations expressed in terms of the variogram becomes:

$$\sum_{j=1}^{N} \lambda_i \gamma(x_i, x_j) + \mu = \bar{\gamma}(x_i, V), \text{ where i = 1,2,…,N} \qquad \textbf{Eq. 57}$$

$$\sum_{i=1}^{N} \lambda_i = 1 \qquad \textbf{Eq. 58}$$

$\bar{\gamma}$ (x_i,V) is the average variogram value between all points within volume V and point x_i.

γ (x_i,x_j) is the variogram value between point x_i and point x_j.

The size and shape of the search neighbourhood used in the estimation is dependent on the ranges of variogram, amount of available geodata, required number of geodata in the estimation and the ratio between the nugget effect and the sill.

4.8.7. Incorporation of soft data

Soft data is data that can be used as an indicator of the content of some element or mineral (e.g. Goovaerts 1997). Hard data is a precisely analysed content.

The lithology log provides such soft data.

Soft data can be assigned to the different lithologies based on the lithology log and hard data. The cluster analysis gives valuable input to the interval quantification through the definition of a mean value and possible minimum and maximum values for the different lithologies.

Once intervals are defined they can be incorporated in the kriging process by using functionality in Isatis. The functionality is called kriging with inequalities where the soft data correspond to an inequality (Bleines et al. 2001).

The kriging with inequalities consist of five steps:

1. Normal score transformation to obtain Gaussian hard data.
2. Variography of the Gaussian data obtained in point 1.
3. Generation of realisations through simulation at soft data locations using a Gibbs sampler (see e.g. Vose 2000, Ross 2003). The generated realisations obey the structural model and the upper and lower limit of the defined intervals. Realisations are produced until the average of the realisations at each location stabilise.
4. The average is called the conditional expectation. The dispersion variance of the realisations quantifies the degree of confidence.
5. Normal kriging is then used with the conditional expectation and the dispersion variance as input (kriging with measurement error).

4.8.8. Grade tonnage curves

Grade tonnage curves are used to assess how the mean grade and tonnage are dependent on the applied cut-off. In case of underground mining where no dense sampling campaigns are executed prior to excavation and decision on whether a SMU is ore or waste, grade tonnage curves can simply be obtained by computing the average grade and tonnage of the blocks having an estimated grade above the cut-off. The estimation can in such a case be performed by linear geostatistics. If diamond borehole geodata will be supplemented with densely collected drill cutting data, then the grade tonnage curves should be obtained using non-linear geostatistics (e.g. Dagbert et al. 2003). Non-linear and linear geostatistics differ in that the weights allocated to samples in non-linear geostatistics are not only dependent on the location, but also on the sample value themselves.

4.8.9. Conditional simulation

If the objective is to study the dispersion of the true grades, conditional simulation provides a more suitable approach than estimation with kriging. The realisations of the Monte Carlo type simulation will have comparable mean and covariance/variogram and the same histogram, as the true grades. One single realisation is not the best estimate of the true grade at one certain location; estimation is not the objective of simulation. The estimation variance calculated from one single realisation is two times higher than the kriging variance (Journel and Huijbregts 1978).

The simulation is performed on a relatively small-meshed block model of the deposit. The results of simulation of the block model represent equiprobable images of the in-situ variability and are here used in subsequent analysis and assessment of the mining process. Figure 73 shows four images of one section of the deposit used to assess the ore variability in one particular mining stope:

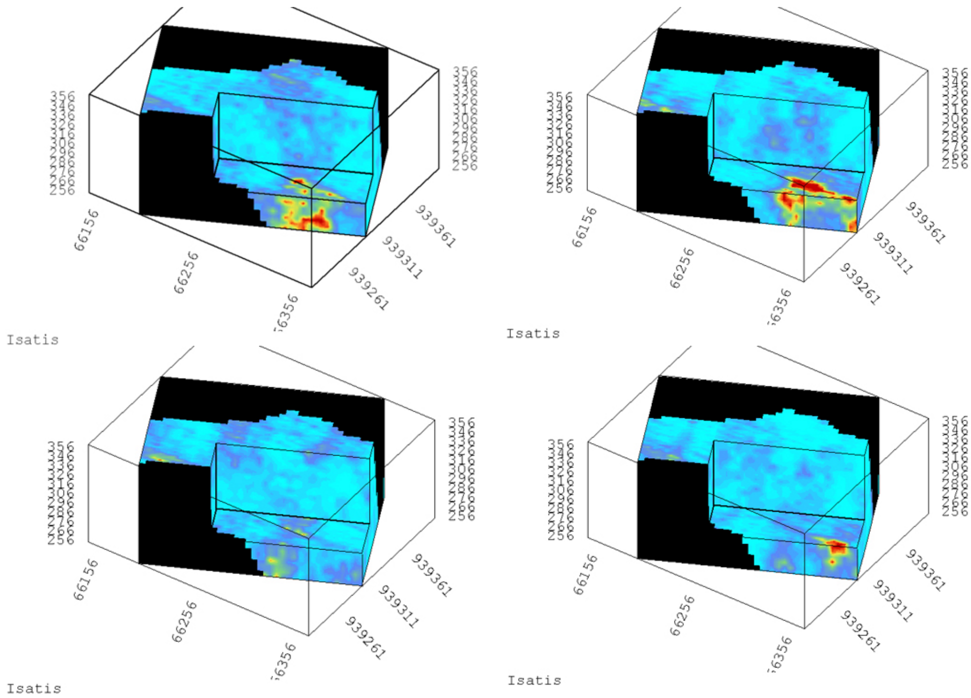

Figure 73 Four possible images of a section of the deposit. Bright blue colour indicate low grade, whereas red indicates high grade.

This class of simulation is called conditional simulation because the realisations are conditioned on the experimental data and already simulated values. A number of algorithms for conditional simulation have been proposed, including the turning band method (Journel and Huijbregts 1978), probability field simulation (Srivastava 1992 in Dimitrakopoulos 1998), simulated annealing, sequential indicator simulation and sequential Gaussian simulation (Journel 1994 and Johnson 1987 in Dimitrakopoulos 1998).

SGS

The sequential Gaussian simulation (SGS) algorithm is commonly used in the mining industry (Coombes et al. 2000). The algorithm consists of six main steps (Dimitrakopoulos 1998; Godoy et al. 2001):

1. Random selection of a grid node not yet simulated
2. Estimation of a conditional probability distribution of the grades at the grid node
3. Draw a random value from the conditional probability distribution
4. Include the simulated value from point 3 in the conditional data set
5. Repeat points 1 to 4 until all nodes have been simulated
6. Repeat points 1 to 6 until the required number of images of the deposit or the section has been generated.

In Isatis, the SGS algorithm is implemented for grid files only (see Figure 74).

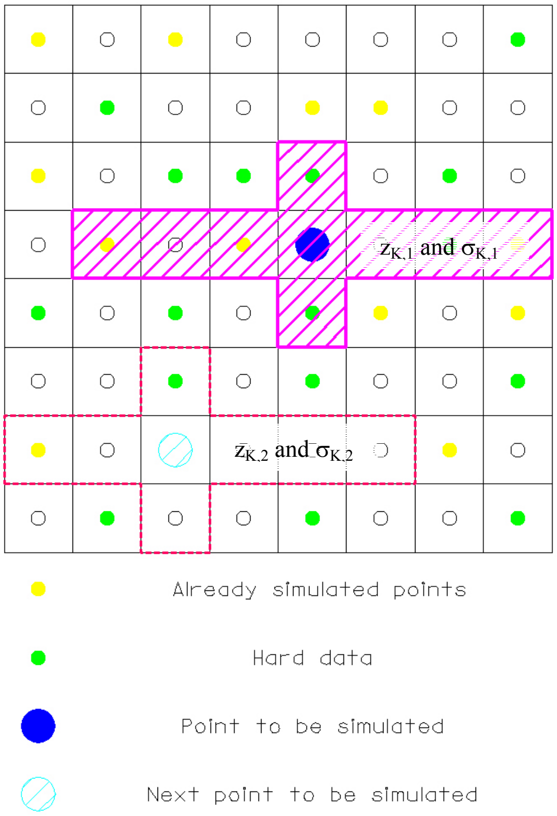

Figure 74 Principle of simulation using the SGS algorithm as implemented in Isatis. Orthogonal shape illustrates the search neighbourhood. Simulated values and hard data inside the neighbourhood are used to estimate the conditional probability distribution.

The randomisation is ensured by 1) the random selection of values from the conditional probability distribution and 2) random and for each run different paths along which the nodes are selected.

As implemented in Isatis the simulation is initiated by a migration of hard data to the nearest grid node. The hard data is indicated with a green point in Figure 74.

Using the SGS algorithm the simulated value z_{sc} is obtained by the kriged value z_K and the corresponding kriging variance σ_K:

$$z_{sc} = z_K + \sigma_K U$$

U is a random normal function with a zero mean and a standard deviation of one.

The simulation requires normally distributed data. Prior to simulation the data must therefore be transformed into normal scores.

Turning band

In the turning band method the idea is to simulate the multidimensional random field by summing contributions from a one-dimensional simulation process. Matheron (1973) developed the method. The method produces realisations z_i on N lines distributed in 3D. Each realisation is projected onto the points to be simulated and averaged to produce a realisation z_s in three dimensions (Journel and Huijbregts 1978):

$$z_s = \frac{1}{\sqrt{N}} \sum_{i=1}^{N} z_i(x) \qquad \textbf{Eq. 59}$$

The conditioning is performed through a separate kriging step (Chilès and Definer 1999).

The lines are distributed regularly (Lantuéjoul 2002), independently and uniformly (Journel 1973) or according to sequences with weak discrepancy (Bouleau (1986) in Lantuéjoul 2002) on the unit sphere.

The method replicates the variogram especially good and it produces non-conditional simulations very efficient (Vann et al. 2002).

The turning band method has been used in the simulation in Section 5.7.3.

4.9. Risk

4.9.1. Definition of risk

Generally, risk is perceived as something negative. Hansson (1999), points out that risk has its scientific meaning and its non-technical meaning. The scientific meaning of the term is that it is something quantifiable:

$$Risk_1 = Consequence \times Probability \qquad \textbf{Eq. 60}$$

Risk must be seen in relationship with an event. The “Consequence” is what happens if the event takes place whereas the “Probability” is the probability that the event actually will take place. Standards Australia (1999) states this relationship when they define risk, as *”the chance of something happening that will have an impact upon objectives. It is measured in terms of consequence and likelihood.”*

The probability is sometimes replaced by frequency, i.e. the number of times the event will occur during one unit of time. One unit of time could be for example minutes, months or years.

Burnup (2003) emphasises the division of risk into a scientific and non-technical, or public, meaning of the term in her discussion on why it is often difficult to discuss risk with communities. Burnup (2003) makes reference to Sandman (1993) and defines risk as

$$Risk_2 = Hazard + Outrage = Risk_1 + Outrage \qquad \textbf{Eq. 61}$$

In Equation (61) the term “Hazard” is equal to consequence multiplied with the probability, i.e. the scientific definition of risk. By including “Outrage”, the communities “feelings” about the issue in question is included into the equation.

Norwegian Standard 5814 (1991) defines risk as *“the danger that undesired events represent for humans, the environment or material values.”* They use the scientific definition given in Equation (60).

4.9.2. Risk management process

Standards Australia (1999) defines risk management as *"the culture, processes and structures that are directed towards the effective management of potential opportunities and adverse effects."*

Risk management is an iterative process and consists of a number of steps including the establishment of risk context, identification, analysis and evaluation of risk, risk treatment, risk monitoring and reviewing and lastly communication of the risk elements (Standards Australia 1999). The process is illustrated in Figure 75.

Risk analysis is defined as *"a systematic use of available information to determine how often specified events may occur and the magnitude of their consequences."*

Risk evaluation is defined as *"the process used to determine risk management priorities by comparing the level of risk against predetermined standards, target risk levels or other criteria."*

Risk assessment embrace risk analysis and risk evaluation.

Vose (2000) uses risk analysis as the *"quantification, either qualitatively or quantitatively, of the probability and the potentially impact of some risk."* In his introduction he states that this definition is sometimes used for "risk assessment" and that "risk analysis" consider the whole process from identification via assessment to communication of risks. This would be what Standards Australia call "risk management".

The complete risk assessment process consist of the following steps (Vose 2000):

1. Identification
2. Qualitative description of the risks, including why it may happen and what can be done to increase or reduce the probability or impact
3. Quantitative or semi-quantitative analysis and associated management options available to control the risks
4. Implementing the risk management strategy
5. Communicate the decisions to interested parties (stakeholders, employees etc.)

The same process can be used on opportunities (Vose 2000).

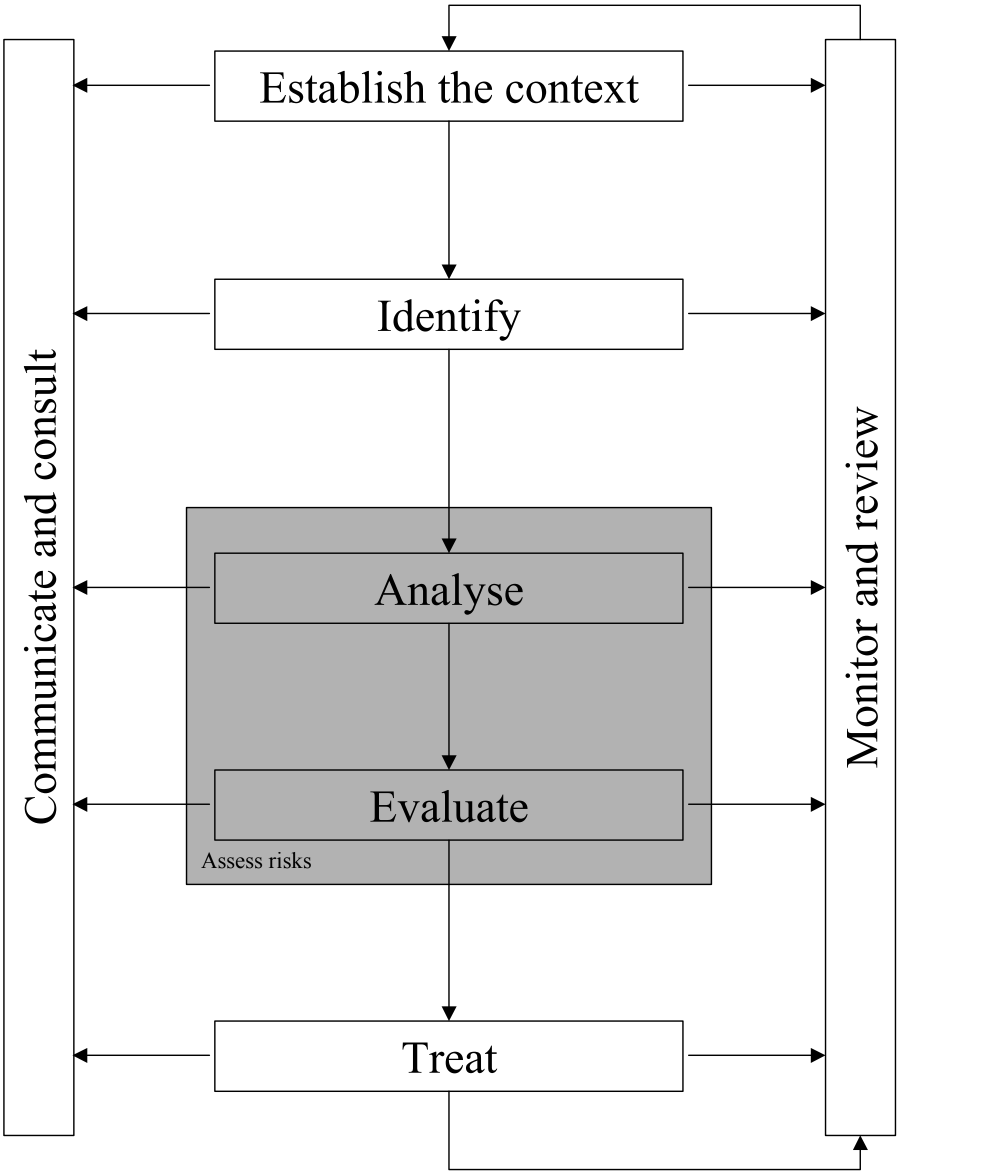

Figure 75 Risk management process. From Standards Australia (1999).

Norwegian Standard 5814 (1991) defines risk analysis as *"systematic approach for describing and / or calculating risk."* It is emphasised that "*Risk analysis involves the identification of undesired events, and the causes and consequences of these events."* Risk evaluation is defined as the comparison between results from the risk analysis with acceptance criteria for risk and other decision criteria.

Risk can be categorised according to what part of an operation they concern. Given a mining operation, or in relation to Figure 75 a mining context, the following risk types may be defined:

- Technical risk
  - Geological, resources and reserve risks
  - Geotechnical risks
- Economic risks
  - Prices
  - Inflation
  - Costs
  - Taxation
- Investment risks
- Market risks
- Political risks
- Closure risks
- Environmental risks
- Reputation risks
- Social risks

4.9.3. Mining risk profile

The risk management process must take all the risks listed in Section 4.9.2 into consideration. Combined they form the risk profile of the mining operation. Considering technical-, investment- and economic risks a simplified risk profile can be constructed (see Figure 76).

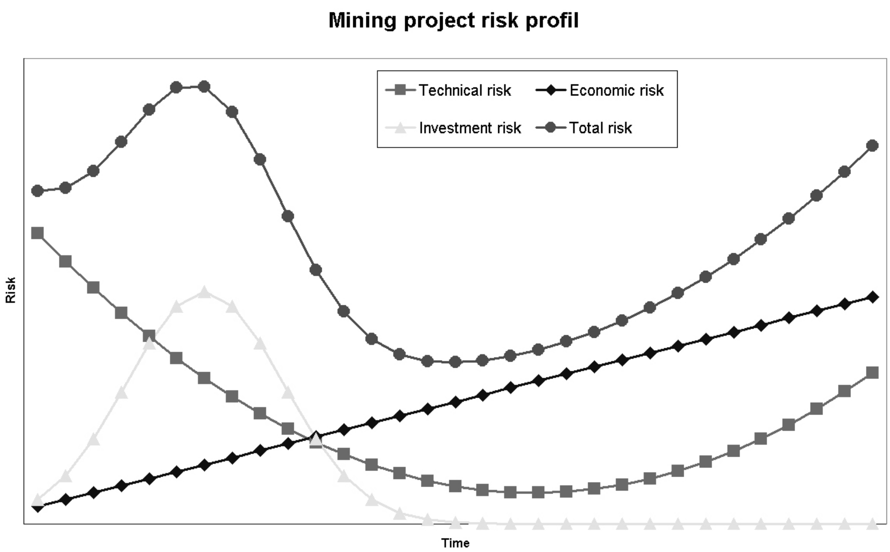

Figure 76 A simplified risk profile for a mining operation.

At the beginning of the project the technical risk is high because the ore variations, the implementation of the mining method and the ore dressing technology is uncertain. The economic risk is relatively low because the taxation regime, the prices etc. can be estimated with a high degree of certainty. The investment risk is low until the initial investments have been done. Then as the complete investments have been done and before the operation starts to generate revenue, the investment risk is at its peak. With time revenue is generated and the investment risk returns to zero because the pay back time has been reached. With time information about the quality variations in the ore, the mining method and the performance of the ore dressing plant have been collected and assessed. The technical risks are thereby reduced. Towards the end of the mine lifetime the technical risks would increase in case of for example pillar mining. That is also the case with the economic risks since it becomes more and more difficult to predict the prices and cost fluctuations as the time frame is increased.

By focusing on the technical risk it is possible to reduce the total risk profile of the operation. Reduced technical risk would have positive side effects on for example the economic risk due to more reliable cost and price estimates and on the investment risks due to more reliable reserve estimations.

4.9.4. Identification of events and their possible consequences

The process map includes processes and the blue boxes, the inputs and outputs. The blue boxes might be information, material or events (see Figure 77).

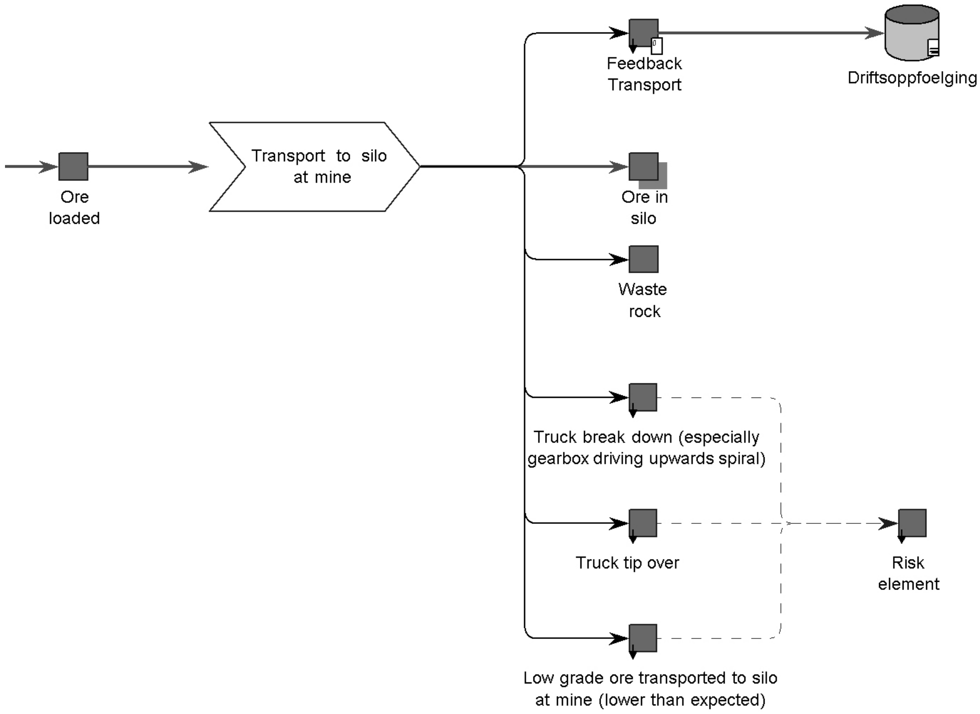

Figure 77 Different types of output from a process: “Feedback transport” is information going into the application “Driftsoppfoelging”, “Ore in silo” is flow of material and the three outputs of type “Risk element” are possible events.

Process analysis has been used to identify these possible events. The possible risk elements along the value chain with related consequences have been identified by discussion and brainstorming among the mining staff.

For qualitative and / or a more quantitative assessment of the risk elements, they can be placed inside a risk matrix with superimposed isorisk curves (see Figure 78).

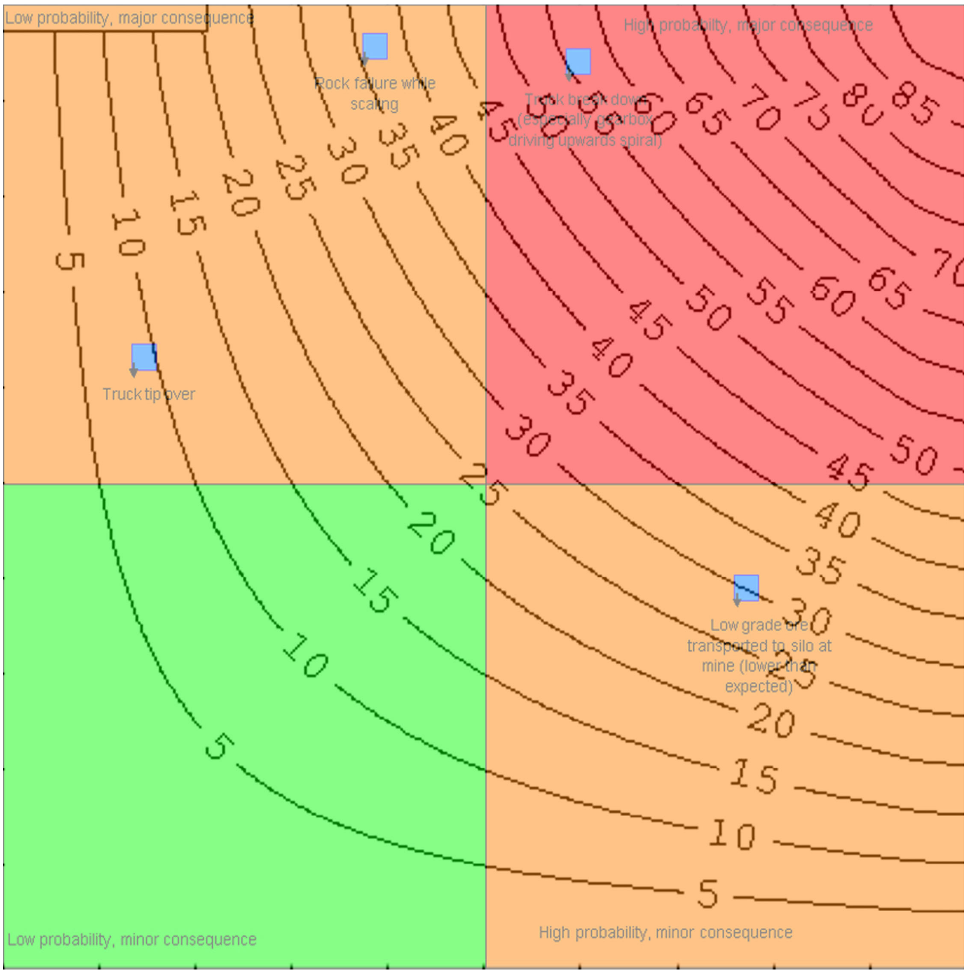

Figure 78 Risk matrix with superimposed isorisk curves. Isorisk curve 100 would indicate a maximum consequence and a probability equal to 1, i.e. the event is certain to take place. Horisontal axis: probability increasing from left to right; vertical axis: consequence increasing from the bottom to the top.

A risk matrix like the one in Figure 78 without the isorisk curves will only be qualitative and the usefulness will depend on the resolution. With a resolution of four pixels the usefulness is limited. This becomes apparent when isorisks are superimposed onto the matrix.

4.9.5. Probability quantification

The different events can be broken down into a consequence and probability (see Figure 79).

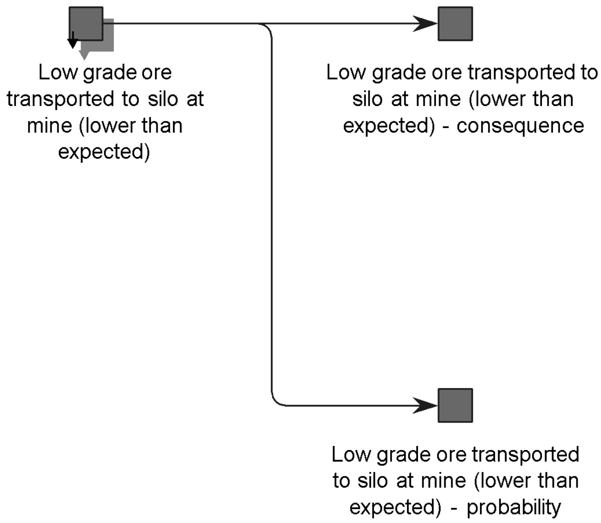

Figure 79 Event break down into consequence and probability. The consequence and probability must be quantified to be able to quantify the risk attached to the event.

The probability that the kind of event shown in Figure 79 can take place can be quantified using geostatistical simulation.

A mining stope in the Kvannevann Iron Ore is approximately 40 metres wide, 60 to 100 metres long and about 105 metres high. Production is executed on two levels. The smallest mining unit (SMU) considered is one blast, which contains 4 rounds, each separated by 2.5 metres. The dimension of the SMU is therefore 40x10x50. To assess the variability of each SMU, small blocks with dimensions 5x2x5 metres can be defined. The variability of each SMU has been deduced from the realisations on the small blocks by recombining the small blocks into the SMUs as described in Journel and Huijbregts (1978). Block models are shown in Appendix I.

The simulation has been performed with 100 iterations.

The result is 100 images of the SMUs in the stopes. Figure 80 shows one of these images for FeTot, FeMagn and dry bulk density for one of the stopes:

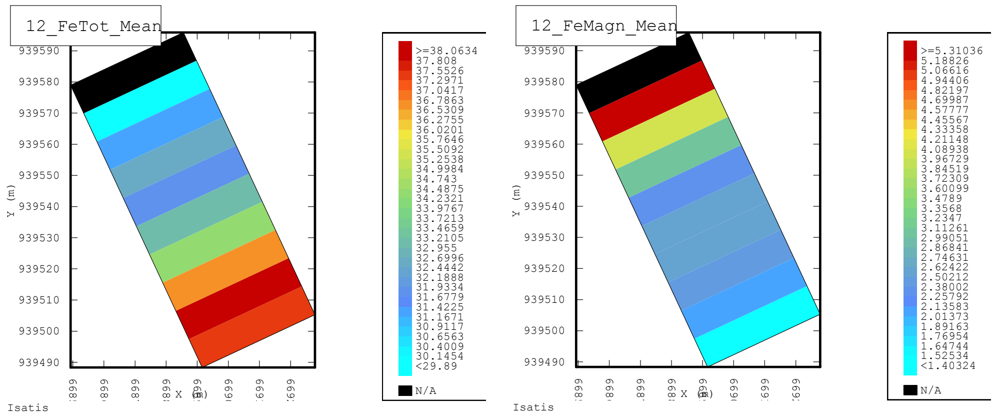

Figure 80 One image illustrating the possible content of a stope to be mined. Left: FeTot, right: FeMagn. "12" in the two figure headings simply means the 12th realisation out of one hundred.

Given the 100 images of the stopes, the probability that the grade is above a certain cut-off value can be estimated simply by counting how many realisations that are above this value and divide this number by the total number of realisations.

If A_n is the event that SMU number n contains more Fe than some cut-off value g. As will be shown in Section 4.10.2, there is a correlation between the Fe content in two adjacent SMUs. Therefore, given A_n, the probability that SMU number n+1 also contain more Fe than some cut-off value could be formalised by Bayes' Theorem:

$$P(A_{n+1} \mid A_n) = \frac{P(A_{n+1})P(A_n \mid A_{n+1})}{P(A_n)} \qquad \textbf{Eq. 62}$$

Or:

$$P(A_{n+1} \mid A_n) = \frac{P(A_{n+1})P(A_n \mid A_{n+1})}{P(A_{n+1})P(A_n \mid A_{n+1}) + P(\overline{A}_{n+1})P(A_n \mid \overline{A}_{n+1})} \qquad \textbf{Eq. 63}$$

Both the conditional probabilities in Equation (63) can be calculated directly from the experimental simulation results by counting the number of times both SMUs have a content above their respective cut-off values and dividing this result by the number of times each of the SMU isolated have a content above the cut-off value. An example will illustrate this:

SMU (n)	1	2	3	4
Limit value, g	34	34	34	34
# > g_n	55	42	59	73
$P(A_n)$	55 %	42 %	59 %	73 %
# > [g_n and g_{n+1}]	35	33	51	
$P(A_{n+1}\|A_n)$	64 %	79 %	86 %	
$P(A_n\|A_{n+1})$	83 %	56 %	70 %	

Realisation 1	37.09	33.88	35.31	37.01
Realisation 2	30.66	31.83	32.84	36.06
Realisation 3	34.58	31.71	30.33	33.49
Realisation 4	34.49	32.91	35.35	35.63
Realisation 5	37.39	35.29	36.12	33.68
Realisation 6	30.88	31.41	33.28	33.90
Realisation 7	34.85	33.93	33.36	33.67
Realisation 8	30.35	30.18	31.60	33.12
Realisation 9	36.06	36.30	37.17	37.58
Realisation 10	38.46	35.25	35.74	36.35
Realisation 11	37.60	36.14	34.84	33.30
:	:	:	:	:
:	:	:	:	:
Realisation x	35.608	35.733	36.007	35.679

$$P(A_2|A_1) = \frac{35}{55} = \underline{\underline{64\ \%}}$$

$$P(A_1|A_2) = \frac{35}{42} = \underline{\underline{83\ \%}}$$

Figure 81 Example illustrating conditional probability. Implemented in a spreadsheet it can be used as a tool to update the probability that the next SMU contains required iron; presupposing that it has been possible to quantify the content in the one just produced.

The example in Figure 81 illustrates how the probability that the iron content in a SMU is above a certain cut-off value can be updated as information about adjacent SMUs is collected.

4.10. Value chain modelling and simulation

4.10.1. Introduction

The value chain from in-situ ore to products illustrates the path that leads the material through the different value adding processes. This can be modelled followed by a simulation to assess consequences of different actions like investments, collection of more geodata etc. The point is to use the process analysis and the blue boxes in particular, to identify key value chain nodes where the responsibility for the node content changes and where actions may influence the properties of the node content. Once the key nodes have been selected a model can be built.

4.10.2. Value chain modelling in @RISK

@RISK is a MS Excel based modelling tool. Values are entered into a normal spreadsheet as distributions or single (tabulated) values and the Monte Carlo type simulation can be run as pure Monte Carlo or Latin Hypercube. Latin Hypercube provides a better result with fewer iterations.

The n images of the deposit or the stopes can be organised in tables. These images could be implemented in the model by defining a distribution fitted to the realisations followed by a sampling from this distribution. However, doing this would make it difficult to preserve the correlation between, for example, the FeTot values in each SMU in each stope. This correlation is illustrated in Figure 82. As illustrated, the correlation between two adjacent SMUs is noticeable, whereas the correlation between the simulated FeTot values in SMUs separated by one SMU is negligible.

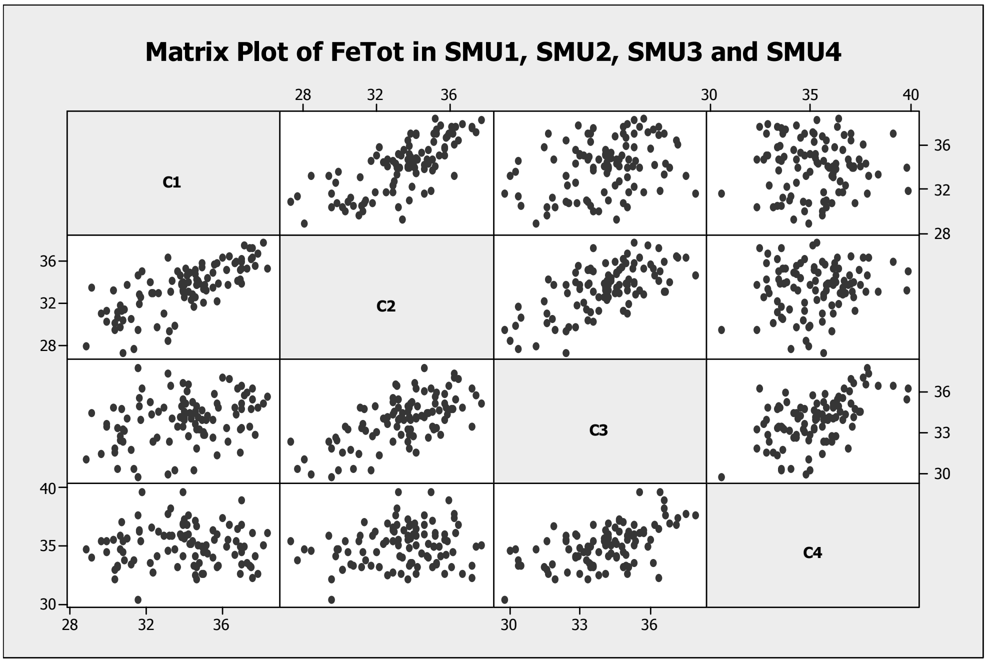

Figure 82 Matrix plot showing the correlation between the FeTot content in four SMUs. SMU C1 is followed by C2 and so on. The correlation between FeTot values in adjacent SMUs is noticeable.

Better it is then to use tabulated values, where the tables consist of the actual SMU realisations. To model the probable outcome from one stope, the model would be built according to the following logic:

1. Pick the first realisation containing information about the dry bulk density, the FeTot and the FeMagn of all the SMUs in the stope.
2. Simulate the first possible outcome in terms of produced product tonnages from each SMU by defining the recovery in the mine and in the processing plant and the content of iron in the products, as distributions.
3. Repeat 1 and 2 for all the realisations.

With 100 SMU realisations and for example 200 iterations in point 2 the total amount of data reaches 20000 for each SMU.

The final result from this simulation is two-fold:

- Distribution showing possible product tonnages from each SMU.
- Distribution showing possible product tonnages from the whole stope.

Having established the stope variability and possible product tonnages, the value chain simulation can be extended to include costs, product prices, taxation and required profit.

5. Results

5.1. Process analysis

5.1.1. The general process model

Figure 83 shows the general process model for Rana Gruber AS. It sums up controlling and the supporting elements. It also states the business focus of the company:

"Manufacturing of iron ore based iron oxide products".

The formulation "iron ore based" is included to emphasise the use of iron ore and not scrap iron.

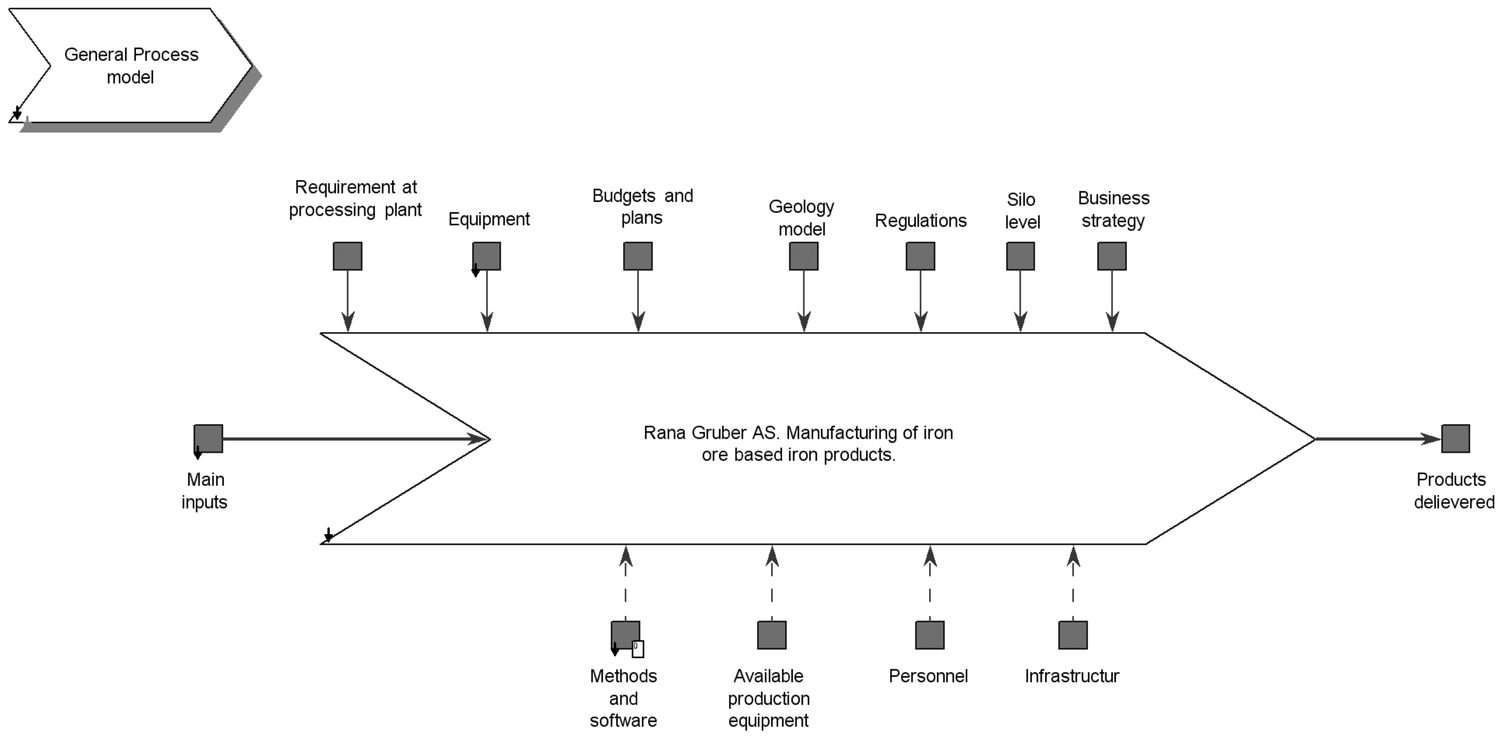

Figure 83 IDEF0 general process model for Rana Gruber AS with input, output and controlling- and supporting elements.

Table 14 sums up the first breakdown of the general process model. The responsible party is included.

Process	Input	Output	Responsibility
Find get and develop deposit	Some requirement, e.g. "increase ore base"	Deposit ready for production	Mining department
Production	Deposit ready for production	Ore in train wagons	Mining department
Tramming	Ore in train wagons	Ore at processing plant	CargoNet / NSB
Unloading	Ore at processing plant	Ore in silo ready for processing	Ore dressing plant
Ore dressing	Ore in silo ready for processing	Products	Ore dressing plant
Packing, sale and distribution	Products	Products delivered	Sales

Table 14 First break down of the general process model

A sub-process in the primary process "Find, get and develop deposit" is "Exploration". This process could be defined as both a primary- and a development process. The reason for this is that once performed successfully as a primary process a deposit is found and the exploration process is carried through as a development process to increase the probability for future success.

In the following, special focus is on the production process and the related inputs and outputs.

5.1.2. The Production Process

"Production" is used to term the process with "Deposit ready for production" as input and "Ore in silo at ore dressing plant" as output, i.e. it constitutes the activities taking place in and around the mine.

The production process consists of the main activities drilling, charging, blasting, loading and transport out of the mine (haulage) and to the ore dressing plant (tramming) (see Figure 84).

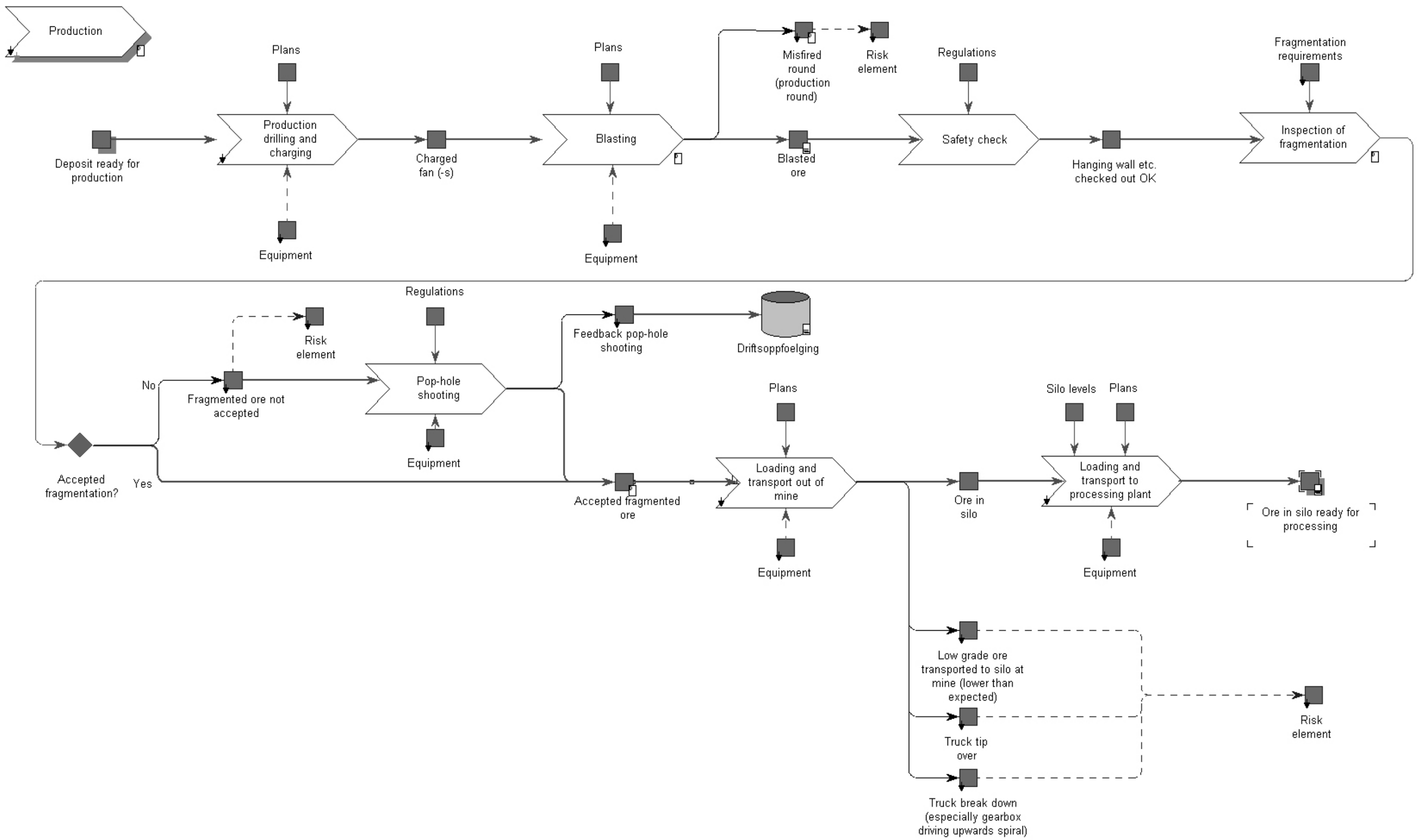

Figure 84 Production process breakdown.

With reference to Figure 84, the mining part of the value chain starts with the process production drilling and charging. In Figure 84, this process has a small arrow in the lower left corner. This arrow indicates, that the process is broken down further. Equipment and plans are supporting and controlling elements respectively. The output from the process is charged blasts (one blast typically consists of four rounds). This output is input into the blasting process. The primary output from this process is “Blasted ore”. A possible secondary output is a risk element, termed “Misfired round”. The next processes are safety check and inspection of fragmentation. The output from the fragmentation inspection consists of two possible outcomes. If the fragmentation is accepted (primary output), the loading and transportation can start as soon as the controlling element “Plans” initiate the process. If the fragmentation is not accepted (secondary output), the block sizes must be reduced through pop-hole shooting. This process has a primary output that the fragmentation is accepted and information as secondary output. The information must be handled by the application “Driftsoppfoelging”. The primary output from the loading and transport ore out of mine (haulage) is “Ore in silo”, whereas secondary output consists of risk elements. The primary output is input into the process loading and transport to processing plant (tramming). The final output is “Ore in silo ready for processing”. This is the main input into the ore dressing process.

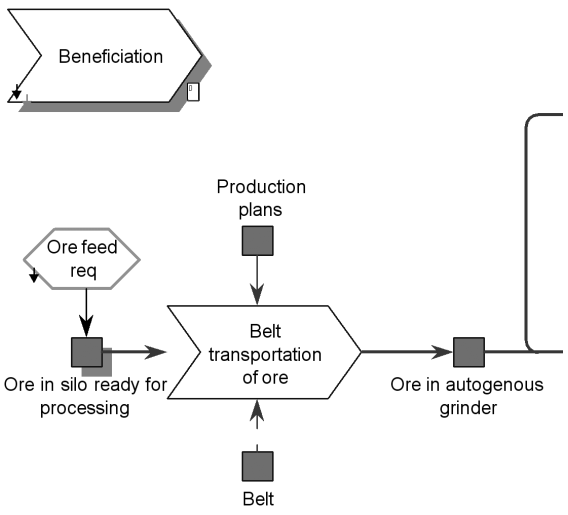

Figure 85 The main input of the ore dressing process is “Ore ready for processing”. The ore dressing plant has defined certain requirements to this input.

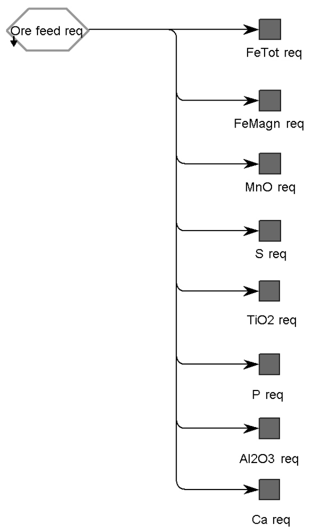

Figure 86 Breakdown of the requirements defined by the ore dressing plant. In addition comes a certain amount of tonnage.

The ore dressing plant has defined requirements to the ore coming into the plant (see Figure 85 and 86). The requirements include of cut-offs relevant to FeTot, FeMagn, MnO, S, P, TiO_2, Al_2O_3 and Ca. At the present time, Rana Gruber AS regards FeTot, FeMagn and MnO as the most important. In addition comes the requirement to a certain amount of ore tonnage per unit of time.

All symbols in the process model with a small black arrow in the lower left corner are broken further down. Above, in Figure 85 and 86, this is illustrated for the element "Ore feed requirements".

5.2. Ore density

5.2.1. Grain density

Figure 87 shows the correlation between the reciprocal density estimations, and total iron (FeTot).

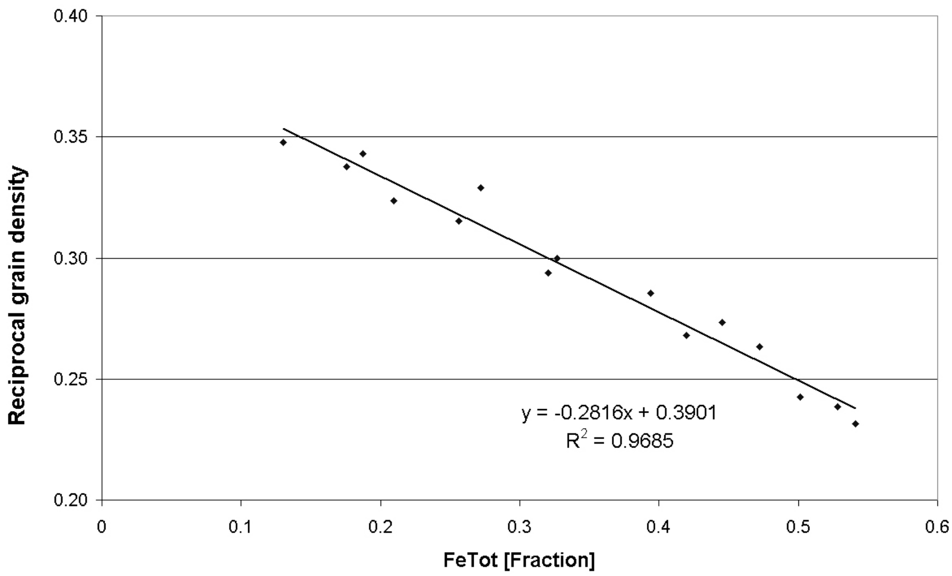

Figure 87 Plot showing the correlation between the reciprocal density estimations using the water pycnometer method and FeTot

To test the reproducibility of the water pycnometer method used to estimate the grain density, ten of the duplicate samples were tested.

As seen in Figure 88 the regression fit is good and almost entirely coincident with the line y = x.

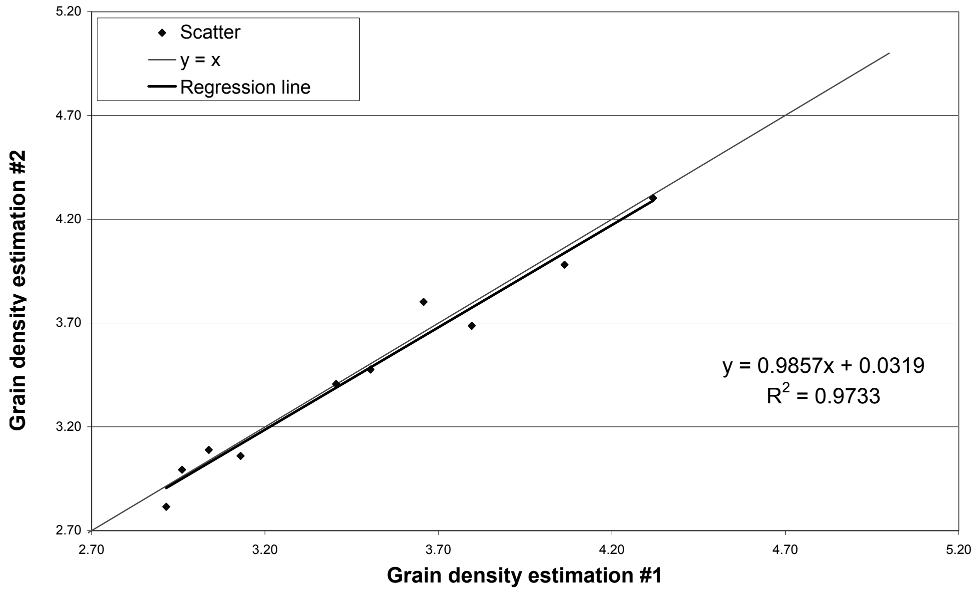

Figure 88 Original and duplicate samples of grain density

To test the water pycnometer method further a T-test was performed. Since values in the two data sets come from the same sample material, or the same reference population with mean m and standard deviation s, they cannot be considered to be independent. The T-test therefore has to take the correlation between the values into consideration.

Summary statistics of the original grain density values and the duplicates are given with the correlation coefficient in Table 15.

	Original	Duplicates
Mean	3.48	3.46
Standard deviation s	0.48	0.48
# of samples	10	10
Correlation coefficient r	0.99	

Table 15 Summary statistics of original and duplicate estimates of grain density.

As can be seen, the mean is different. The question is whether the difference is statistically significant.

Statistical theory provides the solution. If the reference population can be assumed to be normally distributed, then the distribution of differences between the mean of any two sub-populations follows a Student T distribution. The Student T distribution is close to a normal distribution if the number of values is large. The variance s^2 of differences of means is calculated using Equation (64) (Dagbert et al. 2003):

$$s^2 = \frac{s^2_{Original} + s^2_{Duplicates} - 2 * s_{Original} * s_{Duplicates} * r}{n-1} \quad \textbf{Eq. 64}$$

Inserting the values in given in Table 15 into Equation (64) gives:

$$s^2 = \frac{0.48^2 + 0.48^2 - 2 * 0.48 * 0.48 * 0.99}{9} = 0.00072 \quad \textbf{Eq. 65}$$

This gives s = 0.027, which in turn gives a standardised difference of means (3.48-3.46)/0.027 = 0.66. With $n_1+n_2-2 = 18$ degrees of freedom the limit for acceptance on a 95% confidence level is 2.101. Since 0.66 < 2.101 the assumption that the two sub-populations come from the same reference population cannot be rejected, i.e. the method has an acceptable reproducibility.

5.2.2. Dry bulk density

The dry bulk density of the cores was measured. The iron grade of the crushed cores was analysed. The correlation between FeTot and the reciprocal density based on these measurements is given in Figure 89.

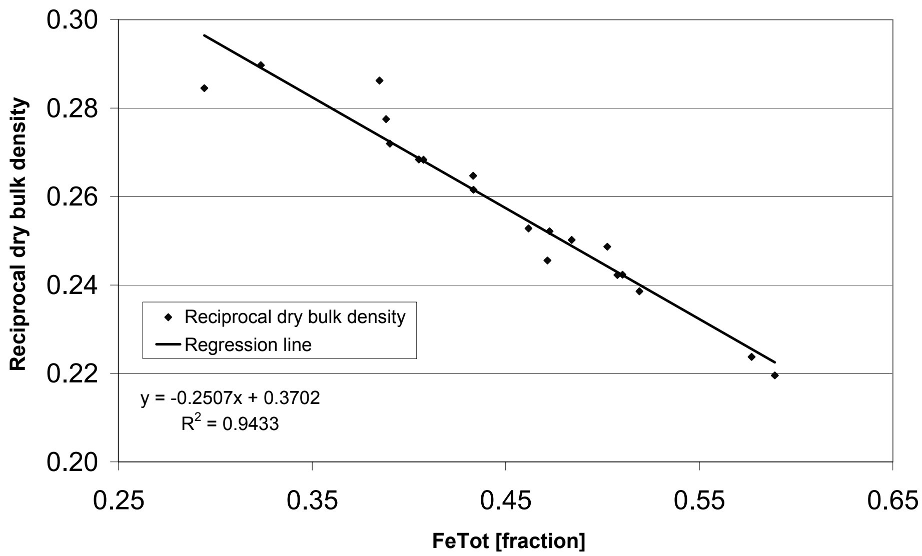

Figure 89 Correlation between FeTot [fraction] and the measured reciprocal dry bulk of the cores.

Given the correlation in Figure 89 and that corresponding regression line, prediction and confidence intervals can be calculated. 68% prediction- and confidence intervals have been calculated for 20%, 30% and 40% FeTot from the regression. Between these values, the intervals have been interpolated linearly for illustration. The result is presented in Figure 90.

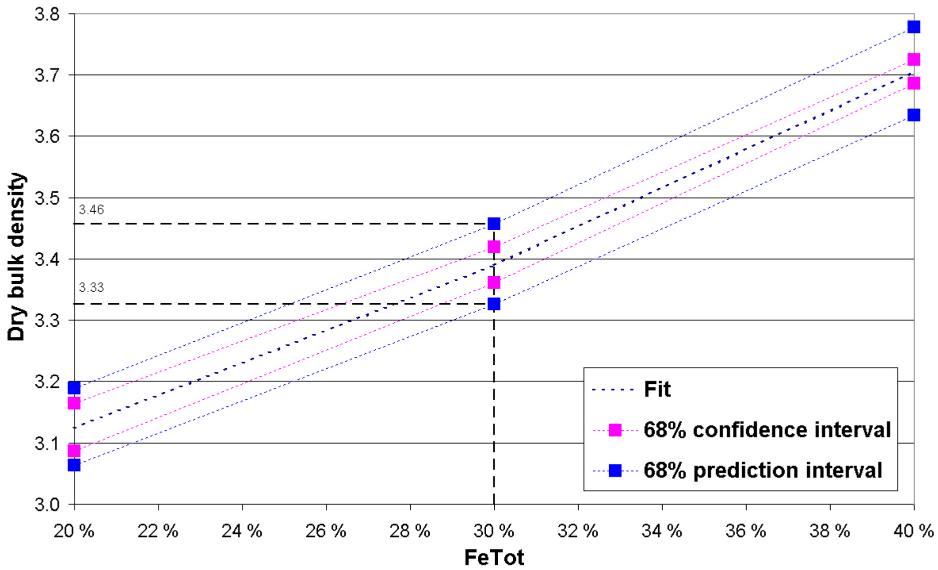

Figure 90 68% prediction and confidence interval calculated for FeTot equal to 20%, 30% and 40%. By FeTot = 30%, we can be 68% certain that the dry bulk density is between 3.33 and 3.46.

From Figure 90, it can be seen that given FeTot equal to 30%, the corresponding density is, with 68% confidence between 3.33 and 3.46 with a most probable value equal to 3.39.

The dry bulk density was measured both using the water replacement method and the calliper method. The results from the two methods are compared in Figure 91.

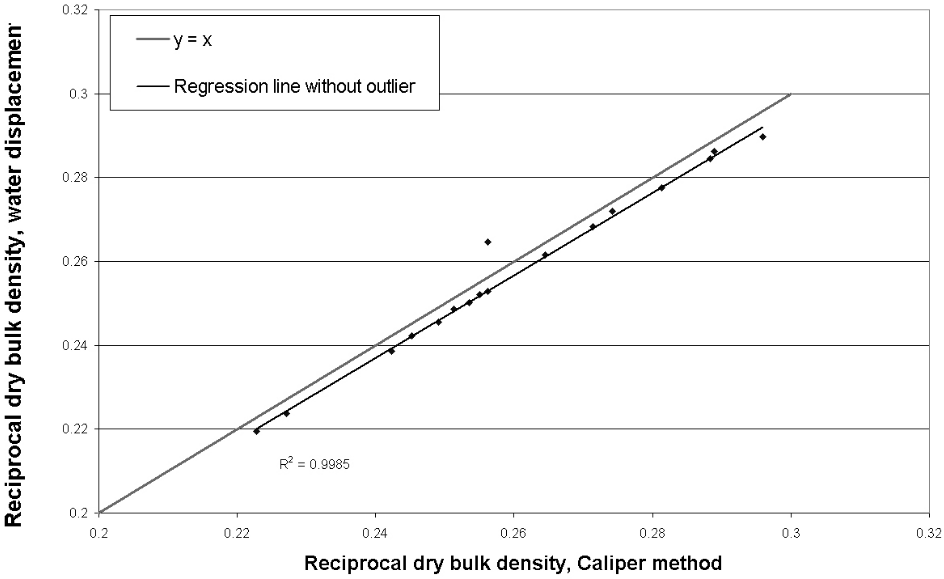

Figure 91 Reciprocal dry bulk density measured using the water replacement method vs. the reciprocal dry bulk density measured using the calliper method.

Statistics	Value
Mean	1.28 %
Standard deviation	0.28 %
Min	0.83 %
Max	2.11 %

Table 16 Summary statistics for the estimated porosity. Outlier disregarded.

From Figure 91 it can be seen that the calliper method underestimates the density compared to the water replacement method. As described in Section 4.3.3 this could be used to estimate the porosity of the rock. The summary statistics of the estimated porosity is given in Table 16. The outlier has been disregard in the calculation of this summary statistics. The porosity obtained here is comparable with the porosity of most igneous and metamorphic rocks, which have porosity between 1% and 2% (e.g. Press and Siever 1986, Broch and Nilsen 2001).

From the porosity, the difference between the in-situ bulk density and the dry bulk density can be estimated by assuming the level of natural water saturation. Assuming the water saturation to be equal to 50%, the difference is 0.17%. For a e.g. 320.000 m^3 large stope and a dry bulk density equal to 3.5, the difference between in-situ and produced tonnage is about 2000 tonnes.

5.2.3. Estimated average mineral density

Following the procedure presented in Chapter 4 the average density of the main iron minerals and the gangue can be estimated. With the parameters given in the linear equation in Figure 89 and with an average a factor equal to 1.427 (see Equation (23), Section 4.3.2), the theoretical equation presented in Section 4.3.2 becomes:

$$\frac{1}{\rho_r} = 0.3702 - 0.2507 * Fe_{Tot} \qquad \textbf{Eq. 66}$$

This gives:

$$\frac{1}{\rho_g} = 0.3702 \Leftrightarrow \rho_g = \underline{2.70\, g/cm^3} \qquad \textbf{Eq. 67}$$

And:

$$a * \left(\frac{1}{\rho_{mh}} - \frac{1}{\rho_g} \right) = -0.2507 \Leftrightarrow \rho_{mh} = \underline{5.14\, g/cm^3} \qquad \textbf{Eq. 68}$$

The same can be done with the grounded ore data (water pycnometer method), but due to different hematite / magnetite content the average a factor becomes 1.426:

$$\frac{1}{\rho_r} = 0.3901 - 0.2816 * Fe_{Tot} \qquad \textbf{Eq. 69}$$

This gives:

$$\frac{1}{\rho_g} = 0.3901 \Leftrightarrow \rho_g = \underline{2.56\, g/cm^3} \qquad \textbf{Eq. 70}$$

And:

$$a * \left(\frac{1}{\rho_{mh}} - \frac{1}{\rho_g} \right) = -0.2816 \Leftrightarrow \rho_{mh} = \underline{5.19\, g/cm^3} \qquad \textbf{Eq. 71}$$

5.2.4. Other density calculations and observations

Detailed density calculations based on average ore mineralogy (mainly Kvannevann-, Vestmalmen and Erik Iron Ore, NGU 2003a) are given in Appendix G. The average density based on this average mineralogy is estimated to 3.55 g/cm^3.

Nilsen (1979) have made density measurement on the Vestmalmen Iron Ore. The average density for this ore with an average iron content of 32% is 3.44 g/cm^3.

Muurmans (1976?) states that an average ore (mainly Kvannevann-, Vestmalmen and Erik Iron Ore) with 33.5% FeTot, 6% FeMagn and 0.16% P has a specific gravity equal to 3.45 g/cm^3.

5.2.5. Density of hematite and magnetite

To verify the procedures above, the density of the hematite and magnetite has been analysed. The tests were performed on hematite and magnetite concentrates with the helium pycnometer.

The test results are given in Table 17:

Sample	Mineral	Weight [g]	Mineral density [g/cm^3]
11 hm	Hematite	16.993	5.16
5 mt	Magnetite	13.782	5.15
5 hm	Hematite	17.498	5.18
10 hm	Hematite	14.708	5.17
6 mt	Magnetite	4.245	5.15
6 hm	Hematite	18.562	5.12

Table 17 Densities for six samples of mineral concentrate.

This gives an average density for hematite and magnetite of 5.16 and 5.15 respectively.

The hematite concentrates were checked in a microscope for impurities. In four thin sections one magnetite grain was found. A circle in Figure 92 indicates this magnetite grain. Figure 93 shows the same part of the thin section as illustrated in Figure 92, but in transmitted light. Coloured grains are gangue rock minerals.

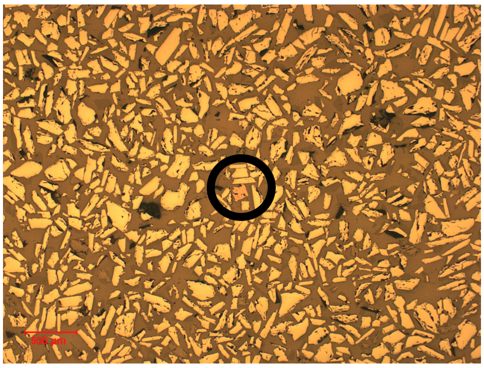

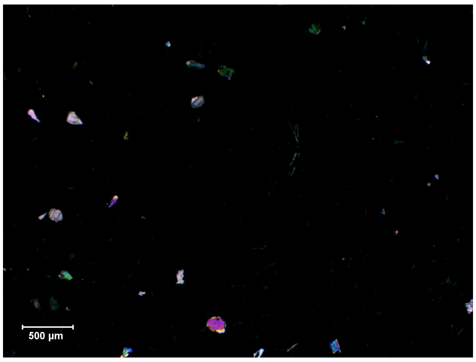

Figure 92 Hematite concentrate with one magnetite grain. Picture taken in reflected light. Magnetite grain indicated by the circle. Light brownish grains are hematite.

Figure 93 Same section of the thin section as Figure 93, but in transmitted light. Coloured minerals are gangue rock minerals.

5.2.6. Equations for density / grade relationship

Given the obtained equations for the relationship between the grade and the reciprocal dry bulk density for the cores the relationship between dry bulk density and the grade becomes:

$$\rho_r = \frac{1}{0.3702 - 0.2507 * Fe_{Tot}} \qquad \textbf{Eq. 72}$$

This relationship has been used in the resource and reserve estimations in this thesis.

5.3. Magnetic susceptibility

Figure 94 shows the correlation between wt% magnetite and magnetic susceptibility, k, for the Kvannevann Iron Ore. For comparison, the results of Clark (1997) are included.

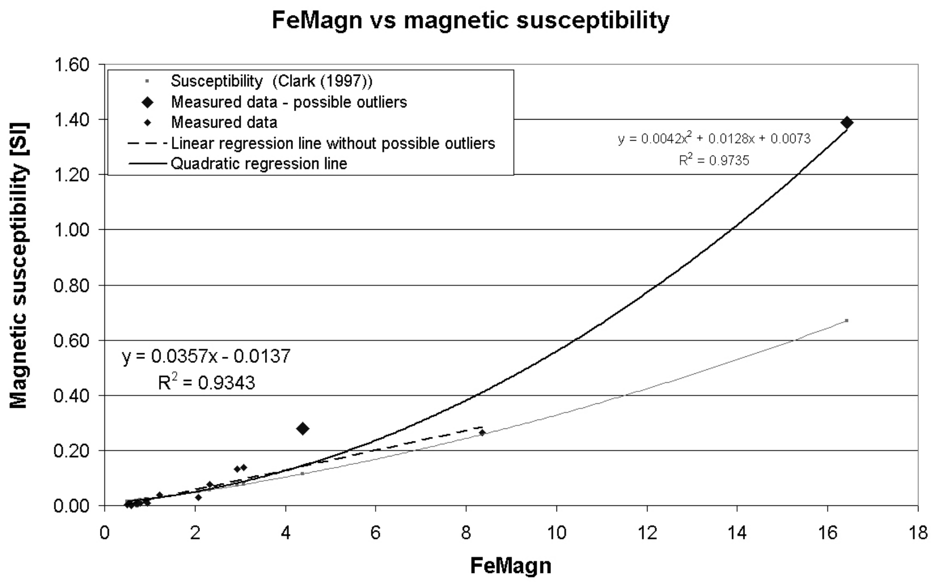

Figure 94 Correlation between wt% mt and magnetic susceptibility.

To be in accordance with Clark (1997) two values have been excluded. Given the data, without the outliers, a linear regression line has been calculated:

$$\kappa = 0.036 * \text{FeMagn [\%]} - 0.014$$

Rearranged:

$$\text{FeMagn [\%]} = 26.18 * \kappa + 0.47$$

68% prediction intervals can been calculated based on the data and the regression line (Table 18):

	FeMagn 68% prediction interval	
Magnetic susceptibility	Lower limit	Upper limit
0.05	1.24	2.31
0.10	2.54	3.63
0.15	3.82	4.97
0.20	5.10	6.31

Table 18 68% prediction intervals for FeMagn given the magnetic susceptibility.

5.4. Cut-off estimation

5.4.1. Deterministic approach to calculate the economic cost break-even

The economic cost break-even, g, can be calculated using the formula presented in Section 4.2.2:

$$g = \frac{h + \frac{(f + F)}{H}}{py} \qquad \textbf{Eq. 73}$$

This must be done for both hematite and magnetite:

$$g_{hm} = \frac{h + \frac{(f + F)}{H}}{p_{hm} y_{hm}} \qquad \textbf{Eq. 74}$$

$$g_{mt} = \frac{h + \frac{(f + F)}{H}}{p_{mt} y_{mt}} \qquad \textbf{Eq. 75}$$

With realistic input values for costs, product prices, and recovery, results for FeHm and FeMagn are given in Table 19 are obtained.

Mineral	Cost break-even cut-off (iron in the minerals)	a	b
Hematite, g_{hm}	31.8	-0.44	14.1
Magnetite, g_{mt}	14.1		

Table 19 Cost break-even cut-off for hematite and magnetite and corresponding a and b, being the parameters in the linear equation if FeHm and FeMagn is the ore decisive parameters.

Parameter	Value
a	-0.80
b	25.45

Table 20 Parameters a and b in case where FeTot and FeMagn are the decisive ore parameters.

The results given in Table 19 must be recalculated to be valid for the case where FeTot and FeMagn are the decisive ore parameters. Using equations in Section 4.2, corresponding results to the results in Table 19 becomes a = - 0.80 and b = 25.45, i.e. the linear equation FeMagn = - 0.80 * FeTot + 25.45 can be used to describe the relationship between FeTot and FeMagn above which the value of the mineralisation exceed the production costs. See Table 20. Figure 95 illustrates a linear equation with parameters a and b from Table 20.

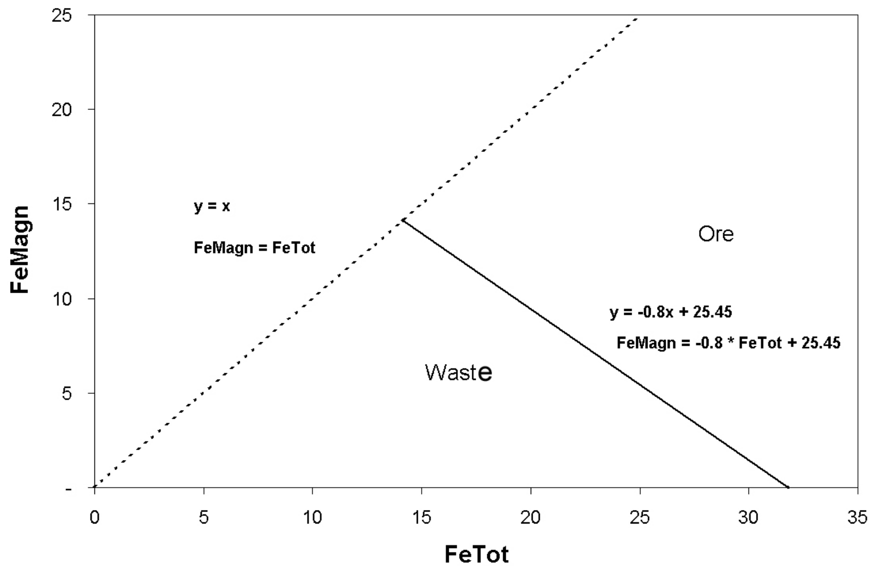

Figure 95 Linear equation defining combinations of FeTot and FeMagn that can be considered as ore.

5.4.2. Probabilistic approach

With the probabilistic approach, most likely values of the input parameters are quantified. In addition, some possible minimum- and maximum values are defined. Correlations between input parameters are also quantified.

By doing this, the same economic cost break-even as in the deterministic approach can be calculated. However, the output is no single value, but a range of possible values. In this case the main simulation output is the required FeHm (g_{hm}) and FeMagn (g_{mt}).

Histograms for these two main outputs given that the FeMagn is above 1.2% are shown in Figure 96 and 97.

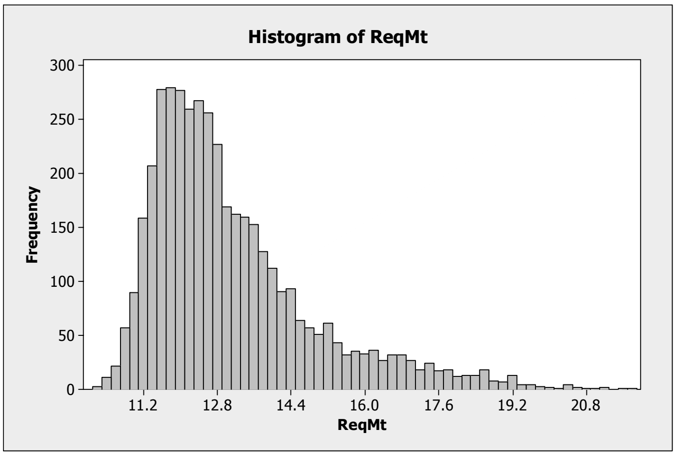

Figure 96 Histogram showing required FeMagn.

The reason for excluding realisations where FeMagn is below 1.2% is that below this value, the recovery of FeMagn is so low, that practically no magnetite-based products are produced. This makes the application of the equations above (in particular Equation (75), Section 5.4.1) unstable.

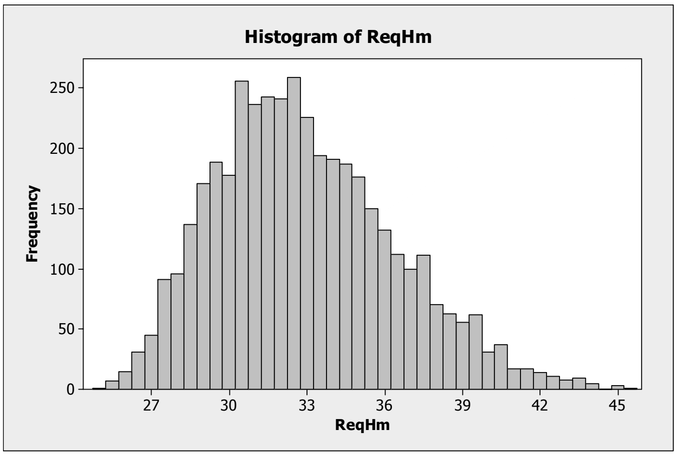

Figure 97 Histogram showing required FeHm.

Since the recovery of magnetite is highly correlated with the magnetite grade of the feed, the required FeMagn and FeHm are separated into intervals according to FeMagn realisations. Using the first quartile (Q25), the median and the third quartile (Q75) in each group of required FeHm and FeMagn as the representative value gives Figure 98.

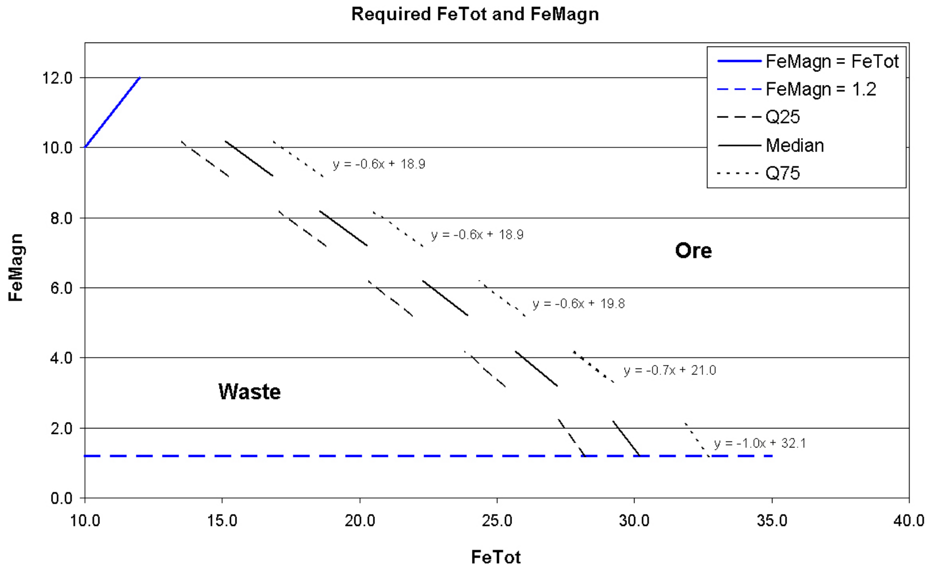

Figure 98 Relationships describing the required FeTot and FeMagn to cover costs. Q25 and Q75 given to illustrate the dispersion.

The illustration in Figure 98 shows that if the FeMagn value is between 1.2 and 2.2, the proper linear equation to use is:

FeMagn = -1.0 * FeTot + 32.1

The Q25 and the Q75 value illustrate the uncertainty in the estimate. The Q75 line should be used if the required probability for covering costs is 75%. Similarly, if 25% probability is sufficient, then the Q25 line should be used.

Above FeMagn = 6, the proper equation to use is indicatively independent of the FeMagn:

FeMagn = -0.6 * FeTot + 18.9

This point is illustrated in Figure 99, where the required additional FeHm, if FeMagn is lowered by one %-point, is plotted against FeMagn.

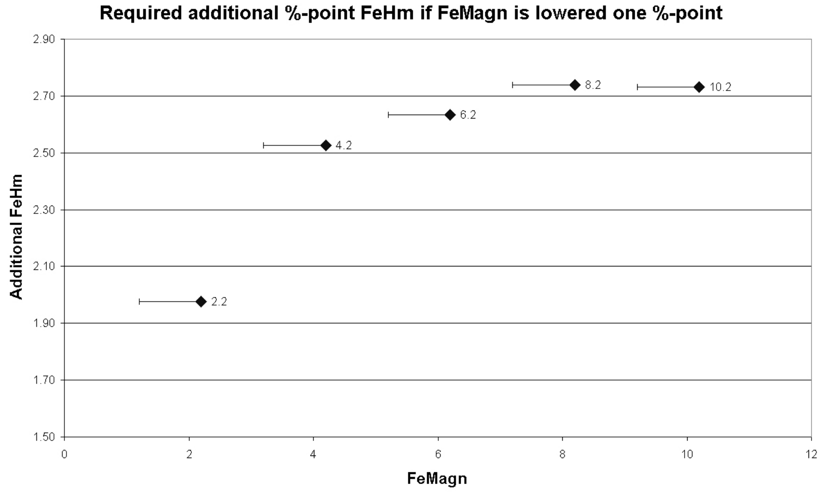

Figure 99 Relationship illustrating how much more FeHm is required if the FeMagn-value decreases with one %-point; e.g. if the FeMagn-value decreases from 4.2 to 3.2 additional 2.55 FeHm is required.

Both parameters a and b decrease with increasing FeMagn. The varying a could be seen as an indicator of the importance of FeMagn. With decreasing a (in absolute value), the more important FeMagn becomes.

5.5. Geochemical characterisation of the ore types

5.5.1. Isatis

The results from the ore type characterisation performed in Isatis is given in Table 21:

	MnO		
Ore / rock type	Average	Stdv	N
Hm_Malm	0.43	0.34	14
Mt_Hm_Malm	0.32	0.56	14
GrFels_Malm	1.56	0.61	7
Garnetfels	4.55	1.32	4
Impregnasjon	0.17	0.05	4

Table 21 % MnO summary statistics for different rock- and ore types. N is the number of samples.

Due to the availability of few samples in each type (see Table 21) it is difficult to conclude decisively, but the analysis indicates, as expected, that rock- or ore types containing garnet are high in MnO and that the ore is relatively low in MnO.

Complete summary statistics for each ore and rock type is given in Appendix I.

5.5.2. MS Access

The results from the approach using the raw assay data from the boreholes and the core length weighted averages are given in the Table 22.

	MnO		
Rock type	Weighted average	Weighted stdev	N
Hm_Malm	0.547	0.583	81
Mt_Hm_Malm	0.340	0.352	135
GrFels_Malm	2.171	2.591	18
Impregnasjon	0.348	1.030	10
Glimskif	0.791	1.981	45

Table 22 Core length weighted summary statistics for different rock- and ore types. Other relevant ore types suffered from a lack of assigned assays. N is number of samples.

Focusing on the ore types in Table 22 (rock types with “Malm” in the type name), it is indicated that the magnetite – hematite ore type has a lower content of MnO relative to the hematite ore. This is supported by the result presented in Table 21. The other ore types defined in Table 9 Section 3.3.3 suffer from a lack of assigned assays.

To decide whether the differences between the averages in Table 22 are significant a two-tailed rank-sum test was performed. Details on hypothesis testing can be found in textbooks on statistics (e.g. Dougherty 1990). The averages were found to be unequal on a 95% level of confidence.

5.6. Geodata collection

Drill cuttings were collected using the collector presented in Section 4.4.

Test runs were performed to check the repeatability of the collection method. The repeatability is illustrated the two plots in Figure 100:

1. FeMagn vs. FeTot showing the FeTot and FeMagn repeatability and
2. MnO vs. S showing the S and MnO repeatability.

The different symbols in Figure 100 indicate different tests, i.e. only identical symbols should be compared.

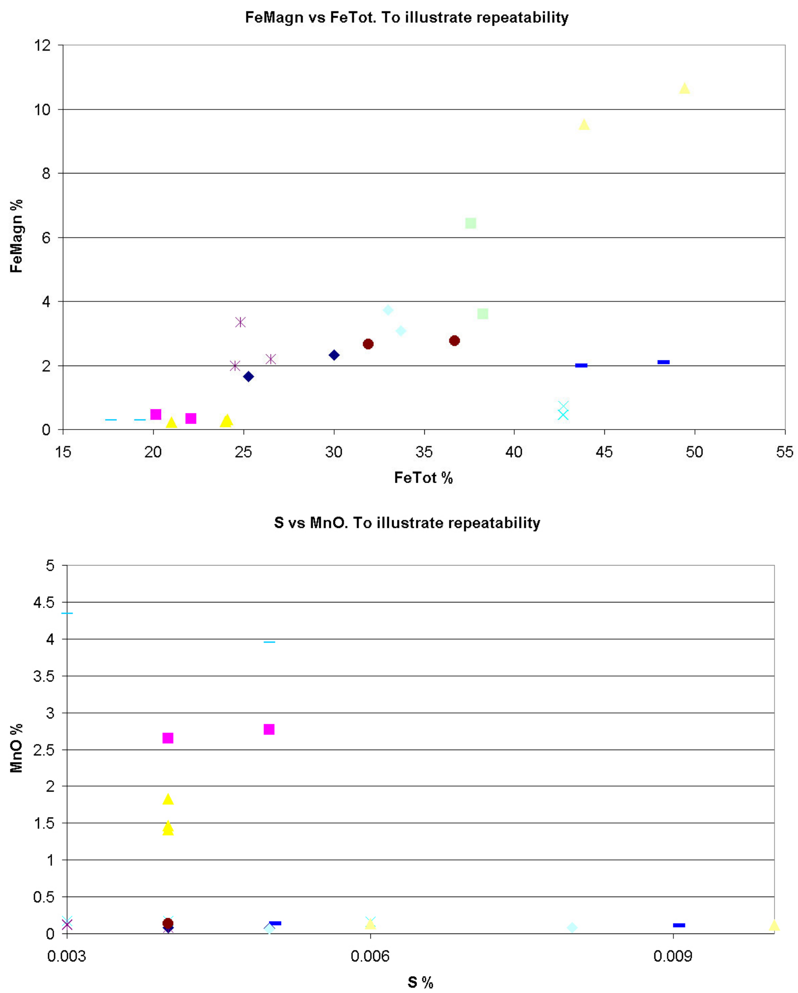

Figure 100 FeTot vs. FeMagn and S vs. MnO to illustrate repeatability of collection of drill cuttings. In both graphs, extremes have been removed to enhance readability. However the extremes are included in the CV estimations. See text.

Extremes excluded in Figure 100 to enhance readability are:

	FeTot	FeMagn	S	MnO
Teat 1	43.2	31.68	0.14	0.16
Teat 2	42.1	32.42	0.10	0.16

Table 23 Extreme values excluded in Figure 99 to enhance readability.

	CV
FeTot	**6 %**
FeMagn	**21 %**
MnO	**14 %**
S	**29 %**

Table 24 Calculated CV for MnO, S, FeTot and FeMagn.

Based on the test results, the coefficient of variation (CV) can be calculated using the formula given in Section 4.4.3. The calculated CV is given in Table 24. For MnO this gives a sampling precision of 28 % at a 95% confidence level.

5.7. Geodata mining

Torture numbers, and they will confess to anything.

Gregg Easterbrook

5.7.1. Structural analysis

Anisotropy

To investigate the degree of anisotropy, variogram maps have been calculated. In Figure 101 the horisontal- and vertical variogram maps are given.

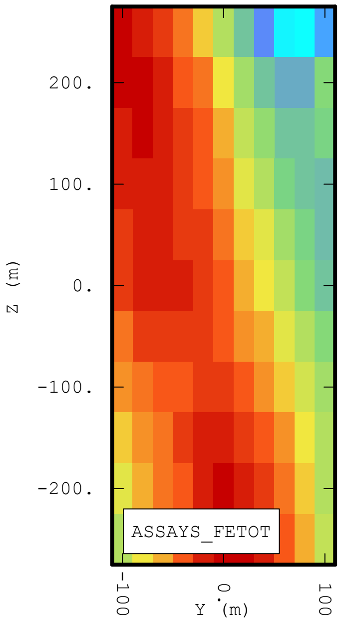

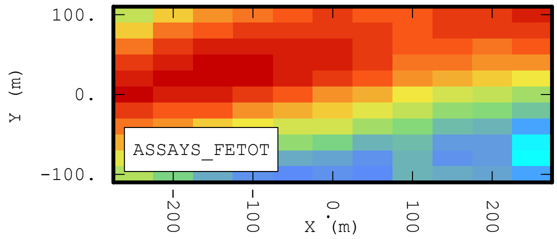

Figure 101 Vertical (left) and horisontal (above) variogram map for total iron, FeTot, indicating the main directions for which separate experimental variograms should be calculated. Red colour indicates low variogram value, i.e. a relative high degree of correlation between sample values.

The main directions can be measured directly from the variogram maps. Variogram maps similar to the one given in Figure 101 have been prepared for all geochemical variables (FeTot, FeMagn, S, TiO_2, P and MnO) and for the joint density. See Figure 102 for the joint density variogram map. The results from the structural analysis are given in Table 25.

Parameter	Rotation around z-axis	Azimuth	Rotation around x-axis	Dip of horisontal reference plane
FeTot	20	N 70° E	10	10° south east
FeMagn	10	N 80° E	0	0° south east
GaussFeTot	14	N 76° E	16	16° south east
GaussFeMagn	10	N 80° E	10	10° south east
GaussMnO	10	N 80° E	10	10° south east
MnO_IncludingSoftData	10	N 80° E	10	10° south east
Joint density	20	N 70° E	30	30° south east

Table 25 Main directions for calculation of experimental variograms. "GaussFeTot" means Gaussian transformed FeTot geodata.

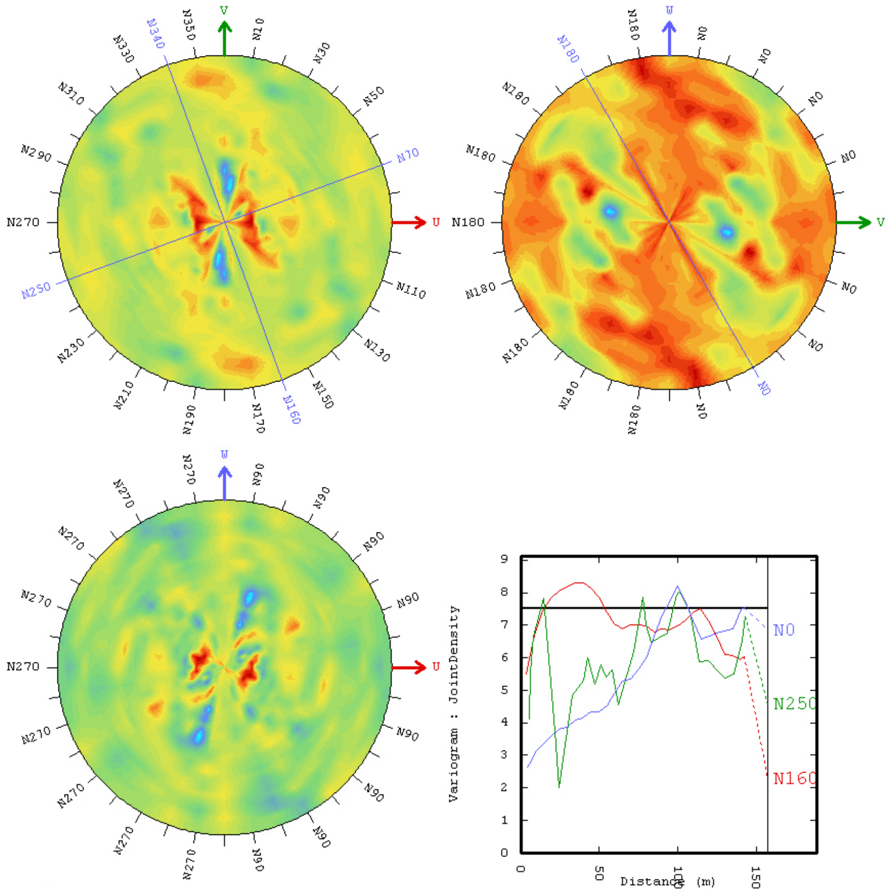

Figure 102 Joint density variogram maps. Upper left: horisontal plane. Upper right: vertical plane N-S. Lower left: vertical plane E-W.

Nugget effect

The nugget effect of a variogram is the apparent discontinuity at h = 0.

The nugget effect has been established by calculating an omni-directional (average) variogram with short lag values, i.e. small h (see Figure 104). The nugget effect has then been quantified by extrapolating the two variogram values with the two smallest lag value h back to h = 0. This presupposes that sufficient number of points is included in the calculation of the variogram values. The calculation of the nugget effect is exemplified with the joint density in Figure 103 and Figure 104.

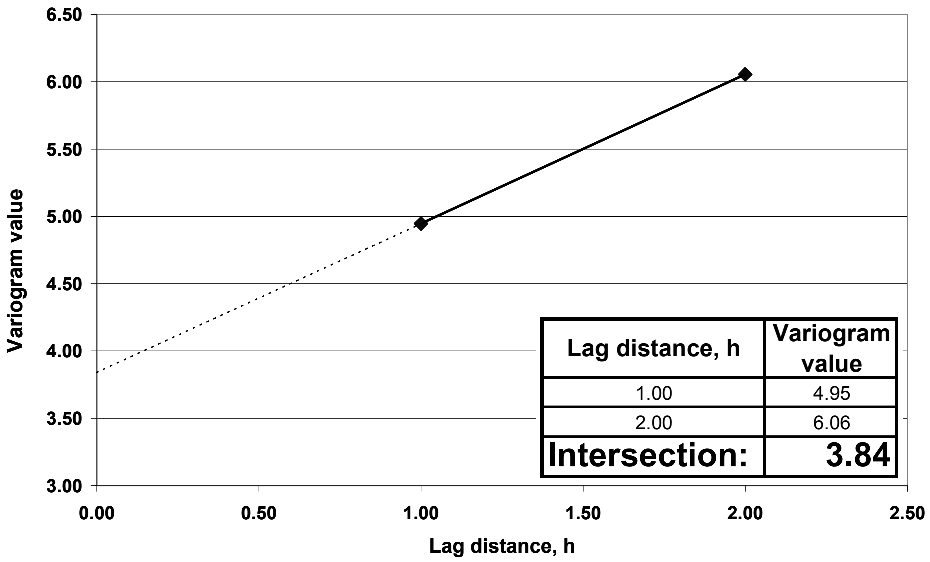

Figure 103 Isolated variogram values for the two smallest lag distances. Lag distances given in metre.

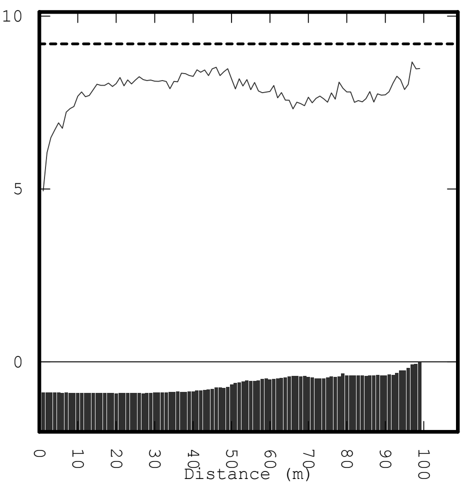

Figure 104 Omni-directional variogram for joint density used in the calculation of joint density nugget effect.

The same procedure has been used for the elements used in estimation or simulation. See Table 26.

Parameter	Nugget effect
FeTot	20.00
FeMagn	2.20
GaussFeTot	0.20
GaussFeMagn	0.15
Joint density	3.84
GaussMnO	0.00
MnO_InclSoftData	0.10

Table 26 Estimated and applied nugget effect.

Variography

The variogram models for FeTot and Gaussian FeMagn are given in Figure 105 and 106 respectively.

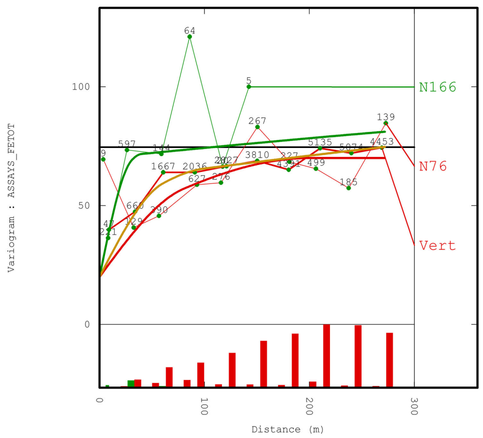

Figure 105 Experimental variogram and variogram model for FeTot used in the block estimation of FeTot.

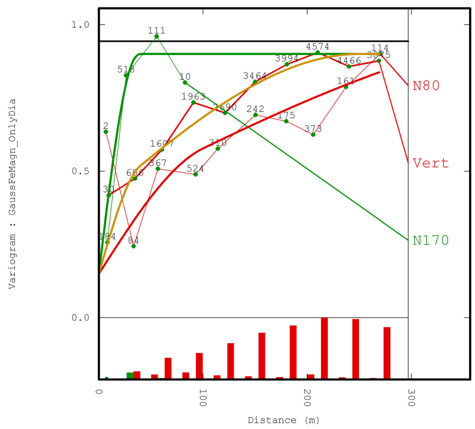

Figure 106 Experimental variogram and variogram model for Gaussian FeMagn used in simulation.

Using the representation form given in Section 4.8.5, the applied models are:

FeTot:

$$\gamma(h) = 20 + 20 \times Sph(80,30,60) + 30 \times Sph(200,40,800)$$
$$+ 20 \times Sph(N/A,700,100)$$

This model indicates that the spatial variogram of FeTot is described by a nugget effect equal to 20, one spherical model with sill 20 at range 80 metres in direction N76°E, range 30 metres in direction N166°E and range 60 metres in direction perpendicular to the reference plane. The model is completed by additional two spherical structures with sills 30 and 20 respectively and with ranges as indicated. “N/A” is used to indicate that the structure is undefined.

As seen, the range in direction N166°E (approximately perpendicular to the ore strike) is relatively short. This short range is indicated in Figure 82, Section 4.10.2.

Other models used in the estimations and simulations are:

FeMagn

$$\gamma(h) = 2.2 + 3 \times Sph(90,40,120) + 2.6 \times Sph(N/A,150,90)$$

GaussFeTot

$$\gamma(h) = 0.2 + 0.4 \times Sph(70,25,60) + 0.3 \times Sph(400,35,200)$$
$$+ 0.15 \times Sph(N/A,100,N/A)$$

GaussFeMagn

$$\gamma(h) = 0.15 + 0.25 \times Sph(100,35,40) + 0.6 \times Sph(500,N/A,N/A)$$
$$+ 0.5 \times Sph(N/A,40,250)$$

GaussMnO used in the estimation of the conditional expectations

$$\gamma(h) = 0.99 \times Sph(160,30,120)$$

The conditional expectations of MnO

$$\gamma(h) = 0.1 + 0.4 \times Sph(140,38,80)$$

All experimental variograms and variogram models are given in Appendix M and N respectively.

Joint density

The average horisontal distance between the boreholes is 25 to 50 metres. The experimental variogram values for horisontal lag distances below 50 metres are therefore not well structured. This can be seen in the upper left part of Figure 107.

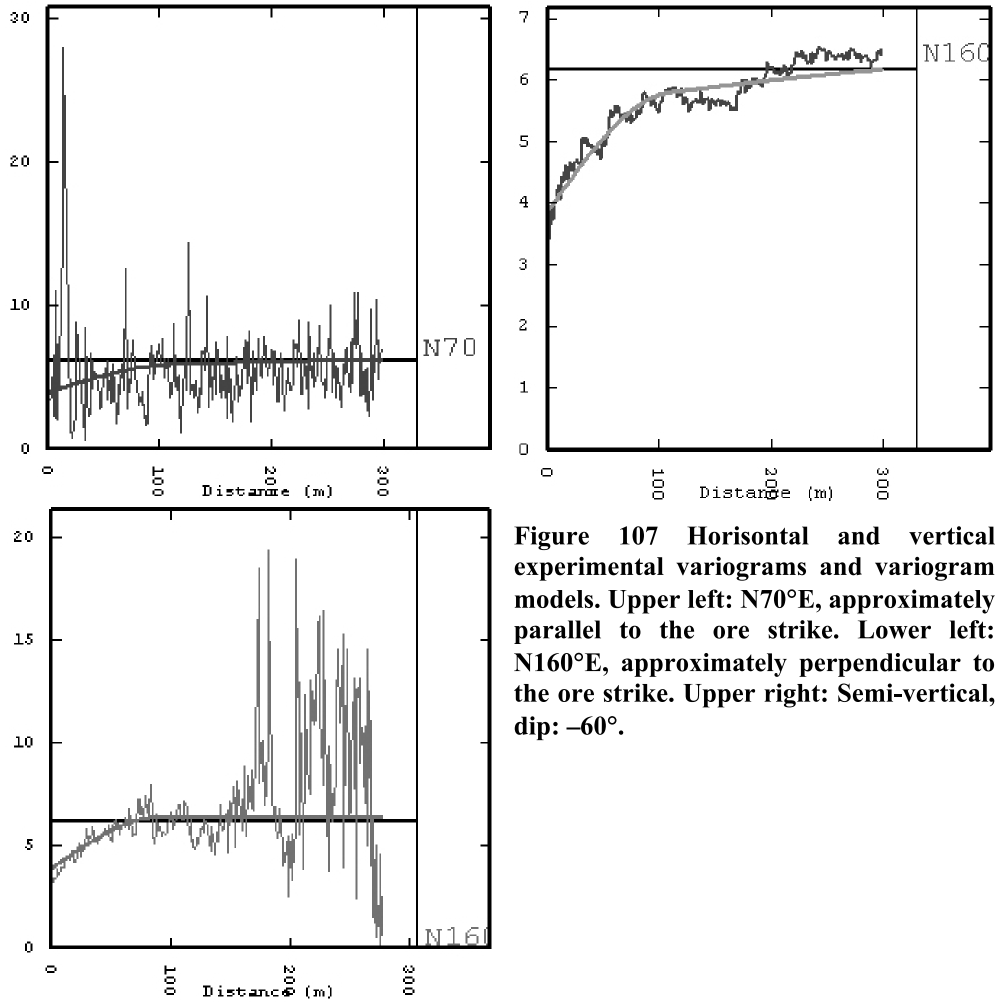

Figure 107 Horisontal and vertical experimental variograms and variogram models. Upper left: N70°E, approximately parallel to the ore strike. Lower left: N160°E, approximately perpendicular to the ore strike. Upper right: Semi-vertical, dip: –60°.

However, the semi-vertical experimental variogram is well structured.

The dominating joint set is the foliation joints, parallel to the ore strike. The foliation of the ore is steeply dipping. Therefore, a variogram structure found for the vertical direction, could also be applicable to the horisontal direction parallel to the ore strike. Applying this as a modelling principle the following variogram model for the joint density is obtained:

$$\gamma(h) = 3.84 + 1.7 \times Sph(110,90,110) + 0.8 \times Sph(500,90,500)$$

This model is shown in Figure 107.

5.7.2. Estimation

Fe

Grade tonnage curves

FeTot and FeMagn grade tonnage curves for the underground operation in question are given in Figure 108 and 109.

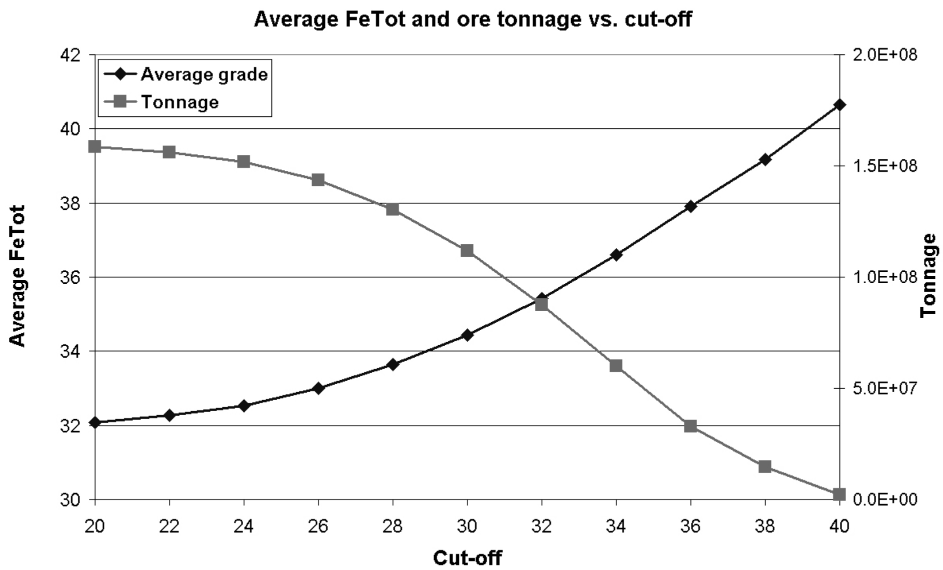

Figure 108 Average grade and ore tonnage vs. cut-off for total iron.

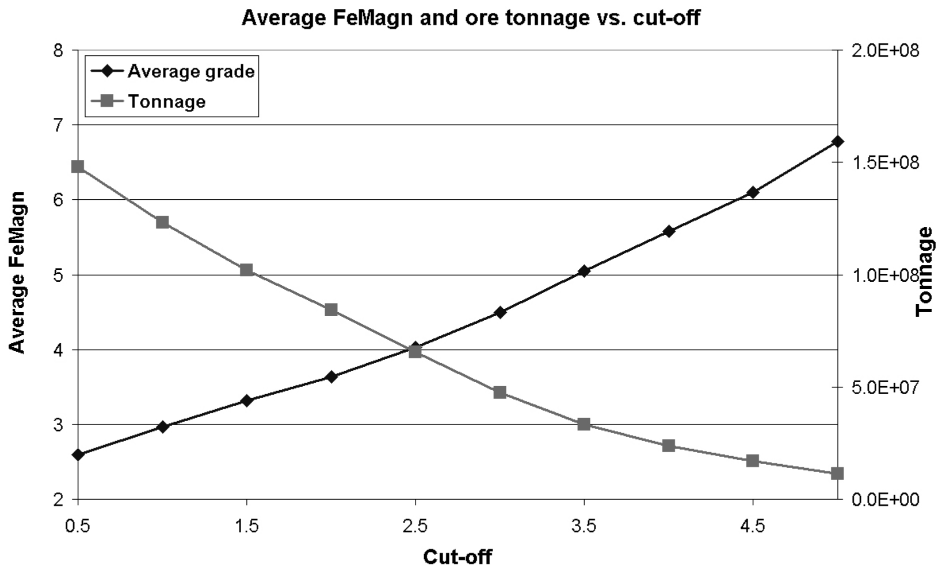

Figure 109 Average grade and ore tonnage vs. cut-off for magnetic iron.

The curves indicate that if a total iron cut-off equal to 20 where used, then there is 160 million tonnes of ore within the mineralised envelope with an average grade of about 32 % total iron. If the cut-off were increased to 30%, then the corresponding numbers would be 110 million tonnes of ore with an average grade of 34.4 %.

Histograms and summary statistics

Histograms showing the block dispersion for blocks with dimensions 40 x 10 x 50 metres for FeMagn and FeTot are given in Appendix J. The block model with colour coding according to total iron content and three horisontal planes through the block model are also given in Appendix J. Summary statistics given in Table 27:

Estimate					
	# of blocks	Mean	Stdv	Min	Max
FeTot	2332	31.84	4.72	13.68	41.97
FeMagn	2333	2.42	1.79	0.06	16.30

Estimation standard deviation					
	# of blocks	Mean	Stdv	Min	Max
FeTot	2332	4.77	1.08	1.82	7.69
FeMagn	2333	1.49	0.39	0.61	2.66

Table 27 Block summary statistics

To compare estimation results and drill cutting collection during open pit operation, the estimation results can be imposed onto the blast definition presented in the Section 3.5 (see Figure 110).

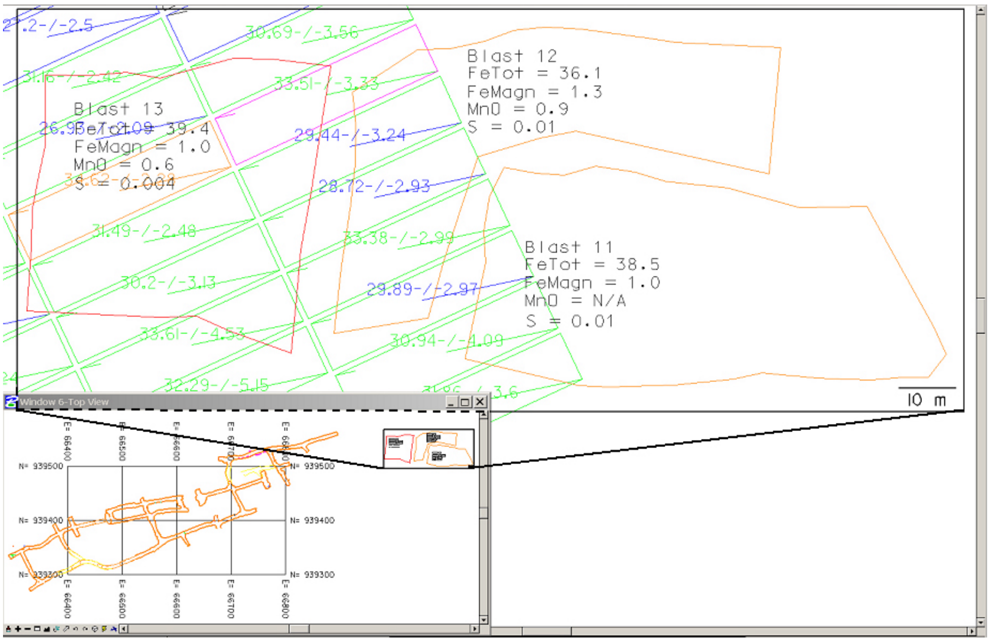

Figure 110 Blast information imposed onto estimation results.

From Figure 110, we can see that only blast 13 is within the estimated area. The average FeTot value of blast 13 is 39.4%. The blast contour is surrounded by blocks estimates in the range 30% to almost 35%. The corresponding kriging standard deviation is in the range from 2.5 to 5.15 at the edge of the mineralised envelope. One must however keep in mine that the estimated blocks visualised here goes from 360 metres above sea level and down to 310, whereas the blasts goes (only) from 360 to 345.

MnO

The MnO content of the ore has been estimated through kriging. The summary statistics for three approaches are given in Table 28. The three approaches include 1) estimation with hard- and soft data, 2) estimation with only hard data and 3) estimation with a varying search neighbourhood and an inclusion of soft data only in the estimation of those blocks that could not be estimated by the hard data. In the incorporation of soft data, the minimum and maximum MnO values needed for the different lithologies in the kriging with inequalities routine (see Section 4.8.7) have been derived from the non-hierarchical cluster analysis.

Estimate					
	# of blocks	Mean	Stdv	Min	Max
MnO; hard- and soft data	1760	0.60	0.50	0.04	3.24
MnO; hard data	975	0.50	0.44	0.08	3.41
MnO; varying neighbh	1766	0.47	0.40	0.08	3.41

Estimation standard deviation					
	# of blocks	Mean	Stdv	Min	Max
MnO; hard- and soft data	1760	0.38	0.11	0.15	0.73
MnO; hard data	975	0.30	0.07	0.15	0.54
MnO; varying neighbh	1766	0.37	0.12	0.15	0.71

Table 28 Block summary statistics for MnO [%]

The meaning of hard- and soft data is discussed in Section 4.8.7.

Figure 111 and 112 below show the block histogram for estimated MnO content.

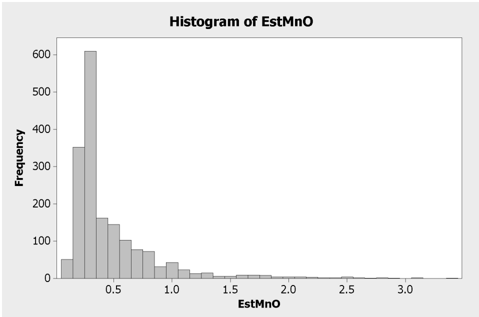

Figure 111 Block histogram for MnO estimated with a varying search neighbourhood and a partly inclusion of the soft data.

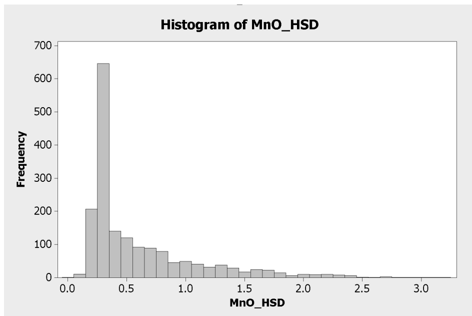

Figure 112 Block histogram for MnO estimated with hard- and soft data. Estimation results are positioned in Figure 113.

The summary statistics show that the number of estimated blocks have increased from 975 with the use of the hard data to 1760 if the soft data is included. The average MnO value increases from 0.5% to 0.6%. The corresponding standard deviation also increases. The increase in standard deviation is as expected since uncertain soft data is included in the estimation.

Figure 113 illustrate the estimation results implemented into the IT planning system.

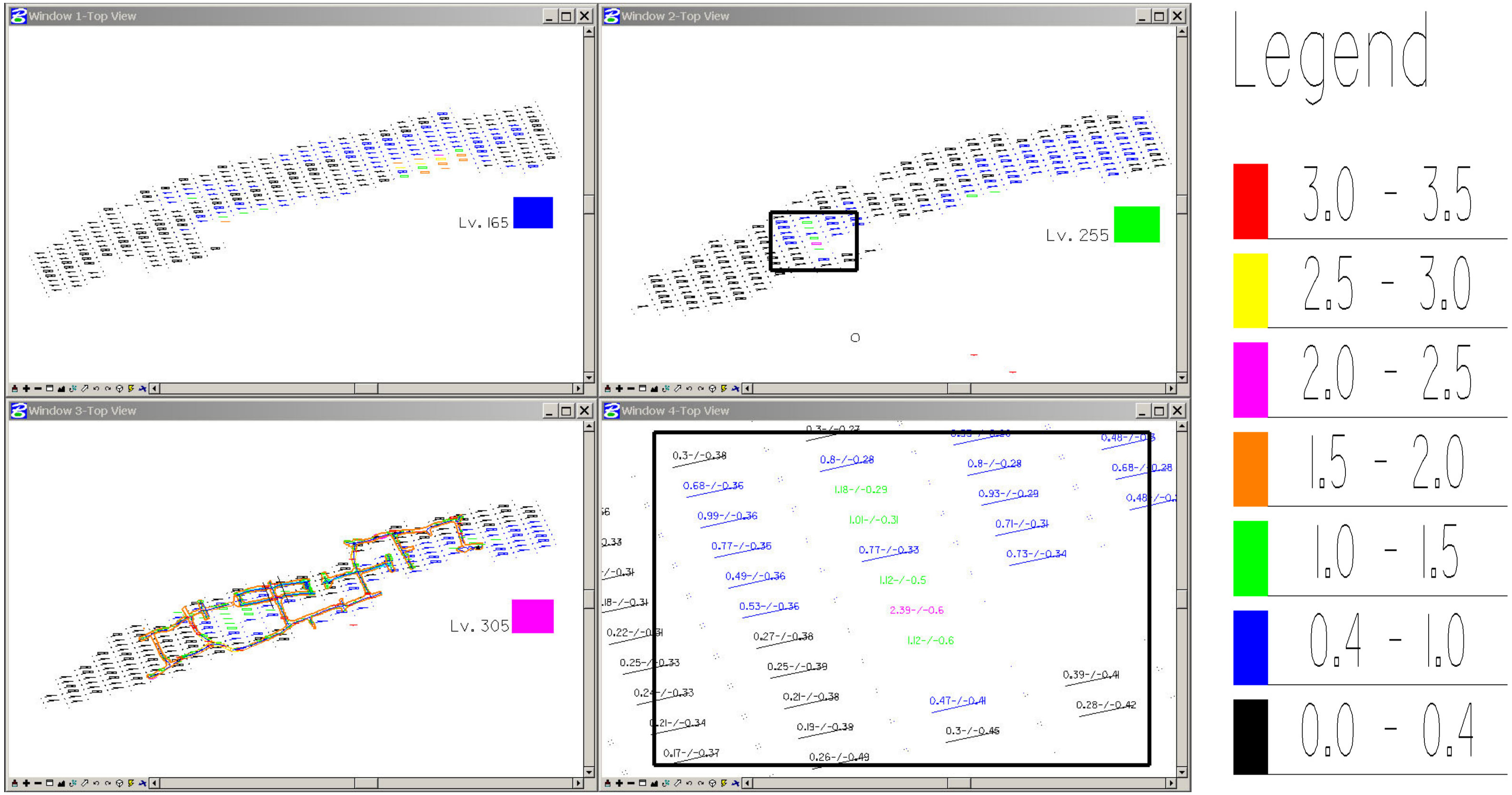

Figure 113 MnO at three different levels. MnO estimated using approach 3 above (this section), i.e. both hard- and soft data have been used. The numbers represent the estimate and the corresponding estimation standard deviation.

Joint density, RQD and RMi

The average joint density in blocks of size 25 x 10 x 25 metres has been estimated using kriging (see Figure 114).

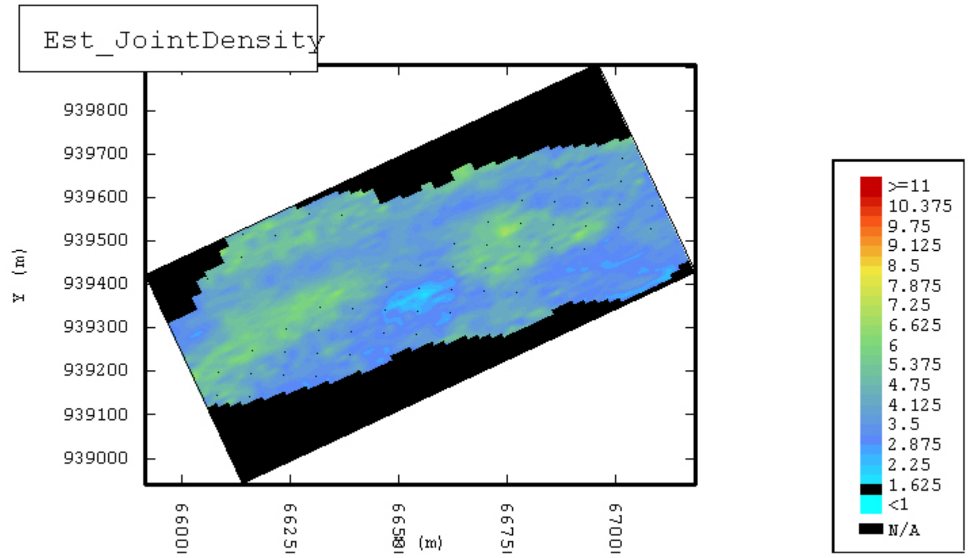

Figure 114 Estimated joint density values, level 255.

The average joint density in the blocks of size 25 x 10 x 25 metres varies from 1.7 to 10.2.

The RQD-value can be estimated from the joint density. See Section 4.5.2. Histogram and summary statistics for joint density and estimated RQD are given in Figure 115 and 116.

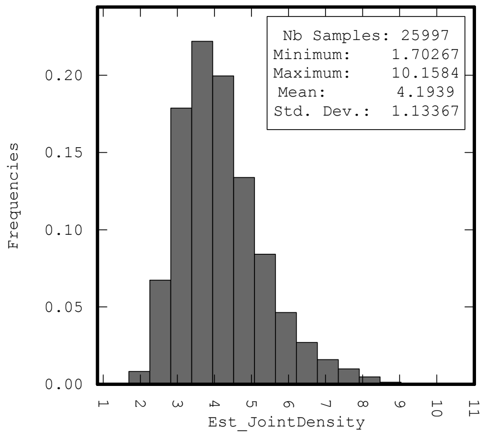

Figure 115 Histogram and summary statistics for estimated joint density (foliation joints).

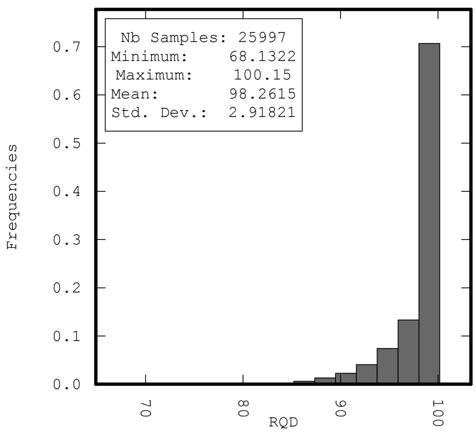

Figure 116 Histogram and summary statistics for estimated RQD.

The histograms and the summary statistics are of low value without coordinates if the aim is to predict potential stability problems. Figure 117 shows the estimated RQD at level 255 (i.e. 255 metres above sea level) across the area of interest.

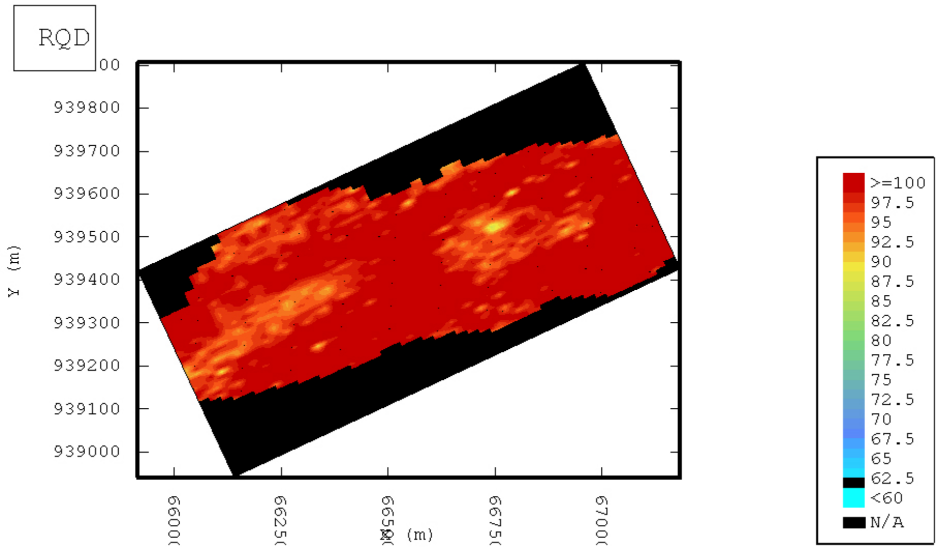

Figure 117 Estimated RQD values.

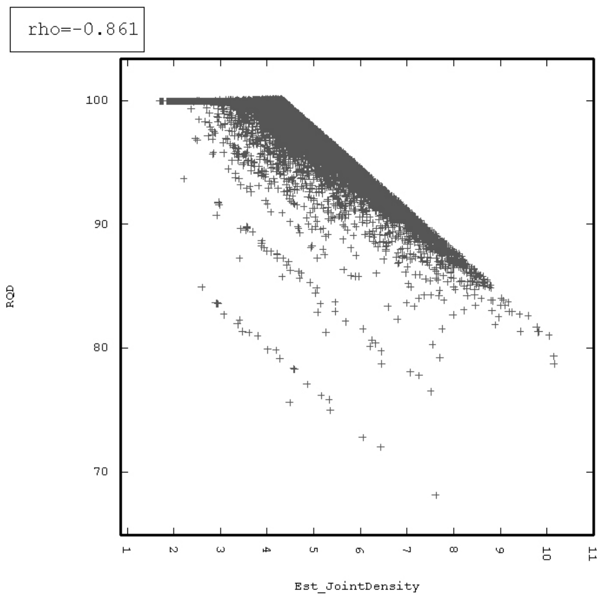

Figure 118 Scatter plot joint density vs RQD.

The RQD varies from 68.13 to 100.15. The few RQD values above 100 are an artefact due to rounding of the input parameters used in the equation defining the relationship between volumetric joint count and RQD (see Equation (37)).

The estimated RQD value is rather high all over the area; however, there are zones where the RQD value is lower indicating a higher concentration of joints. This is also seen if Figure 114 and 117 are compared.

The scatter plot in Figure 118 shows the relationship between estimated joint density and RQD. The plot shows that the RQD value is more or less independent of the joint density as long as the joint density is below 3.

Given the joint characteristics in Section 3.6, the following joint data input has been used in the RMi calculations. These factors are based on quantification sheets in Palmström (1996):

Joint alternation, jA	1.5
Joint roughness, jR	2
Joint size, jL	0.875
Joint cond factor, jC	1.17
Uniaxial compr strength, sigma c	60
Beta value	41

Table 29 RMi-input.

In Table 29, the beta value has been obtained using Equation (36) in Section 4.5.2 and expected block dimensions. The uniaxial compressive strength (Sigma c in Table 29) is based on tests performed on core samples (Sintef Bergteknikk 1993, Myrvang 2001, Nilsen 2003).

Given the joint density and the other input parameters in Table 29, the RMi value can be estimated according to equations presented in the Section 4.5.2. The results are presented in Figure 119.

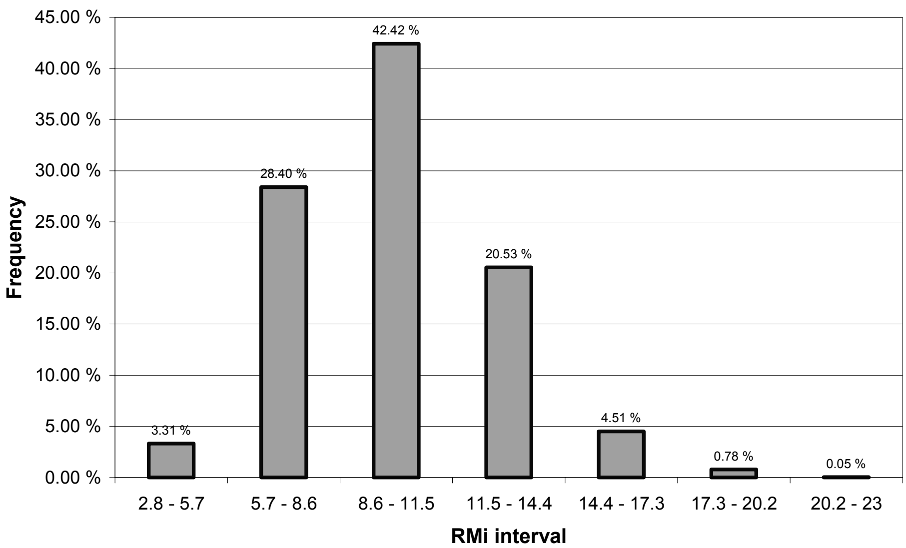

Figure 119 Percentage of blocks with estimated RMi interval within interval.

These results have been implemented in the production planning system and illustrated in Figure 120 and 121:

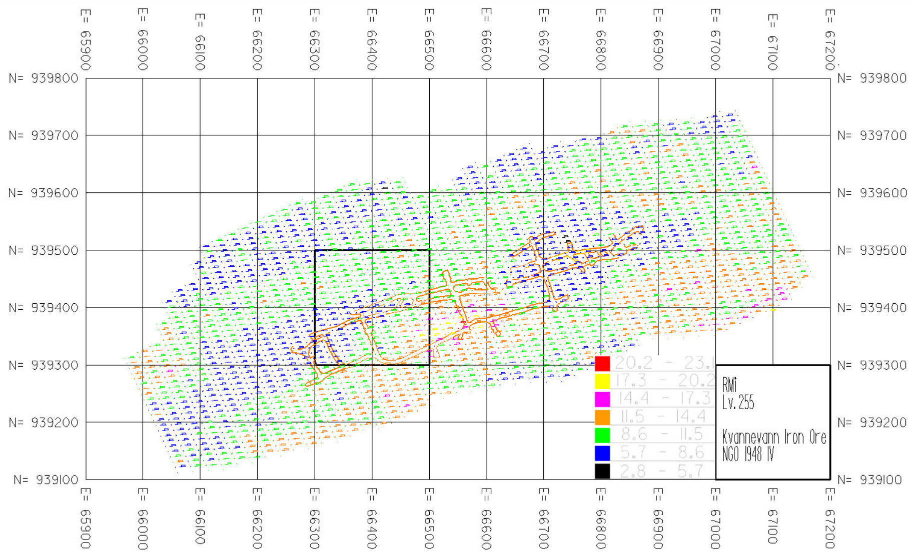

Figure 120 RMi-variations at level 255. Square enlarged in the next figure.

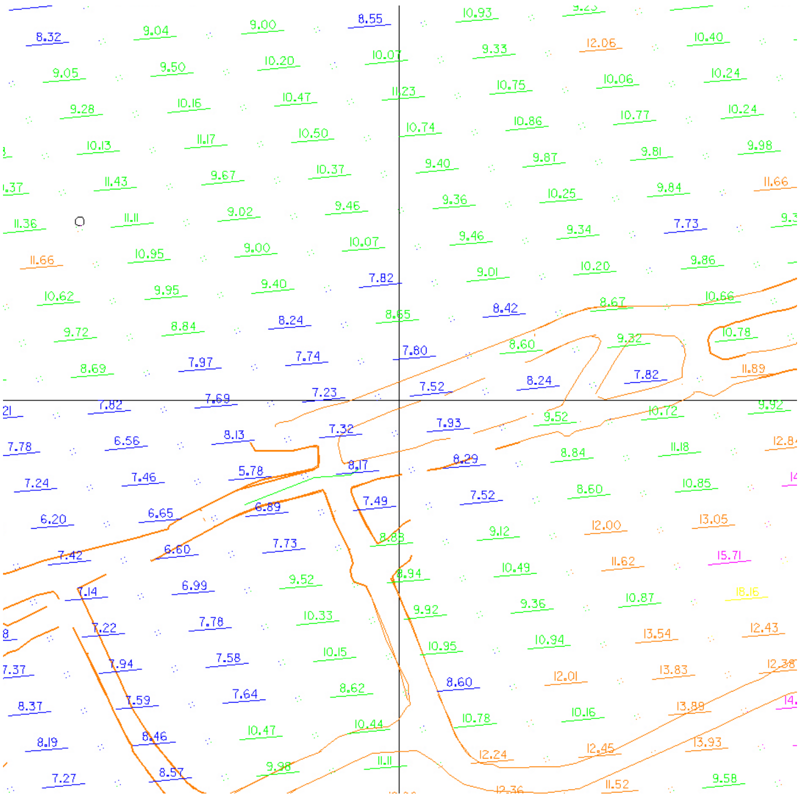

Figure 121 RMi-variation at level 255; blow up.

The CAD system used in the production planning can be used to draw attention to certain aspects of the geoinformation at hand. The geoinformation is organised in layers in the CAD system. Each RMi interval defined in the legend in Figure 120 is assigned to one specific layer in the CAD file. Information of special interest can thereby be emphasised by turning off layers that contain information not interesting for the problem in question.

Figure 122 illustrates a mine map at level 320 with superimposed information about the RMi value in the range 2.8 to 5.7. Figure 123 shows a map where zones with RMi values in the interval between 2.8 to 5.7 at level 180 is highlighted. Violet lines in Figure 123 represent the mineralised envelope.

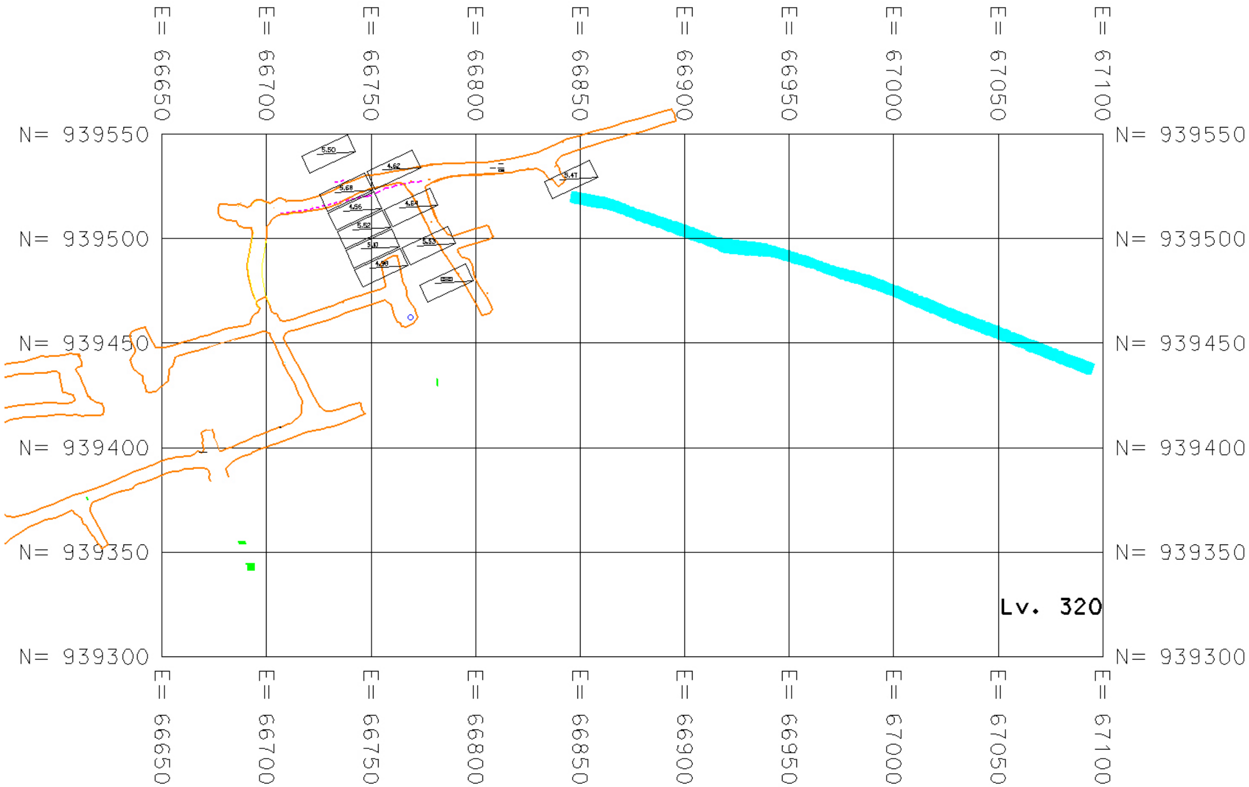

Figure 122 Black blocks indicating RMi-values in interval from 2.8 to 5.7 between level 300 and 330. Mine map at level 320. Weakness zone from Nilsen (1979) extended down to level 320 indicated in light blue colour. Core loss indicated in green.

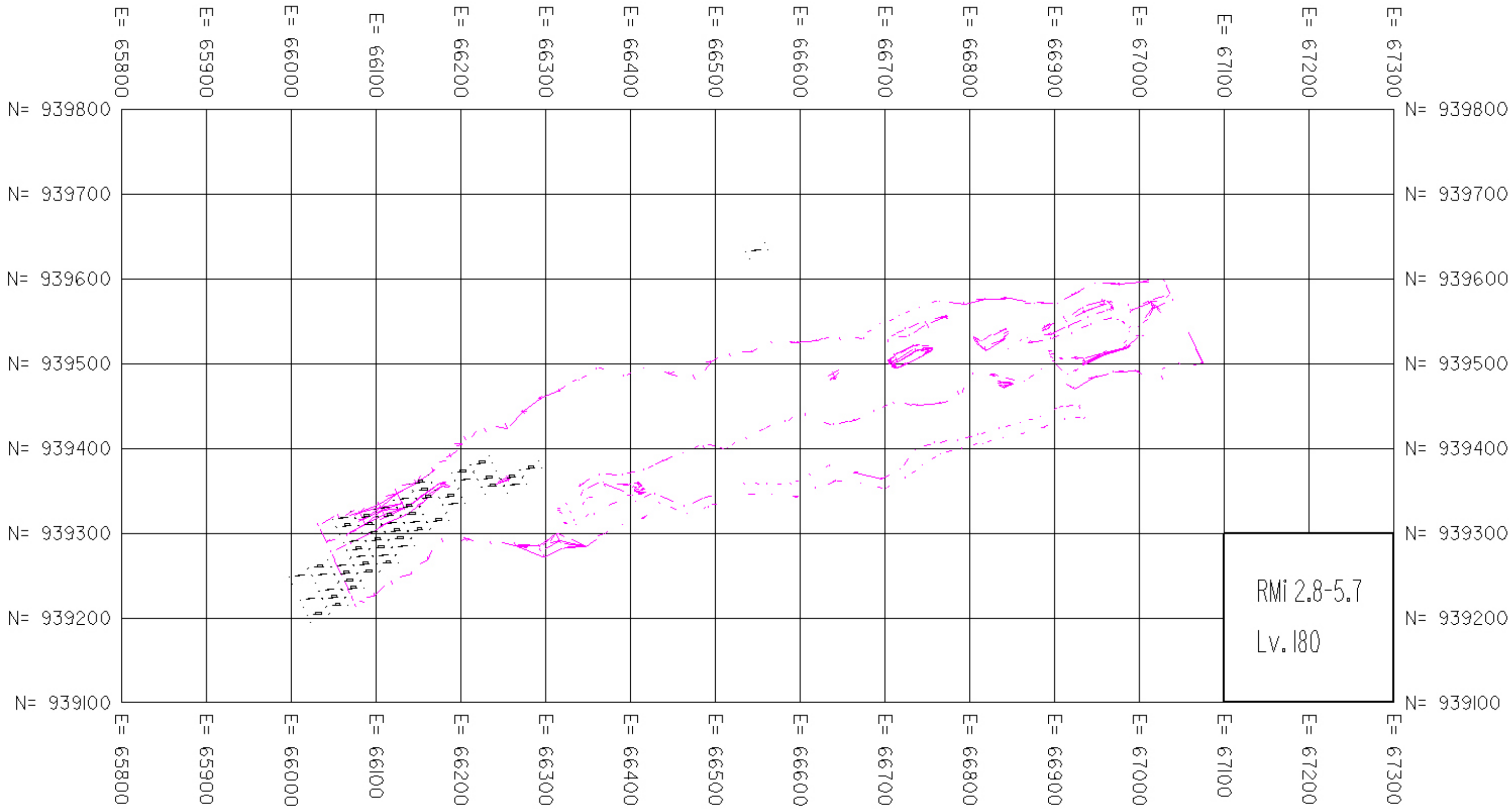

Figure 123 Black "dots" indicating an estimated RMi value between 2.8 and 5.7 at level 180. Violet lines represent the mineralised envelope.

5.7.3. Simulation

Based on simulation realisations in small blocks (5x2x5 meter) the average value in each large block (SMU, 40x10x50 meter) in both planned and already produced stopes have been computed. Stope 4 has been selected for illustration. Stope 4 is parallel to stope 3 shown in Figure 130.

FeTot and FeMagn

For illustration, a selection of fifteen realisations has been plotted against SMU number in Figure 124.

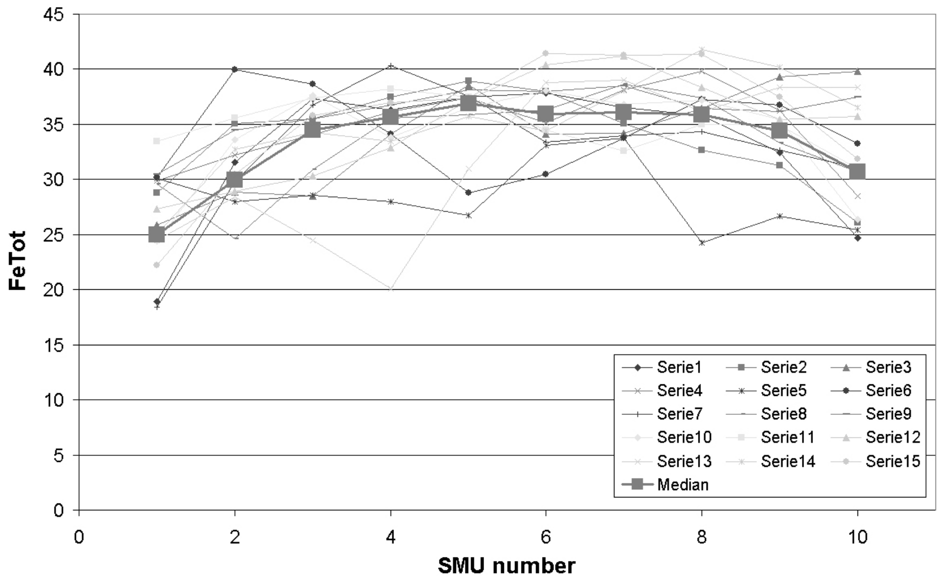

Figure 124 Fifteen out of one hundred possible realisations of SMU averages along stope 4 at level 279, i.e. between 254 and 304. Median indicated by the thick blue line.

The long axis of the stope is directed perpendicular to the ore, approximately N155°E. The SMU numbering starts at the southern end of the stope.

From Figure 124, it can be seen that the iron grade varies across the stope. The SMUs in the middle of the stope (SMU number 5 to 8) have the highest expected FeTot content. With a slightly higher decrease at the southern end, the FeTot grade decreases towards both ends of the stope.

In Figure 125, the FeMagn content across stope 4 is shown.

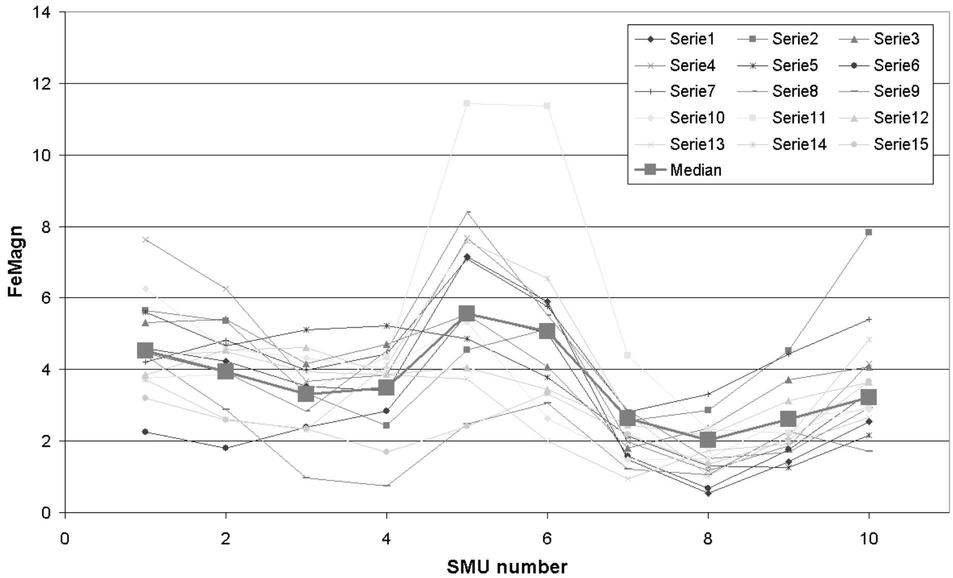

Figure 125 Simulation results for FeMagn in the same stope as in the Figure 125.

Compared to FeTot, the FeMagn content varies considerably more. A slight increase in value can be seen towards each end of the stope (SMU 1 and SMU 10). In addition, a peak is reached in the middle of the stope (SMU 5 and 6). There seems to a general decreasing trend from SMU 1 to SMU 10, i.e. from the southern end of the stope and northwards.

Summary statistics for the simulations of FeTot and FeMagn of each SMU in the stope 4 are given in the Table 30 and 31.

FeTot	4				
Level / SMU	Lv. 279		Lv. 329		
	Mean	Stdv	SMU	Mean	Stdv
1	24.5	6.3	11	25.7	3.2
2	29.8	4.9	12	30.6	3.0
3	33.4	4.0	13	34.8	2.5
4	35.0	3.6	14	37.3	2.2
5	35.8	3.4	15	37.2	2.3
6	35.5	3.4	16	38.0	1.9
7	35.9	3.0	17	37.7	1.6
8	36.2	3.0	18	34.6	1.6
9	34.1	3.7	19	31.0	2.5
10	30.1	4.7	20	28.0	4.6

Table 30 Summary statistics for the total iron content organised according to SMU number.

FeMagn	4				
Level / SMU	Lv. 279		Lv. 329		
	Mean	Stdv	SMU	Mean	Stdv
1	4.9	1.8	11	6.1	1.5
2	4.0	1.4	12	3.8	0.9
3	3.4	1.2	13	4.0	1.0
4	3.6	1.3	14	5.4	1.2
5	6.0	2.0	15	4.8	1.1
6	5.2	1.8	16	3.6	0.8
7	2.7	1.0	17	3.1	0.7
8	2.1	0.8	18	2.6	0.6
9	2.8	1.1	19	3.4	0.8
10	3.5	1.5	20	3.4	1.1

Table 31 Summary statistics for the magnetic iron content organised according to SMU number.

Having the simulation results for the SMUs in the stope, the probability that a SMU has a content of total iron (for example) above some cut-off value can be estimated simply by counting the number of realisations above this cut-off and dividing this number by the total number of realisations. This has been done and the result from the same stope as in Figure 124 and 125 is illustrated in Figure 126.

In Figure 126 the cut-off value is for illustration purposes set to 34 % total iron. The probability that the SMU value at level 279 is above this cut-off increases from below 10% to almost 80% from SMU 1 to SMU 8. SMU number 13 on level 329 has an estimated probability of about 60% to be above 34%. Moving north in the stope, the probability approach 100% for SMU 14, 15, 16 and 17.

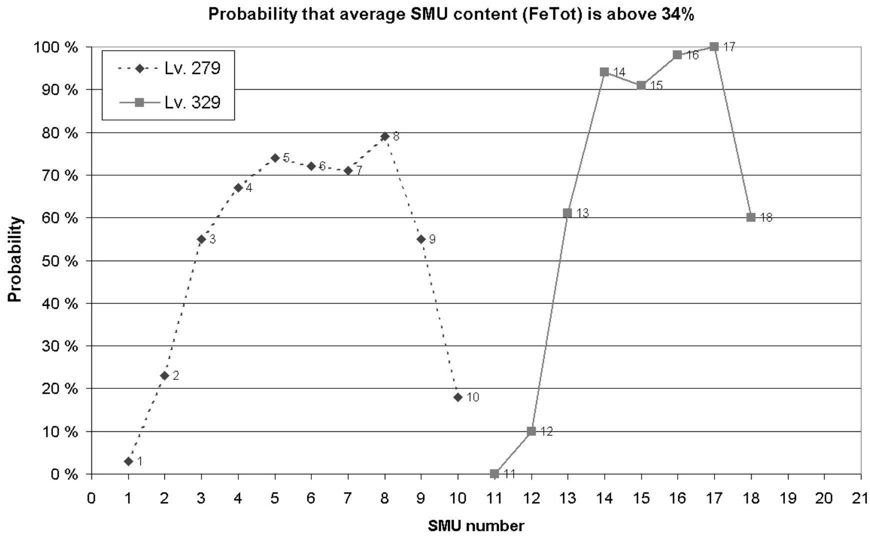

Figure 126 Probability estimate that the average content of a SMU is above the given cut-off. The probability estimate is obtained from simulation realisations.

Similarly the probability that the SMU average is below some cut-off or within an interval can be estimated. The probability that the average FeTot is below 25% is illustrated in Figure 127.

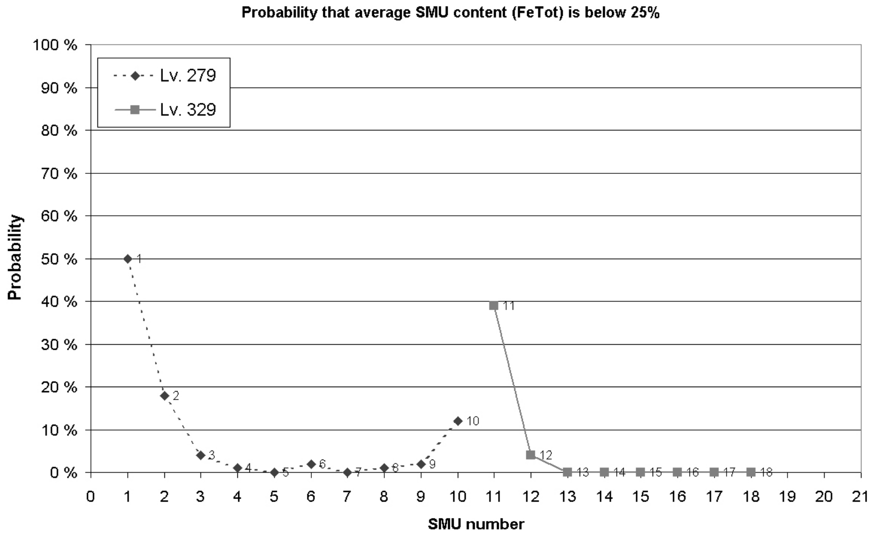

Figure 127 Probability estimate that the average content of a SMU is below 25%. The probability estimate is obtained from simulation realisations.

As shown in Figure 127, the probability that the average FeTot content is below 25% is almost zero for all SMUs except for the first SMUs on each level and the last SMU on level 279.

This could also be used as a dynamic tool to assess how the probability that the average content of a SMU is changing as a function of the cut-off. This is illustrated in Figure 128.

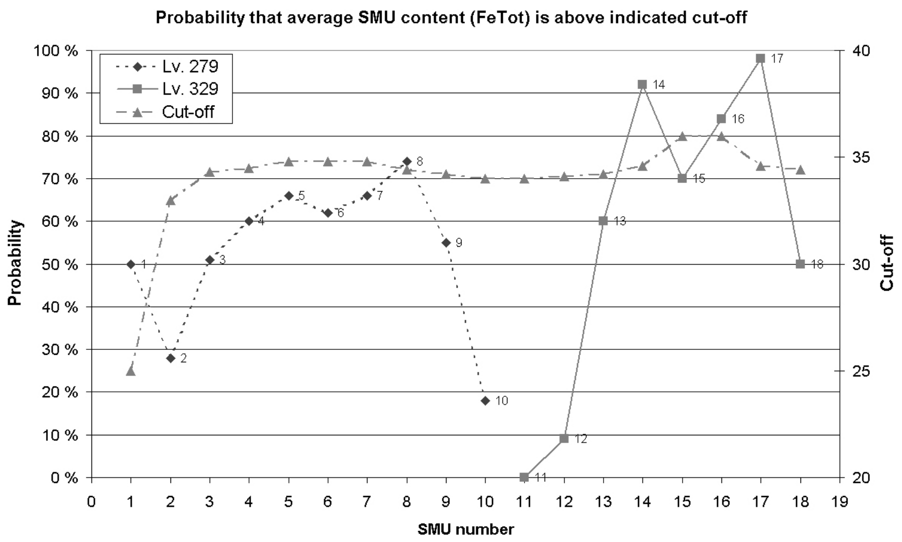

Figure 128 Probability that the SMUs are above a dynamic cut-off changing across the stope.

From Figure 128 it can be seen that the probability that SMU 1 (Level 279) has an average content above 25% is 50%. Further it can be seen that there is a probability equal to 70% and 82% that the content of SMU 15 and 16 respectively exceed 36%.

5.7.4. Density estimations based on simulation results

As illustrated in Section 4.3.2, the average density of an iron ore cannot be obtained from the average content of iron unless the distribution of iron is known. This fact is demonstrated in this section.

The density has been estimated with two different approaches: 1) from the mean FeTot in the SMUs by using the non-linear relationship between iron grade and density defined in Section 5.2.6, and 2) from the mean of density estimations based on each FeTot realisation in each SMU.

Approach 1

The basis of this density estimation is the average FeTot value of the SMU. This average value has been retrieved from the small blocks within the SMU. The density is then estimated using Equation (76). This equation is a modification of the general Equation (15) from Section 4.3.2.

$$\rho_{SMU} = \frac{1}{0.3702 - 0.2507 * Fe_{Tot,\, SMU\, mean}} \qquad \textbf{Eq. 76}$$

Approach 2

The basis of this density estimation is each single simulation result attached to the small blocks within each SMU. The density of n small block is estimated using Equation (76), and the average density of the SMU is computed from these estimations using Equation (77). This equation is a modification of the general Equation (15) from Section 4.3.2.

$$\rho_{SMU} = \frac{1}{n}\sum_{i=1}^{n} \frac{1}{0.3702 - 0.2507 * Fe_{Tot,\, small\, block}} \qquad \textbf{Eq. 77}$$

Approach 1 vs. approach 2

To compare the two approaches described above, the results from one SMU can be plotted in a scatter plot. The plot in Figure 129 shows 100 estimations of the density in SMU 5, stope 4. This is based on 100 realisations of the total iron content in the SMU.

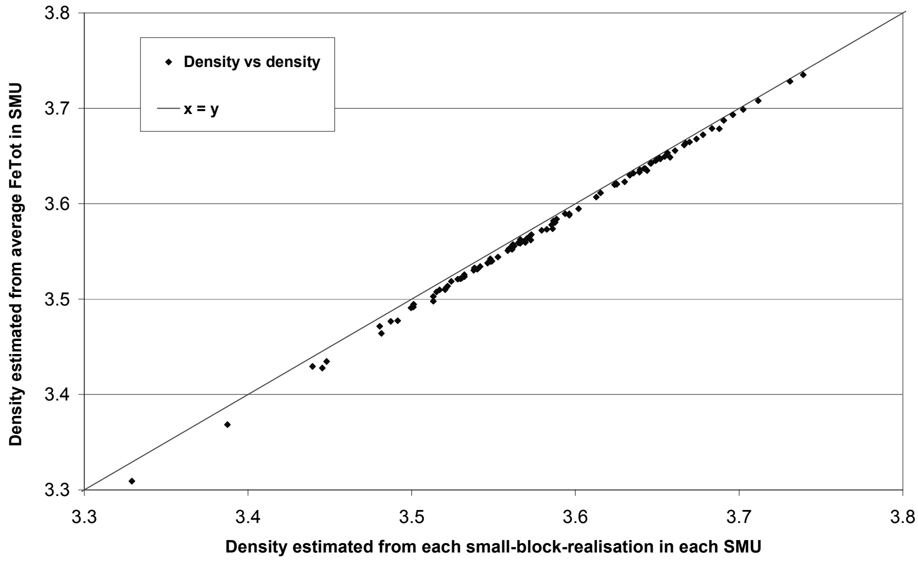

Figure 129 Estimation of density based on single simulation results vs. density estimated from mean FeTot in the SMU.

The straight line in Figure 129 is the first bisector line y = x. All values plot below this line. This means that approach 1 using the average total iron content in the SMU underestimates the density compared to approach 2. This is in accordance with illustrations in Section 4.3.2.

This means that approach 2 should, whenever possible, be used.

5.8. Cluster analysis of ore assays

5.8.1. Introduction

To utilise the advantages of both hierarchical and non-hierarchical cluster analysis, they have been used in combination.

See Section 4.6.4 for description of the input data.

5.8.2. Hierarchical cluster analysis

Results from the hierarchical cluster analysis are given in Appendix K.

Five clusters were formed based on similarity level. Their summary statistics are given in Appendix K.

5.8.3. Non-hierarchical cluster analysis

The cluster centroids of the five clusters defined in the hierarchical cluster analysis were used as seeds. The summary statistics from the non-hierarchical analysis is included in Appendix L.

The final cluster centroids from the non-hierarchical analysis are in accordance with the result from the hierarchical analysis.

5.8.4. Interpretation

To interpret the results the standardised average for each cluster, as defined from the non-hierarchical cluster analysis, is given in Table 32. The standardised mean is used because the difference in magnitude between the variables is large. See Section 4.6.4. A standardised average below zero means that the cluster is characterised by an average value below the grand average. For example, the standardised average for FeMagn in cluster 1 is -0.51. This means that cluster 1 contains observations relatively low on FeMagn.

Variable	Cluster 1	Cluster 2	Cluster 3	Cluster 4	Cluster 5
FeMagn	-0.51	-0.15	-0.74	1.27	1.47
MnO	-0.04	-0.33	3.34	-0.38	-0.21
P	1.06	-0.34	-0.73	-0.79	-1.29
S	-0.10	-0.20	-0.007	0.01	6.66
FactorScore	-0.24	-0.66	0.97	1.25	0.81

Table 32 The standardised mean for each cluster illustrating their characteristics

The factor score is used instead of FeTot and TiO_2 due to the correlation between these two variables. See Section 4.6.4. A high factor score indicates a low FeTot value and a high TiO_2 and vice versa.

Based on the standardised mean given in Table 32, the clusters can be interpreted. The interpretation is given in the list below, by naming the clusters. Geochemical characteristics are included.

- Cluster 1 – Hematite ore
    - This cluster is characterised by a high level of P, a high level of FeTot and a low level of TiO_2.
- Cluster 2 – Magnetite – hematite ore

    - This cluster is high in FeTot, low in TiO_2 and high in FeMagn relative to cluster 1 and 3. It is low in P.
- Cluster 3 – Manganese – hematite impregnation
    - This cluster is very high in MnO
- Cluster 4 – Magnetite impregnation
    - This cluster is relatively high in FeMagn and very low in FeTot and high in TiO_2.
- Cluster 5 – Sulphurous magnetite impregnation
    - This cluster is very high in FeMagn and extremely high in S.

5.8.5. Validating and profiling

A second non-hierarchical analysis with different seed values was performed to validate the results. Similar clusters were obtained.

Profiling was not performed since all variables are included in the cluster analysis.

5.9. Value chain simulation

The final outputs from the value chain of Rana Gruber AS are the hematite- and magnetite products. The expected product tonnage can be estimated using the probabilistic approach described in Section 4.10.2. Here exemplified with stope 3 (see Figure 130).

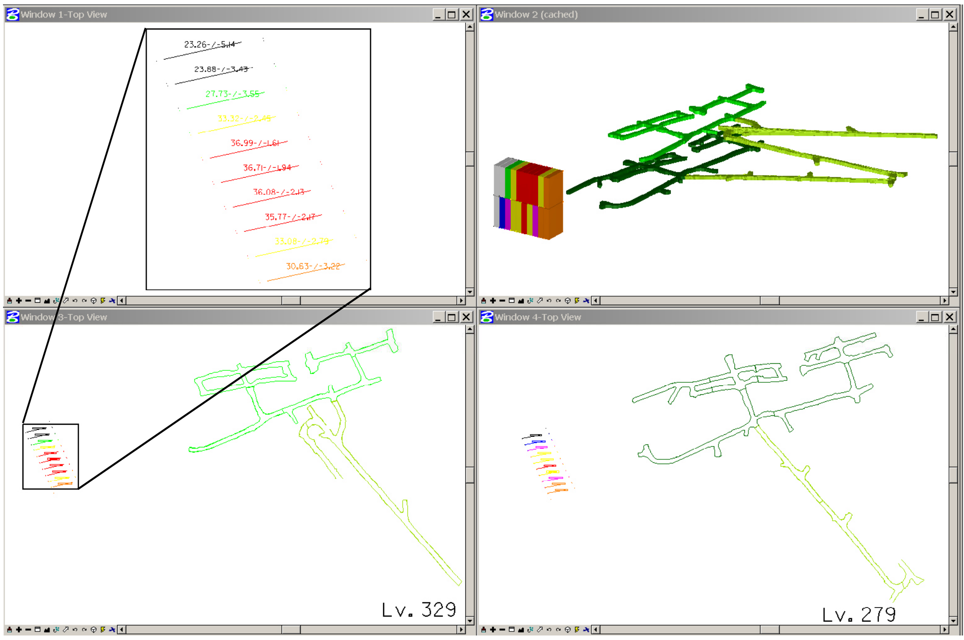

Figure 130 Planned stope 3 relative to the mine map with estimated SMU FeTot average (average of 100 average SMU realisations) and corresponding dispersion standard deviation of the 100 SMU averages.

Using the FeTot and FeMagn realisations from the stope, the plots in Figure 131 and 132 are obtained. They show cumulative distributions quantifying the expected product tonnages from SMUs at level 329 in the planned stope 3. The steepness of these curves indicates the degree of uncertainty. A steep curve indicates a high degree of certainty. It can be seen that the uncertainty is at the greatest, both for magnetic based products and hematite based products, at the start and the end of stope 3. This corresponds to plot marked c31 and c40 (magnetite product) and c11 and c20 (hematite products).

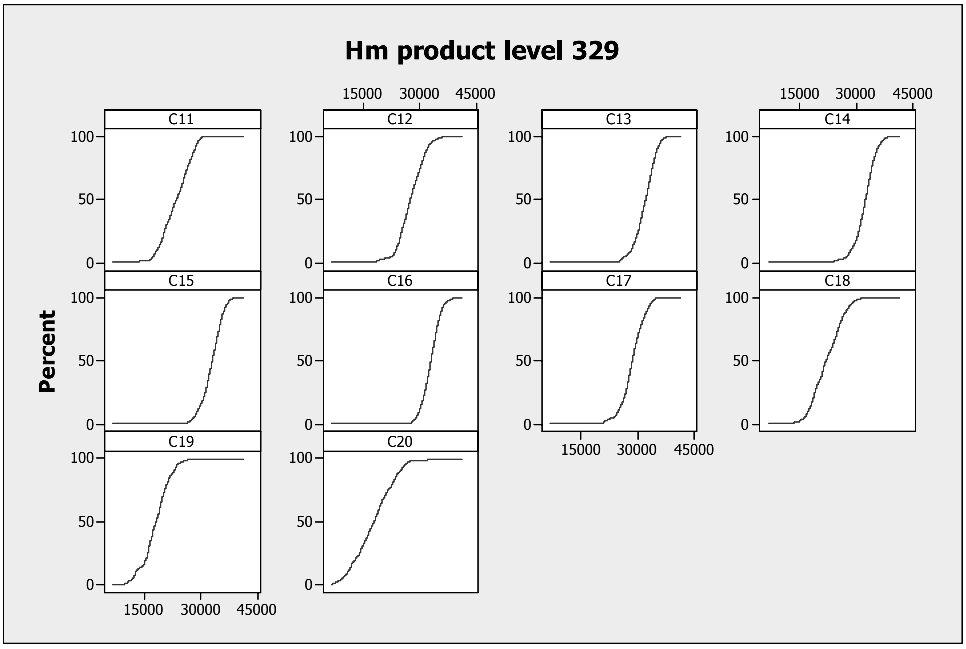

Figure 131 Expected product tonnages from SMU 1 (C11) to SMU 10 at level 329 (C20) from the planned stope 3.

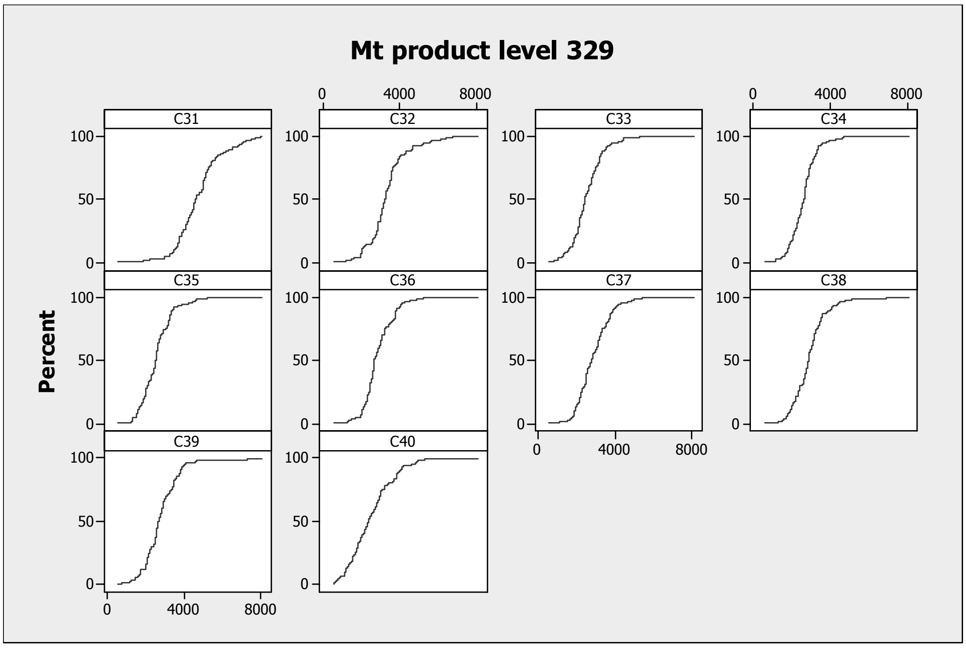

Figure 132 Expected product tonnages from SMU 1 (C31) to SMU 10 (C40) at level 329 from the planned stope 3.

Percentile	Product tonnage
5%	27671
50%	32203
95%	36736

Table 33 Percentile and corresponding product tonnages. There is a 5% chance that the product tonnage is lower than 27671 and there is a 95% chance that the product tonnage is below 36736.

Each of the cumulative distributions can be further investigated by fitting a parametric distribution to the experimental data. Below, a normal distribution has been fitted to the data in Figure 131. The 5%, the 50% and the 95% percentile have been calculated and are given in Table 33. The graph in Figure 133 illustrates that there is a 5% probability that the Hm-product tonnage from SMU 4 will be lower than 27700 (rounded) tonnes. Similar for 50% and 95%, i.e. there is a 50% probability and a 95% probability that the Hm-product tonnage from SMU 4 will be lower that 32200 (rounded) and 36700 tonnes respectively.

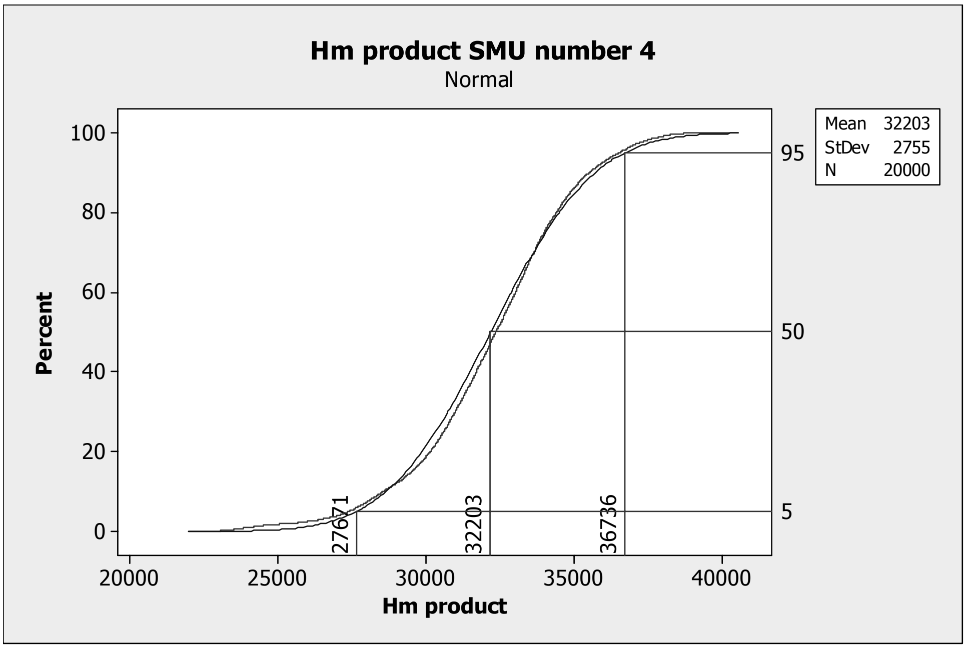

Figure 133 Expected product tonnages from one single SMU at level 329 from the planned stope 3.

5.10. Risk

5.10.1. Events

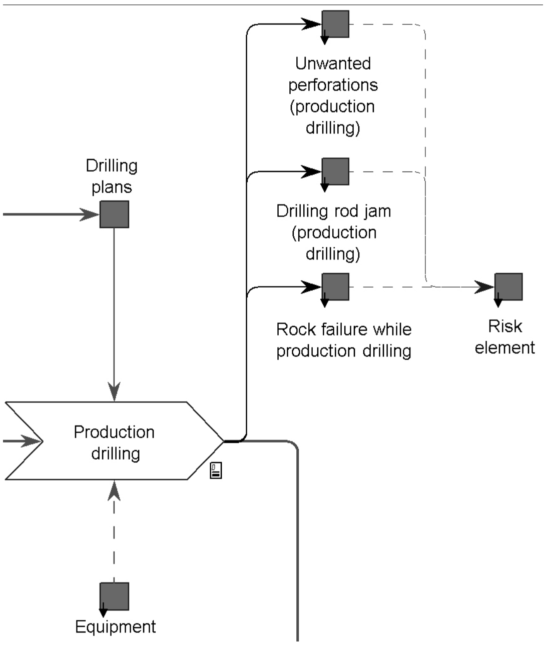

Figure 134 Possible block fall / rock failure during production drilling.

Possible events related to the mining value chain of Rana Gruber AS have been identified along the value chain:

1. An SMU does not on average contain ore with the required specifications when it comes to
   - FeTot
   - FeMagn
2. Block fall / rock failure.

The event related to rock failure is also given and illustrated as a secondary output from the production drilling process in Figure 134.

In particular, the following events have been defined:

- FeTot:
  - The average FeTot content of a SMU is between 25 and 34%. As can be seen in Figure 98, 34% represent the approximate Q75 cut-off required if FeMagn is equal to zero.
- FeMagn
  - The average FeMagn content of a SMU is between 1.2 and 2.5%. 1.2% approximates the lowest grade where any magnetite products are produced, whereas 2.5% approximates the average in the deposit.

5.10.2. Consequences

The economic consequence related to the event that iron ore that is not in accordance to the ore requirements is produced, could be quantified by an evaluation of the resulting decrease in recovery, product price and product tonnage. The economic consequences related to the events defined in 5.10.1 are:

- FeTot:
    - NOK 1.3 million
- FeMagn
    - NOK 0.9 million

The related economic risk is illustrated in Figure 135.

The consequence related to rock failure is more difficult to estimate. Firstly, a rock failure may have fatal consequences. It is difficult, if not impossible to assign a monetary value to such an accident. Secondly, the rock failure may lead to destruction of equipment. In turn this might lead to stop in production and increased repair costs.

5.10.3. Estimated economic risk

Based on the estimated probabilities in Section 5.7.3 and the above economic consequences the economic risk has been estimated from Equation (78), also given in Section 4.9.1.

$$Risk = Consequence\ x\ Probability \qquad \textbf{Eq. 78}$$

Figure 135 shows the economic risk related to the events that the ore does not contain the required amount of FeTot and FeMagn in stope 3, i.e. the average SMU content is between 25 and 34% for FeTot and between 1.2 and 2.5% for FeMagn.

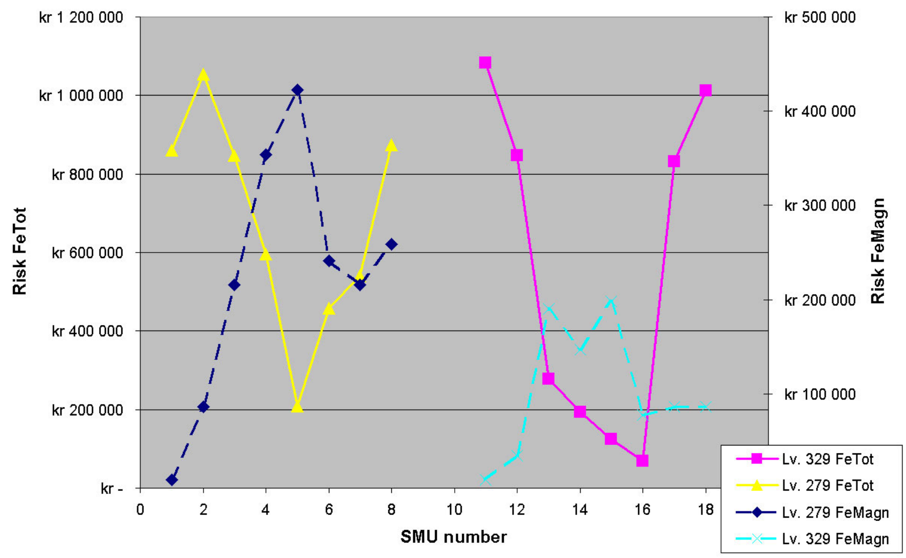

Figure 135 Estimated risk related to the event that FeTot is between 25 and 34% (below required) and that FeMagn is between 1.2 and 2.5% (below required) in stope 3.

In Figure 135, SMUs with a high probability that the content is below the lower limit have been excluded. This applies to SMU 9 and 10 and SMU 19 and 20.

Having estimated more risks, the risk matrix presented in the Section 4.9.4 could have been used to compare risks and thereby be able to prioritise which risk to reducing.

6. Discussion

There are three kinds of lies: lies, damned lies and statistics

Mark Twain

6.1. Introduction

Can we ever, within a reasonable cost and timeframe, completely know our deposit? Can we ever know the ore variations? Can we ever know it's behaviour when it comes to stability?

It is depressing that the answer to all these questions are negative. However it is always possible to know it better than we do at a given time. That is called continuous improvement. If continuous improvement is taken seriously and implemented in the mining value chain, the deposit will be known at the time of depletion.

Implementation of continuous improvement would include collection, storing and analysis of geodata. This comprises geological observations in the mine, ore feed grades, and rock failures and joints.

We must simply "let the ore body speak", listen, react and perform. The problem is to know what to listen for and when to react.

6.2. Process analysis

The process analysis identifies and visualises processes, inputs and outputs and can be used to define the person or people who are responsible for the process execution. Further, if executed correctly it can be used to elucidate bottlenecks and thereby bring improvement. By including information or data as a major output, the process analysis can be used to identify necessary computer systems.

However, the potential that lies in the method can only be realised with the involvement of the organisation as a whole or at least representatives from the organisation.

6.3. Grade estimation and simulation

A decision based on relevant information is probably good. A decision that is not based on reliable information is probably erroneous. That is why estimation and simulation techniques are used to turn geodata into useful geoinformation. However, simple approach could be sufficient. That is why a reasonable prediction of TiO_2 can be obtained from the good correlation between TiO_2 and FeTot.

The estimated value obtained using kriging at an unsampled point is the most probable value given the data, the data configuration and the variogram model. If the question is what is the most probable value, then estimation is the correct technique to use. If a "what if" is requested, then simulation and not estimation will provide the answer. The reason is that the simulation gives an indication of how far from the expected value the real outcome may be. This indication can then be used as valuable input in a risk- and uncertainty analysis. The aim of such an analysis would be to improve the mining risk profile presented in Section 4.9.3.

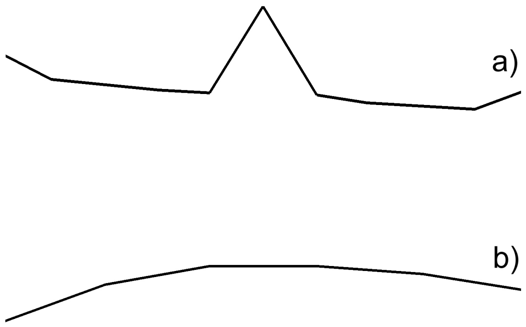

Figure 136 Generalised shapes showing how a) the FeMagn- and b) the FeTot grade varies along the stope.

From the simulation results presented in Section 5.7.3, it can be seen that the FeMagn- and FeTot grades vary along the stope according to the general shapes illustrated in Figure 136 a and b respectively. The FeMagn grade is highest in the middle of the stope with a small increase towards the ends. The FeTot grade is highest in the middle of the stope. The simulation results also indicate that the verity is considerable. Deviations from the general shapes can therefore not be excluded. More geodata could and should be collected to reduce this verity. This could be accomplished through the use of the drill cutting collector during drift drilling or and perhaps preferably, through the collection of cuttings during production drilling, possibly supplemented by borehole geophysics. A collection of drill cuttings along the drifts would supplement the existing geodata and possibly contribute to an uncertainty reduction.

The simulation output can also be used in a Bayesian manner. The basis is the many possible realisations and the correlation between them. If the content of the first SMU is quantified, then the probable content of the second SMU can be quantified with a higher degree of confidence than before. Theoretically this would also account for the third SMU, but figures given in Section 4.10.2 show that the correlation between SMUs not in direct contact with each other is negligible. This means that as the stope is produced, one is in position to be more and more certain about the mineral or grade content. However, this requires thorough production follow-up.

Simulations implemented for FeTot and FeMagn may produce unrealistic realisations. They are unrealistic in the sense that single realisations of FeMagn may be larger than the corresponding realisation of FeTot. Since total iron is the sum of iron bound in magnetite, hematite and silicates, this is not realistic. If there had been a correlation between FeMagn and FeTot, co-simulation could provide a solution. However, the scatter plot shown in Section 3.3.2 shows that if the whole mineralised envelope is taken into account such correlation is non-existing. A way of avoiding this problem is to consider averages of several realisations instead of single realisations. This is feasible in the present case where hematite dominates over magnetite, these averages obey the total sum constrains indicated above. If magnetite and hematite were more equally proportioned, the approach applied here to overcome the problem would not correct it. Research has been done on this area. The stepwise conditional transformation has been proposed (Leuangthong and Deutsch 2003). This handles also the problem at the level of single realisations. Although tested for one realisation, neither the time nor the capacity was sufficient to automate this technique. Automation is necessary to handle more than one realisation within a reasonable timeframe.

The simulation results also provide the foundation for management- and analysis of risks through probability quantification, and value chain simulations through the quantification of grade distributions. These grade distributions are the main input in the quantification of expected product outcome from the different stopes.

The drill cutting analyses from open pit blasts were not very consistent with the estimated values in the blocks (see Figure 110, Section 5.3.2). One major source of error in this comparison is the unequal spatial range of the blocks versus the blasts. If more blasts were available, a more thorough comparison could be made.

6.4. Stability issues

Both grade and stability are of major importance when it comes to mining. Stability problems may lead to the destruction of expensive mining equipment that may be difficult to replace. One might have insurance that covers any financial losses, but it is difficult to insure the operation against lost opportunities.

Although geostatistics have been used in rockmass classification, it does not seem to have been used to any great extent. The reason for this is at least two fold. First, there is probably an insufficient amount of geoinformation available at sites. This point would be especially valid at construction sites. Core drilling is expensive, and the amount of geodata required to use geostatistics might exceed the amount that can be collected within the financial framework available for the developer. However, at mine sites, where the ore body has been explored by core drilling, there should not be any excuse. Second, there might be an insufficient awareness among technical staff about how geostatistics can be applied to joint data.

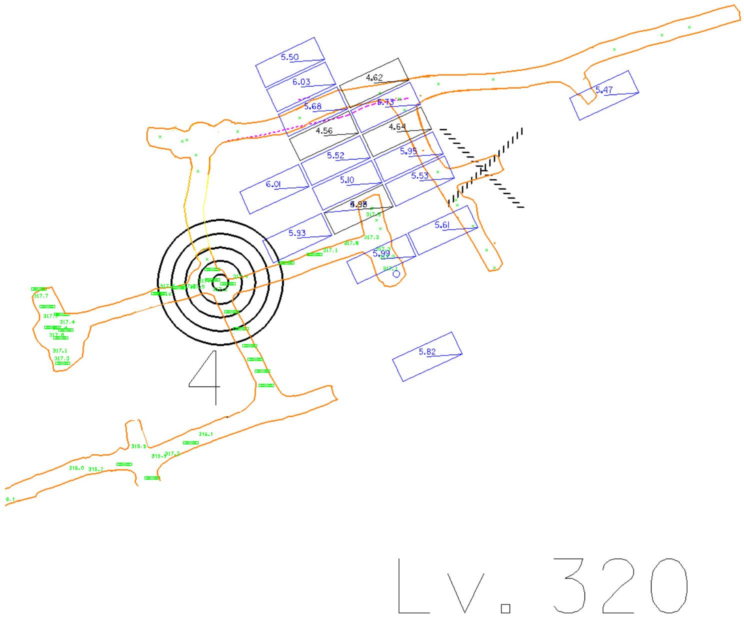

Figure 137 Area exposed to instability indicated by circles. RMi-estimates indicated by blue (5.0 to 6.1) and black blocks (2.8 to 5.0). Dashed cross indicates location on level 255, where rock stress measurements gave extremely high stresses.

Classification systems and the division into classes are based on empirical data, as for the RMi system. A strong and stable rock-mass at one site is not necessarily strong enough and thereby stable if it was placed at another site. The strength is relative to exposed human activities and rock stresses. Therefore the RMi classes need to be correlated to actual events at the relevant site in order to be of future value. Rana Gruber AS has had stability problems in the mine. In Figure 137 circles indicate one of these areas. Blocks indicate estimated RMi values between 2.8 and 5 (black) and between 5 and 6.1 (blue). These intervals contain 1% and 4% of the estimated blocks respectively, i.e. 5% of the lowest RMi-values. Dashed cross indicates location on level 255 where stress measurements gave very high stresses (Nilsen 2003).

A very low RMi value indicates that the rock is highly jointed, i.e. joint density and RMi are inversely proportional. Jointed rock masses do not have the same capability to absorb stress. Therefore, if parts of the rock masses are highly jointed, this will increase the load on the surrounding less jointed rock masses, possibly to a level that exceeds rock strength. Suggestively, this is what can be observed in Figure 137.

Stability problems have also been observed in stope 4. Stope 4 is parallel to stope 3 in Figure 130. Blocks of waste rock from the north wall of the stope are falling into the stope. Since this material blends with the ore, the result is an unintentional dilution. With these problems at hand it is interesting to see that the joint density near the north wall of stope 4 is high. In Figure 121 under the heading “Joint density, RQD and RMi”, Section 5.7.2 it can be seen that the RMi values are low in this area. The western most approximately north-south trending drift in this figure is the drilling drift in stope 4.

6.5. Density

The density is of great importance in the resource and reserve estimation. This yields not only the average value, but also its dependency on the iron content.

The density – iron content dependency can be modelled using a second-degree equation. If such an equation is used, an extrapolation must be performed to estimate the density of the ore- and gangue minerals. Extrapolation can be dangerous because assumptions are made about the dependency outside the data range. However, it is possible to deduce a theoretical dependency between the reciprocal density and the iron content. This dependency does not suffer from the same constraints and can be used to estimate the density of the ore- and gangue minerals.

As shown, the non-linear dependency between density and iron content has the consequence that the average density cannot be estimated correctly from an average FeTot, without knowing the distribution of iron. Using the average would consistently underestimate the real density. The solution is to simulate the iron content on a small grid followed by an estimation of the density from all FeTot realisations rather than estimate the density from a FeTot average.

The iron content – density dependency can be used to estimate the density, if the iron content is at hand. The density could also be used as an iron content indicator. This is illustrated in Table 34.

		68 % prediction interval FeTot		
Reciprocal density	Density	Lower limit	Estimate	Upper limit
0.27	3.70	38.2	40.2	42.3
0.28	3.57	34.4	36.5	38.5
0.29	3.45	30.6	32.7	34.9

Table 34 68% prediction intervals for FeTot.

The absolute mineral density was estimated using a helium pycnometer. These measurements were performed on mineral concentrates obtained through crushing, sieving, gravitational- and magnetic separation using a shaking table and permroll separator respectively. Finally a magnetic bar was used to obtain the magnetite concentrate. The density was estimated using measurements on wet and dry cores and on powder. As they all gave different, but similar, results the statement is underlined: *"there is no such thing as a true value…There exists only results from a procedure"* (Deming 1986). However, the method involving the wet cores provided the best results compared to the measurements of the mineral density. The dependency found from these measurements has therefore been used in Table 32. If another method for density determination was to be used routinely, another density – iron content dependency should be used.

6.6. Cut-off estimation

Cut-off is simply the value used to tag a mineralisation as ore or waste.

The algorithm used to estimate the cut-off is highly dependent on the main goal of the operation. If the main goal is to maximise the profit of the operation, an algorithm should be chosen, which makes it possible to determine the cut-off that maximises the preferred profit indicator. This could for example be the internal rate of return (IRR) or the net present value (NPV).

The cost break-even as applied here, does not maximise the profit. It might maximise the lifetime of the mine, but the operation as a whole, will probably be vulnerable to (unexpected) price or cost changes if this cut-off was used in the long run.

A thorough and well thought-through estimation and utilisation of a cut-off, or a cut-off policy, is a prerequisite to increase the probability for future success. However, without an organisation and routines with sufficient resources to follow-up the cut-off, no future success can be ensured.

6.7. Magnetic properties of the ore and the hematite

As expected, the magnetic susceptibility of the ore shows a strong correlation with the content of FeMagn. The relationship found in Section 5.3 coincides with previous reported results within a limited FeMagn range. The deviations at high FeMagn values probably originate from very coarse-grained magnetite in these samples. However, at the present time this issue remains unsolved. More samples could be collected to confirm the deviations.

Once tested and established the FeMagn – magnetic susceptibility dependency could be implemented in Isatis given the estimated FeMagn and a corresponding measurement of error given by the regression and the prediction intervals. Preferably the kriging with inequalities functionality could be used to produce the conditional expectation and the dispersion variance. Having these two parameters, an estimation or simulation technique could be exploited to incorporate the magnetic susceptibility measurements.

In addition to the measurements of the magnetite susceptibility of the ore, the magnetic susceptibility of the hematite in the ore and the remanence of the ore have been measured. The remanence measurements were performed using the equipment and methodology described in Section 4.7.3. The measurements of magnetic susceptibility on hematite were performed using a Frantzen magnetic separator. The hematite concentrate was obtained through crushing, sieving, grinding and magnetic separation of ore samples collected from the Kvannevann Iron Ore. Both the remanence measurements and the susceptibility measurements for hematite were performed to investigate the in-situ magnetic properties of the ore. The aim was two-fold: 1) search for ore quality indicators and 2) correlate in-situ magnetic properties with expected magnetic properties of the products. Although interesting preliminary results were obtained, more work must be done to further assess and validate these results. Unfortunately, there was insufficient time to do this within the timeframe of this work.

6.8. Selectivity

The mining method applied at the present time does not allow a high degree of selectivity. Once a stope has been opened for production, the whole stope must be produced. The smallest mining unit (SMU) considered contains about 70 000 tonnes of ore. This represents approximately one week of production. Except from the last one, none of the SMUs in the stope can be left where they are. The question could be whether the blasted SMU should be transported to the ore dressing plant or not. Without a detailed knowledge of the ore variations, this question is impossible to answer.

Selective mining with sub-level stoping would constitute a blending procedure. To blend, one would have to have at least two stopes in production at the same time. During the last few years, this has been one of the main concerns of this mining company. Neither the development- nor the production activities have been able to produce enough ore, i.e. the production from the mine is the limiting capacity. The question has not been which qualities to blend, but where do we have any quality at all.

Having said this, one company goal is now to produce ore from more than one stope. If the goal is to stabilise the grade of the ore entering into the ore dressing plant, a more detailed production follow-up needs to be performed. Ore feed data need to be transferred back into the mine to determine the probability that a SMU in fact contains a certain FeTot level, given that the estimated value is above this level.

Given the present IT-systems in the mining company, blending would be subjective, based on estimated and simulated stope content stored in MS Excel worksheets and visualisation of the SMUs, colour coded according to estimated grade. With a limited number of stopes in production at the same time, for example two, this would probably be sufficient. This presupposes that the organisation is capable of performing the blending process. If the number of stopes exposed to production at the same time could be increased further, then software could be considered that automates the blending process in the mine.

7. Conclusions and recommendations

7.1. Conclusions

The following conclusions can be made from this thesis:

1. The process approach to the value chain provides an overview and sufficient possibilities to perform a detailed process breakdown to identify and assess IT-requirements, bottlenecks, input / output requirements and role- and competence requirements.
2. The process approach requires devoted management and workers as well as an organisation that has the resources to perform a thorough follow-up of the results.
3. Collected geodata must be stored for future reference and reuse.
4. Simulation of ore variations provides a powerful tool to predict the variations in plant feed. The quantification of these variations provides valuable input into the prediction of future costs, recovery, product prices. Further it increases the probability to fulfil the delivery obligations.
5. Geostatistics modelling and estimation of rockmass parameters give valuable information for the prediction of potential stability problems.

6. Density can be used as an iron grade indicator.
7. Collection of drill cuttings, using the developed drill-cutting collector gives precise results. However, the accuracy is questionable. More testing is recommended.
8. Magnetic susceptibility can be used as an indicator for FeMagn, but more research is needed to gain complete confidence in the dependency valid for the Kvannevann Iron Ore.
9. Incorporation of soft data increases the volume that can be estimated, but at the cost of a relatively large estimation variance.
10. Implementation of IT-systems to generate blending plans should be considered, as they would stabilise the ore feed grade. Although complex IT-systems exist, the engineering constraints on the site point to the simpler tools using MS Excel in combination with reserve estimation-, simulation- and visualisation systems.

7.2. Recommendations

The following recommendations are stressed:

1. Review the company goals to establish a basis for cut-off policy determination instead of a cost break-even.
2. Focus on preservation and utilisation of existing and new geodata (e.g. diamond borehole cores, feed analysis and in-mine lithology observations) to ease the possibility to reanalyse collected and stored ore material and to extend the longevity of the geodata.
3. Improve the analysis of ore feed data to make a quantification of the probability that a SMU has a certain content of FeTot, for example, given that the estimation has predicted this content.
4. Develop and implement a system to handle the stepwise conditional transformation. This will further improve the FeTot / FeMagn simulation.
5. Use a distribution input, or at least a multi-single value input, instead of single value input in the calculation of RMi. This would be especially important for the uniaxial compression strength, which is highly variable within the ore.
6. A further development would be to calculate the RMi value with input data that are distinctly dependent on the rock type.

8. References

Ackoff, R.L. 1989. From data to Wisdom. Journal of Applied System Analysis. Vol. 16, pp. 3-9.

AME 2004. AME's latest Iron Ore Industry Market Update. Retrieved from http://www.minebox.com/story.asp?articleId=4949, 1/12-04.

Armstrong, M. 1998 Basic linear geostatistics. Springer-Verlag Berlin Heidelberg. 139p.

Baecher, G.B., Christian, J.T. 2003. Reliability and Statistics in Geotechnical Engineering. John Wiley & Sons, Ltd. 554p.

Barton, N, Lien, R and Lunde, J. 1974. Engineering classification of rock masses for the design of rock support. Rock mechanics, 6, pp. 189-236.

Berg, A.E. 1995. Dunderland Iron ore company, Limited i Rana. Forspillet og første driftsperiode. Post-graduate thesis in history. University in Trondheim, Norway. 137p.

Bieniawski, Z. T. 1973. Engineering classification of jointed rock masses. Trans. S. African Instn. Civ. Engrs., Vol. 15, no. 12, pp. 335-344.

Bieniawski, Z. T. 1989. Engineering rock mass classifications. New York. Wiley & Sons. 251p.

Bleines, C., Deraisme, J., Geoffroy, F., Perseval, S., Rambert, F.: Renard, D., Touffait, Y. 2001. Isatis Software Manual. Geovariances & Ecole Des Mines De Paris. 526p.

Blum, P. 1997, Physical properties handbook: a guide to the shipboard measurement of physical properties of deep-sea cores. ODP Tech. Note, 26 [Online]. Available from World Wide Web: <http://www-odp.tamu.edu/publications/tnotes/tn26/INDEX.HTM>. [Cited 2004-08-13]

Bouleau, N. 1986. Probabilités de l'Ingéniur, Herman, Paris.

Box, G. 1979. Robustness in the strategy of scientific model building. In: Launer, R.L., Wilkinson, G.N., (eds.) Robustness in statistics. New York (NY). Academic Press.

Brandt, R.T., Dorr, J.V.N., II, Gross, G.A., Gruss, H. and Semenenko, N.P. 1973. Problems of nomenclature for banded ferruginous-cherty sedimentary rocks and their metamorphic equivalents. In: Genesis of Precambrian Iron and Manganese Deposits. Proc. Kiev Symp. (1970), UNESCO, Paris vol. 9, pp. 377-380.

Brattli, B, Tørudbakken, B.O., Ramberg, I.B. 1982. Resetting of a Rb-Sr total rock system in Rödingfjället Nappe Complex, Nordland, North Norway. Norsk Geologisk Tidsskrift, vol. 62, pp. 219-224.

Broch, E. and Nilsen, B. 2001. Ingeniørgeologi – Berg. Compendium engineering geology. Department of Geology and Resources Engineering, NTNU. 294p.

Braathen, A. and Gabrielsen, R.H. 2000. Bruddsoner i fjell. Oppbygning og definisjoner. Gråstein 7. Norges Geologiske Undesøkelse.

Brundtland, G.H. 1987. Our common future. World commission on Environment and Development. Oxford University Press.

Bugge, J.A.W. 1948. Rana Gruber. Geologisk beskrivelse av jernmalmfeltene i Dunderlandsdalen. Norges Geologiske Undersøkelse, no. 171.

Bugge, J.A.W. 1978. Mineral Deposits in Norway. In: Bowie, S. H. U., Kvalheim, A., Haslam H.W. (eds.). Mineral Deposits of Europe, Norwest Europe, vol. 1, pp. 199-247. The Inst. of Mining and Metallurgy.

Burnup, C. 2003. Reflections on Risk and Uncertainty. Proc. Mining Risk Management Conference. Sydney, NSW, 9. - 12. Sept. 2003, pp. 11-13.

BVLI 1980. Geofysiske metoder for detaljkartlegging av malmforekomster. Tekniske rapport no. 19. Bergverkenes Landssammeslutnings industrigruppe.

Chilès, J.P., Delfiner, P. 1999. Geostatistics: modeling Spatial Uncertainty. John Wiley & Sons, Inc. 635p.

Chilès, J.P. 1988. Fractal and Geostatistical Methods for Modelling of a Fracture Network. Mathematical Geology, vol. 20, no. 6, pp. 631-654.

Clark, D.A. 1997. Magnetic petrophysics and magnetic petrology: aids to geological interpretation of magnetic surveys. AGSO Journal of Geology & Geophysics, Vol. 17, no. 2, pp. 83-103.

Cleveland, H. 1982. Information as Resource. The Futurist. Dec. 1982, pp. 34-39.

Coombes, J., Thomas, G., Glacken, I. and Snowden, V. 2000. Conditional simulation – which method for mining?. In: Geostats 2000. Kleingeld, W.J. and Krige, D.G. (eds.). Cape Town. Retrieved from http://snowden.pretzel.com.au/getBinary.aspx?documentid=766, 2/7-02.

Craig, J. R., Vaughan, D. J. 1994. Ore microscopy & Ore petrography. Second edition. John Wiley & Sons. Inc. 348p.

Dagbert, M., Dimitrakopoulos, R., Stoker, P 2003. Geostatistical Mineral Resources / Ore reserve Estimation and meeting JORC requirements. Step by step from sampling to Grade Controll. Seminar notes. 309p.

Dahlø, T.S. 1994. Kvannevann underjordsgruve. Vurdering av sikringsbehov. Prosjektrapport 361571.16. 10p.

Deere, D. and Miller, R.D. 1966. Engineering classification and index properties for intact rock. Univ. of Illinois, Tech Rept. No. AFWL-TR-65-116.

Deming, W. E. 1986. Hors de la crise / Out of the Crisis. Economica, Paris. In English, Cambridge University Press, Cambridge. 352p.

Dimitrakopoulos, R. 1998. Conditional simulation algorithms for modelling orebody uncertainty in open pit optimisation. International Journal of Surface Mining, Reclamation and Environment, vol. 12, no. 4, pp. 173-179.

Dougherty, E. R. 1990. Probability and statistics for the engineering, computing and physical sciences. Prentice-Hall International, Inc. 714p.

Downs, B., Bartelmehs, K., Sinnaswamy, K.. 2003. Software XtalDraw. Program to draw crystal structures and molecules. Email: downs@geo.arizona.edu.

Easterbrook, G. Quote retrieved from “The quote garden”. http://www.quotegarden.com/index.html, 21/5-04.

Eichler, J. 1976. Origin of the Precambrian Banded Iron formations, pp. 157-201. In: Handbook of strata-bound and stratiform Ore Deposits. Wolf. K.H. (Ed.). Volume 7.

Einstein, H.H. 2003. Uncertainty in Rock Mechanics and Rock Engineering – Then and Now, pp. 281-293. ISRM 2003 – Technology Roadmap for rock mechanics, South African Institute of Mining and Metallurgy.

Eliot, T.C. 1934. The Rock. Faber & Faber.

Eloranta, J.W. 1983. Determination of magnetite content through the use of magnetic susceptibility in large diameter blast holes. A master of science thesis, University of Wisconsin – Madison. 26p.

Evans, A.M. 1994. Ore Geology and Industrial Minerals. An Introduction. Blackwell Scientific Publications. 344p.

Fallon, G.N, Fullagar, P.K, Sheard, S.N. 1997. Application of geophysics in metalliferous mines. Australian Journal of Earth Sciences. Vol. 44, nr. 4, pp. 391-409.

Foslie, S. 1949. Håfjellmulden i Ofoten og dens sedimentære jern-mangan-malmer. Norges Geologiske Undersøkelse nr. 174. 129p.

Gabrielsen, R.H, Braathen, A., Dehls, J. and Roberts, D. 2002. Tectonic lineaments of Norway. Norsk Geologisk Tidsskrift, vol. 82, pp. 153-174.

Gether, Harald 2002. Strategy as a Contribution to Prosperity and Sustainability. Overall Optimisation of Technological Value Sequences. Doctor Technicae Thesis. Norwegian University of Science and Technology. 331p.

Gingele, J., Childe, S.J., Miles, M.E. 2002. A modelling technique for re-engineering business processes controlled by ISO 9001. Computers in Industry, vol. 49, nr. 3, pp. 235-251.

Godoy, M. C., Dimitrakopoulos, R and Felipe Costa, J. 2001. Economic functions and Geostatistical Simulation Applied to Grade Control, pp. 591 - 600. In: Mineral Resource and Ore Reserve Estimation - The AusIMM Guide to Good Practise. Monograph 23. Edwards, A.C. (ed).

Goovaerts, P. 1997. Geostatistics for Natural Resources Evaluation. Applied Geostatistics Series. Oxford University Press Inc. 442p.

Grenne, T, Ihlen, P.M., Vokes, F.M. 1999. Scandinavian Caledonide Metalogeny in a plate tectonic perspective. Mineral Deposita nr. 34, pp. 422-471.

Gross, G. A 1966. Principal Types of Iron-Formation and Derived Ores. The Canadian Mining and Metallurgical Bulletin for February, vol. 59, pp. 41-44.

Gross, G.A. 1983. Tectonic systems and the deposition of iron-formation. Precambrian research vol. 20, pp. 171-187.

Gross, G.A. 1991. Genetic concepts for iron-formation and associated metalliferous sediments. Econ. Geol. Monogr. 8, pp. 51-81.

Guo, W., Dentith, M.C., Bird, R.T., and Clark, D.A., 2000. Systematic error analysis of demagnetisation and implications for magnetic interpretation. Geophysics, vol. 66, no. 2, pp. 562-570.

Henry, D.J.. and Guidotti, C.V. 2002. Titanium in biotite from metapelitic rocks: Temperature effects, crystal-chemical controls and petrologic applications. American Mineralogist, vol. 87, no. 4, pp. 375-382.

Hair Jr, J.F., Anderson, R.E., Tatham, R.L., Black, W.C. 1995. Multivariate data analysis with readings. Fourth edition. Prentice Hall. 706p.

Hall, B.E. and Vries, J.C. 2003. Quantifying the Economic Risk of Suboptimal Mine Plans Strategies. Proc. Mining Risk Conference. Sydney, NSW, 9-12 Sept. 2003, pp. 59-69.

Hansson, S. O. 1999. A Philosophical Perspective on Risk. Ambio vol. 28, no. 6, pp. 539-542.

Harland, W.B. 1964. Critical evidence for a great infra-Cambrian glaciation. Geol. Rundsch., vol 54, pp. 232-235.

Haugen, S. 1998. Optimising the mining process according to external performance requirements, pp. 355-360. In Mine Planning and Equipment Selection 1998, Singhal (ed.). Proceedings of the Seventh International Symposium on Mine Planning and Equipment Selection. Calgary, Canada 6. - 9. October 1998.

Haugen, S. 1999. Operational planning and control of industrial minerals extraction. A process analysis approach to improvement. Doctoral Thesis. Norwegian University of Science and Technology. 161p.

Hoek, E, Kaiser, P.K., Bafden, W.F. 1995. Support of Underground Excavations in Hard Rock, Rotterdam: A.A. Balkema.

Houlding, S.W. 1994. 3D geoscience modelling. Compter techniques for geological characterization. Springer-Verlag Berlin Heidelberg. 297p.

Hoffman, P.F., Schrag D.P. 2002. The snowball Earth hypothesis: testing the limits of global change. Terra Nova, vol 14, no 3, pp. 129-155.

Hunt, C.P., Moskowitz, B.M., Banerjee, S.K. 1995. Rock Physics and Phase Relations. A handbook of Physical Constants. American Geophysical Union. Retrieved from http://www.agu.org/reference/rock/15_hunt.pdf, 7/1-02.

Hunt, V.D. 1996. Process mapping: how to reengineer your business processes, Wiley, New York, USA. 274p.

IDEF0 1994. Integration Definition for Functional Modeling (IDEF0). Standard describing the IDEF0 modelling language. Federal Information Processing Standard (FIPS) Publication 183. Issued by the National Institute of Standards and Technology, USA.

Info Comm 2004. The Iron Ore Market. Abstract. Retrieved from http://r0.unctad.org/infocomm/Iron/covmar04.htm, 2/12-04.

James, H.L. 1954. Sedimentary facies of iron-formation. Econ. Geol. vol. 49, no. 3, pp. 235-293.

James, H.J. 1983. Distribution of banded iron-formation in space and time, pp. 471-490. In: Iron formation: Facts and problems, Trendall, A.F. and Morris, R.C. (Eds), Elsevier, Amsterdam.

Johnson, M 1987. Multivariate Statistical Simulation. New York: John Wiley & Sons.

Johnson, R.A., Wichern, D.W. 1992. Applied multivariate statistical analysis. Third edition. Prentice-Hall Internation, Inc. 626p.

Journel A.G. 1994. Modelling uncertainty: Some conceptual thoughts, pp. 30-45. In: Geostatistics for the next century. Dimitrakopoulos, R. (ed), Dodrect: Kluwer Academic Publisher.

Journel, A. G., Huijbregts, Ch. J. 1978. Mining geostatistics. Academic Press. 580p.

Kelly, T.D. and Jorgenson, J.D 2004. Iron Ore statistics. U.S. Geological Survey. Retrieved from http://minerals.usgs.gov/minerals/pubs/of01-006/ironore.pdf., 4/12-04.

Kimberley, M.M. 1978. Paleoenvironmental Classification of Iron Formations. Economic Geology, vol. 73, nr. 2.

Kimberley, M.M. 1989a. Nomenclature for Iron Formations. Ore Geol. Rev., vol. 5: pp. 1-12.

Kimberley, M.M. 1989b. Exhalative Origins of Iron Formation. Ore Geol. Rev., vol. 5: pp. 13-145.

Kimberley, Michael M. 1994. Debate about ironstone: has solute supply been surficial weathering, hydrothermal convection, or exhalative of deep fluids? Terra Nova, vol. 6, no. 2, pp. 116-132.

Kirscvink, J.L. 1992. Late Proterozoic low.latitude global glaciation: the Snowball Earth, pp. 51-52. In: Schopf, J.W. and Klein, C. (eds). The Proterozoic Biosphere. Cambridge University Press, Cambridge.

Klein, C., Beukes, N.J. 1993. Sedimentology and geochemistry of the glaciogenic Late Proterozoic Rapitan iron-formation in Canada. Economic Geology, vol. 88, no. 3, pp. 542-565.

Koch, G. S Jr, Link, R. F. 1971. Statistical Analysis of Geological Data. Vol. 2. John Wiley & Sons. Inc. 417p.

Krige, D. 1951. A Statistical Approach to Some Mine Valuation and Allied Problems on Witwatersrand. M. Sc. thesis, University of Witwatersrand, South-Africa.

Kuchta, M, Newman, A, Topal, E. 2003. Production Scheduling at LKAB's Kirunas Mine Using Mixed Integer Programming. Mining Engineering April 2003, pp. 35-40.

Lane, K.F. 1988. The Economic Definition of Ore. Cut-off grades in theory and practise. Mining Journal Books Limited. 97p.

Lantuéjoul, C. 2002. Geostatistical simulation. Models and algorithms. Springer. 239p.

La Pointe, P. R. 1980. Analysis of the spatial variations in rock mass properties through geostatistics. Proceedings of the 21st Symposium on Rock Mechanics, 570-580.

Leuangthong, O. and Deutsch, C.V. 2003. Stepwise Conditional Transformation for Simulation of Multiple Variables. Mathematical Geology, vol 35, no. 2.

Lipton, I. 2001. Measurements of Bulk Density for Resource Estimation, pp. 57-66. In: Mineral Resource and Ore Reserve Estimation - The AusIMM Guide to Good Practise. Monograph 23. Edwards, A.C. (Ed).

Ludvigsen, E. 1997. Mine surveying in Norway. What are the challenges. Proc X. ISM Congress, Fremantle, Australia. 1997.

Lund, Ø., Bilov-Olsen, J., Lilleås, J.E., Johansen, T.E. 2001. Håndbok i Prosessmodellering i Forsvaret. 57p.

Malvik, T. 1997. Innhold av sporelementer i hematitt fra underjordsmalm, Kvannevann. Sintef Rapport STF22 F97034. 6p.

Malvik, T. 1999. Mikroskopbeskrivelse av malmprøver fra Kvannevann. Sintef Rapport STF22 F99035. 6p.

Matheron, G. 1963. Principles of Geostatistics. Economic Geology, vol. 58, pp. 1246-1266.

Matheron, G. 1973. The intrinsic random functions and their application. Advances in Applied Probability, vol. 5, pp. 439-468.

Maynard, J.B. 1983. Geochemistry of Sedimentary Ore Deposits. Springer-Verlag New York Inc. 239p.

Melezhik, V. A., Gorokhov, I. M., Fallick, A. E., Roberts, D, Kuznetsov, A. B., Zwaan, K. B., Pokrovsky, B.G. 2002. Isotopic stratigraphy suggests Neoproterozoic ages and Laurentian ancestry for high-grade marbles from North-Central Norwegian Caledonides. Geological Magazine, vol. 139, no. 4, pp. 375-393.

Menzel, C., Mayer, R. J., Edwards, D. D. 1994. IDEF3 process description and their semantics. In Dagli, C.H. and Kusiak, A. Intelligent systems in design and manufacturing, pp. 172-212. New York: Asme Press.

Mito, Y, Yamamoto, T, Shirasagi, S, Aoki, K. 2003. Prediction of geological conditions ahead of the tunnel face in TBM tunnels by geostatistical simulation technique, pp. 833-836. ISRM 2003 - Technology roadmap for roch mechanics, South African Institute of Mining and Metallurgy.

Mortimer, G.J. 1950. Grade Control, Trans. Inst. Min. Metall, vol. 59, pp. 357-359.

Morley, C, Snowden, V, Day, D. 1999. Financial impact of resource / reserve uncertainty. Journal of South African Institute of mining and metallurgy, vol 99, nr. 6, Okt-Des 1999, pp. 293-301.

Mutton, AJ. 2000. The Application of geophysics during evalution of the Century zinc deposit. Geophysics, vol 65, no. 6, Nov-Des 2000, pp. 1946-1960.

Muurmans, J (1976?). Tyngdemåling Ørtfjell Jernmalmforekomst. A/S Norsk Jernverk, Rana Gruber. 15p.

Myrvang, A. 2001. Bergmekaniske undersøkelser i Ørtfellet underjordsgruve ved Rana Gruber AS. STF22 F01111. Sintef Bygg og miljøteknikk. 12p.

NGU 2003a. Transcript from database Norwegian ores. Unpublished.

NGU 2003b. Lineament map. Retrieved from http://www.ngu.no/, 21/10-03.

NGU 2005. Geology map. Retrieved from http://www.ngu.no/ 25/1-05.

Nilsen, B.1979. Stabilitet av høye fjellskjæringer. Report 11, Geol. Inst., NTH, Trondheim. 271p.

Nilsen, B, Palmstrøm A. 2000. Engineering geology and rock engineering. Handbook 2. Norwegian Group for Rock Mechanics (NBG). 201p.

Nilsen, B, Shresta, K. K., Panthi, K. H., Holmøy, K. 2003 RMR vs Q vs RMi. Tunnels and Tunneling International, vol. 35, nr. 5, pp. 45-48..

Nilsen, O. 1990. Et utvalg nordiske mineralforekomster. Intern skriftserie nr. 58. Institutt for Geologi, Universitetet i Oslo, pp.53-54.

Nilsen, P. 2003. 2D bergspenningsmåling ved Ørtfjell gruve. STF22 F03109. Sintef Berg og geoteknikk. 5p.

NIST 2004. National Institute of Standards and Technology, USA. Reference manual DATAPLOT. Retrieved from http://www.itl.nist.gov/div898/software/dataplot/refman2/, 23/9-03.

Nordvik, Egil 2000. Ny framtid for Rana Gruber, pp. 158-159. In Halfdan Carstens (ed.) ...bygger i berge, en beretning om norsk bergverksdrift. Utgivere: Norsk Bergindustriforening og Den Norske Bergingeniørforening.

Norwegian Standard 5814. 1991. Risk Analysis Requirements.

Oftedahl, C. 1981. Norges Geologi. 2. utgave. Tapir.203p.

Osland, R. 1998. Modelling of variations in Norwegian olivine deposits. Causes of variation and estimation of key quality factors. PhD-thesis. Norwegian University of Science and Technology.

Palmström, A. 1995. RMi – a rock mass characterization system for rock engineering purposes. Ph.D. thesis, Univ. Oslo, Norway. 400p.

Palmström, A. 1996. Characterizing Rock Masses by Rmi for Use in Practical Rock Engineering. Part 1: The development of the Rock Mass index (RMi). Journal of Tunneling and Underground Space Technology, vol. 11, no. 2, pp. 175-188.

Palmström, A. 2000a. Recent developments in rock support estimates by the RMi. Journal of Rock Mechanics and Tunneling Technology, vol 6, no. 1. May 2000, pp. 1-19.

Palmström, A. 2000b. Block size and Block size distribution. Paper presented at the workshop on Reliability of classification systems in connection with the GeoEng2000 conference, Melbourne, 18.-24. November 2000.

Park, R.G. 1989. Foundations of structural geology. 2nd ed. Blackie Academic & Professionals. 140p.

Petruk, W. 1965. Relationship between the specific magnetic susceptibility and the iron plus manganese content of chlorite. The Canadian Mineralogist vol. 8, part 3, pp. 372-376.

Poniewierski, J, MacSporran, G, Sheppard, I. 2003. Optimisation of Cut-off Grade at Mount Isa Mines Limited's Enterprise Mine. Conference Proceedings. Twelfth International Symposium on Mine Planning and Equipment Selection.

Porter, M.E. 1985. Competitive advantages. The Free Press. New York.

Prestvik, T. 1992. Mineralogi. En innføring i krystallografi og mineralogi. Vett & Viten AS. 178p.

Press, F. and Siever R. 1986. Earth. Fourth edition. W. H. Freeman and Company. 648p.

Priest, S.D., Hudson, J.A. 1981. Estimation of discontinuity Spacing and Trace Length Using Scanline Surveys. Int. J. Rock Mech. Min. Sci. & Geomech. Abstr., vol. 18, pp 183-197.

Ramdohr, P. 1980. The ore minerals and their intergrowths. Second edition, vol.2, pp. 441-1123. Pergamon Press.

Rana Gruber AS 1984. Beskrivelse av Rana Gruber. Internal report. 10p.

Ringdalen, E. 1983. Variasjon i kjemi og mineralogy i malmene i Ørtfjell. Internrapport AS Norsk Jernverk divisjon Rana Gruber AS. 3p

Ringdalen, E. 1984 Granatfels, mineralogi, mineralkjemi, utbredelse Internrapport AS Norsk Jernverk divisjon Rana Gruber AS. 15p.

Ross, S.M. 2003. Introduction to probability models. Eight edition. Academic Press. 707p.

Sandman P. M. 1993. Responding to Community Outrage: Strategies for Effective Risk Communication (American Industrial Hygiene Association: Fairfax, VA).

Sandøy, R. 1996. En beskrivelse av mineralogiske og geokjemiske omvandlinger fra gabbro til skapolittførende bergart (ødegårditt) fra Ødegaarden i Bamle, Telemark. Diploma thesis NTNU.

Sheldon, Richard P. 1964. Relation Between Specific Gravity and Iron Content of Rocks From the Red Mountain Formation, Alabama. Geological Survey Bulletin 1182-D.

Shibli, Syed Abdul Rahman. 2004. Geostatistics FAQ - Frequently Asked Questions. Retrieved from http://ai-geostats.jrc.it/Geostats_Faq/Syed/index.html, 3/5-04.

Sinclair, J. 1998. Geological Controls in Resource / Reserve Estimation. Explor. Mining Geol, vol. 7, no. 1 and 2, pp. 29-44. Canadian Institute of Mining, Metallurgy and Petroleum.

Sintef Bergteknikk 1993. Bergmekaniske undersøkelser i forbindelse med underjordsdrift ved Rana Gruber AS. STF36 F93002. Sintef Bergteknikk.

Standards Australia 1999. AS4360 - Risk Management. Standards Association of Australia.

Stephens, M.B., Gustavson, M., Ramberg, I.B, Zachrisson, E. 1985. The Caledonides of central - north Scandinavia - a tectonostratigraphic overview, pp. 135-162. In: Gee D.G and Sturt B.A. (eds.), 1985. The Caledonide Orogen – Scandinavia and Related areas, part 1.

Svinndal, S. 1977. The Iron Ore deposits of Norway. pp. 237-244. In: Zitzmann, A. (ed.). Iron ore deposit of Europe and adjacent areas, vol. 1.

Søvegjarto, U. 1972. Berggrunnsgeologiske undersøkelser i Dunderlandsdalen, Nordland. Post-graduate thesis, University of Oslo. 139p.

Søvegjarto, U. 197?. Joint mapping in the exploration drift. Internal report, Rana Gruber AS.

Søvegjarto, U. 1986. Ørtfjell jernmalmfelt. Ny geologisk 1:1000 dagkartlegging 1973-81. Internal rapport AS Norsk Jernverk divisjon Rana Gruber AS.

Søvegjarto, U., Marker, M., Gjelle, S. 1989. STORFORSHEI 2027 IV, berggrunnskart, M=1:50.000 Norges geologiske undersøkelse.

Søvegjarto, U. 1990. Jernmalmene i Rana, pp. 154-176. In: Rui, I.J. (ed). Deformasjon og remobilisering av malmer. Report nr. 76, BVLI-project.

Syrjänen, P. and Lovén, P. 2003. 3-D modeling of rock mass quality, pp. 1175-1178. ISRM 2003 – Technology roadmap for rock mechanics, South African Institute of Mining and Metallurgy, 2003.

Telford, W.M, Geldert, L.P., Sheriff, R..E 1994. Applied geophysics. Cambidge Uni Press. 726p.

Torsvik, T. H., Olesen, O. 1988. Petrophysics and paleomagnetism. Initial report of the Norwegian Geological Survey Laboratory. NGU report 88.171

Trendall, A.F. 1983. Introduction. In: Trendall, A.F. and Morris, R.C. (Eds.), Iron formation: Facts and problems. Elsevier, Amsterdam, p. 1-12.

Trendall, A.F. 2002. The significance of iron-formation in the Precambrian Stratigraphic record, pp. 33-66. In: Altermann, W. and Corcoran, P.L. Precambrian Sedimentary Environments: A modern Approach to Ancient Depositional Systems. Special publication number 33. International Association of Sedimentologists. Blackwell Science.

U.S. Geological Survey, Mineral Commodity Summaries. 2003. Retrieved from: http://minerals.usgs.gov/minerals/pubs/commodity/iron_ore/340303.pdf, 22.03.2004.

Ulltveit-Moe, J. 2004. Paragraph in Dagens Næringsliv 13/10-04.

US Environmental Protection Agency 1998. Guidance for data quality assessement. Practical methods for data analysis. EPA QA/G-9. Office of Research and Development Washington, D.C. 20460. Retrieved from: http://www.epa.gov/swerust1/cat/epaqag9.pdf, 13/6-02.

Vann, J, Bertoli, O, Jackson S. 2002. An overview of geostatistical Simulation for Quantifying risk, pp. 13-29. In: Searston, S.M. and Warner, R.J. Proceedings from Quantifying Risk and Error Symposium. Geostatistical Association of Australia.

Vernadat, F.B. 1996. Enterprise Modeling and Integration: principles and applications. Chapman & Hall. 513p.

Vose, D. 2000. Risk analysis. A quantitative guide. Second edition. John Wiley & Sons LTD. 406p.

Yeary, L.W. 2004. An Overview of Spinels. Retrieved from: http://www.tntech.edu/chemistry/Inorganic/Chem4110/Student/16%20Spinels.ppt, 15/8-04.

Yu, Y.F., Mostyn, G.R. 1993. Spatial correlation of rock joints, pp. 241-255. In: Li, K.S. and Lo S-C.R. (eds). Probabilistic Methods in Geotechnical Engineering. Balkema, Rotterdam. 331p.

Zablocki, C. J. 1974. Magnetite assays from magnetite susceptibility measurements in taconite production blast holes, Northern Minnesota. Geophysics vol. 39, no. 2, pp. 174-189.

Zakarian, A., Kusiak, A. 2001. Process analysis and reengineering. Computer & Industrial Engineering, vol. 41, pp. 135-150.

9. Appendices

Declustered summary statistics

FeMagn

	raw variable	weight variable	raw var normalized
Number of defined samples	1060	1060	1060
Minimum of the variable	0.10000000149	0.0003	0.10000000149
Maximum of the variable	32.1890411377	0.0101	32.1890411377
Mean of the variable	2.59529579043	0.0009	2.73695789213
Variance of the variable	9.84	0.00	9.06
Standard Deviation	3.14	0.00	3.01

FeTot

	raw variable	weight variable	raw var normalized
Number of defined samples	1070	1070	1070
Minimum of the variable	5.31527662277	0.0003	5.31527662277
Maximum of the variable	48.1057052612	0.0100	48.1057052612
Mean of the variable	32.0275479116	0.0009	30.513082734
Variance of the variable	74.56	0.00	88.44
Standard Deviation	8.64	0.00	9.40

MnO

	raw variable	weight variable	raw var normalized
Number of defined samples	257	257	257
Minimum of the variable	0.0500000007451	0.0012	0.0500000007451
Maximum of the variable	6.40521287918	0.0183	6.40521287918
Mean of the variable	0.616887346823	0.0039	0.737255407161
Variance of the variable	1.14	0.00	1.67
Standard Deviation	1.07	0.00	1.29

P

	raw variable	weight variable	raw var normalized
Number of defined samples	1021	1021	1021
Minimum of the variable	0.0722950026393	0.0003	0.0722950026393
Maximum of the variable	0.582727789879	0.0116	0.582727789879
Mean of the variable	0.212720195472	0.0010	0.202963279764
Variance of the variable	0.00	0.00	0.00
Standard Deviation	0.05	0.00	0.05

S

	raw variable	weight variable	raw var normalized
Number of defined samples	1031	1031	1031
Minimum of the variable	0.0010000000475	0.0003	0.0010000000475
Maximum of the variable	0.322230964899	0.0097	0.322230964899
Mean of the variable	0.00605469837443	0.0010	0.0102098646459
Variance of the variable	0.00	0.00	0.00
Standard Deviation	0.02	0.00	0.03

TiO2

	raw variable	weight variable	raw var normalized
Number of defined samples	624	624	624
Minimum of the variable	0.0900000035763	0.0006	0.0900000035763
Maximum of the variable	0.848500847816	0.0109	0.848500847816
Mean of the variable	0.309286905536	0.0016	0.328639409867
Variance of the variable	0.02	0.00	0.03
Standard Deviation	0.15	0.00	0.16

Table 35 Summary statistics of declustered data

Block size in declustering

	dx [metre]	dy [metre]	dz [metre]	Average
FeMagn	141	30	130	Maximised
FeTot	142	30	128	Minimised
MnO	145	31	145	Maximised
P	142	35	128	Minimised
S	141	29	130	Maximised
TiO_2	145	32	129	Maximised

Jointing in Erik open pit

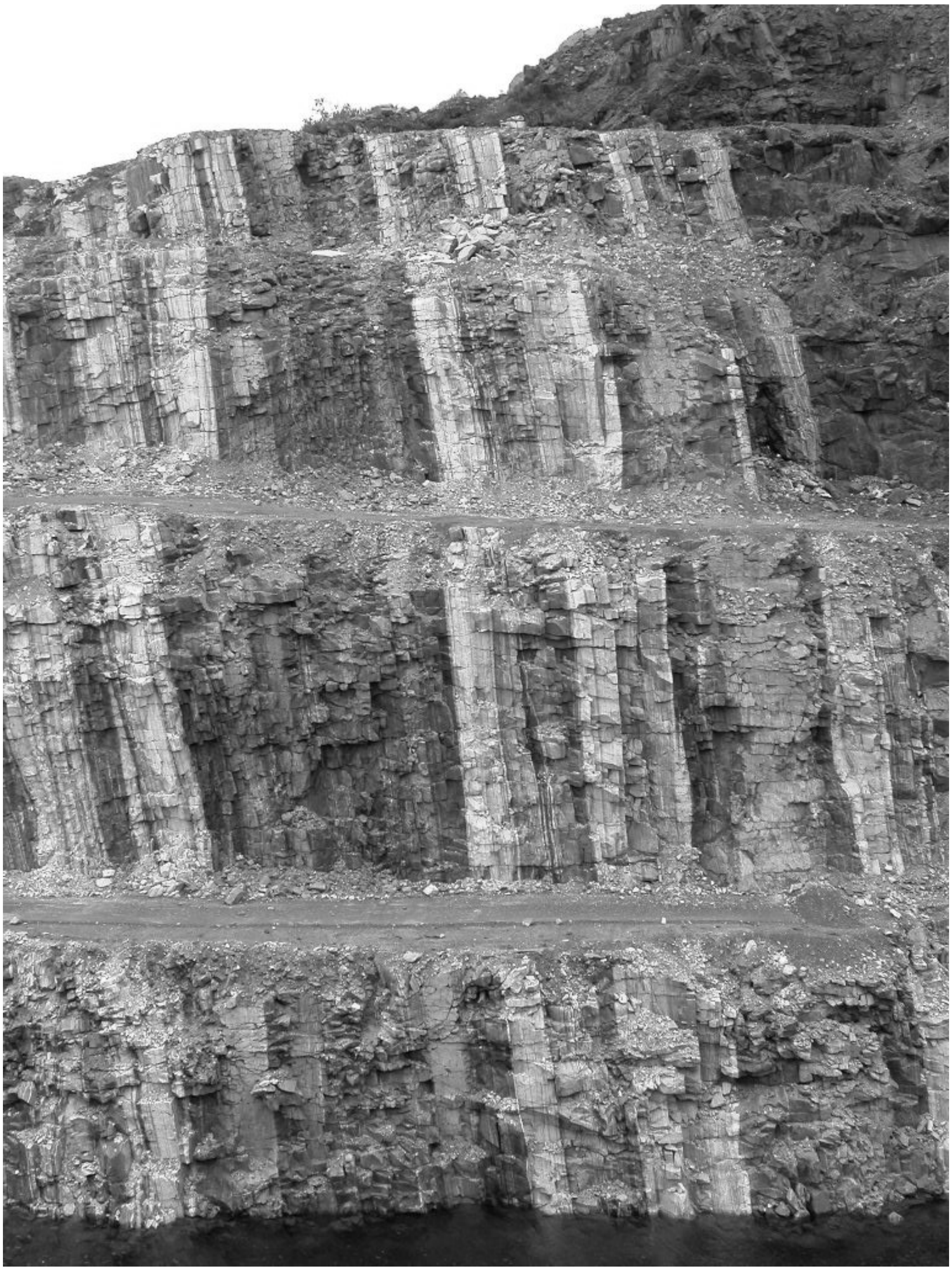

Figure 138 Steeply dipping lithologies. Western wall of ramp into Erik open pit. Joint set 1.

Lineament map, Rana

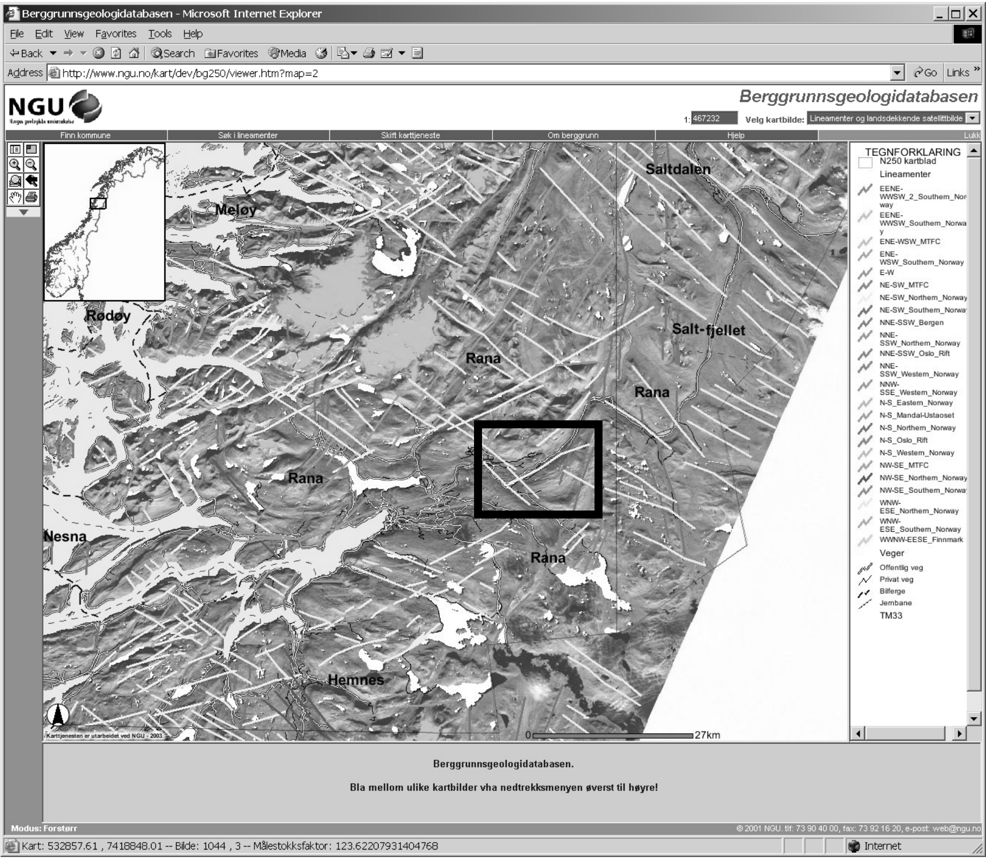

Figure 139 Lineament map, Rana (NGU 2003b). Mining area within square. Direction of foliation joints indicated by the NE-SW striking line within square.

North wall of Kvannevann open pit

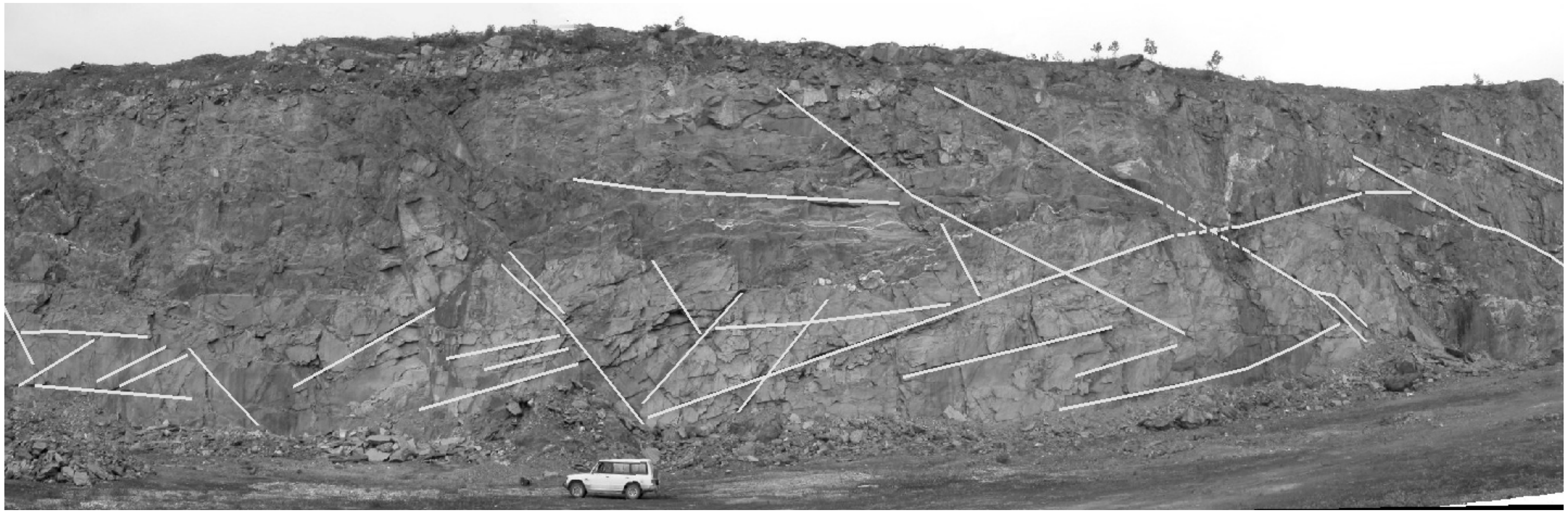

Figure 140 North wall of Kvannevann open pit. Joints from joint set two and three indicated by yellow lines. Pit wall orientated N75^{o}E. This direction corresponds to the strike of the ore.

Summary statistics of joint density along borehole

```
root  -  Jun 22 2004   10:09:27


Univariate Statistics
=====================
                     Count    Minimum    Maximum       Mean   Variance
Joint density        14961     0.0000    40.0000     4.2349     9.2010



Histogram
=========

Variable : Joint density
**********************
       Lower    Frequencies(%)
       Bound    All   Mask   High
 Below  -2.00   0.00   0.00   0.00
     1   0.00  29.67   0.00   0.00
     2   2.00  35.70   0.00   0.00
     3   4.00  18.49   0.00   0.00
     4   6.01   8.13   0.00   0.00
     5   8.01   4.18   0.00   0.00
     6  10.01   1.70   0.00   0.00
     7  12.01   0.98   0.00   0.00
     8  14.01   0.37   0.00   0.00
     9  16.02   0.31   0.00   0.00
    10  18.02   0.21   0.00   0.00
    11  20.02   0.09   0.00   0.00
    12  22.02   0.06   0.00   0.00
    13  24.02   0.03   0.00   0.00
    14  26.03   0.01   0.00   0.00
    15  28.03   0.05   0.00   0.00
    16  30.03   0.00   0.00   0.00
    17  32.03   0.00   0.00   0.00
    18  34.03   0.01   0.00   0.00
    19  36.04   0.00   0.00   0.00
    20  38.04   0.01   0.00   0.00
 Above  40.04   0.00   0.00   0.00
```

Figure 141 Summary statistics of joint density along borehole.

Major weakness zones extended into 3D

Figure 142 Zones of weakness observed on the surface extended into 3D and their position relative to where the mining activity takes / has taken place.

Density estimation based on mineralogy

Mineral	Weight %	Density Min	Density Mean	Density Max
Hematite	43.00	4.90	5.10	5.30
Magnetite	4.80	4.90	5.12	5.20
Apatite	1.30	3.16	3.19	3.22
Pyrite	0.03	5.00	5.10	5.20
Quartz	28.20	2.60	2.62	2.65
Oligoclase	1.00	2.64	2.65	2.66
Biotite	1.10	2.70	2.90	3.10
Muscovite	1.50	2.76	2.82	2.88
Chlorite	4.60	2.60	3.00	3.40
Hornblende	3.20	3.02	3.24	3.45
Epidote	4.80	3.38	3.38	3.38
Garnet	0.10	3.40	4.00	4.60
Calcite / dolomite	6.40	2.70	2.70	2.70
	100.03			

Table 36 Average mineral content and density range of the minerals.

Ore [gram]:	1000	Volume 1000 gram ore [cm3]		
Mineral	Gram mineral in 1000 gram ore	Min	Mean	Max
Hematite	429.87	87.729	84.288	81.108
Magnetite	47.99	9.793	9.372	9.228
Apatite	13.00	4.113	4.074	4.036
Pyrite	0.30	0.060	0.059	0.058
Quartz	281.92	108.429	107.601	106.383
Oligoclase	10.00	3.787	3.772	3.758
Biotite	11.00	4.073	3.792	3.547
Muscovite	15.00	5.433	5.318	5.207
Chlorite	45.99	17.687	15.329	13.525
Hornblende	31.99	10.593	9.889	9.273
Epidote	47.99	14.197	14.197	14.197
Garnet	1.00	0.294	0.250	0.217
Calcite / dolomite	63.98	23.697	23.697	23.697
	1000	289.884	281.638	274.234

Table 37 Considering one kilogram of ore. Calculated volume each mineral occupies given the min, mean and max density values.

Density Min	Density Mean	Density Max
3.45	**3.55**	**3.65**

Table 38 Calculated average density based on the average ore mineralogy.

Sample coordinates, grain density

		NGO 48 IV				
Sample	Fraction	X	Y	Z	Grain density	FeTot
1	F	66377	939383	320	3.3	32.7
1	M	66377	939383	320	3.7	42.0
1	C	66377	939383	320	3.4	32.0
2	F	66401	939321	320	3.7	44.6
2	M	66401	939321	320	4.2	52.8
2	C	66401	939321	320	4.3	54.1
3	F	66442	939406	320	3.8	47.2
4	F	66707	939469	320	3.5	39.4
5	C	66328	939285	250	4.1	50.1
6	F	66352	939369	250	3.0	27.2
6	M	66352	939369	250	3.2	25.6
6	C	66352	939369	250	2.9	13.0
7	F	66433	939383	255	2.9	18.8
7	M	66433	939383	255	3.1	21.0
7	C	66433	939383	255	3.0	17.5

Table 39 Coordinates for samples used in the grain density determination.

Core sample coordinates

# of samples	X	Y	Z	Remark
2	66379	939369	321	Transportation drift lv. 320
3	66544	939419	321	Pilar between stope 7 and 8
9	66624	939401	390	Kvannevann open pit
5	66627	939435	321	Pilar between stope 8 and 9

Table 40 Coordinates for core samples used in the determination of magnetic susceptibility and magnetic remanence and dry bulk density.

Block models

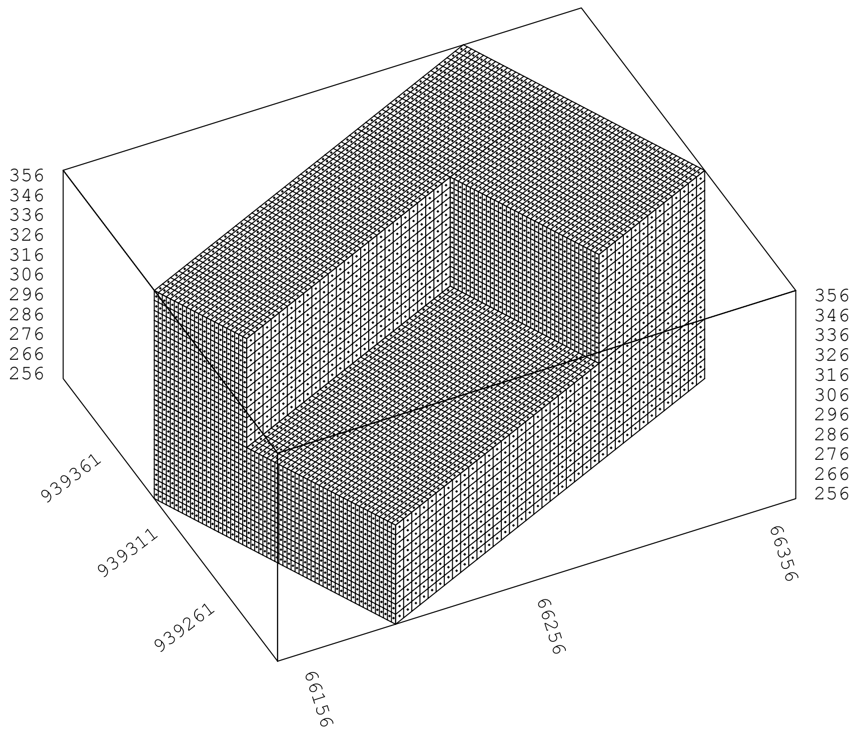

Figure 143 Block model 5x2x5 metre.

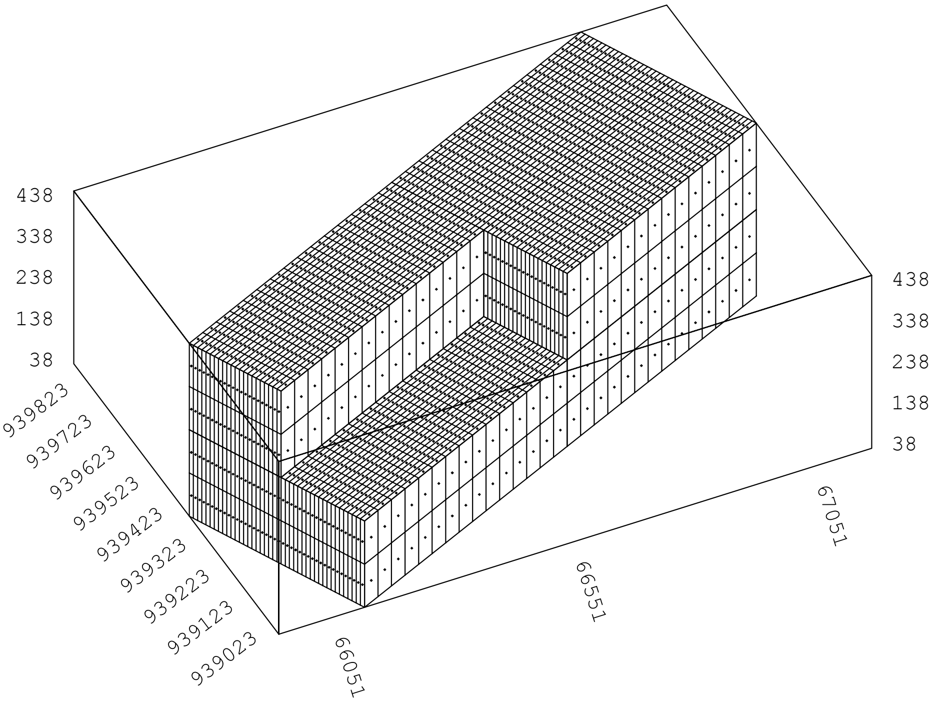

Figure 144 Block model 40x10x50 metre.

Geochemical characteristics of different ore types

steinare - Jun 02 2004 09:08:48

Mt_hm_Malm:

Univariate Statistics

	Count	Minimum	Maximum	Mean	Variance
ASSAYS_FEMAGN	73	0.1000	14.7049	2.8301	6.0474
ASSAYS_FETOT	73	17.2104	44.4136	34.9105	34.9429
ASSAYS_MNO	14	0.1128	0.6631	0.3282	0.0314
ASSAYS_P	73	0.1400	0.3229	0.2114	0.0015
ASSAYS_S	73	0.0010	0.1289	0.0079	0.0004
ASSAYS_TIO2	48	0.1295	0.5749	0.2651	0.0085

Hm_Malm:

Univariate Statistics

	Count	Minimum	Maximum	Mean	Variance
ASSAYS_FEMAGN	51	0.1000	20.8735	1.9169	16.2400
ASSAYS_FETOT	51	10.2155	44.0000	34.2054	40.6432
ASSAYS_MNO	14	0.1237	1.4044	0.4320	0.1135
ASSAYS_P	51	0.0800	0.4068	0.2331	0.0030
ASSAYS_S	51	0.0010	0.3222	0.0093	0.0020
ASSAYS_TIO2	26	0.1234	0.5102	0.2396	0.0066

Impregnasjon:

Univariate Statistics

	Count	Minimum	Maximum	Mean	Variance
ASSAYS_FEMAGN	35	0.3000	9.7000	4.6347	4.7792
ASSAYS_FETOT	35	6.5151	37.2653	18.9704	51.7151
ASSAYS_MNO	4	0.1100	0.2531	0.1651	0.0028
ASSAYS_P	34	0.1095	0.5827	0.1824	0.0056
ASSAYS_S	34	0.0010	0.0439	0.0065	0.0001
ASSAYS_TIO2	20	0.1982	0.6845	0.5115	0.0187

GrFels_Malm:

Univariate Statistics

	Count	Minimum	Maximum	Mean	Variance
ASSAYS_FEMAGN	25	0.1000	3.4000	0.6468	0.7147
ASSAYS_FETOT	25	13.0000	38.3772	24.6295	48.5846
ASSAYS_MNO	7	0.3200	2.2900	1.5682	0.3704
ASSAYS_P	25	0.1700	0.2952	0.2267	0.0011
ASSAYS_S	25	0.0010	0.0120	0.0033	0.0000
ASSAYS_TIO2	14	0.2300	0.5200	0.4197	0.0076

Granatfels:

Univariate Statistics

	Count	Minimum	Maximum	Mean	Variance
ASSAYS_FEMAGN	18	0.1000	2.4000	0.4420	0.3011
ASSAYS_FETOT	18	9.4256	36.7000	18.4843	49.5493
ASSAYS_MNO	4	2.5489	5.8544	4.5527	1.7541
ASSAYS_P	18	0.1106	0.2900	0.1882	0.0017
ASSAYS_S	18	0.0010	0.0560	0.0050	0.0002
ASSAYS_TIO2	9	0.3100	0.6311	0.4756	0.0080

Mt_Malm:

Univariate Statistics
=====================

	Count	Minimum	Maximum	Mean	Variance
ASSAYS_FEMAGN	8	2.7138	14.2962	6.2804	11.5948
ASSAYS_FETOT	8	21.2829	42.6899	33.4229	43.9124
ASSAYS_MNO	1	0.2588	0.2588	0.2588	0.0000
ASSAYS_P	8	0.2011	0.2700	0.2260	0.0004
ASSAYS_S	8	0.0010	0.0229	0.0046	0.0001
ASSAYS_TIO2	3	0.1600	0.3232	0.2394	0.0045

Annen_Malm:

Univariate Statistics
=====================

	Count	Minimum	Maximum	Mean	Variance
ASSAYS_FEMAGN	7	0.1492	4.9547	1.1034	2.5742
ASSAYS_FETOT	7	22.0082	41.8045	30.3404	38.5172
ASSAYS_MNO	3	0.3407	2.2969	1.0173	0.8196
ASSAYS_P	7	0.1558	0.2975	0.2170	0.0025
ASSAYS_S	7	0.0010	0.0060	0.0023	0.0000
ASSAYS_TIO2	6	0.1697	0.4300	0.2926	0.0064

Blanding_Malm:

Univariate Statistics
=====================

	Count	Minimum	Maximum	Mean	Variance
ASSAYS_FEMAGN	7	3.8059	19.1991	9.9478	34.9720
ASSAYS_FETOT	7	15.1000	40.8623	29.3515	75.5486
ASSAYS_MNO	2	0.1100	0.1300	0.1200	0.0001
ASSAYS_P	7	0.1400	0.2261	0.1774	0.0008
ASSAYS_S	7	0.0010	0.0279	0.0053	0.0001
ASSAYS_TIO2	5	0.2075	0.6300	0.3969	0.0269

Block estimations implemented into the planning system

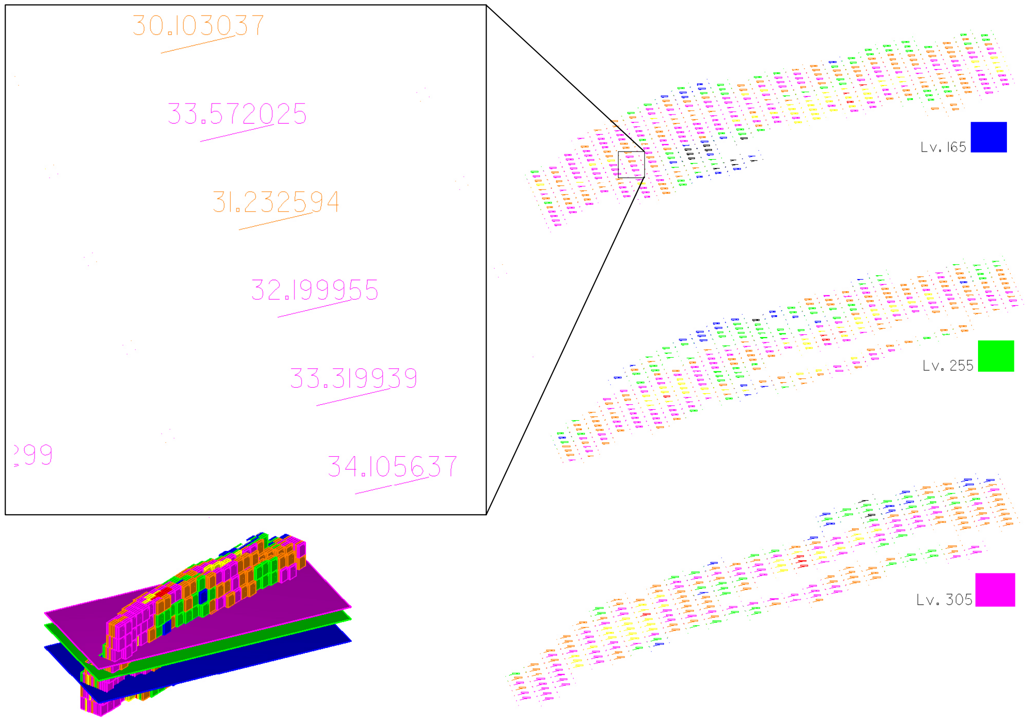

Figure 145 Three levels (horisontal planes) through the total iron block model. The blow up image illustrates the grade presentation.

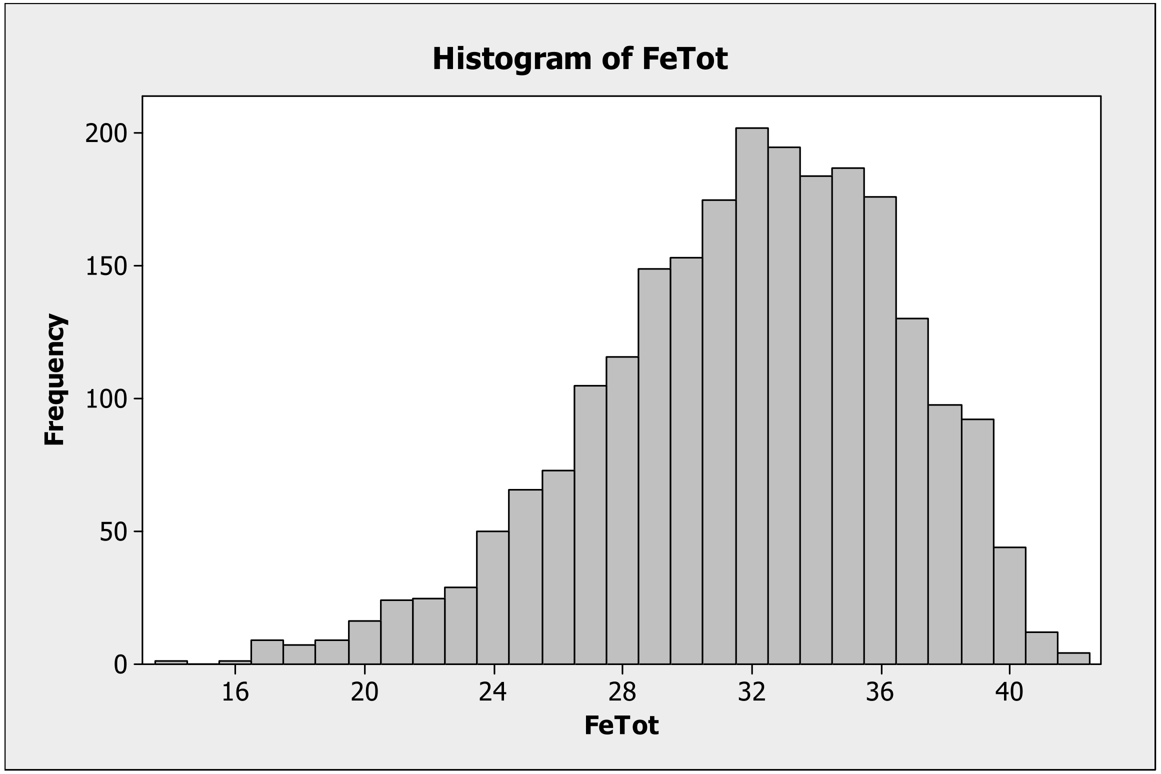

Figure 146 FeTot histogram. Estimated blocks with dimensions 40x10x50.

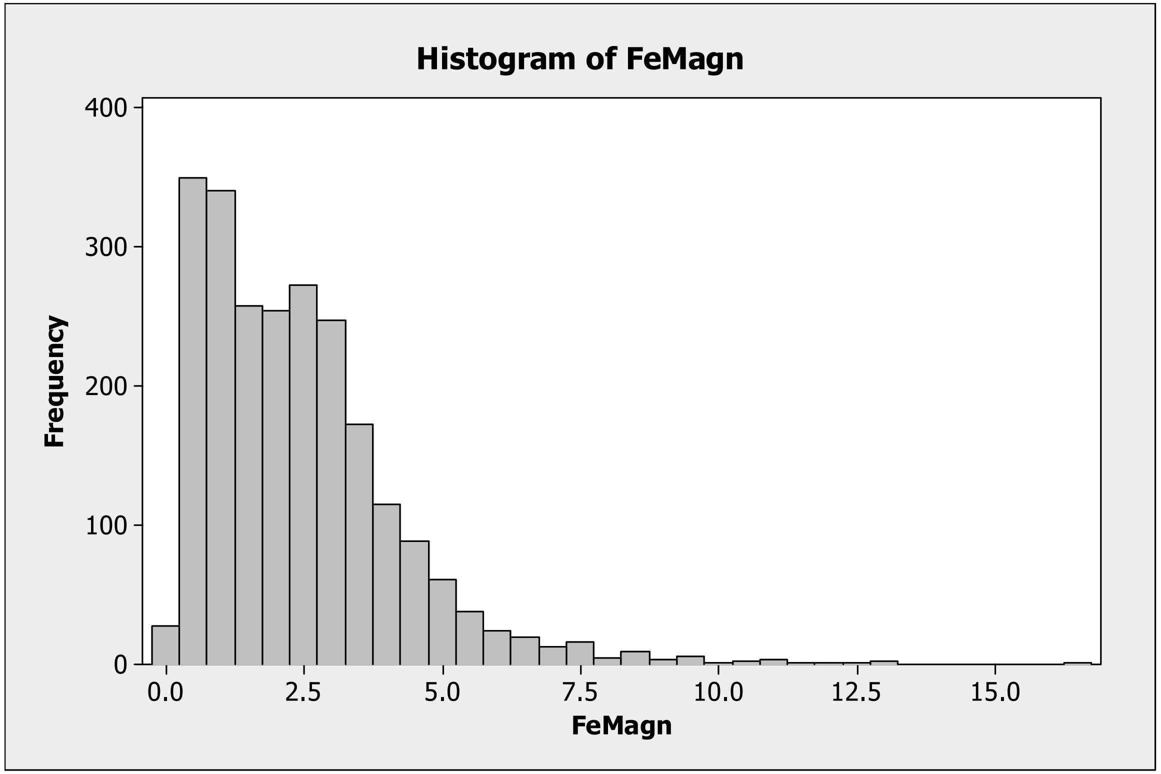

Figure 147 FeMagn histogram. Estimated blocks with dimensions 40x10x50.

Summary statistics – hierarchical cluster analysis

Cluster Analysis of Observations: FEMAGN; MNO; P; S; FactorScore

Standardized Variables, Squared Euclidean Distance, Ward Linkage
Amalgamation Steps

Step	Number of clusters	Similarity level	Distance level	Clusters joined		New cluster	Number of obs. in new cluster
1	238	99.990	0.013	170	206	170	2
2	237	99.989	0.014	43	49	43	2
3	236	99.981	0.024	116	220	116	2
4	235	99.978	0.027	92	214	92	2
5	234	99.977	0.029	57	62	57	2
6	233	99.975	0.031	185	236	185	2
7	232	99.975	0.031	66	67	66	2
8	231	99.974	0.032	8	43	8	3
9	230	99.973	0.033	157	203	157	2
10	229	99.972	0.035	89	102	89	2
11	228	99.970	0.037	117	174	117	2
12	227	99.969	0.039	53	148	53	2
13	226	99.967	0.041	83	129	83	2
14	225	99.965	0.044	13	149	13	2
15	224	99.962	0.048	170	216	170	3
16	223	99.961	0.049	3	114	3	2
17	222	99.957	0.054	52	156	52	2
18	221	99.955	0.056	218	222	218	2
19	220	99.955	0.057	81	223	81	2
20	219	99.954	0.058	151	152	151	2
21	218	99.953	0.059	195	197	195	2
22	217	99.948	0.065	59	72	59	2
23	216	99.948	0.065	231	232	231	2
24	215	99.945	0.069	96	237	96	2
25	214	99.939	0.076	42	145	42	2
26	213	99.938	0.078	13	204	13	3
27	212	99.935	0.082	25	155	25	2
28	211	99.933	0.084	130	188	130	2
29	210	99.933	0.084	104	172	104	2
30	209	99.932	0.085	14	131	14	2
31	208	99.926	0.092	167	215	167	2
32	207	99.926	0.093	136	202	136	2
33	206	99.924	0.095	189	190	189	2
34	205	99.923	0.097	36	50	36	2
35	204	99.919	0.102	107	201	107	2
36	203	99.918	0.103	82	219	82	2
37	202	99.917	0.104	5	144	5	2
38	201	99.916	0.106	135	158	135	2
39	200	99.913	0.108	218	221	218	3
40	199	99.913	0.109	101	143	101	2
41	198	99.911	0.111	19	20	19	2
42	197	99.907	0.116	41	78	41	2
43	196	99.902	0.122	8	77	8	4
44	195	99.901	0.124	93	106	93	2
45	194	99.897	0.129	88	132	88	2
46	193	99.896	0.131	9	22	9	2

47	192	99.894	0.133	35	127	35	2
48	191	99.893	0.134	83	116	83	4
49	190	99.891	0.136	52	141	52	3
50	189	99.890	0.138	16	17	16	2
51	188	99.886	0.143	44	55	44	2
52	187	99.883	0.146	27	40	27	2
53	186	99.882	0.148	123	217	123	2
54	185	99.880	0.150	53	205	53	3
55	184	99.880	0.150	29	30	29	2
56	183	99.880	0.151	10	12	10	2
57	182	99.876	0.155	48	65	48	2
58	181	99.876	0.155	147	157	147	3
59	180	99.875	0.157	150	159	150	2
60	179	99.873	0.160	91	184	91	2
61	178	99.868	0.166	104	213	104	3
62	177	99.861	0.174	107	207	107	3
63	176	99.860	0.176	79	137	79	2
64	175	99.856	0.181	166	183	166	2
65	174	99.856	0.181	115	224	115	2
66	173	99.853	0.184	28	128	28	2
67	172	99.853	0.185	60	111	60	2
68	171	99.844	0.196	23	87	23	2
69	170	99.838	0.202	39	73	39	2
70	169	99.838	0.203	90	118	90	2
71	168	99.835	0.207	26	76	26	2
72	167	99.834	0.207	112	231	112	3
73	166	99.830	0.213	142	154	142	2
74	165	99.829	0.214	96	187	96	3
75	164	99.829	0.214	146	176	146	2
76	163	99.829	0.214	27	54	27	3
77	162	99.825	0.219	82	211	82	3
78	161	99.821	0.224	63	69	63	2
79	160	99.817	0.229	29	199	29	3
80	159	99.813	0.235	25	52	25	5
81	158	99.807	0.242	53	117	53	5
82	157	99.805	0.244	18	140	18	2
83	156	99.796	0.255	3	105	3	3
84	155	99.788	0.265	4	27	4	4
85	154	99.786	0.268	180	228	180	2
86	153	99.784	0.271	90	91	90	4
87	152	99.777	0.280	38	41	38	3
88	151	99.771	0.287	10	80	10	3
89	150	99.771	0.287	23	198	23	3
90	149	99.771	0.287	133	182	133	2
91	148	99.770	0.289	167	189	167	4
92	147	99.769	0.289	200	208	200	2
93	146	99.758	0.303	177	192	177	2
94	145	99.757	0.305	15	71	15	2
95	144	99.755	0.307	82	168	82	4
96	143	99.753	0.309	57	135	57	4
97	142	99.744	0.321	14	84	14	3
98	141	99.740	0.326	16	139	16	3
99	140	99.734	0.333	92	104	92	5
100	139	99.732	0.335	97	185	97	3
101	138	99.732	0.336	101	160	101	3
102	137	99.729	0.340	31	123	31	3
103	136	99.728	0.340	46	66	46	3
104	135	99.728	0.341	11	98	11	2

105	134	99.714	0.358	181	196	181	2
106	133	99.703	0.371	93	170	93	5
107	132	99.701	0.375	32	88	32	3
108	131	99.696	0.381	95	108	95	2
109	130	99.693	0.384	113	166	113	3
110	129	99.690	0.389	45	51	45	2
111	128	99.687	0.391	13	130	13	5
112	127	99.685	0.395	6	7	6	2
113	126	99.667	0.417	46	47	46	4
114	125	99.667	0.418	61	64	61	2
115	124	99.658	0.428	23	24	23	4
116	123	99.658	0.428	3	21	3	4
117	122	99.645	0.444	89	218	89	5
118	121	99.642	0.448	14	142	14	5
119	120	99.642	0.449	2	169	2	2
120	119	99.641	0.450	42	238	42	3
121	118	99.629	0.465	36	63	36	4
122	117	99.622	0.473	81	93	81	7
123	116	99.621	0.475	60	151	60	4
124	115	99.605	0.495	90	191	90	5
125	114	99.602	0.499	9	107	9	5
126	113	99.573	0.534	134	229	134	2
127	112	99.571	0.537	48	74	48	3
128	111	99.564	0.546	53	147	53	8
129	110	99.551	0.562	177	239	177	3
130	109	99.534	0.584	85	193	85	2
131	108	99.523	0.597	5	150	5	4
132	107	99.513	0.610	3	115	3	6
133	106	99.489	0.641	179	230	179	2
134	105	99.487	0.643	2	35	2	4
135	104	99.482	0.649	58	113	58	4
136	103	99.457	0.680	112	165	112	4
137	102	99.445	0.696	48	56	48	4
138	101	99.441	0.700	9	53	9	13
139	100	99.441	0.701	59	101	59	5
140	99	99.435	0.707	122	195	122	3
141	98	99.424	0.722	125	126	125	2
142	97	99.424	0.722	11	138	11	3
143	96	99.408	0.741	8	57	8	8
144	95	99.387	0.768	19	29	19	5
145	94	99.372	0.786	81	83	81	11
146	93	99.369	0.790	10	90	10	8
147	92	99.325	0.845	97	99	97	4
148	91	99.324	0.846	175	177	175	4
149	90	99.317	0.856	32	194	32	4
150	89	99.304	0.871	136	200	136	4
151	88	99.294	0.885	85	153	85	3
152	87	99.278	0.905	1	234	1	2
153	86	99.276	0.907	48	96	48	7
154	85	99.189	1.016	82	171	82	5
155	84	99.175	1.033	4	89	4	9
156	83	99.160	1.052	18	146	18	4
157	82	99.131	1.089	161	225	161	2
158	81	99.117	1.106	124	180	124	3
159	80	99.075	1.158	16	37	16	4
160	79	99.071	1.163	59	164	59	6
161	78	99.071	1.164	13	25	13	10
162	77	99.037	1.206	42	167	42	7

163	76	98.984	1.273	6	173	6	3
164	75	98.980	1.277	5	28	5	6
165	74	98.980	1.278	97	212	97	5
166	73	98.954	1.310	33	125	33	3
167	72	98.844	1.448	110	134	110	3
168	71	98.810	1.490	94	209	94	2
169	70	98.792	1.513	14	112	14	9
170	69	98.779	1.530	85	133	85	5
171	68	98.731	1.589	8	42	8	15
172	67	98.694	1.636	44	59	44	8
173	66	98.546	1.821	60	181	60	6
174	65	98.450	1.942	15	45	15	4
175	64	98.408	1.994	4	58	4	13
176	63	98.369	2.043	38	97	38	8
177	62	98.339	2.080	2	6	2	7
178	61	98.315	2.110	36	61	36	6
179	60	98.244	2.200	19	31	19	8
180	59	98.205	2.249	119	227	119	2
181	58	98.157	2.309	10	39	10	10
182	57	98.045	2.449	5	13	5	16
183	56	97.955	2.561	10	92	10	15
184	55	97.927	2.597	11	163	11	4
185	54	97.901	2.629	103	235	103	2
186	53	97.864	2.675	8	82	8	20
187	52	97.848	2.696	122	124	122	6
188	51	97.778	2.783	23	210	23	5
189	50	97.776	2.786	70	100	70	2
190	49	97.433	3.215	1	178	1	3
191	48	97.422	3.230	103	186	103	3
192	47	97.334	3.339	86	233	86	2
193	46	97.322	3.354	9	81	9	24
194	45	97.316	3.362	26	36	26	8
195	44	97.130	3.594	32	122	32	10
196	43	96.970	3.795	11	95	11	6
197	42	96.869	3.922	18	175	18	8
198	41	96.868	3.924	3	119	3	8
199	40	96.784	4.029	38	136	38	12
200	39	96.707	4.125	44	60	44	14
201	38	96.471	4.421	70	110	70	5
202	37	96.008	5.000	79	94	79	4
203	36	95.648	5.452	34	121	34	2
204	35	95.523	5.608	46	75	46	5
205	34	95.414	5.744	15	85	15	9
206	33	95.348	5.827	5	19	5	24
207	32	95.306	5.880	161	162	161	3
208	31	95.035	6.219	46	68	46	6
209	30	94.642	6.711	1	3	1	11
210	29	94.593	6.774	10	48	10	22
211	28	94.396	7.019	2	4	2	20
212	27	93.589	8.031	14	32	14	19
213	26	93.562	8.065	120	226	120	2
214	25	93.352	8.327	16	103	16	7
215	24	93.165	8.562	33	179	33	5
216	23	93.109	8.632	5	23	5	29
217	22	91.898	10.149	8	10	8	42
218	21	91.187	11.039	11	79	11	10
219	20	90.978	11.301	9	18	9	32
220	19	90.644	11.719	70	86	70	7

221	18	89.015	13.761	109	120	109	3
222	17	88.868	13.944	8	38	8	54
223	16	87.376	15.813	44	70	44	21
224	15	87.032	16.244	2	26	2	28
225	14	78.116	27.413	5	9	5	61
226	13	73.380	33.345	1	8	1	65
227	12	72.308	34.688	33	34	33	7
228	11	72.163	34.870	15	44	15	30
229	10	60.849	49.042	2	14	2	47
230	9	56.173	54.899	1	46	1	71
231	8	54.830	56.581	16	161	16	10
232	7	51.140	61.204	2	5	2	108
233	6	29.163	88.732	11	16	11	20
234	5	-43.126	179.282	15	33	15	37
235	4	-62.429	203.462	1	2	1	179
236	3	-143.441	304.940	15	109	15	40
237	2	-214.426	393.857	11	15	11	60
238	1	-297.449	497.854	1	11	1	239

Final Partition
Number of clusters: 5

	Number of observations	Within cluster sum of squares	Average distance from centroid	Maximum distance from centroid
Cluster1	71	90.276	0.97553	3.60203
Cluster2	108	127.727	1.00626	2.10972
Cluster3	20	96.816	2.05966	4.14738
Cluster4	37	164.213	1.74987	5.86903
Cluster5	3	10.913	1.89097	2.14169

Cluster Centroids

Variable	Cluster1	Cluster2	Cluster3	Cluster4	Cluster5	Grand centroid
FEMAGN	-0.61025	-0.001487	-0.51028	1.33124	1.47927	0.0000000
MNO	-0.03874	-0.343994	2.84650	-0.44384	-0.20197	0.0000000
P	1.08653	-0.268307	-0.63509	-0.85343	-1.29598	-0.0000000
S	-0.01242	-0.225101	0.24194	-0.04412	7.32894	0.0000000
FactorScore	-0.28011	-0.453869	0.67908	1.42457	0.87158	-0.0000000

Distances Between Cluster Centroids

	Cluster1	Cluster2	Cluster3	Cluster4	Cluster5
Cluster1	0.00000	1.54103	3.50476	3.25636	8.08029
Cluster2	1.54103	0.00000	3.47482	2.38533	7.87967
Cluster3	3.50476	3.47482	0.00000	3.86041	7.99693
Cluster4	3.25636	2.38533	3.86041	0.00000	7.41243
Cluster5	8.08029	7.87967	7.99693	7.41243	0.00000

Results for: Cluster1 – hematite ore

Descriptive Statistics: FEMAGN; FETOT; MNO; P; S; TIO2

Variable	Total Count	Mean	StDev	Minimum	Q1	Median	Q3
FEMAGN	71	0.9405	0.7206	0.1000	0.3739	0.7521	1.2493
FETOT	71	36.038	3.671	24.100	33.413	36.452	38.953
MNO	71	0.5868	0.4159	0.1535	0.3046	0.4234	0.7758
P	71	0.25618	0.03349	0.20206	0.23943	0.25000	0.26339
S	71	0.003840	0.003747	0.001000	0.001000	0.002093	0.005000
TIO2	71	0.21991	0.05447	0.09000	0.18306	0.21849	0.25661

Variable	Maximum
FEMAGN	3.9141
FETOT	41.900
MNO	2.0624
P	0.41000
S	0.016301
TIO2	0.37869

Results for: Cluster2 – Magnetite – hematite ore

Descriptive Statistics: FEMAGN; FETOT; MNO; P; S; TIO2

Variable	Total Count	Mean	StDev	Minimum	Q1	Median	Q3
FEMAGN	108	2.411	1.422	0.100	1.260	2.176	3.581
FETOT	108	35.606	4.625	23.599	31.889	36.450	38.790
MNO	108	0.2540	0.1552	0.1026	0.1642	0.2100	0.2883
P	108	0.19296	0.03055	0.13000	0.16989	0.19871	0.21262
S	108	0.002468	0.001705	0.001000	0.001000	0.002000	0.003934
TIO2	108	0.25501	0.08326	0.11175	0.18998	0.25055	0.30289

Variable	Maximum
FEMAGN	5.947
FETOT	44.500
MNO	1.0617
P	0.27949
S	0.008425
TIO2	0.59000

Results for: Cluster3 – Garnet - hematite impregnation

Descriptive Statistics: FEMAGN; FETOT; MNO; P; S; TIO2

Variable	Total Count	Mean	StDev	Minimum	Q1	Median	Q3	Maximum
FEMAGN	20	1.182	2.101	0.100	0.234	0.300	0.587	7.310
FETOT	20	21.36	6.17	9.43	16.13	22.59	26.83	29.76
MNO	20	3.732	1.641	1.383	2.292	3.740	5.329	6.405
P	20	0.17584	0.03033	0.11065	0.15889	0.17613	0.19922	0.22863
S	20	0.00548	0.00724	0.00100	0.00100	0.00200	0.00686	0.02373
TIO2	20	0.4277	0.0746	0.3131	0.3558	0.4337	0.4904	0.5639

Results for: Cluster4 – Magnetite impregnation

Descriptive Statistics: FEMAGN; FETOT; MNO; P; S; TIO2

Variable	Total Count	Mean	StDev	Minimum	Q1	Median	Q3
FEMAGN	37	5.629	3.499	2.104	3.507	4.329	6.744
FETOT	37	20.72	8.62	8.77	14.30	19.02	24.37
MNO	37	0.14521	0.05544	0.08908	0.11000	0.12688	0.14572
P	37	0.16566	0.03090	0.11000	0.14739	0.15688	0.18500
S	37	0.003636	0.003656	0.001000	0.001000	0.002016	0.005080
TIO2	37	0.5303	0.1662	0.1862	0.4493	0.5350	0.6572

Variable	Maximum
FEMAGN	17.700
FETOT	42.30
MNO	0.30361
P	0.25377
S	0.015575
TIO2	0.8426

Results for: Cluster5 – Sulphurous magnetite impregnation

Descriptive Statistics: FEMAGN; FETOT; MNO; P; S; TIO2

Variable	Total Count	Mean	StDev	Minimum	Q1	Median	Q3	Maximum
FEMAGN	3	5.986	1.619	4.133	4.133	6.700	7.126	7.126
FETOT	3	17.90	11.01	8.98	8.98	14.50	30.21	30.21
MNO	3	0.409	0.271	0.100	0.100	0.520	0.606	0.606
P	3	0.1450	0.0264	0.1215	0.1215	0.1400	0.1735	0.1735
S	3	0.05121	0.00867	0.04450	0.04450	0.04815	0.06100	0.06100
TIO2	3	0.491	0.239	0.257	0.257	0.480	0.735	0.735

Summary statistics – non-hierarchical cluster analysis

K-means Cluster Analysis: FEMAGN; MNO; P; S; FactorScores1

Standardized Variables

Final Partition

Number of clusters: 5

	Number of observations	Within cluster sum of squares	Average distance from centroid	Maximum distance from centroid
Cluster1	83	109.484	1.012	3.662
Cluster2	92	77.993	0.851	2.197
Cluster3	16	44.867	1.552	2.729
Cluster4	49	184.823	1.639	5.478
Cluster5	4	9.260	1.307	1.972

Cluster Centroids

Variable	Cluster1	Cluster2	Cluster3	Cluster4	Cluster5	Grand centroid
FEMAGN	-0.5148	-0.1529	-0.7373	1.2797	1.4736	-0.0000
MNO	-0.0418	-0.3314	3.3386	-0.3803	-0.2058	-0.0000
P	1.0550	-0.3428	-0.7297	-0.7998	-1.2905	-0.0000
S	-0.1026	-0.2016	-0.0067	0.0105	6.6624	0.0000
FactorScores1	-0.2375	-0.6571	0.9652	1.2543	0.8149	-0.0000

Distances Between Cluster Centroids

	Cluster1	Cluster2	Cluster3	Cluster4	Cluster5
Cluster1	0.0000	1.5345	4.0146	3.0023	7.5070
Cluster2	1.5345	0.0000	4.0780	2.4417	7.2691
Cluster3	4.0146	4.0780	0.0000	4.2412	7.8908
Cluster4	3.0023	2.4417	4.2412	0.0000	6.6895
Cluster5	7.5070	7.2691	7.8908	6.6895	0.0000

Results for: Cluster1 – Hematite ore

Descriptive Statistics: FEMAGN; FETOT; MNO; P; S; TIO2

Variable	Total Count	Mean	StDev	Minimum	Q1	Median	Q3
FEMAGN	82	1.192	1.107	0.100	0.387	0.894	1.570
FETOT	82	35.455	4.033	24.100	32.504	35.709	38.862

```
MNO           82    0.5955    0.4785    0.1400    0.2684    0.4151
0.7853
P             82   0.25421   0.03224   0.21000   0.23913   0.24910
0.26073
S             82  0.003384  0.003353  0.001000  0.001000  0.002000
0.004450
TIO2          82   0.23143   0.06378   0.09000   0.18355   0.22680
0.26643

Variable   Maximum
FEMAGN       4.729
FETOT       41.900
MNO         2.3187
P          0.41000
S         0.016000
TIO2       0.39000
```

Results for: Cluster2 – Magnetite – hematite ore

Descriptive Statistics: FEMAGN; FETOT; MNO; P; S; TIO2

```
          Total
Variable  Count      Mean     StDev   Minimum        Q1    Median
Q3
FEMAGN       91     2.058     1.226     0.100     1.163     1.980
2.724
FETOT        91    36.501     4.263    19.695    33.765    37.213
39.588
MNO          91    0.2712    0.1816    0.1026    0.1714    0.2300
0.2949
P            91   0.18910   0.02409   0.13000   0.17010   0.19650
0.21000
S            91  0.002692  0.002152  0.001000  0.001000  0.002100
0.004000
TIO2         91   0.23597   0.06399   0.12880   0.18620   0.22440
0.28000

Variable   Maximum
FEMAGN       5.500
FETOT       44.500
MNO         1.3833
P          0.22640
S         0.016300
TIO2       0.43210
```

Results for: Cluster3 – Manganese – hematite impregnation (Garnet fels)

Descriptive Statistics: FEMAGN; FETOT; MNO; P; S; TIO2

```
          Total
Variable  Count     Mean    StDev  Minimum       Q1   Median
Q3  Maximum
FEMAGN       15    0.617    0.960    0.100    0.221    0.300
0.546    3.934
FETOT        15    19.87     6.19     9.43    14.56    21.99
23.70    29.76
```

MNO	15	4.340	1.421	2.290	2.718	4.370	5.632	6.405
P	15	0.17081	0.03198	0.11060	0.14960	0.16770	0.19550	0.22860
S	15	0.00397	0.00524	0.00100	0.00100	0.00200	0.00500	0.01920
TIO2	15	0.4501	0.0698	0.3235	0.4098	0.4814	0.4967	0.5639

Results for: Cluster4 – Magnetite impregnation

Descriptive Statistics: FEMAGN; FETOT; MNO; P; S; TIO2

Variable	Total Count	Mean	StDev	Minimum	Q1	Median	Q3
FEMAGN	48	5.516	3.103	2.105	3.800	4.520	6.217
FETOT	48	22.31	8.17	8.77	15.72	23.20	28.28
MNO	48	0.2187	0.3665	0.0891	0.1131	0.1300	0.1655
P	48	0.16790	0.03266	0.11000	0.14518	0.15845	0.18560
S	48	0.004200	0.004996	0.001000	0.001000	0.002100	0.005150
TIO2	48	0.5027	0.1584	0.1862	0.3726	0.5117	0.5992

Variable	Maximum
FEMAGN	17.700
FETOT	42.30
MNO	2.2653
P	0.25380
S	0.023700
TIO2	0.8426

Results for: Cluster5 – Sulphurous magnetite impregnation

Descriptive Statistics: FEMAGN; FETOT; MNO; P; S; TIO2

Variable	Total Count	Mean	StDev	Minimum	Q1	Median	Q3	Maximum
FEMAGN	3	5.986	1.619	4.133	4.133	6.700	7.126	7.126
FETOT	3	17.90	11.01	8.98	8.98	14.50	30.21	30.21
MNO	3	0.409	0.271	0.100	0.100	0.520	0.606	0.606
P	3	0.1450	0.0264	0.1215	0.1215	0.1400	0.1735	0.1735
S	3	0.05120	0.00868	0.04450	0.04450	0.04810	0.06100	0.06100
TIO2	3	0.491	0.239	0.257	0.257	0.480	0.735	0.735

Experimental variograms

```
========== Parameter File Print ==========
---> Set name   : VarFeMagnOnlyDiaHoles
     Directory name ........ Kvannevann
     File name ............ Comp_S_DL_8m_New
     Selection name ........ DiamondDrillHoles
     Number of variables ... 1
       ASSAYS_FEMAGN
     Total number of samples in File 1413
     Number of samples in Selection  1381

Variogram
=========
 Calculated in 3 directions using 1381 active samples.
 Reference Plane: Horizontal

Direction 1 : N80
*****************
 Width of the slicing       =  10.000000m
 Height of the slicing      =  10.000000m
 Calculation lag            =  30.000000m
 Tolerance (perc. of lag)   = 50.00%
 Number of lags             = 10
 Angular tolerance          = 22.500000
 Direction                  = Azimuth=N80.00

Variable : ASSAYS_FEMAGN
------------------------
 Mean of variable           = 2.548825
 Variance of variable       = 8.454173

 Rank    Number        Average          Value
         of pairs      distance
   0       2           6.747673       0.307800
   1      87          33.545082       3.387278
   2     368          56.587445       4.621926
   3     526          92.760564       5.741349
   4     330         114.001225       4.038605
   5     250         149.857674       6.692644
   6     176         179.711412       6.079292
   7     372         205.738888       5.796694
   8     158         237.184181       3.882038
   9     117         269.947457       9.483396

Direction 2 : N170
******************
 Width of the slicing       =  10.000000m
 Height of the slicing      =  10.000000m
 Calculation lag            =  30.000000m
 Tolerance (perc. of lag)   = 50.00%
 Number of lags             = 10
 Angular tolerance          = 22.500000
 Direction                  = Azimuth=N170.00

Variable : ASSAYS_FEMAGN
------------------------
 Mean of variable           = 2.548825
 Variance of variable       = 8.454173

 Rank    Number        Average          Value
         of pairs      distance
   0     268           8.125063       3.325100
```

1	747	25.860081	6.019036
2	169	56.584816	5.036843
3	54	86.165324	8.335161
4	3	117.763777	6.738878
5	5	148.054922	7.777954

Direction 3 : Vert
****
Calculation lag = 30.000000m
Tolerance (perc. of lag) = 50.00%
Number of lags = 10
Angular tolerance = 22.500000
Direction = Azimuth=N0.00 Dip=-90.00

Variable : ASSAYS_FEMAGN

Mean of variable = 2.548825
Variance of variable = 8.454173

Rank	Number of pairs	Average distance	Value
0	18	12.054049	5.721051
1	583	35.465352	4.584484
2	1524	60.348085	6.393115
3	1778	90.667397	10.433931
4	2523	121.135772	7.806422
5	2928	149.957662	7.209501
6	3189	180.366117	6.579986
7	3367	209.932984	7.504325
8	3057	239.915847	6.366185
9	2563	268.292274	6.096982

========== End of Parameter File Print ==========

========== Parameter File Print ==========
---> Set name : VarFeTotOnlyDia
Directory name .... Kvannevann
File name .... Comp_S_DL_8m_New
Selection name .... DiamondDrillHoles
Number of variables ... 1
ASSAYS_FETOT
Total number of samples in File 1413
Number of samples in Selection 1381

Variogram
=========
Calculated in 3 directions using 1381 active samples.
Reference Plane: Az = 20.00 Ay = 0.00 Ax = 10.00

Direction 1 : N70
****
Width of the slicing = 10.000000m
Height of the slicing = 10.000000m
Calculation lag = 30.000000m
Tolerance (perc. of lag) = 50.00%
Number of lags = 10
Angular tolerance = 22.500000
Direction = Azimuth=N70.00

Variable : ASSAYS_FETOT

Mean of variable = 31.958972
Variance of variable = 74.182467

Rank Number Average Value

	Number of pairs	Average distance	Value
0	2	6.747673	118.058082
1	103	35.668785	42.108849
2	381	56.159349	60.384925
3	604	93.155658	62.290511
4	241	117.916312	78.499544
5	313	150.205235	79.217587
6	263	181.471597	67.834952
7	523	205.843448	83.815282
8	179	240.977073	94.179199
9	203	271.089946	77.047214

Direction 2 : N160
****
Width of the slicing = 10.000000m
Height of the slicing = 10.000000m
Calculation lag = 30.000000m
Tolerance (perc. of lag) = 50.00%
Number of lags = 10
Angular tolerance = 22.500000
Direction = Azimuth=N160.00 Dip=10.00

Variable : ASSAYS_FETOT

Mean of variable = 31.958972
Variance of variable = 74.182467

Rank	Number of pairs	Average distance	Value
0	253	8.250007	40.654893
1	727	26.687006	74.821971
2	286	56.776704	83.372913
3	93	87.269132	107.547082
4	41	118.797221	129.185842
5	13	144.705203	232.689762
6	1	167.232934	51.866267

Direction 3 : Vert
****
Calculation lag = 30.000000m
Tolerance (perc. of lag) = 50.00%
Number of lags = 10
Angular tolerance = 22.500000
Direction = Azimuth=N160.00 Dip=-80.00

Variable : ASSAYS_FETOT

Mean of variable = 31.958972
Variance of variable = 74.182467

Rank	Number of pairs	Average distance	Value
0	30	9.727624	52.016703
1	624	34.433342	46.872952
2	1632	60.727489	63.371702
3	2005	90.809768	64.352630
4	2808	121.046750	66.828226
5	3551	150.193269	66.433551
6	4128	180.334230	65.128296
7	4518	210.147915	72.963544
8	4603	240.212871	75.776424
9	4116	269.072457	75.708296

========== End of Parameter File Print ==========

========== Parameter File Print ==========
---> Set name : VarGaussFeMagn_OnlyDia
Directory name .... Kvannevann
File name .... Comp_S_DL_8m_New
Selection name .... None
Number of variables ... 1
GaussFeMagn_OnlyDia
Total number of samples in File 1413
Number of samples in Selection 1413

Variogram
=========
Calculated in 3 directions using 1413 active samples.
Reference Plane: Az = 10.00 Ay = 0.00 Ax = 10.00

Direction 1 : N80
****
Width of the slicing = 10.000000m
Height of the slicing = 10.000000m
Calculation lag = 30.000000m
Tolerance (perc. of lag) = 50.00%
Number of lags = 10
Angular tolerance = 22.500000
Direction = Azimuth=N80.00

Variable : GaussFeMagn_OnlyDia

Mean of variable = -0.065913
Variance of variable = 0.943773

Rank	Number of pairs	Average distance	Value
0	2	6.747673	0.634539
1	84	33.368403	0.244331
2	367	56.746205	0.508342
3	524	92.879091	0.489025
4	310	114.218867	0.576930
5	242	150.339198	0.692121
6	175	179.876638	0.670472
7	373	205.666432	0.624738
8	161	237.175414	0.787710
9	114	269.947271	0.900421

Direction 2 : N170
****
Width of the slicing = 10.000000m
Height of the slicing = 10.000000m
Calculation lag = 30.000000m
Tolerance (perc. of lag) = 50.00%
Number of lags = 10
Angular tolerance = 22.500000
Direction = Azimuth=N170.00 Dip=10.00

Variable : GaussFeMagn_OnlyDia

Mean of variable = -0.065913
Variance of variable = 0.943773

Rank	Number of pairs	Average distance	Value
0	184	8.209178	0.257305
1	518	26.152183	0.827265
2	111	55.472575	0.960011

```
 3      10          82.708375      0.802591

Direction 3 : Vert
*****************
 Calculation lag          =  30.000000m
 Tolerance (perc. of lag)  = 50.00%
 Number of lags           = 10
 Angular tolerance        = 22.500000
 Direction                = Azimuth=N170.00 Dip=-80.00

Variable : GaussFeMagn_OnlyDia
------------------------------
 Mean of variable         = -0.065913
 Variance of variable     = 0.943773

 Rank   Number       Average         Value
        of pairs     distance
  0       30         9.505458       0.417753
  1      606        34.565743       0.474635
  2     1607        60.620342       0.573786
  3     1963        90.785931       0.734746
  4     2690       121.088281       0.699048
  5     3464       150.024043       0.805312
  6     3994       180.496108       0.864953
  7     4574       210.138328       0.905274
  8     4466       240.055577       0.857519
  9     3875       268.748802       0.876842

========== End of Parameter File Print ==========

========== Parameter File Print ==========
---> Set name   : VarGaussFeTot
     Directory name ........ Kvannevann
     File name ............. Comp_S_DL_8m_New
     Selection name ........ None
     Number of variables ... 1
       GaussFeTot
     Total number of samples in File 1413
     Number of samples in Selection  1413

Variogram
=========
 Calculated in 3 directions using 1413 active samples.
 Reference Plane: Az = 14.00  Ay = 0.00  Ax = 16.00

Direction 1 : N76
*****************
 Width of the slicing      =  10.000000m
 Height of the slicing     =  10.000000m
 Calculation lag           =  30.000000m
 Tolerance (perc. of lag)  = 50.00%
 Number of lags            = 10
 Angular tolerance         = 22.500000
 Direction                 = Azimuth=N76.00

Variable : GaussFeTot
---------------------
 Mean of variable          = 0.157192
 Variance of variable      = 0.903551

 Rank   Number       Average         Value
        of pairs     distance
  0        9         3.560005       0.971790
  1      129        32.609894       0.635820
  2      394        56.729021       0.584343
```

3	621	92.805541	0.757215
4	277	115.781831	0.706423
5	265	150.552202	1.030610
6	227	181.031430	0.834582
7	499	206.298590	0.845519
8	183	237.669686	0.729826
9	139	273.056988	1.188890

Direction 2 : N166
****
Width of the slicing = 10.000000m
Height of the slicing = 10.000000m
Calculation lag = 30.000000m
Tolerance (perc. of lag) = 50.00%
Number of lags = 10
Angular tolerance = 22.500000
Direction = Azimuth=N166.00 Dip=16.00

Variable : GaussFeTot

Mean of variable = 0.157192
Variance of variable = 0.903551

Rank	Number of pairs	Average distance	Value
0	216	8.301645	0.475179
1	574	25.992616	0.909748
2	149	59.050294	0.895358
3	66	85.906976	1.232022
4	19	117.091794	0.955377
5	3	140.526289	2.793579

Direction 3 : Vert
****
Calculation lag = 30.000000m
Tolerance (perc. of lag) = 50.00%
Number of lags = 10
Angular tolerance = 22.500000
Direction = Azimuth=N166.00 Dip=-74.00

Variable : GaussFeTot

Mean of variable = 0.157192
Variance of variable = 0.903551

Rank	Number of pairs	Average distance	Value
0	48	8.952542	0.543183
1	659	33.799297	0.593391
2	1653	60.824281	0.754992
3	2020	90.800026	0.755699
4	2787	121.043894	0.817558
5	3812	150.340189	0.870982
6	4420	180.276463	0.811762
7	5136	210.270799	0.921069
8	5125	240.089493	0.878065
9	4491	269.064011	0.894590

========== End of Parameter File Print ==========

========== Parameter File Print ==========
---> Set name : VarGaussMnOBeforeCondExp
Directory name .... Kvannevann
File name .... MnO_Merged_ForCondExp
Selection name .... None

Number of variables ... 1
GaussMnO
Total number of samples in File 2506
Number of samples in Selection 2506

Variogram
=========
Calculated in 3 directions using 2506 active samples.
Reference Plane: Az = 10.00 Ay = 0.00 Ax = 10.00

Direction 1 : N80
****
Width of the slicing = 10.000000m
Height of the slicing = 10.000000m
Calculation lag = 30.000000m
Tolerance (perc. of lag) = 50.00%
Number of lags = 10
Angular tolerance = 22.500000
Direction = Azimuth=N80.00

Variable : GaussMnO

Mean of variable = -0.000000
Variance of variable = 0.988453

Rank	Number of pairs	Average distance	Value
0	7	3.205957	0.337461
1	18	22.984869	0.199537
2	61	57.072756	0.533192
3	53	90.268198	0.370058
4	46	114.658612	1.058668
5	21	148.485102	1.656608
6	30	183.046203	0.929960
7	29	209.930278	1.072002
8	4	232.807078	0.661610
9	7	272.341941	3.190689

Direction 2 : N170
****
Width of the slicing = 10.000000m
Height of the slicing = 10.000000m
Calculation lag = 30.000000m
Tolerance (perc. of lag) = 50.00%
Number of lags = 10
Angular tolerance = 22.500000
Direction = Azimuth=N170.00 Dip=10.00

Variable : GaussMnO

Mean of variable = -0.000000
Variance of variable = 0.988453

Rank	Number of pairs	Average distance	Value
0	56	8.115577	0.318482
1	82	24.768155	1.006517
2	8	49.986488	1.592956

Direction 3 : Vert
****
Calculation lag = 30.000000m
Tolerance (perc. of lag) = 50.00%

Number of lags = 10
Angular tolerance = 22.500000
Direction = Azimuth=N170.00 Dip=-80.00

Variable : GaussMnO

Mean of variable = -0.000000
Variance of variable = 0.988453

Rank	Number of pairs	Average distance	Value
2	11	65.544554	0.375858
3	166	92.355591	1.452700
4	186	120.574660	0.579919
5	313	150.232358	0.640686
6	265	180.248537	0.949335
7	264	209.835630	1.755752
8	138	242.195462	1.072819
9	247	268.804479	0.817893

========== End of Parameter File Print ==========

========== Parameter File Print ==========
---> Set name : VarJointDensity_Lag1m
Directory name .... Kvannevann
File name .... BreaksLines
Selection name .... None
Number of variables ... 1
JointDensity
Total number of samples in File 15038
Number of samples in Selection 15038

Variogram
=========
Calculated in 5 directions using 14809 active samples.
Reference Plane: Az = 20.00 Ay = 0.00 Ax = 30.00

Direction 1 : N70
****
Width of the slicing = 5.000000m
Height of the slicing = 5.000000m
Calculation lag = 1.000000m
Tolerance (perc. of lag) = 50.00%
Number of lags = 300
Angular tolerance = 22.400000
Direction = Azimuth=N70.00

Variable : JointDensity

Mean of variable = 4.025115
Variance of variable = 6.173955

Rank	Number of pairs	Average distance	Value
2	2	1.945883	3.250000
3	0	0.000000	0.000000
4	0	0.000000	0.000000
5	14	5.214040	3.535714
6	72	6.055240	6.534722
7	19	6.811663	2.368421
8	20	8.126427	2.125000
9	41	8.922248	10.963415
10	23	9.901123	3.586957

11	1	10.536842	2.000000
12	0	0.000000	0.000000
13	10	13.458882	9.750000
14	73	13.918880	11.869863
15	32	14.889565	13.171875
16	4	15.624364	28.000000
17	0	0.000000	0.000000
18	0	0.000000	0.000000
19	0	0.000000	0.000000
20	0	0.000000	0.000000
21	22	21.192510	1.545455
22	39	22.021489	1.423077
23	35	22.991934	0.671429
24	41	24.112707	1.414634
25	67	25.003583	1.873134
26	58	25.920751	1.913793
27	14	26.786149	8.750000
28	0	0.000000	0.000000
29	0	0.000000	0.000000
30	0	0.000000	0.000000
31	0	0.000000	0.000000
32	0	0.000000	0.000000
33	0	0.000000	0.000000
34	2	34.419624	0.500000
35	101	35.101593	8.470297
36	107	35.952052	4.565421
37	66	37.068127	3.446970
38	157	38.063519	2.283439
39	240	39.009855	2.381250
40	362	40.116667	6.538674
41	217	40.954767	5.815668
42	444	41.871975	4.186937
43	237	43.090432	5.369198
44	276	43.878611	5.014493
45	423	45.159387	5.172577
46	422	45.928433	4.411137
47	194	47.010388	3.610825
48	155	47.976277	2.780645
49	337	49.154895	2.838279
50	1088	49.997615	3.931985
51	1265	50.943414	4.560870
52	512	51.983048	5.062500
53	708	53.013590	5.035311
54	973	54.027525	6.060637
55	811	54.903893	3.395808
56	262	55.960979	4.444656
57	372	57.011574	4.919355
58	426	57.972337	3.153756
59	383	58.984299	3.236292
60	452	59.967190	5.787611
61	237	60.924696	4.092827
62	121	61.985437	2.206612
63	109	63.028908	1.766055
64	188	64.052121	4.438830
65	187	64.959910	2.339572
66	158	66.073946	4.955696
67	249	67.047357	5.232932
68	109	67.816081	5.802752
69	8	68.655142	4.062500
70	0	0.000000	0.000000
71	1	71.369229	12.500000
72	22	72.100910	2.681818
73	33	72.996175	2.893939
74	121	74.201963	4.752066
75	357	75.023722	4.490196

76	434	75.998328	6.652074
77	489	76.990976	6.460123
78	1126	78.071886	7.488011
79	986	78.930052	5.367140
80	281	79.920061	4.339858
81	147	80.970683	4.091837
82	110	81.980964	3.577273
83	188	83.020930	2.944149
84	183	84.003610	3.275956
85	166	84.971605	3.840361
86	138	86.008062	3.833333
87	143	87.004920	2.118881
88	152	88.013498	2.996711
89	173	89.017423	1.546243
90	166	89.979120	1.734940
91	120	90.993114	3.945833
92	137	92.053071	6.160584
93	366	93.120565	7.090164
94	451	93.992601	6.009978
95	321	94.965099	6.419003
96	610	96.127818	4.809836
97	914	97.003239	5.313457
98	1325	98.077676	6.688302
99	2792	99.064690	6.068052
100	3434	99.965616	6.883372
101	2568	100.984566	7.190421
102	2569	101.903994	5.994940
103	1252	102.942573	6.571086
104	1338	104.107898	7.682362
105	1067	104.957180	4.876757
106	461	105.938325	5.131236
107	298	107.008987	5.823826
108	369	107.956846	6.199187
109	274	108.988143	5.490876
110	264	110.012078	3.880682
111	323	111.011649	3.527864
112	255	111.959938	3.958824
113	170	113.000232	5.129412
114	174	113.935938	8.681034
115	37	114.822782	4.378378
116	75	116.197946	4.066667
117	537	116.966915	4.833333
118	129	117.786413	5.058140
119	47	119.163579	2.680851
120	78	119.958266	1.448718
121	21	120.990887	1.119048
122	31	122.159541	4.709677
123	227	123.119493	4.903084
124	739	124.053977	5.747632
125	164	124.792672	4.560976
126	28	125.878501	4.089286
127	18	127.026706	14.305556
128	70	128.074684	4.985714
129	201	129.097684	3.733831
130	163	129.990026	4.432515
131	217	130.992447	3.555300
132	135	131.954249	4.370370
133	232	133.096001	4.306034
134	336	133.989036	4.633929
135	154	134.998787	2.464286
136	147	135.960846	3.030612
137	89	136.941786	4.219101
138	283	137.833532	3.772085
139	31	139.086345	6.725806
140	72	140.001003	6.597222

141	327	141.079383	6.961774
142	237	142.131444	5.457806
143	438	142.882386	7.711187
144	55	144.033768	10.554545
145	251	145.099977	2.840637
146	340	146.102078	5.938235
147	337	146.822133	5.077151
148	257	148.261739	3.414397
149	316	148.908521	4.276899
150	409	149.976124	5.654034
151	356	150.978982	3.769663
152	452	151.984439	7.327434
153	226	152.997927	6.634956
154	563	154.046767	5.094139
155	289	154.988128	4.159170
156	265	156.009604	3.543396
157	522	157.092911	5.048851
158	713	157.962152	4.478261
159	593	158.971666	3.508432
160	169	159.875347	3.834320
161	121	160.972026	7.772727
162	78	162.073888	2.121795
163	357	163.003002	5.546218
164	295	163.924960	4.283051
165	163	164.958342	3.159509
166	127	165.991567	1.795276
167	134	167.020886	2.977612
168	145	167.995754	3.496552
169	177	169.043325	5.025424
170	346	170.006745	6.291908
171	282	170.953245	3.264184
172	175	171.975184	5.074286
173	172	173.026284	3.674419
174	192	174.020995	4.544271
175	519	175.069889	4.501927
176	326	175.899038	6.492331
177	228	177.008497	7.557018
178	311	178.042427	6.471061
179	383	178.965882	4.593995
180	154	180.008317	6.662338
181	110	180.892872	8.136364
182	23	182.145359	1.869565
183	52	183.011585	4.057692
184	74	184.011104	3.777027
185	198	185.055734	6.732323
186	246	185.994121	4.717480
187	243	186.998287	4.884774
188	289	188.006499	4.051903
189	446	189.075090	7.586323
190	403	189.979144	7.363524
191	633	191.058067	5.161927
192	428	191.903591	4.982477
193	387	193.126366	5.108527
194	493	194.027286	7.810345
195	457	195.071874	6.766958
196	783	195.978747	6.348659
197	754	196.995327	5.108090
198	877	197.977308	5.347206
199	1099	199.007605	5.653321
200	1622	200.033722	6.601726
201	2500	201.034688	6.800200
202	3317	201.986516	6.780826
203	1062	202.925918	4.368644
204	238	203.883600	6.747899
205	533	205.063974	3.350844

206	713	206.017722	3.212482
207	609	206.970685	3.246305
208	422	207.980310	4.658768
209	479	209.026581	6.637787
210	479	210.007255	6.073069
211	693	211.044865	4.898990
212	560	211.926771	2.628571
213	284	213.035034	3.466549
214	212	213.924008	3.726415
215	360	215.086292	5.584722
216	327	216.002635	4.480122
217	376	217.002191	4.597074
218	371	217.984300	4.061995
219	347	219.019960	4.083573
220	364	219.997078	4.711538
221	332	220.999072	7.537651
222	365	222.020582	7.119178
223	454	223.039397	6.674009
224	989	223.955104	5.676441
225	277	224.748425	8.976534
226	188	226.108884	8.069149
227	537	226.985865	5.257914
228	126	227.963398	3.797619
229	124	228.999135	3.814516
230	120	229.998598	6.145833
231	111	230.988998	6.085586
232	102	231.997211	5.529412
233	98	233.008500	2.704082
234	94	233.989902	8.755319
235	88	234.989649	6.920455
236	86	235.989694	5.941860
237	173	236.879549	4.930636
238	88	237.990268	6.568182
239	213	239.011667	4.286385
240	106	239.990310	4.915094
241	298	241.204295	5.036913
242	513	241.936071	5.429825
243	280	242.998245	8.542857
244	385	244.050737	7.987013
245	395	244.981779	4.994937
246	208	245.941716	4.963942
247	322	247.044524	4.361801
248	313	248.030246	4.782748
249	168	248.962703	3.482143
250	310	249.903557	4.319355
251	245	250.902301	6.400000
252	217	252.062251	6.502304
253	170	252.851218	8.950000
254	229	253.967693	9.949782
255	100	255.015530	3.835000
256	155	256.033521	6.622581
257	195	256.995356	4.930769
258	187	258.103027	5.687166
259	376	258.991480	3.496011
260	188	259.917706	5.555851
261	191	261.064576	3.421466
262	184	261.960567	4.603261
263	296	263.036069	3.211149
264	206	263.890367	2.868932
265	149	265.051465	5.805369
266	189	266.007354	5.174603
267	376	267.027242	6.820479
268	177	267.802710	6.932203
269	84	269.032438	5.785714
270	86	269.995236	4.686047

271	107	271.007867	3.906542
272	122	272.005277	7.348361
273	152	273.011775	4.572368
274	168	274.037280	10.818452
275	271	275.055315	7.365314
276	549	276.071503	6.934426
277	550	276.904430	7.180909
278	143	277.865252	10.800699
279	104	279.035239	3.629808
280	82	279.901339	5.457317
281	76	280.996957	3.703947
282	74	281.993187	6.560811
283	71	282.991723	4.190141
284	73	284.034871	3.287671
285	141	285.141573	5.453901
286	181	285.840737	5.555249
287	50	287.093783	2.970000
288	111	288.026988	2.220721
289	172	289.021349	5.665698
290	236	290.049676	9.627119
291	219	290.929965	3.424658
292	296	292.133414	7.173986
293	296	292.969685	6.858108
294	289	293.999693	7.435986
295	289	294.996963	10.337370
296	414	296.096783	4.789855
297	597	297.006867	5.453099
298	382	298.004463	6.366492
299	541	299.060346	7.017560

Direction 2 : N111
****
Width of the slicing = 5.000000m
Height of the slicing = 5.000000m
Calculation lag = 1.000000m
Tolerance (perc. of lag) = 50.00%
Number of lags = 300
Angular tolerance = 22.400000
Direction = Azimuth=N110.89 Dip=20.70

Variable : JointDensity

Mean of variable = 4.025115
Variance of variable = 6.173955

Rank	Number of pairs	Average distance	Value
1	1	1.482072	8.000000
2	3	2.166231	1.000000
3	6	2.972161	1.333333
4	9	3.981019	3.722222
5	12	5.039777	8.500000
6	12	6.027053	8.875000
7	38	7.096079	8.289474
8	54	8.065914	4.370370
9	76	8.981081	5.598684
10	84	9.994686	3.839286
11	91	10.991734	3.989011
12	84	12.005623	4.511905
13	91	13.007940	5.560440
14	87	14.023545	4.482759
15	93	14.976610	4.666667
16	82	15.992228	3.750000
17	68	16.984986	4.757353
18	46	17.987310	2.652174

19	47	18.996898	2.765957
20	70	20.135489	1.600000
21	99	20.989358	1.035354
22	70	21.976389	1.600000
23	42	22.917750	3.035714
24	18	23.917829	1.500000
25	13	24.922074	1.538462
26	15	25.941870	2.533333
27	15	27.094110	3.100000
28	24	28.013532	1.208333
29	27	29.016320	1.759259
30	24	30.012084	1.562500
31	24	30.962641	2.395833
32	23	32.016083	2.086957
33	22	32.999810	0.977273
34	52	34.127735	2.576923
35	135	35.029093	5.525926
36	124	35.984488	5.608871
37	110	36.990265	5.268182
38	109	38.020887	6.463303
39	92	38.946609	5.608696
40	50	40.004802	7.460000
41	59	41.004092	6.864407
42	60	41.990320	10.750000
43	172	43.052342	7.081395
44	114	43.930400	6.877193
45	50	45.023155	7.630000
46	49	45.995102	3.632653
47	45	46.993500	3.988889
48	43	48.025673	4.209302
49	51	49.043413	3.823529
50	61	50.030128	3.672131
51	99	51.035230	5.646465
52	113	51.995187	4.969027
53	100	52.999663	6.870000
54	192	54.016758	5.005208
55	185	54.999143	5.732432
56	207	55.996207	4.403382
57	166	56.965315	6.804217
58	127	57.974444	6.614173
59	88	59.017706	9.420455
60	78	59.993885	6.147436
61	88	61.005094	6.892045
62	80	61.997651	6.168750
63	90	63.059967	6.927778
64	147	64.000557	5.047619
65	144	64.976621	6.670139
66	114	66.018916	5.543860
67	112	67.019821	5.763393
68	77	67.941040	4.707792
69	96	68.985993	5.062500
70	180	70.020277	5.452778
71	221	70.993648	4.945701
72	247	71.990843	5.534413
73	291	72.996033	5.336770
74	331	74.017680	5.468278
75	425	74.983564	5.457647
76	426	75.970469	7.780516
77	408	76.982308	8.922794
78	481	78.038451	5.746362
79	485	79.032197	3.821649
80	400	79.985438	4.345000
81	360	80.940233	4.688889
82	239	81.975480	4.891213
83	228	82.999889	5.942982

84	220	83.983196	4.895455
85	201	84.980231	6.447761
86	177	85.989053	5.742938
87	169	86.992107	5.644970
88	138	87.980477	7.452899
89	118	88.996487	5.122881
90	102	90.004263	9.794118
91	49	91.000360	6.193878
92	47	92.019406	2.404255
93	55	93.051554	4.372727
94	112	94.058645	10.821429
95	130	94.965836	7.734615
96	75	96.026434	5.386667
97	93	97.037637	7.301075
98	121	98.009319	6.677686
99	132	99.010202	7.518939
100	132	100.003558	4.166667
101	106	100.970772	8.660377
102	106	102.000096	10.485849
103	95	102.993810	8.536842
104	89	104.018038	7.157303
105	101	105.006349	5.301980
106	96	105.970760	5.416667
107	85	107.000703	4.605882
108	84	107.995623	4.267857
109	81	109.008102	5.030864
110	73	109.988542	11.828767
111	70	110.979089	8.692857
112	70	111.995865	6.385714
113	67	112.998957	7.149254
114	62	113.928437	6.516129
115	37	114.947084	2.594595
116	35	115.997438	2.414286
117	35	117.018642	3.514286
118	37	117.997190	2.229730
119	41	118.996060	3.378049
120	92	120.102910	3.478261
121	149	121.000644	4.738255
122	162	122.024596	6.487654
123	151	122.953292	9.821192
124	72	123.895105	9.451389
125	49	124.998583	6.306122
126	78	126.022896	14.435897
127	101	127.003191	14.777228
128	94	127.990870	11.686170
129	81	128.989461	11.043210
130	93	130.034329	8.241935
131	104	131.002739	7.480769
132	106	132.007725	6.448113
133	94	132.987600	6.680851
134	76	133.979373	5.730263
135	76	135.006842	5.276316
136	64	135.996059	5.976562
137	99	137.030423	5.156566
138	125	137.982709	4.976000
139	143	139.020074	3.804196
140	149	139.996958	3.140940
141	168	141.026951	2.672619
142	228	141.992424	3.028509
143	253	143.001436	3.918972
144	242	144.004452	3.514463
145	257	145.010111	4.204280
146	212	145.997232	4.084906
147	206	147.021213	3.750000
148	202	148.016638	5.995050

149	183	148.977499	5.382514
150	135	149.958642	7.166667
151	118	150.963478	6.555085
152	121	151.979531	8.880165
153	84	152.967873	16.226190
154	42	154.014116	18.892857
155	36	155.033359	7.472222
156	52	155.975325	9.413462
157	61	156.996637	13.221311
158	77	158.048210	8.538961
159	66	159.034924	15.469697
160	56	159.965687	14.473214
161	52	161.012120	7.846154
162	59	162.068786	8.211864
163	58	162.988499	5.241379
164	67	163.939224	4.126866
165	60	165.015328	5.433333
166	53	165.993583	4.028302
167	48	167.068094	5.135417
168	67	168.017269	6.716418
169	67	168.982976	6.582090
170	65	169.946553	3.584615
171	50	170.984182	2.060000
172	28	171.994837	3.267857
173	12	172.830433	1.041667
174	14	173.919413	1.035714
175	8	175.048440	1.062500
176	4	176.023823	1.000000
177	3	176.809807	0.833333
178	2	177.597892	0.250000
179	0	0.000000	0.000000
180	0	0.000000	0.000000
181	0	0.000000	0.000000
182	0	0.000000	0.000000
183	0	0.000000	0.000000
184	0	0.000000	0.000000
185	0	0.000000	0.000000
186	0	0.000000	0.000000
187	0	0.000000	0.000000
188	0	0.000000	0.000000
189	5	189.047886	10.000000
190	13	190.008590	7.653846
191	17	190.966314	9.264706
192	21	191.964936	10.500000
193	23	193.035554	8.608696
194	29	194.040339	7.568966
195	31	194.998602	6.629032
196	40	196.025011	5.462500
197	50	196.989590	5.140000
198	53	198.019331	6.801887
199	49	199.036299	5.887755
200	43	199.986811	6.569767
201	39	201.013720	4.102564
202	29	201.989494	4.672414
203	34	202.983087	3.838235
204	27	204.008290	1.888889
205	20	204.919820	3.200000
206	20	205.969763	2.850000
207	8	206.930894	1.062500
208	0	0.000000	0.000000
209	0	0.000000	0.000000
210	0	0.000000	0.000000
211	0	0.000000	0.000000
212	0	0.000000	0.000000
213	0	0.000000	0.000000

214	115	214.063519	3.752174
215	133	214.980142	4.308271
216	49	215.887665	1.887755
217	36	216.950421	3.430556
218	44	218.015740	6.681818
219	71	219.051957	7.598592
220	90	220.046255	8.061111
221	129	221.026910	8.217054
222	146	222.005661	10.205479
223	138	222.988797	9.644928
224	117	223.988492	10.252137
225	102	224.952033	7.485294
226	42	225.917833	7.976190
227	10	227.140941	4.650000
228	14	227.993107	3.321429
229	26	229.005163	1.269231
230	31	230.073774	2.419355
231	13	230.949810	1.423077
232	15	231.980506	2.133333
233	12	233.074851	3.541667
234	12	233.969323	2.291667
235	14	234.976957	3.464286
236	10	235.958477	2.800000
237	15	236.908971	3.133333
238	22	238.111461	8.750000
239	28	239.029705	2.535714
240	31	239.943216	1.903226
241	22	241.015656	0.568182
242	22	242.000782	0.522727
243	22	242.997732	13.704545
244	14	244.012953	11.071429
245	14	245.044700	18.821429
246	14	246.004109	10.250000
247	13	247.018590	7.153846
248	14	247.948604	15.892857
249	16	249.008255	9.531250
250	13	249.990816	12.192308
251	9	250.910689	10.444444
252	10	252.049729	6.650000
253	24	253.004753	8.062500
254	42	253.991830	9.869048
255	44	255.008937	11.738636
256	42	256.007464	13.476190
257	45	257.019590	9.577778
258	43	258.006955	7.755814
259	45	258.963912	6.422222
260	44	260.005919	5.056818
261	27	261.031669	7.129630
262	22	261.963919	7.727273
263	19	262.980505	4.657895
264	20	263.971028	4.850000
265	18	264.991758	4.694444
266	11	266.039277	3.318182
267	4	266.925368	8.625000
268	0	0.000000	0.000000
269	0	0.000000	0.000000
270	0	0.000000	0.000000
271	0	0.000000	0.000000
272	0	0.000000	0.000000
273	0	0.000000	0.000000
274	0	0.000000	0.000000
275	0	0.000000	0.000000
276	0	0.000000	0.000000
277	0	0.000000	0.000000
278	0	0.000000	0.000000

279	0	0.000000	0.000000
280	0	0.000000	0.000000
281	0	0.000000	0.000000
282	0	0.000000	0.000000
283	0	0.000000	0.000000
284	0	0.000000	0.000000
285	1	285.448785	0.500000
286	8	286.133982	3.687500
287	21	287.056064	2.809524
288	29	288.029292	1.465517
289	32	288.972446	2.453125
290	34	289.992179	3.000000
291	31	290.996193	2.290323
292	33	291.988619	6.712121
293	29	293.000083	6.155172
294	29	294.002527	3.396552
295	30	295.030053	4.900000
296	28	296.026775	2.178571
297	33	297.027327	2.530303
298	28	297.993599	3.482143
299	12	298.868480	3.250000

Direction 3 : N160
****

Width of the slicing = 5.000000m
Height of the slicing = 5.000000m
Calculation lag = 1.000000m
Tolerance (perc. of lag) = 50.00%
Number of lags = 300
Angular tolerance = 22.400000
Direction = Azimuth=N160.00 Dip=30.00

Variable : JointDensity

Mean of variable = 4.025115
Variance of variable = 6.173955

Rank	Number of pairs	Average distance	Value
1	1458	0.999778	2.682442
2	1460	2.000539	3.044863
3	1498	3.002994	3.215955
4	1546	4.003565	3.382600
5	1594	5.004051	3.389586
6	1661	6.002029	3.454846
7	1722	7.001401	3.811266
8	1769	8.001956	3.537592
9	1823	8.999869	3.738343
10	1881	10.002784	3.912015
11	1945	11.000429	3.928792
12	1997	12.001983	3.881322
13	2074	13.000461	4.224204
14	2100	13.999289	4.208333
15	1964	14.997715	4.358961
16	1880	15.995546	4.304255
17	1851	17.000041	4.293625
18	1767	17.996025	4.465195
19	1770	18.997407	4.695763
20	1733	19.998316	4.672533
21	1676	20.995392	4.167661
22	1630	21.994693	4.159202
23	1546	22.996238	4.313389
24	1523	23.994470	4.660867
25	1481	24.998146	5.093856
26	1386	26.001543	4.450577

27	1344	26.996803	4.968006
28	1300	27.994036	4.711154
29	1241	28.996645	4.887994
30	1202	29.997521	4.784526
31	1159	30.997431	5.760569
32	1149	32.003111	5.019147
33	1130	33.000744	5.384956
34	1137	33.997718	5.293316
35	1100	35.000668	5.535909
36	1067	35.991681	5.840675
37	1030	36.988400	5.559709
38	1015	37.994818	5.166010
39	978	38.992882	5.158487
40	1008	40.003821	5.019345
41	1006	40.997707	5.283300
42	1021	41.997390	5.275220
43	967	43.000324	5.284385
44	935	44.001822	5.490909
45	955	45.003829	5.459686
46	955	45.996172	5.801047
47	957	46.994401	5.516719
48	917	47.983917	5.540894
49	958	48.989352	5.914927
50	919	49.997287	5.501632
51	909	50.993663	5.292629
52	892	51.994403	5.154709
53	886	52.996085	5.893341
54	867	53.993605	6.092849
55	879	54.990281	5.875995
56	901	56.000314	6.209767
57	908	57.000986	6.001101
58	914	57.994689	5.699125
59	936	59.002675	5.539530
60	924	59.994803	5.816017
61	897	60.989165	5.983835
62	868	61.987164	5.984447
63	848	62.985967	5.823703
64	759	63.995138	6.330698
65	754	64.994887	6.187003
66	710	66.002142	5.759859
67	688	66.987910	6.748547
68	649	68.000194	6.086287
69	635	68.995642	5.670079
70	626	69.993287	5.412939
71	599	70.988287	5.470785
72	597	71.993676	5.506700
73	589	72.993768	5.809847
74	596	73.999577	7.177013
75	567	74.992555	6.513228
76	591	75.996026	7.198816
77	578	76.994196	6.554498
78	579	77.991238	6.263385
79	569	78.989965	6.353251
80	557	79.993073	7.182226
81	546	80.991225	7.419414
82	540	81.987050	6.672222
83	547	82.989122	6.518282
84	533	83.995018	6.474672
85	525	84.990738	7.925714
86	532	85.985454	6.198308
87	522	86.980519	5.601533
88	531	87.981725	5.026365
89	492	88.983582	5.548780
90	537	89.990588	6.502793
91	562	91.001329	5.653025

92	578	91.995770	5.723183
93	570	92.985167	5.854386
94	563	93.982891	5.401421
95	569	94.992651	5.573814
96	566	95.993666	5.549470
97	540	96.986077	5.489815
98	509	97.980308	5.601179
99	462	98.978572	6.044372
100	422	99.977933	6.090047
101	396	100.982038	6.463384
102	388	101.986153	6.534794
103	377	102.988847	5.733422
104	371	103.984291	6.312668
105	367	104.976974	5.946866
106	372	105.975936	6.413978
107	372	106.979774	6.366935
108	381	107.988245	6.906824
109	360	108.980403	6.930556
110	346	109.971328	6.437861
111	319	110.972287	6.253918
112	299	111.967216	6.215719
113	279	112.965255	7.127240
114	258	113.962245	7.029070
115	241	114.966879	6.800830
116	213	115.949421	6.424883
117	192	116.953273	5.520833
118	179	117.955695	6.265363
119	178	118.956797	5.148876
120	177	119.963733	5.265537
121	175	120.962484	4.942857
122	169	121.962263	4.822485
123	162	122.962792	4.966049
124	158	123.963757	5.348101
125	145	124.961067	5.100000
126	133	125.934717	5.609023
127	134	126.942537	5.813433
128	127	127.955042	5.818898
129	123	128.952329	5.613821
130	116	129.940039	6.293103
131	121	130.950563	6.028926
132	111	131.956963	5.927928
133	104	132.943782	5.673077
134	99	133.922873	5.272727
135	103	134.931011	4.699029
136	95	135.947487	5.873684
137	91	136.941964	5.351648
138	86	137.921807	4.924419
139	94	138.946792	4.537234
140	79	139.956043	5.632911
141	77	140.924890	5.285714
142	77	141.939636	5.175325
143	70	142.945861	6.957143
144	67	143.931619	6.246269
145	66	144.900969	5.689394
146	71	145.921635	6.070423
147	62	146.931276	5.758065
148	60	147.909189	6.291667
149	60	148.916815	6.650000
150	54	149.913800	4.574074
151	51	150.911798	7.068627
152	49	151.914329	7.020408
153	50	152.893478	6.150000
154	50	153.873981	7.820000
155	54	154.897327	6.898148
156	52	155.921366	4.903846

157	47	156.920984	7.542553
158	48	157.886915	8.052083
159	51	158.873243	7.411765
160	56	159.898742	6.446429
161	51	160.930529	6.441176
162	48	161.917298	5.677083
163	46	162.871338	8.804348
164	46	163.846228	7.304348
165	50	164.868465	5.410000
166	48	165.915326	8.041667
167	43	166.912105	8.360465
168	43	167.868607	7.151163
169	42	168.832110	8.642857
170	48	169.866364	6.802083
171	46	170.915114	6.673913
172	41	171.910735	9.719512
173	42	172.873347	9.892857
174	41	173.827327	13.560976
175	47	174.866416	18.500000
176	44	175.916583	7.977273
177	41	176.899955	9.890244
178	39	177.871557	10.064103
179	39	178.823540	9.205128
180	44	179.859448	6.909091
181	41	180.887979	8.768293
182	40	181.892051	7.412500
183	38	182.870163	10.657895
184	37	183.821447	19.391892
185	41	184.846476	10.573171
186	41	185.880758	10.280488
187	38	186.896121	7.500000
188	36	187.872170	6.388889
189	36	188.820622	6.833333
190	38	189.833313	5.947368
191	39	190.861571	5.346154
192	38	191.889953	5.789474
193	34	192.876743	6.750000
194	34	193.822461	5.808824
195	35	194.798844	4.971429
196	38	195.834370	3.960526
197	37	196.888967	4.175676
198	33	197.881300	5.166667
199	32	198.827290	4.531250
200	32	199.780793	5.437500
201	38	200.834470	2.460526
202	35	201.881310	5.114286
203	32	202.879705	3.234375
204	31	203.832884	5.500000
205	31	204.785160	4.161290
206	34	205.808789	6.294118
207	35	206.874591	18.885714
208	31	207.889894	12.225806
209	29	208.843887	12.879310
210	29	209.793298	5.517241
211	32	210.799115	10.421875
212	34	211.859571	3.779412
213	30	212.895136	5.250000
214	28	213.854787	8.589286
215	18	214.728348	12.305556
216	29	215.790044	8.948276
217	32	216.849501	7.953125
218	29	217.878223	7.431034
219	17	218.719939	13.000000
220	16	219.717406	12.125000
221	16	220.715515	11.187500

222	16	221.713641	10.875000
223	15	222.711127	13.200000
224	15	223.709246	11.066667
225	15	224.707425	15.566667
226	15	225.705621	16.166667
227	14	226.703077	10.857143
228	14	227.701264	10.535714
229	14	228.699495	7.928571
230	13	229.696955	16.423077
231	13	230.695205	9.730769
232	13	231.693471	9.153846
233	13	232.691721	5.423077
234	12	233.689209	9.833333
235	12	234.687495	3.750000
236	12	235.685796	8.875000
237	12	236.684090	6.125000
238	11	237.681601	7.272727
239	11	238.679931	6.909091
240	11	239.678226	8.545455
241	10	240.675715	11.450000
242	10	241.674074	14.550000
243	10	242.672407	10.950000
244	10	243.670738	11.100000
245	9	244.668194	12.222222
246	9	245.666577	15.277778
247	9	246.664944	3.888889
248	9	247.663324	11.722222
249	8	248.660725	10.750000
250	8	249.659175	14.562500
251	8	250.657606	6.375000
252	8	251.655999	6.562500
253	7	252.653463	8.142857
254	7	253.651972	11.928571
255	7	254.650492	10.142857
256	7	255.649023	13.071429
257	6	256.646511	2.333333
258	6	257.644965	12.583333
259	6	258.643565	12.166667
260	5	259.641120	13.100000
261	5	260.639662	9.000000
262	5	261.638134	10.700000
263	5	262.636750	10.200000
264	4	263.634326	8.500000
265	4	264.632795	7.000000
266	4	265.631276	14.500000
267	4	266.629932	5.000000
268	3	267.627301	12.500000
269	3	268.625980	4.000000
270	3	269.624671	11.000000
271	3	270.623237	1.500000
272	2	271.620515	4.250000
273	2	272.619177	1.250000
274	2	273.617721	5.000000
275	2	274.616347	0.500000
276	1	275.613805	2.000000
277	1	276.612498	0.000000
278	1	277.610797	4.500000
279	1	278.609654	0.500000

Direction 4 : N209
****
Width of the slicing = 5.000000m
Height of the slicing = 5.000000m
Calculation lag = 1.000000m
Tolerance (perc. of lag) = 50.00%

Number of lags = 300
Angular tolerance = 22.400000
Direction = Azimuth=N209.11 Dip=20.70

Variable : JointDensity

Mean of variable = 4.025115
Variance of variable = 6.173955

Rank	Number of pairs	Average distance	Value
1	3	1.359767	2.166667
2	12	2.071847	6.458333
3	9	3.077139	4.000000
4	15	4.105371	5.300000
5	18	4.971034	3.055556
6	30	5.997334	1.550000
7	104	6.969405	6.365385
8	76	7.994778	4.092105
9	70	8.986033	4.828571
10	62	9.964322	3.169355
11	65	11.019379	5.469231
12	51	12.001018	6.137255
13	47	13.042718	7.393617
14	46	14.010761	7.630435
15	47	15.021984	9.000000
16	43	16.045191	4.197674
17	54	17.042222	4.435185
18	58	18.025992	3.646552
19	60	19.024182	3.208333
20	55	19.981530	5.545455
21	60	20.999483	3.975000
22	54	21.992871	2.962963
23	58	22.997168	4.327586
24	54	23.962830	9.351852
25	56	24.966160	10.821429
26	53	26.029529	6.349057
27	61	27.034761	6.163934
28	59	28.024520	8.593220
29	59	28.981267	13.728814
30	89	30.022601	6.219101
31	93	31.008914	4.677419
32	99	31.982072	5.464646
33	92	32.971708	6.163043
34	93	33.963461	4.935484
35	78	34.949803	7.000000
36	68	35.983236	5.625000
37	65	37.003356	3.330769
38	58	37.968409	4.000000
39	67	38.964941	3.246269
40	57	39.992674	4.447368
41	51	40.980148	3.039216
42	57	41.978420	4.105263
43	56	43.043134	5.428571
44	52	44.010569	4.644231
45	69	44.996504	4.471014
46	66	46.005781	4.196970
47	39	47.021402	8.128205
48	45	48.017583	9.522222
49	89	49.022913	4.758427
50	101	50.008319	5.767327
51	135	51.043572	5.314815
52	202	52.042803	3.997525
53	194	52.957853	3.832474
54	100	53.936592	3.915000

55	81	54.986452	5.512346
56	74	56.017787	4.641892
57	91	57.014118	3.730769
58	96	57.981798	3.916667
59	86	58.982577	5.860465
60	108	60.040801	6.120370
61	214	61.115269	5.628505
62	284	61.927391	6.044014
63	197	63.015677	5.555838
64	1292	64.146709	3.708978
65	608	64.995305	3.646382
66	573	66.010149	5.268761
67	695	67.021488	4.998561
68	734	67.978417	3.919619
69	403	68.970399	5.162531
70	324	69.996540	6.587963
71	311	71.003172	6.696141
72	250	71.970533	6.280000
73	214	72.984652	5.684579
74	208	73.998077	5.651442
75	205	75.002488	5.782927
76	223	76.005705	4.147982
77	219	76.996579	4.036530
78	184	77.998126	3.855978
79	338	79.115322	7.736686
80	335	79.949729	7.302985
81	145	80.958266	6.320690
82	98	81.977874	6.193878
83	98	83.021944	5.377551
84	104	83.982829	4.927885
85	61	84.954514	3.975410
86	22	85.978818	3.227273
87	27	87.005466	3.870370
88	31	88.036114	4.112903
89	35	88.992471	2.757143
90	45	89.994371	4.066667
91	30	90.995002	2.666667
92	39	92.003336	2.589744
93	63	93.073754	5.841270
94	109	94.006995	9.119266
95	123	94.993479	8.325203
96	114	95.979346	5.122807
97	86	96.955565	9.151163
98	44	97.942931	8.000000
99	37	99.017604	7.189189
100	51	99.996364	5.392157
101	66	101.017961	4.757576
102	84	102.074140	6.196429
103	111	103.012235	5.878378
104	135	103.982130	7.459259
105	130	105.024730	8.730769
106	116	105.998467	7.500000
107	120	107.003058	7.150000
108	109	107.998361	8.697248
109	106	108.982564	11.330189
110	117	109.991416	12.461538
111	125	111.015096	11.476000
112	176	112.028038	8.710227
113	176	112.975748	7.724432
114	136	113.985585	7.272059
115	135	115.006602	9.455556
116	131	115.980901	7.893130
117	85	116.952789	5.700000
118	65	118.014069	4.100000
119	65	119.022004	3.361538

120	105	120.036017	4.704762
121	148	121.012517	5.226351
122	152	121.996311	5.723684
123	175	122.992670	6.808571
124	193	124.021067	5.689119
125	250	125.022930	5.104000
126	314	126.008384	5.542994
127	368	126.993015	5.394022
128	355	127.988117	4.338028
129	330	128.996767	5.831818
130	322	129.996135	7.167702
131	294	130.984363	4.702381
132	273	131.977490	4.985348
133	228	133.000436	5.162281
134	210	133.994494	3.919048
135	227	134.999911	5.281938
136	188	135.974705	4.944149
137	163	136.983601	4.858896
138	162	138.007194	5.098765
139	221	139.002180	4.828054
140	243	139.994974	5.940329
141	291	141.012770	5.457045
142	298	141.997930	4.627517
143	275	142.999748	4.514545
144	266	143.997653	4.236842
145	227	144.996224	4.955947
146	177	145.992149	6.514124
147	151	146.978653	6.079470
148	122	147.973172	7.577869
149	98	148.955063	6.489796
150	72	149.971053	8.006944
151	52	150.988032	8.471154
152	49	152.000548	6.112245
153	42	152.995126	3.952381
154	39	154.011876	4.987179
155	37	155.006134	6.175676
156	38	155.988525	4.763158
157	39	157.003261	5.474359
158	36	158.001507	4.513889
159	37	158.988785	5.202703
160	37	159.992107	4.891892
161	41	160.998418	5.926829
162	33	161.957350	8.348485
163	31	163.000577	7.274194
164	31	163.998378	8.129032
165	31	164.976259	10.741935
166	32	166.007004	8.546875
167	30	167.001491	9.966667
168	41	168.000098	10.829268
169	39	168.951854	10.166667
170	32	170.067011	10.015625
171	61	171.048669	11.786885
172	69	171.999910	8.333333
173	64	172.992733	7.296875
174	68	173.958347	5.375000
175	62	174.995352	8.177419
176	35	175.934013	5.157143
177	11	176.841871	6.318182
178	0	0.000000	0.000000
179	0	0.000000	0.000000
180	0	0.000000	0.000000
181	0	0.000000	0.000000
182	0	0.000000	0.000000
183	7	183.133032	8.500000
184	12	184.096044	8.708333

185	26	184.971465	7.153846
186	16	185.995452	6.000000
187	16	187.042861	15.062500
188	14	188.028224	16.357143
189	20	189.069119	9.725000
190	46	189.965726	6.076087
191	45	190.999042	2.833333
192	45	192.022056	2.888889
193	64	193.013031	5.648438
194	78	193.990743	7.019231
195	71	194.950726	5.823944
196	64	195.940768	4.984375
197	36	197.027320	4.944444
198	43	198.072657	6.697674
199	59	199.085998	6.677966
200	80	200.065997	6.731250
201	109	201.017832	5.889908
202	117	202.004342	4.393162
203	126	203.005257	3.301587
204	121	203.995450	3.512397
205	90	204.994206	3.927778
206	61	205.998967	2.844262
207	64	207.017460	3.804688
208	72	207.980761	4.062500
209	62	208.970576	6.701613
210	56	210.007130	4.848214
211	62	211.000928	8.766129
212	50	211.996663	11.130000
213	40	212.981228	15.475000
214	37	213.996799	9.824324
215	34	215.003383	13.838235
216	30	215.964413	4.350000
217	16	216.946393	4.187500
218	9	217.898704	17.000000
219	0	0.000000	0.000000
220	0	0.000000	0.000000
221	0	0.000000	0.000000
222	0	0.000000	0.000000
223	0	0.000000	0.000000
224	0	0.000000	0.000000
225	0	0.000000	0.000000
226	0	0.000000	0.000000
227	0	0.000000	0.000000
228	0	0.000000	0.000000
229	0	0.000000	0.000000
230	0	0.000000	0.000000
231	0	0.000000	0.000000
232	0	0.000000	0.000000
233	0	0.000000	0.000000
234	0	0.000000	0.000000
235	3	235.338466	3.500000
236	4	236.088898	1.375000
237	5	236.950957	1.900000
238	4	238.077253	2.250000
239	2	239.006979	7.250000
240	3	239.825663	9.000000
241	2	241.159863	0.250000
242	1	242.105155	4.500000
243	0	0.000000	0.000000
244	7	244.105380	3.142857
245	12	245.057880	8.083333
246	13	245.908692	15.307692
247	9	247.019308	17.777778
248	8	248.038944	42.250000
249	16	249.020875	35.593750

250	16	249.970492	15.000000
251	18	250.991336	3.361111
252	16	252.022255	7.656250
253	16	253.013870	14.625000
254	16	254.000599	5.125000
255	16	254.986146	7.718750
256	12	255.869918	14.958333
257	0	0.000000	0.000000
258	0	0.000000	0.000000
259	0	0.000000	0.000000
260	0	0.000000	0.000000
261	0	0.000000	0.000000
262	0	0.000000	0.000000
263	0	0.000000	0.000000
264	0	0.000000	0.000000
265	0	0.000000	0.000000
266	0	0.000000	0.000000
267	0	0.000000	0.000000
268	0	0.000000	0.000000
269	0	0.000000	0.000000
270	0	0.000000	0.000000
271	2	271.299369	26.500000
272	10	272.107442	7.200000
273	15	273.051081	11.300000
274	18	273.989637	14.500000
275	18	275.003876	3.555556
276	17	276.049461	4.411765
277	16	276.999738	16.531250
278	18	278.023086	34.416667
279	11	278.913601	19.818182
280	6	279.814809	6.000000

Direction 5 : N160
****
Calculation lag = 1.000000m
Tolerance (perc. of lag) = 50.00%
Number of lags = 300
Angular tolerance = 22.500000
Direction = Azimuth=N160.00 Dip=-60.00

Variable : JointDensity

Mean of variable = 4.025115
Variance of variable = 6.173955

Rank	Number of pairs	Average distance	Value
1	3047	0.999705	2.795372
2	3044	2.000247	3.407194
3	3056	3.000765	3.642997
4	3074	4.001065	3.872479
5	3096	5.000419	3.973676
6	3138	5.999665	3.725303
7	3171	6.999794	3.993062
8	3233	8.000226	4.048562
9	3251	9.001786	4.128730
10	3306	10.000085	4.218693
11	3349	11.000490	4.281577
12	3386	12.000497	4.065121
13	3431	13.000470	4.349315
14	3476	13.999472	4.428078
15	3566	15.000345	4.338054
16	3592	15.999880	4.512945
17	3677	16.999896	4.608104
18	3731	18.001199	4.388770

19	3799	19.000785	4.384180
20	3870	20.001354	4.495995
21	3920	21.000867	4.671939
22	3994	21.998772	4.515148
23	4057	22.995904	4.554843
24	4147	23.997378	4.530504
25	4198	24.998928	4.670319
26	4266	25.998433	4.676512
27	4336	27.000280	4.716328
28	4393	28.001332	4.671523
29	4466	29.001192	4.647000
30	4546	30.001326	4.663880
31	4600	31.000154	4.845217
32	4681	31.997717	5.040483
33	4765	32.996234	5.061070
34	4841	33.995277	4.961372
35	4908	34.995353	5.058578
36	4980	35.995854	4.976004
37	5104	36.995501	4.928292
38	5226	37.994830	4.952545
39	5369	38.996450	4.928385
40	5470	39.997472	4.889122
41	5575	40.995881	4.948341
42	5676	41.997293	4.830603
43	5816	42.998200	4.919790
44	5959	43.997769	4.830425
45	6145	44.993080	4.773230
46	6207	45.995569	4.792734
47	6266	46.995223	4.882222
48	6354	47.994349	4.709081
49	6403	48.994128	4.815399
50	6496	49.994660	4.981604
51	6591	50.995854	4.969276
52	6632	51.996946	4.922120
53	6636	52.996063	5.031646
54	6616	53.994740	5.082527
55	6637	54.991317	5.093114
56	6697	55.991777	5.392191
57	6702	56.994428	5.504327
58	6731	57.993607	5.415243
59	6789	58.992833	5.391884
60	6854	59.993294	5.493726
61	6900	60.993325	5.587391
62	6969	61.991650	5.471373
63	7062	62.992925	5.527896
64	7094	63.993680	5.578024
65	7129	64.994123	5.466265
66	7208	65.994217	5.377497
67	7233	66.994729	5.363542
68	7328	67.994022	5.439820
69	7343	68.991644	5.444641
70	7448	69.991077	5.474356
71	7445	70.992327	5.353727
72	7457	71.989633	5.320638
73	7487	72.987389	5.393950
74	7519	73.985904	5.472403
75	7590	74.988378	5.293808
76	7552	75.992528	5.426178
77	7556	76.990821	5.331260
78	7621	77.989851	5.370949
79	7648	78.990645	5.379380
80	7628	79.989471	5.590915
81	7642	80.987411	5.539257
82	7680	81.988060	5.498307
83	7695	82.990038	5.430734

84	7651	83.989308	5.524376
85	7720	84.988873	5.576360
86	7735	85.988234	5.767679
87	7816	86.987722	5.793820
88	7902	87.987044	5.766388
89	8000	88.988045	5.666125
90	8047	89.987396	5.665838
91	8127	90.987699	5.645626
92	8161	91.988772	5.657211
93	8180	92.988340	5.612347
94	8247	93.986891	5.590457
95	8319	94.986339	5.696839
96	8315	95.984623	5.649429
97	8428	96.983283	5.563301
98	8365	97.982296	5.520143
99	8448	98.981687	5.523556
100	8461	99.983041	5.469212
101	8508	100.984157	5.609426
102	8532	101.983579	5.659576
103	8586	102.984464	5.645353
104	8508	103.982842	5.790139
105	8581	104.982396	5.787146
106	8604	105.981679	5.842922
107	8660	106.981168	5.811778
108	8666	107.981774	5.816986
109	8763	108.981563	5.869508
110	8807	109.982301	5.847564
111	8865	110.980093	5.837338
112	9026	111.981031	5.775094
113	9201	112.982605	5.876916
114	9219	113.983903	5.865604
115	9282	114.981127	5.869209
116	9350	115.978922	5.802460
117	9476	116.978544	5.728789
118	9573	117.980249	5.827745
119	9579	118.980613	5.775551
120	9720	119.981880	5.866049
121	9751	120.983484	5.749923
122	9835	121.984028	5.594509
123	9895	122.985679	5.602021
124	10090	123.982762	5.718484
125	10394	124.983745	5.644747
126	10649	125.985584	5.626819
127	10864	126.983050	5.488954
128	11106	127.981336	5.526472
129	11346	128.983009	5.622290
130	11397	129.983950	5.595200
131	11504	130.982780	5.649600
132	11580	131.982213	5.659283
133	11721	132.984670	5.702670
134	12024	133.986700	5.625250
135	12230	134.989067	5.665904
136	12290	135.988608	5.625671
137	12373	136.986062	5.816011
138	12526	137.984665	5.646775
139	12841	138.988582	5.617631
140	13246	139.985631	5.598181
141	13164	140.982871	5.688696
142	13012	141.982046	5.683331
143	12845	142.980539	5.698793
144	12843	143.982932	5.708440
145	12693	144.983573	5.503782
146	12746	145.982333	5.644987
147	12833	146.984209	5.685771
148	12933	147.985028	5.711397

149	12918	148.983649	5.625406
150	12964	149.982924	5.597655
151	13058	150.984053	5.583703
152	13089	151.982325	5.657346
153	13167	152.977522	5.679046
154	13307	153.977046	5.644736
155	13357	154.981821	5.572733
156	13344	155.984534	5.669215
157	13368	156.985238	5.624102
158	13395	157.988717	5.598320
159	13412	158.990489	5.661870
160	13472	159.990250	5.580129
161	13601	160.995309	5.601059
162	13570	161.998039	5.633493
163	13691	162.997600	5.599774
164	13752	163.995960	5.512398
165	13837	164.995245	5.520958
166	13859	165.995655	5.559312
167	14304	166.997354	5.536913
168	14940	167.994602	5.515696
169	15183	168.996279	5.525324
170	15391	169.996869	5.745728
171	15708	170.998811	5.826012
172	16140	172.003518	5.768587
173	16519	172.998066	5.876143
174	16819	173.998801	5.997622
175	16955	175.001860	5.993040
176	16935	176.002297	5.979451
177	17184	177.002245	5.792743
178	17232	178.000084	5.909587
179	17244	178.999857	6.005973
180	17241	179.997353	5.898991
181	17320	180.998421	5.859931
182	17378	182.001091	5.932530
183	17531	182.999726	5.913867
184	17770	183.999780	6.017755
185	17955	185.001091	5.993400
186	18126	186.001340	5.971257
187	18050	187.001698	6.036260
188	18194	188.000894	5.990217
189	18192	189.001263	5.934916
190	18310	190.001806	5.984926
191	18372	191.002711	5.915932
192	18535	192.002497	5.898220
193	18632	193.004312	5.988219
194	18827	194.006273	6.016492
195	19127	195.006805	6.095441
196	19316	196.005154	6.184769
197	19585	197.002258	6.288946
198	19764	198.002223	6.249696
199	19909	199.001080	6.184766
200	20111	200.000567	6.191661
201	20314	201.002136	6.217559
202	20565	202.003152	6.186385
203	20740	203.003548	6.113380
204	20969	204.002447	6.089465
205	21115	205.002581	6.096969
206	21256	206.001915	6.145441
207	21461	207.001716	6.111947
208	21738	208.002341	6.071833
209	22082	209.003606	6.147360
210	22562	210.002862	6.203550
211	22915	211.003279	6.112328
212	23093	212.002931	6.232408
213	23099	213.002648	6.193688

214	23280	214.002298	6.168149
215	23257	215.002427	6.066303
216	23479	216.002320	6.106457
217	23590	217.003160	6.097181
218	23702	218.002157	6.140874
219	24015	219.000844	6.229128
220	24196	220.000917	6.245888
221	24384	221.001508	6.361508
222	24408	222.000846	6.451942
223	24607	223.000120	6.435953
224	24715	224.000156	6.377200
225	24905	224.999950	6.438546
226	25095	226.000214	6.370293
227	25227	227.000145	6.444444
228	25387	228.000068	6.464470
229	25588	228.998554	6.358781
230	26010	229.997571	6.400192
231	26092	230.997936	6.372681
232	26396	231.998723	6.298757
233	26452	232.999651	6.253062
234	26552	233.997995	6.306531
235	26793	234.997897	6.423917
236	26949	235.999193	6.418067
237	26932	236.997142	6.257612
238	27122	237.995299	6.419143
239	27514	238.997267	6.403158
240	27485	239.998928	6.350900
241	27638	240.998764	6.413579
242	27641	242.000255	6.490756
243	27615	243.000051	6.537371
244	27767	243.998752	6.492041
245	27889	244.998549	6.474757
246	27909	245.998243	6.479003
247	28024	246.997180	6.500892
248	28264	247.998446	6.470722
249	28199	248.999216	6.405387
250	28551	250.000317	6.316048
251	28819	250.998783	6.427582
252	28999	251.998837	6.478189
253	29191	252.999929	6.417338
254	29502	254.001003	6.391380
255	29513	255.000991	6.390320
256	29699	255.999347	6.393953
257	30045	256.999781	6.341638
258	30081	258.001648	6.361025
259	30260	259.000001	6.377743
260	30286	260.000035	6.402661
261	30554	261.001923	6.370606
262	30561	262.000926	6.400232
263	30771	263.000022	6.381544
264	30940	264.001410	6.418536
265	30929	265.002039	6.341071
266	31011	266.002501	6.381203
267	31083	267.001795	6.461217
268	31262	268.001903	6.417104
269	31392	269.001466	6.339959
270	31525	270.000276	6.475607
271	31784	270.999561	6.517698
272	31948	272.000541	6.472033
273	31789	273.000550	6.480166
274	31912	273.998486	6.473960
275	32067	274.998730	6.399601
276	32062	275.999601	6.393768
277	31956	277.000357	6.347040
278	31910	278.001795	6.348088

279	31602	279.000638	6.428755
280	31660	279.998954	6.280496
281	31659	280.998149	6.343394
282	31772	281.998849	6.378006
283	31781	283.001073	6.386741
284	31762	284.001188	6.387271
285	31920	285.001788	6.390351
286	31914	286.002580	6.381431
287	31835	287.001844	6.306110
288	31800	287.999640	6.303475
289	32012	288.998793	6.216278
290	32082	289.999674	6.277492
291	32126	290.999915	6.312395
292	32275	291.999504	6.300945
293	32597	293.000986	6.316778
294	32510	294.000899	6.443233
295	32748	294.999734	6.435706
296	32792	296.000114	6.467004
297	32849	297.002004	6.419800
298	32822	298.003014	6.492916
299	32718	299.001364	6.415521

========== End of Parameter File Print ==========

========== Parameter File Print ==========
---> Set name : VarMnO_CondExp
Directory name .... Kvannevann
File name .... MnO_Merged_ForCondExp
Selection name .... None
Number of variables ... 1
MnO_CondExp
Total number of samples in File 2506
Number of samples in Selection 2506

Variogram
=========
Calculated in 3 directions using 2502 active samples.
Reference Plane: Az = 10.00 Ay = 0.00 Ax = 10.00

Direction 1 : N80
****
Width of the slicing = 10.000000m
Height of the slicing = 10.000000m
Calculation lag = 30.000000m
Tolerance (perc. of lag) = 50.00%
Number of lags = 10
Angular tolerance = 22.500000
Direction = Azimuth=N80.00

Variable : MnO_CondExp

Mean of variable = 0.487911
Variance of variable = 0.500926

Rank	Number of pairs	Average distance	Value
0	7	3.205957	0.002074
1	89	30.801082	0.305318
2	373	57.698098	0.252887
3	379	91.675950	0.418139
4	323	115.373196	0.534101
5	212	149.335028	0.403029
6	153	182.030577	0.659658

7	285	206.968187	0.441210
8	100	237.969694	0.741050
9	77	268.390636	0.481403

Direction 2 : N170
****
Width of the slicing = 10.000000m
Height of the slicing = 10.000000m
Calculation lag = 30.000000m
Tolerance (perc. of lag) = 50.00%
Number of lags = 10
Angular tolerance = 22.500000
Direction = Azimuth=N170.00 Dip=10.00

Variable : MnO_CondExp

Mean of variable = 0.487911
Variance of variable = 0.500926

Rank	Number of pairs	Average distance	Value
0	221	7.452661	0.296512
1	365	26.744113	0.458186
2	104	55.064688	0.628621
3	7	77.709482	0.313575

Direction 3 : Vert
****
Calculation lag = 30.000000m
Tolerance (perc. of lag) = 50.00%
Number of lags = 10
Angular tolerance = 22.500000
Direction = Azimuth=N170.00 Dip=-80.00

Variable : MnO_CondExp

Mean of variable = 0.487911
Variance of variable = 0.500926

Rank	Number of pairs	Average distance	Value
0	19	9.748770	0.126316
1	483	35.038521	0.386924
2	1308	60.607035	0.439603
3	1853	90.879249	0.584887
4	2164	120.582296	0.528351
5	2877	150.603151	0.504697
6	3189	180.256091	0.485747
7	3404	210.199206	0.443424
8	2755	239.798027	0.585979
9	2524	268.778328	0.619278

========== End of Parameter File Print ==========

Variogram models

```
========== Parameter File Print ==========
---> Set name   : VarModelFeMagnOnlyDiaHoles
     Directory name ........ Kvannevann
     File name ............. Comp_S_DL_8m_New
     Selection name ........ DiamondDrillHoles
     Number of variables ... 1
       ASSAYS_FEMAGN
     Total number of samples in File 1413
     Number of samples in Selection  1381

Model : Covariance part
=======================
Number of variables        = 1
- Variable 1 : ASSAYS_FEMAGN
Number of basic structures = 3
Global Rot (mathematician) = (  10.00,    0.00,    0.00)
Global Rot (geologist)     = (  80.00,    0.00,    0.00)
S1 : Nugget effect
     Sill =        2.2
S2 : Spherical - Range = 40.000000m
     Sill =          3
     Directional Scales = ( 90.000000m, 40.000000m,120.000000m)
S3 : Spherical - Range = 90.000000m
     Sill =        2.6
     Directional Scales = ( N/A,150.000000m, 90.000000m)

Model : Drift part
==================
 Number of drift functions  = 1
 - Universality condition

========== End of Parameter File Print ==========

========== Parameter File Print ==========
---> Set name   : VarModelFeTot
     Directory name ........ Kvannevann
     File name ............. Comp_S_DL_8m_New
     Selection name ........ None
     Number of variables ... 1
       ASSAYS_FETOT
     Total number of samples in File 1413
     Number of samples in Selection  1413

Model : Covariance part
=======================
Number of variables        = 1
- Variable 1 : ASSAYS_FETOT
Number of basic structures = 4
Global Rot (mathematician) = (  14.00,    0.00,   15.00)
Global Rot (geologist)     = (  76.00,   15.00,    0.00)
S1 : Nugget effect
     Sill =         20
S2 : Spherical - Range = 30.000000m
     Sill =         20
     Directional Scales = ( 80.000000m, 30.000000m, 60.000000m)
S3 : Spherical - Range = 40.000000m
     Sill =         30
     Directional Scales = (200.000000m, 40.000000m,800.000000m)
S4 : Spherical - Range = 100.000000m
     Sill =         20
     Directional Scales = ( N/A,700.000000m,100.000000m)
```

Model : Drift part
==================
Number of drift functions = 1
- Universality condition

========== End of Parameter File Print ==========

========== Parameter File Print ==========
---> Set name : VarModelGaussFeMagn_OnlyDia
Directory name .... Kvannevann
File name .... Comp_S_DL_8m_New
Selection name .... DiamondDrillHoles
Number of variables ... 1
GaussFeMagn_OnlyDia
Total number of samples in File 1413
Number of samples in Selection 1381

Model : Covariance part
=======================
Number of variables = 1
- Variable 1 : GaussFeMagn_OnlyDia
Number of basic structures = 4
Global Rot (mathematician) = (10.00, 0.00, 10.00)
Global Rot (geologist) = (80.00, 10.00, 0.00)
S1 : Nugget effect
Sill = 0.15
S2 : Spherical - Range = 35.000000m
Sill = 0.25
Directional Scales = (100.000000m, 35.000000m, 40.000000m)
S3 : Spherical - Range = 500.000000m
Sill = 0.6
Directional Scales = (500.000000m, N/A, N/A)
S4 : Spherical - Range = 40.000000m
Sill = 0.5
Directional Scales = (N/A, 40.000000m,250.000000m)

Model : Drift part
==================
Number of drift functions = 1
- Universality condition

========== End of Parameter File Print ==========

========== Parameter File Print ==========
---> Set name : VarModelGaussFeTot
Directory name .... Kvannevann
File name .... Comp_S_DL_8m_New
Selection name .... None
Number of variables ... 1
GaussFeTot
Total number of samples in File 1413
Number of samples in Selection 1413

Model : Covariance part
=======================
Number of variables = 1
- Variable 1 : GaussFeTot
Number of basic structures = 4
Global Rot (mathematician) = (14.00, 0.00, 16.00)
Global Rot (geologist) = (76.00, 16.00, 0.00)
S1 : Nugget effect
Sill = 0.2
S2 : Spherical - Range = 25.000000m
Sill = 0.4

Directional Scales = (70.000000m, 25.000000m, 60.000000m)
S3 : Spherical - Range = 35.000000m
Sill = 0.3
Directional Scales = (400.000000m, 35.000000m,200.000000m)
S4 : Spherical - Range = 100.000000m
Sill = 0.15
Directional Scales = (N/A,100.000000m, N/A)

Model : Drift part
==================
Number of drift functions = 1
- Universality condition

========== End of Parameter File Print ==========

========== Parameter File Print ==========
---> Set name : VarModelGaussMnO
Directory name .... Kvannevann
File name .... Comp_S_DL_8m_New
Selection name .... None
Number of variables ... 1
GaussMnO
Total number of samples in File 1413
Number of samples in Selection 1413

Model : Covariance part
=======================
Number of variables = 1
- Variable 1 : GaussMnO
Number of basic structures = 2
S1 : Nugget effect
Sill = 0.1
S2 : Spherical - Range = 65.000000m
Sill = 0.75

Model : Drift part
==================
Number of drift functions = 1
- Universality condition

========== End of Parameter File Print ==========

========== Parameter File Print ==========
---> Set name : VarModel_MnOCondExp
Directory name .... Kvannevann
File name .... MnO_Merged_ForCondExp
Selection name .... None
Number of variables ... 1
MnO_CondExp
Total number of samples in File 2506
Number of samples in Selection 2506

Model : Covariance part
=======================
Number of variables = 1
- Variable 1 : MnO_CondExp
Number of basic structures = 2
Global Rot (mathematician) = (10.00, 0.00, 10.00)
Global Rot (geologist) = (80.00, 10.00, 0.00)
S1 : Nugget effect
Sill = 0.1
S2 : Spherical - Range = 38.000000m
Sill = 0.4

```
    Directional Scales = (140.000000m, 38.000000m, 80.000000m)

Model : Drift part
==================
 Number of drift functions  = 1
 - Universality condition

========== End of Parameter File Print ==========


========== Parameter File Print ==========
---> Set name   : VarModelJointDensity_Lag1m
    Directory name ........ Kvannevann
    File name ............. BreaksLines
    Selection name ........ None
    Number of variables ... 1
     JointDensity
    Total number of samples in File 15038
    Number of samples in Selection  15038

Model : Covariance part
=======================
Number of variables        = 1
- Variable 1 : JointDensity
Number of basic structures = 3
Global Rot (mathematician) = (  20.00,    0.00,   30.00)
Global Rot (geologist)     = (  70.00,   30.00,    0.00)
S1 : Nugget effect
    Sill =       3.84
S2 : Spherical - Range = 90.000000m
    Sill =        1.7
    Directional Scales = (110.000000m, 90.000000m,110.000000m)
S3 : Spherical - Range = 90.000000m
    Sill =        0.8
    Directional Scales = (500.000000m, 90.000000m,500.000000m)

Model : Drift part
==================
 Number of drift functions  = 1
 - Universality condition
========== End of Parameter File Print ==========
```